Neurotrophin Receptor p75 Affords Clearance of Amyloid Beta in Alzheimer's Disease and Provides Targeting Route to Basal Forebrain Cholinergic Neurons

by
Inga Antyborzec, M.Sc
supervised by Dr.Saak Ovsepian
and Prof.Oliver Dolly

Thesis submitted for the award of
Doctor of Philosophy

September 2016

International Centre for Neurotherapeutics
School of Biotechnology, Dublin City University

Declaration

I hereby certify that this material, which I now submit for assessment on the programme of study leading to the award of Ph.D. is entirely my own work, and that I have exercised reasonable care to ensure that the work is original, and does not to the best of my knowledge breach any law of copyright, and has not been taken from the work of others save and to the extent that such work has been cited and acknowledged within the text of my work.

Signed: _____

Candidate ID No.: 58116711

Date: 8th September, 2016

Table of contents

List of abbreviations:

AA - amino acid
AAV – adeno associated virus
Aβ - amyloid beta
AC - anterior comissure
ACh – acetylcholine
AChEIs - acetylcholinesterase inhibitors
AD - Alzheimer's disease
ADAM – a desintegrin and metalloproteinase-family of enzymes
AICD - APP intracellular domain
AMPA - α-amino-3-hydroxy-5-methyl-4-isoxazolepropionic acid
AlP - alkaline phosphatase
AP - anterio–posterior
Aph – anterior pharynx defective
APOE – apolipoprotein E
APP - amyloid precursor protein
AraC - cytosine-β-D-arabinofuranoside
ATS – Advanced Targeting Systems
α7 nAChRs – α7-type nicotinic acetylcholine receptor
BACE - β-APP cleaving enzyme
B/Akt - protein kinase B also known as Akt
BAS – nucleus basalis
BBB – blood brain barrier
BCIP - 5-bromo-4-chloro-3-indolyl phosphate
BDNF - brain derived neurotrophic factor
BF - basal forebrain
BFCNs – basal forebrain cholinergic neurons
BoNT A – botulinum neurotoxin type A
BoNT B – botulinum neurotoxin type B
BSA - bovine serum albumin
CA 1 – cornu ammonis area 1
CA 2 – cornu ammonis area 2
CA 3 - cornu ammonis area 3
CALHM1 – calcium homeostasis regulator 1
CBPs – calcium binding proteins
CC – corpus callosum
ChAT - choline acetyltransferase
CMV – cytomegalovirus promoter
CNS – central nervous system
CPA – cyclopiazonic acid
CRD - cysteine rich domain
CSF - cerebrospinal fluid
CSPD - disodium 3-(4-methoxyspiro{1,2-dioxetane-3,2' (5'chloro) tricycle [3.3.1.13,7]decan}-4-yl) phenyl phosphate
CTB - cholera toxin binding
CTF – carboxy terminal fragment
DA - dopamine
DAB - 3,3'-diaminobenzidine
DAPI - 4',6-diamidino-2-phenylindole

DBB – diagonal bands of Broca
DG – dentate gyrus
DIC – differential interference contrast
DMEM – Dulbecco's Modified Eagle's Medium
DMN - default mode network
DV – dorso-ventral
EC – enthorinal cortex
EDTA - ethylenediamine tetraacetic acid
EE – early endosomes
EF-1 – elongation factor 1
EGTA - ethylene glycol-bis(2-aminoethylether)-N,N,N′,N′-tetraacetic acid
Epi – epinephrine (adrenaline)
ER – endoplasmic reticulum
ERC – enthorinal cortex
FACS - fluorescence activated cell sorting
FAD – familial AD
FCS - fetal calf serum
FDA - Food and Drug Administration
FITC - fluorescein isothiocyanate
FL-$p75^{NTR}$ - full length $p75^{NTR}$
fMRI -functional magnetic resonance imaging
FX – fornix
GABA – gamma aminobutyric acid
GAD – glutamic acid decarboxylase
GAG – group specific antigen
GFP – green fluorescence protein
GM1 – monosialotetrahexosylganglioside
GSK-3β – glycogen synthase kinase 3 beta
GT1b – trisialoganglioside 1b
GWAS - genome wide association studies
H - hippocampus
HBSS - Hank's balanced salt solution
HDB - horizontal limbs of diagonal band of Broca
HEPES - 4-(2-hydroxyethyl)-1-piperazineethanesulfonic acid
hGlob-pa – human globin poly- adenylation site
Hins-pA – human insulin polyadenylation sequence
HIV-1 - human immunodeficiency virus type 1
HRP – horseradish peroxidase
5-HT3 – 5-hyroxytryptamine (serotonin) receptor
IC - immuno-cytochemistry
ICD - intracellular domain fragment
Icv – intracerebroventricular
IgG - immunoglobulin
i.p. – intraperitoneal
iPSCs - induced pluripotent stem cells
IP3R - inositol trisphosphate receptors
IRES - internal ribosome entry site
JNK - Jun N-terminal kinase
Kd - dissociation constant
kDa - kilodalton

LE – late endosomes
LentiGFP – lentivirus expressing green fluorescent protein
LDT - laterodorsal tegmentum
Life Tech. – Life Technologies
LoC – locus ceruleus
LS - lysosomes
LSM - laser scanning microscope
LTD - long-term depression
LTR – long terminal repeats
LV – lateral ventricle
LVs – lentiviral vectors
mAChR - muscarinic acetylcholine receptors
MAG - myelin associated glycoprotein
MBN – magnocellular basal nucleus
MCI – mild cognitive impairment
MCPO - magnocellular preoptic area
MF – mossy fiber
mGluRs – metabotropic glutamate receptors
MIB- mebefradil
ML – medio-lateral
MRI – magnetic resonance imaging
mRNA – messenger ribonucleic acid
MS - medial septum
MVB – multivesicular cell bodies
MW – molecular weight
nAChRs – nicotinic acetylcholine receptors
NBM – nucleus basalis of Meynert
NBT - nitro blue tetrazolium chloride
NCX - sodium-calcium exchanger
NE – norepinephrine (noradrenaline)
NEP – neprilysin
NF-κB - nuclear factor 'kappa-light-chain-enhancer' of activated B-cells
NFTs – neurofibrillary tangles
NGF - nerve growth factor
NGFR - nerve growth factor receptor
NIRF - neurotrophin receptor interacting factors
NMDA - N-methyl-D-aspartate
NO - nitric oxide
Nogo66 - ligands recognized by 66-amino acid fragment of Nogo
NogoR - neurite outgrowth inhibitory receptor
NRADD - neurotrophin receptor alike death domain protein
NRH1 - neurotrophin receptor homolog-1
NRH2 - neurotrophin receptor homolog-2
NT 3 – neurotrophin 3
NT 4 – neurotrophin 4
NTR– neurotrophin receptor
NTs – neurotrophins
Nuc - nucleus
oAβ – oligomeric amyloid β
OMGP - oligodendrocyte - myelin glycoprotein

PACAP - pituitary adenylate cyclase-activating polypeptide
PBS - phosphate buffered saline
PC – prefrontal cortex
PC1 – pro-convertase 1
PC2 - pro-convertase 2
PEI – polyethylenimine
PEN 2– presenilin enhancer 2
PET – positron emission tomography
PFA - paraformaldehyde
PI3-K - phosphatidylinositol 3-kinase
PLAIDD - p75-like apoptosis-inducing death domain protein
PLCγ - phospolipase Cγ
PMA - phorbol ester 12-myristate 13-acetate
PMCA - plasma membrane calcium ATPase
PP – prefrontal fibers
PPC - posterior cingulate cortex
PPT - pedunculopontine tegmentum
Pro-NGF - pro nerve growth factor
PrP - prion peptides
PSEN 1 – presenilin 1
PSEN 2 – presenilin 2
PSD 95 – postsynaptic density protein 95
P0 - postanatal day 0
$p75^{NTR}$ - p75 neurotrophin receptor
Ras - superfamily of small GTPases
RE – recycling endosomes
REM – rapid eye movement
Rho - subfamily of the Ras superfamily
RIP – regulated intramembrane proteolysis
RNS – reactive nitrogen species
ROS – reactive oxygen species
RRE – reve responsive element
RVG – rabies virus glycoprotein
RyR - ryanodine receptors
SAD – sporadic AD
s.c. – subcutaneous
SC – Schaffer collaterals
SE – signalling endosomes
SERCA – sarco-/endoplasmic reticulum calcium
SHP - septo-hippocampal pathway
SI - substantia innominata
siRNA – small interfering ribonucleic acid
SNARE - "SNAP (Soluble NSF Attachment Protein) REceptor" proteins
SNPs - single nucleotide polymorphism
SOP – standard operating procedure
s-$p75^{NTR}$ - short isoform of $p75^{NTR}$
SSC – side scatter
Sulfo-NHS-SS-biotin – sulfosuccinimidyl-2-[biotinamido]ethyl-1, 3-dithiopropionate
TACE - tumour necrosis factor alpha-converting enzyme
TAT/REV – reverse transcriptase

TeTx - tetanus toxin
ThG - Thapsigargin
TNF – tumour necrosis factor
TNFRSF - tumour necrosis factor receptor superfamily
TRAF - TNF receptor associated factors
Trk - tropomyosin-related tyrosine kinase
Trk A - tropomyosin-related tyrosine kinase A
Trk B – tropomyosin-related kinase B
Trk C – tropomyosin-related kinase C
TRPC - transient receptor potential type C
vAChT – vesicular acetylcholine transporter
VDB - vertical limbs of the diagonal band of Broca
VGCC - voltage-gated calcium channels
Vglut - vesicular glutamate transporters
VP - ventral pallidum
Vps10p - vacuolar protein sorting 10 protein
VSV-G – vesicular stomatitis virus glycoprotein
VTA – ventral tegmental area
WB – western blot
WGA - wheat germ agglutinin
WPRE – woodchuck post-translational regulatory element

List of Tables

Index of Figures

Abstract

I.M. Antyborzec

"Neurotrophin Receptor p75 Affords Clearance of Amyloid Beta in Alzheimer's Disease and Provides Targeting Route to Basal Forebrain Cholinergic Neurons"

Basal forebrain cholinergic neurons (BFCNs) are one of the most affected neuronal populations in Alzheimer's disease (AD). They exclusively express p75 neurotrophin receptor ($p75^{NTR}$) during adulthood, known also to bind non-neurotrophic ligands including amyloid beta (Aβ), which is mainly responsible for neuronal damage in AD.

Immuno-histochemistry and Western blot analysis as well as fluorescent and confocal laser scanning microscopy were utilized in this study to identify and functionally characterize BFCNs in culture and *in vivo*. Stereotactic injections into the rat brain were used to chemically-induce AD and later to introduce lentivirus targeted to BFCNs.

Selective internalization of $p75^{NTR}$ (labelled with 192-IgG-Cy3) and fluorescent (Alexa 488-labelled) Aβ (1-42) was observed in live cultured BFCNs. Parameters of endocytosis and combined trafficking of these two molecules were analyzed as well as their distribution in compartments of BFCNs. Although Aβ entry routes remains elusive, the destination of $p75^{NTR}$ cargo points to lysosomes, suggesting a novel role of $p75^{NTR}$ in Aβ clearance by cholinergic cells. This was also true in saporine-induced (192-IgG-SAP) *in vivo* AD rat model, in which increase of Aβ (1-42) was observed in cortical and hippocampal structures of brain, thus confirming the role of BFCNs in clearance of Aβ. Interestingly in further experiments Aβ (1-42) oligomers significantly reduced $p75^{NTR}$ endocytosis in a dose-dependent manner, suggesting new homeostatic role of $p75^{NTR}$ in Aβ uptake. $P75^{NTR}$ also prove to facilitate transfer of lentiviral vectors to BFCNs *in vitro* and *vivo*. 192-IgG-lentivirus injected into the lateral ventricle of rat brain yielded selective expression of GFP in cholinergic neurons in medial septum and diagonal bands of Brocca regions.

New functions of $p75^{NTR}$ described in this thesis make significant contribution to the knowledge of AD. Also novel strategy described herein can be utilized further for targeted delivery of neurotherapeutics to BFCNs with possible minimal off-side effects.

Chapter I. General introduction to Alzheimer's disease (AD)

1.1. History of Alzheimer's disease

The first case study of AD was presented during a lecture given on the 4th of November 1906 at the Conference in Tübingen (south-west Germany) by a neuropathologist - Dr. Alois Alzheimer. He reported observations made in his patient Auguste D., whose sickness he followed since her admittance to the mental hospital in Frankfurt. Auguste D. experienced devastated symptoms of aphasia, disorientation, paranoia, hallucinations and pronounced psycho-social impairment that progressed to her death at 53 years of age. Dr. Alzheimer took her brain for post-mortem analysis and discovered "peculiar changes" in neurophybrils later called neurophybrillary tangles and "miliary foci" in the cortex, currently known as amyloid beta (Aβ) plaques. His report on these histopathological alterations did not get much attention initially, but was emphasized in Emil Kraeplin's *Handbook of Psychiatry* in 1910 under the acronym of Alzheimer's disease. For the next 50 years, cases similar to Auguste D. were considered as normal part of aging until it was confirmed that synapse loss is the major correlate of cognitive decline and shown that the number of plagues and tangles correlate with severity of the disease (Deutsch 1971; Katzman, 1976). Soon after a reduction in the number of cholinergic neurons of BF was discovered (Bowen et al., 1976; Davies and Maloney, 1976), combined with a decrease of choline acetyltransferase (ChAT) activity in the cerebral cortex (Bartus et al., 1982). This stream of research continued to yield knowledge about other cholinergic markers associated with AD (Bierer et al., 1995). Parallel studies revealed considerable down-regulation of nicotinic cholinergic receptors (nAChRs) in the cortex (Araujo et al., 1988; Sihver et al, 1999). About the same time, nicotinic and muscarinic agonists were developed (Sunderland et al, 1988) and clinical trials began. That resulted in the first drug - tacrine (Cognex) approved by the Food and Drug Administration (FDA), developed by Warner-Lambert in 1993 and followed by Aricept (Donepezil) in 1996. Since then, the era of acetylcholinesterase inhibitors (AChEIs) has started and despite limited success of these drugs, they remain to this day a main FDA-approved option for the treatment of clinical and pre-clinical AD. Apart from AChEIs, FDA approved Memantine in 2003, which acts as an antagonist of N-methyl-D-aspartate (NMDA) receptor (Chapter 1.6). Other potential therapeutics are currently in clinical trials, with their effects largely mediated via modulation of the activity of enzymes involved in the cleavage of amyloid precursor

protein (APP) (β and γ secretase inhibitors) or prevention of the aggregation of toxic Aβ species (anti-aggregants) as well as targeting amyloid plagues directly (through active or passive immunization).

1.2. Risk factors for AD

Both genetic and environmental risk factors can contribute to the development of AD. Genetic factors are mainly accountable for early onset of familial AD (FAD), which is responsible for less than 10% of all AD cases. They follow Mendelian pattern of inheritance, represented more precisely by autosomal dominant mutations in the genes for APP on chromosome 21, presenilin 1 (PSEN 1) on chromosome 14 or presenilin 2 (PSEN 2) on chromosome 1 (Schellenberg et al, 1992; Levy-Lahad et al., 1995; Prince and Sisodia 1998). Point mutations in these three genes lead to over-production of Aβ protein, which accumulates in pathological amounts and forms aggregates in the brains of AD patients. These genetic data have been also considered as the strongest supportive evidence for amyloid hypothesis of AD (Chapter 1.5.).

As regards to the genetic bases for late onset of AD, they are less known and mostly connected to apolipoprotein E (APOE). APOE is polymorphic protein (with three major isoforms APOE 2, APE 3, APOE 4) essential for the normal catabolism of triglyceride-rich lipoprotein constituents (Nishimura et al., 2014). The highest genetic risk of AD is associated with allele 4 of APOE on chromosome 19 (Kingwell, 2013) with around 40 – 80 % of affected patients possessing at least one copy of this allele, which can increase the chance of developing AD 2-5 fold, whereas having two alleles raises this possibility more than 5 times. However, the presence of allele 4 of APOE does not necessarily predispose to developing the disease. There are populations (e.g. Nigerian) that reveal no link between APOE 4 and the incidence of AD (Osuntokun et al., 1995). Moreover and to complicate the apolipoprotein story, another allele of APOE (allele 2) is found to be protective in many AD cases. Currently-running genome wide association studies (GWAS) analyse millions of single nucleotide polymorphism (SNPs) in search of the genes responsible for the disease. A catalogue of these GWAS has been complied and is available to the public at: http://www.alzgene.org/largescale.asp with up-to-date rank list of odd ratios for each genetic risk factor. In addition, meta-analysis has been

performed for each gene, for which there are at least two independent association studies; these data are also available online. They suggest the incomplete penetrance of genetic risk factors associated with late AD, leaving room for epigenetic and environmental stimuli that may contribute to the development of the disease.

On the other hand, the vast majority of sporadic AD cases (almost 95 %) occurs without involving any obvious genetic risks. They develop with time and mostly manifest after 65 years of age. Age as a risk factor actually doubles the possibility of getting AD after 65; therefore, aging is still the main and best known condition for developing the disease (Mattson and Magnus, 2006). The number of AD cases raises rapidly in aging global population according to Alzheimer's association (Fargo, 2014). The group with the highest risk of AD, those older than 85, is currently the fastest growing age group in the developed countries. It is estimated that the number of people with AD actually doubles by mid-century. However, it is essential to remember that AD is not a normal part of aging and advanced age alone is not sufficient to cause the disease. Beside age, the other so-called lifestyle risk factors are also important for the disease process. These may include exercise (Smith et al., 2014), diet (Solfrizzi et al., 2011), education and occupation (Garibotto et al., 2008; 2013) or other putative risks which involve smoking and alcohol consumption, (Piazza-Gardner, 2013; Durazzo et al., 2014) or traumatic brain injury (Weiner et al., 2014).

The above characteristics of risk factors for sporadic and familial AD cases is simplified and it is important to bear in mind the complexity of the disease that allows early onset symptoms to appear without the evidence of Mendelian transmission as well as existence of late symptoms of AD with familial clustering.

1.3. Clinical symptoms, forms of AD and current diagnosis

The memory deficit in AD follows a particular pattern known as Ribot's law (Ribot, 1881) in which recently acquired memories are more vulnerable to loss than longer established ones. The patients show anterograde dementia (difficulty in learning new information) or retrograde amnesia (difficulty in retrieving previously learned information), displaying preserved memory for information from the remote past. Short-term memory deficits begins early in the disease process with common symptoms including asking the same question repeatedly, forgetting important

appointments or difficulties in finding words. However at this stage the person seems to be normal, because the social skills remain largely intact (Solomon and Murphy, 2008). As the disease progresses, working memory becomes impaired. This form of memory is responsible for reasoning and comprehension as well as goal-oriented active monitoring and manipulation of information or behavior in the presence of interfering processes (Becker and Morris, 1999). Spatial memory responsible for real time navigation into familiar or unknown environment also becomes impaired early in AD (Nitz, 2009). Higher cognitive functions, which include the executive (planning, problem solving, verbal and abstract reasoning, multi-tasking, judgment) or attention control (integration, processing, disposal, and retrieval of information) are also affected (Budson and Solomon, 2012). Progressive deterioration of cognition and memory functions cause that patients are usually unable to take care of themselves in later stages of the disease. Their motor coordination and general locomotion become affected and daily activities impaired, which may lead to complete incapacitation. The disease finishes with total loss of cognitive functions and close to complete memory and behavioural loss.

Such developments are devastating not only for the patient but equally difficult for family members or caregivers. A person with AD may eventually fail to recognize one's own spouse and children. The rate of AD progression widely differs from case to case with average 5 years from diagnosis to death, although the neuropathological process itself can start 10-20 years prior to the appearance of first clinical signs. Recognizing the harbingers of AD as opposed to changes associated with normal aging is very important, as an early diagnosis can help in the management of the disease.

By convention, several stages of AD are defined, which include pre-dromal, moderate and severe stages, with borders between these phases, and appropriate guidelines for the clinicians how to qualify them remaining a matter of debate (Dubois et al., 2010). Pre-dromal (pre-symptomatic) stage of dementia also called as mild cognitive impairment (MCI) does not necessarily evolve into clinical AD. Generally, memory tests are performed as indicators of AD severity, followed by magnetic resonance imaging (MRI) to measure the white matter hyper-intensity versus total brain matter as well as intracranial and hippocampal volumes (Borson et al., 2005; Archana and Ramakrishnan, 2014). Also, positron emission tomography

(PET) is used to observe the amyloidosis in brains of AD affected people or those in high risk groups (Grimmer et al., 2009).

Research continues on the developments of cerebrospinal fluid (CSF) or less invasive blood plasma biomarkers for AD diagnosis (Laske 2011; Kang et al., 2014). One of the prime aims and challenges nowadays is to diagnose AD early enough, so that the patient could benefit from the disease modifying therapies available prior to the onset of extensive neurodegenerative alterations with irreversible functional impairments (Nordberg, 2015).

In summary, it is worth stressing that AD, one of the worst chronic progressive neurodegenerative illness accompanied by global intellectual debilitation, followed by death, is largely of unknown origin and further research is urgently needed to find out its underlying causes and provide reliable and effective treatment with rehabilitation.

1.4. Pathological hallmarks of AD and their correlation with the disease

Clinical manifestations of AD are caused by pathological changes in specific brain areas. Among the main neuropathological changes, the senile plaques and neurofibrillary tangles (NFTs) are the most frequently described since Alois Alzheimer's first case study of AD in 1901.

Amyloid plaques are extracellular deposits of aggregated Aβ peptides with two most common variants –Aβ40 and Aβ42 (Glenner et al., 1984). They are surrounded by large dystrophic neurites, which can also be present within the senile plagues (Cras et al., 1991), hypertrophic astrocytes and activated microglia as well as other inflammatory cells. Heparan sulfate proteoglycan and apolipoprotein E also associate with the plaques (Fukuchi et al., 1998; Sanan et al., 1994). Among other elements, the complement cascade like α-1-antichymotrypsin, lysosomal proteases or anti-oxidant enzymes constitute a minority of these structures (Abraham et al., 1988; Lemere et al., 1995; McLellan et al., 2003). Strong staining for AChE activity is also revealed in the plaques due to the local distortion of cholinergic fibers network (Alvarez et al., 1997). Senile plaques deposition occurs early in the disease process and proceeds slowly. The accumulation of amyloid plaques does not always correlate with severity of cognitive deficit and memory loss of AD (McLean et al., 1999, Perez-Nievas et al, 2013).

Deposition of Aβ associated with cerebral vasculature is frequently found in AD (Glenner and Wong, 1984). This so called vascular dementia is caused by blockage or damage and leaking of blood vessels, which deprive small areas of brain from blood and oxygen, often causing local strokes with neurodegeneration and cognitive decline (Iadecola, 2004). It is currently unsolved which proportions of dementia are caused by plaques and associated damage or vascular pathology, with some arguments that the latter accelerates the damage driven by amyloid (Kester et al., 2014). In the past, evidence of vascular dementia was used to exclude a diagnosis of AD (and vice versa). This is no longer valid since pathological evidence shows both types of brain changes commonly co-exist creating so called mixed dementia (Jellinger and Attems, 2007; Schneider et al., 2007).

As opposed to amyloid plaques, NFTs are represented largely by intra-neuronal inclusions, that can be found both in association with fibrilliar amyloid plaques or apart from them (e.g. in frontotemporal dementia). NFTs are composed of microtubule-associated proteins (MAPs) - tau in their hyperphosphorylated form. Normally this protein plays an important role in cytoskeleton formation and stability by reversible phosphorylation and dephosphorylation (Weingarten et al., 1975). If phosphorylated tau is not dephosphorylated, it is unable to bind other microtubules, which results in polymerization of the phosphorylated tau to the straight filaments. These are then cross-linked by glycosylation to form paired helical fragments (PHF), found in NFTs (Grundke-Iqbal et al., 1986). NFTs correlate better than plaques with cognitive decline (Arriagada et al., 1992; Giannakopoulos et al., 2003). However, more recent theories postulate a main role of soluble tau in AD (Berger et al., 2007; Lasagna-Reevers et al., 2011).

In addition to these two mentioned above pathological features, extensive loss of neurons and degeneration of nerve terminals are also reported in AD. Cell death occurs mostly by apoptotic or necrotic processes triggered by proteases such as caspases and calpains (Wang, 2000; Mattson, 2000). BF cholinergic neurons studied in parts of this work are especially vulnerable to AD (Chapter 1.5.3.2.). However, the synaptic changes are observed long before cell loss (Knobloch and Mansuy, 2009; Bosch and Hayashi, 2012). They are central to the disease process and correlate best with the severity of dementia (DeKosky and Scheff, 1990; Arendt 2009, Koffie et al., 2011). Both, Aβ and tau contribute to the synapse degeneration (Bloom 2014).

1.5. Main hypothesis of AD

1.5.1. Amyloid cascade hypothesis

Amyloid cascade hypothesis is the prevailing hypothesis in the field of AD. It views over-production or deficit of Aβ clearance as proximal cause of both SAD and FAD. The production of Aβ and its accumulation into the toxic species deposited in brain in the form of plaques are key elements of this hypothesis (Hardly and Selkoe 2002, Golde and Janus, 2005). Genetic correlation of presenilins and APP mutations (Chapter 1.3.) with AD strongly favours the main role of Aβ in AD. However, the presence of amyloid plaques does not always correlate with cognitive decline. Therefore, the original hypothesis has been modified, emphasizing the pathogenic role of non fibrilliar Aβ in form of oligomers, postulated to be the primary cause of cognitive impairment of AD (Selkoe 2008). This hypothesis is based on observation that mental decline precedes the appearance of fibrilliar Aβ in transgenic mouse models of AD (Billings at all, 2005) and that there is a strong positive correlation between the levels of soluble Aβ and severity of dementia (McLean, 1999). The amyloid cascade hypothesis also implicates Aβ in the initiation of pathological processes associated with impairments of MAP tau functions and cell loss.

1.5.1.1. Generation of amyloid β (Aβ) in brain, its toxicity and clearance

The molecular events that lead to Aβ production in brain are governed by a series of endoproteases that cleave transmembrane amyloid precursor protein (APP). APP can be processed via amyloidogenic pathway, through sequential proteolysis by β and γ secretases (Shoji et al., 1992) as shown in Figure 1. or in a non amyloidogenic way by metalloproteases TACE or ADAM family (ADAM 10 or 17), which possess α-secretase activity. They cleave APP within the Aβ domain to produce soluble sAPPα ectodomain and the membrane-bound C83 fragment; the latter is then cleaved by γ-secretase to produce the non-toxic p3 part (Słomnicki and Leśniak, 2008). It is reported that α and β secretases compete directly for APP cleavage (Skovronsky et al., 2000). β-secretase, also known as BACE-1 (β-APP cleaving enzyme), is membrane bound type 1 protein mainly localized in endosomes, lysosomes and the trans-Golgi network (Capell et al., 2000). The other variant of this aspartyl protease known as BACE-2 shows lower expression in neurons but it is widely expressed in

peripheral tissues (Bennett et al., 2000). β-secretase generates the amino N-terminus of Aβ peptide, leaving membrane-bound carboxy-terminal fragment (CTFβ 99 amino acids long) to be cleaved by γ secretase between 38 and 43 residues. The APP cleavage can occur within the Golgi network as well as during the re-internalization of APP within endosomes (Koo and Squazzo, 1995; Hartman et al., 1997). The γ-secretase itself is a multimeric protein complex consisting of presenilin-1 (PSEN1) and presenilin-2 (PSEN2) catalytic subunits, nicastrin, Aph-1 and PEN-2 (Kimberly et al. 2003). Depending on the exact point of cleavage, different length of amyloid beta peptides are generated.

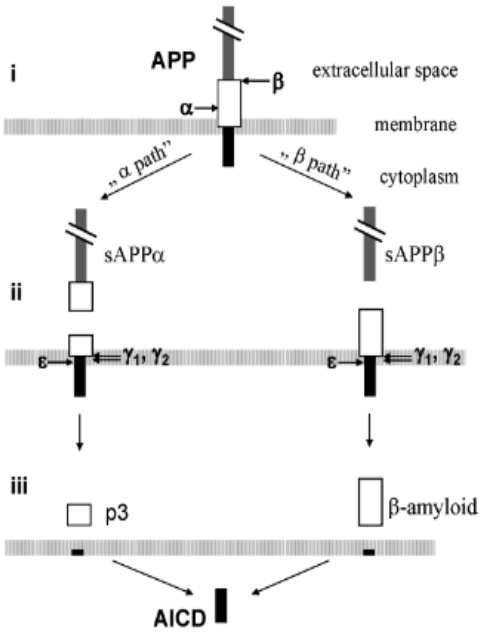

(i) The first cleavage is realized in APP extracellular domain by α or β-secretase activity and releases soluble N-terminal fragments sAPPα or sAPPβ.

(ii) Thereafter, γ-secretase generates p3 or β-amyloid (40-42) as a result of intra-membrane digestion.

(iii) Simultaneously, in both cases, the C-terminal fragment called APP Intracellular Domain (AICD) is released into the cytoplasm.

Figure 1. Proteolytic processing of APP (Słomnicki and Leśniak, 2008).

The Aβ (1-40) is the predominant isoform and accounts for 70 % of total Aβ pool (Fraering, 2007). A smaller proportion of Aβ produced as Aβ(1-42) has a greater tendency for misfolding with oligomerization (into dimers, trimers, tetramers, dodecamers and higher order oligomers). Aβ oligomers subsequently aggregate into soluble protofibrils, which are maturating further into fibrils and forming amyloid plaques (Glabe, 2008). These are mostly found in neocortex and hippocampus of AD affected brains (Masters et al., 1985). It was shown that Aβ oligomerization occurs in the endosomal compartments as well as during interaction with lipid bilayers, especially cholesterol and glycosphingolipid-rich lipid rafts (Takahashi et al., 2004; Kim et al., 2006). However, Aβ aggregation and fibrillization pathways can be independent and distinct (Necula et al., 2007). This means that Aβ oligomers are not

an obligate intermediate of insoluble fibrils. Soluble Aβ oligomeric species are reported to be the most neurotoxic (Selkoe, 2004) and they are a major cause of memory impairment according to the amyloid cascade hypothesis (Chapter 1.5.1).

Excitotoxicity due to over-excitation of NMDA receptors has been implicated as a central mechanism by which Aβ causes neuronal damage; however, there is no proof of direct Aβ binding to these receptors (Lai and McLaurin, 2010). Recent findings indicate that Aβ oligomers influence neurons indirectly, by induction of astrocytic glutamate release, which in turn activates neuronal NMDA receptors. An excessive influx of calcium through these receptors activates nitric oxide synthase, which produces toxic levels of NO that correlate with synaptic spine loss in initial phase of AD (Talantova et al., 2013). Also, other receptors are implicated in Aβ-mediated synaptotoxicity. For example, metabotropic glutamate receptors (mGluRs) facilitate Aβ induction of long term depression (LTD) (Walsh et al., 2002), or α7 nAChRs trigger a down-regulation of the ERK2/MAPK pathway, associated with memory formation (Dineleyetal., 2001). This can suggest that different receptors mediate dissimilar aspects of Aβ toxicity. However, other receptor-mediated mechanism of Aβ toxicity are also possible. For example, Aβ may alter membrane property by forming pores, which promotes calcium influx into neurons, resulting in disruption of Ca^{2+} homeostasis (Kawahara, 2010) (Chapter 1.5.1.2.). It is also possible that Aβ create clusters at the membrane that may reduce the level of scaffolding proteins like PSD-95, which stabilize the glutamate receptors on the membrane (Dinamarca et al., 2012). Additionally, intracellular Aβ is implicated in the disruption of axonal transport mediated by glycogen synthase kinase (GSK-3β) (Decker et al., 2010). The other generic explanation for the toxicity of intracellular Aβ aggregates involves the sequestration of vital proteins for the cell, that results in the cellular dysfunction and apoptosis (Selkoe, 2003). Aβ is also known to trigger hyper-phosphorylation of tau and the formation of NFTs (Amadoro et al., 2011). However, how exactly Aβ causes neurotoxicity in AD remains a matter of debate. The factors known to increase Aβ production and therefore neurotoxicity involve genetic mutations in Aβ precursor (APP) or the enzymes involved in Aβ production (presenilins) (Haass et al., 1995; Jankowsky et al., 2004). Also, some enzymes associated with acetylcholine turnover are known to play an important role in neurotoxicity induced by Aβ. For example, Aβ-AChE complexes associated with amyloid plaques (Alvarez et al., 1997) are

more toxic than amyloid fibrils alone. AChE interacts with the growing amyloid fibrils and accelerates the assembly of Aβ peptides.

It is worth mentioning that Aβ peptides can be generated as a part of normal metabolism of APP (Seubert et al., 1992). They have been implicated in physiological regulation of synaptic activity (Kamenetz et al., 2003). However, their precise function in healthy brains is unclear. It is known that unaggregated Aβ peptides in low concentrations (0.1 – 1 μM) may exert neuro-protective effects as they activate PI-3-K pathway and inhibit GKS-3β (Giuffrida et al., 2009).

The clearance of Aβ from brain is an important process regulating the Aβ homeostasis, with its disruption leading towards pathological accumulation of neurotoxic species of this peptide in AD brain. The mechanisms of removal Aβ peptides have been extensively studied and they involve: receptor-mediated transfer of Aβ to intra-vascular space by LRP receptors, efflux of soluble Aβ from brain parenchyma to the blood by adenosine triphosphate pump (Shibata et al., 2000; Lam 2001) and local break down of Aβ through neprilysin (NEP) (Iwata et al., 2000). However, none of these processes can explain the preferential accumulation of Aβ in certain brain regions and especially the vulnerability of cholinergic neurons in AD (Mesulam 2004). In this study, we provide converging evidence suggesting that BFCNs play an important role in Aβ removal, due to $p75^{NTR}$ being particularly enriched in the axons of these cells. Binding of soluble Aβ by $p75^{NTR}$ promotes its sorting to lysosomes of cholinergic cells for degradation (Chapters 4.7.).

1.5.1.2. Calcium hypothesis of AD

Intracellular calcium (Ca^{2+}) plays crucial role in many processes and is essential for functioning of key enzymes (such as kinases, phosphatases and proteases), so its altered homeostasis can account for age-related aberrations, leading towards neurodegeneration and AD. Physiological levels of free cytoplasmic Ca^{2+} is maintained between 20 to 100 nM in neuron at rest, and when activated it reaches up to 1.5 – 2.0 mM within micro domains (Llinas et al., 1995; Corona et al., 2011). The fine balance of intracellular Ca^{2+} is maintained by its regulated influx and efflux through Ca^{2+} channels and pores as well as by the exchange/sequestration of Ca^{2+} by the internal stores [endoplasmic reticulum (ER) and mitochondria]. In addition, Ca^{2+} binding proteins (CBPs) such as parvalbumin, calbindin or calretinin determine the

dynamics of free Ca^{2+} inside neurons (Schwaller, 2010). The schematic of neuronal Ca^{2+} signalling is shown on Figure 2 (Grienberger and Konnerth, 2012).

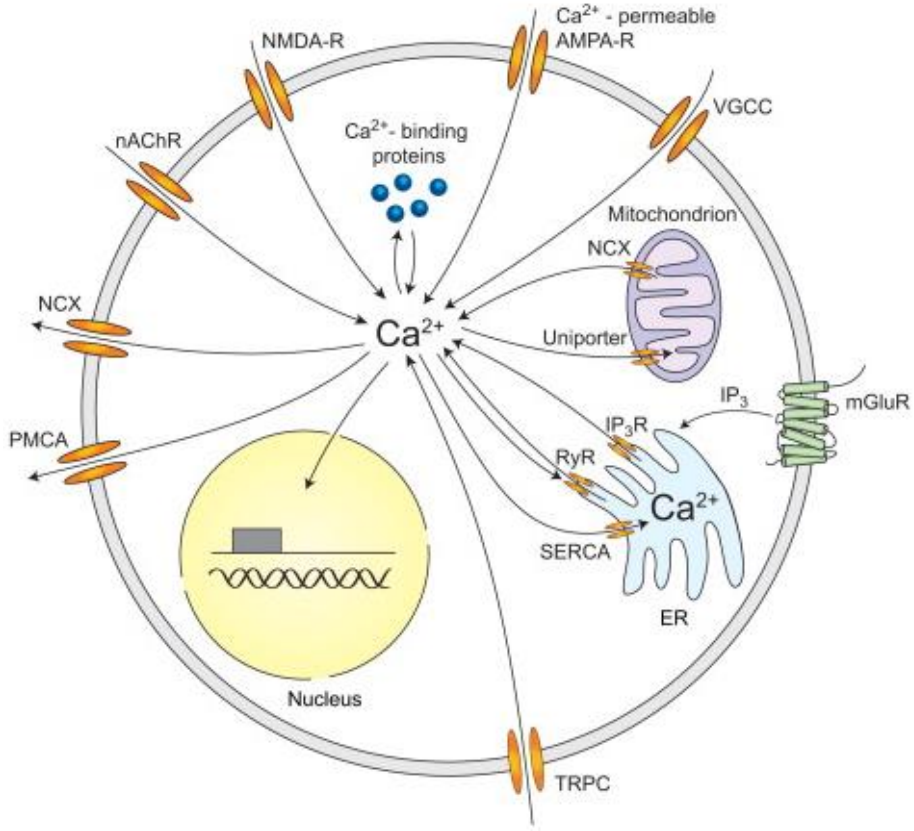

Figure 2. Neuronal calcium signalling (Grienberger and Konnerth, 2012). Sources of Ca^{2+} influx: AMPA, NMDA, nAChR, voltage-gated calcium channels (VGCC), and transient receptor potential type C (TRPC) channels. Calcium release from internal stores is mediated by inositol trisphosphate receptors (IP3R) and ryanodine receptors (RyR). IP3R can be activated by mGluR. Ca^{2+} efflux is mediated by the plasma membrane calcium ATPase (PMCA), the sodium-calcium exchanger (NCX), and the sarco-/endoplasmic reticulum calcium ATPase (SERCA). Also, the mitochondria are important for neuronal calcium homeostasis.

Altered Ca^{2+} homeostasis observed in AD could be the earliest and one of the primary causes of neurodegeneration (Hartmann et al., 1994, Kawahara et al., 2011). It is already known that increase of Ca^{2+} induces changes in the number and morphology of spines and synapses (Kato-Negishi et al., 2003), the alterations widely described in AD (Koffie et al., 2011).

Many studies have shown that Aβ directly interferes with Ca^{2+} and disrupts activity of ionotropic glutamate receptors (Alberdi et al., 2010), nAChRs (Parri and Dineley, 2010), IP3R (Cheung et al., 2010) as well as the P, Q , or L-type channels (Nimmrich et al., 2008; Ueda et al., 1997) or ER-Ca^{2+} stores (Green et al., 2008) and mitochondrial function (Leuner et al., 2007). Reduced Ca^{2+}-buffering capacity by CBPs results in inactivation of calcineurin and calpains pathways by Ca^{2+} influx

through NMDA receptors (Shankar et al., 2007, Cavallucci et al., 2013). These pathways lead to the risk of developing neurofibrillary tangles (NFTs) (Grynspan et al., 1997), dendritic spine loss and swelling of dystrophic neurites (Wu et al., 2010).
Furthermore, recent studies indicate that Aβ oligomers can directly induce Ca^{2+} entry through disturbance of plasma membrane structure and formation of Ca^{2+} permeable pores (Demuro et al., 2010; Kawahara et al., 2010). Consequently, this leads to the creation of reactive oxygen species (ROS) and induce other adverse effects similar to those usually observed after exposure of neurons to Aβ.
Genetic mutations in PSEN (Crusts and Broeckhoven, 1998) causing FAD are also linked to the dysregulation of neuronal Ca^{2+}. The reason for this phenomenon was found recently (Supnet and Bezprozvanny, 2011) as PSEN normally function as low-conductance passive ER Ca^{2+} leak channels, independent of γ-secretase activity. Their mutations therefore, cause loss of ER Ca^{2+} leak function and an exaggerated Ca^{2+} release from overloaded ER stores. This is associated with the increased production of Aβ (Green et al., 2007). Conversely, other passive Ca^{2+} channels called calcium homeostasis modulator 1 (CALHM1), which are mainly associated with ER, promote the α-secretase pathway (Green and LaFerla, 2008).
Altogether these changes indicate that aging neurons experience significant dysregulation of Ca^{2+} handling. Altered Ca^{2+} homeostasis affects production of pathological proteins (Aβ and tau) and these may further exacerbate Ca^{2+} function, having strong impact on the development of AD.

1.5.1.3. Mitochondrial dysfunction and oxidative stress hypothesis

The accumulation of Aβ has been found within structurally-damaged mitochondria isolated from AD brains (Hirai et al., 2001). Key mitochondrial enzymes were found affected; consequently, electron transport, oxygen consumption and ATP production were impaired. These discoveries prompted the hypothesis that mitochondria are focal point for synaptic dysfunction observed in AD (Caspersen et al., 2005). Both Aβ and tau have been implicated in the impairment of mitochondrial respiration. Aβ was found to form complexes with alcohol dehydrogenase (Lustbader et al., 2004) and block complex-III and IV dependent respiration leading to an aggravated mitochondrial impairment, whereas tau was found to preferentially impair complex-I of the respiratory chain (Eckert et al., 2014).

Closely connected with mitochondrial dysfunction is the oxidative stress hypothesis of AD. This is based on the fact that dysfunctional mitochondria release hydrogen peroxide into the cytosol, where it participates in metal ion hydroxyl radical formation. Elevated levels of these metal ions (iron, copper, zinc) and aluminium are linked with the reactive oxygen species that mediate damage and neurodegeneration (Praticco, 2008). Oxidative stress is also defined as an imbalance between the generation of reactive oxygen/nitrogen species (ROS/RNS) and the cells ability to neutralize them by the anti-oxidant defence. The other sources of ROS and RNS in brain are astrocytes and microglia (Akama and Van Eldik, 2000; Colton et al., 2000).

1.5.2. Tau hypothesis of AD

Tau hypothesis of AD links Aβ and tau pathology by postulating that Aβ toxicity is tau dependent. The hypothesis is based on tau and tyrosine protein kinase Fin interaction upon which Fin-kinase, localized to the dendritic compartments, phosphorylates N-methyl-D-aspartate (NMDA) receptors and mediates their interaction with postsynaptic density protein 95 (PSD95), which is required for Aβ toxicity (Ittner and Götz, 2011). On the other hand, the exposure of Aβ triggers progressively increased phosphorylation of tau, causing its accumulation in somato-dendritic compartments of the affected neurons. Hyper-phosphorylated tau has even faster affinity for Fin compared to normal MAP tau. Along with their independent harmful effects, Aβ and tau have been postulated to amplify each other's cytotoxic effects.

1.5.3. Cholinergic hypothesis of the geriatric memory dysfunction

The hypothesis was put forward in 1982 (Bartus et al., 1982) and is based on the fact that functional disturbances in cholinergic activity occurring in the brains of healthy but elderly adults are responsible for learning and memory deficits in demented individuals. These changes are attributed to region-dependent decrease of ChAT activity at both protein and mRNA levels (Bowen et al., 1976; Davies and Maloney 1976) with a decline in the activity of high-affinity choline (Rylett et al., 1983) and ACh release (Nilsson et al., 1986). According to this hypothesis the population of cholinergic cells is the earliest affected in AD (Davies and Maloney, 1976;

Whitehouse et al., 1981; Mesulam et al., 1983; McGeer et al., 1984; Geula et al., 1998; Härtig et al., 2002) and the most vulnerable to neuropathological changes occurring during the disease. Gene expression alterations and impairments in intracellular signalling or cytoskeletal transport may mediate the atrophy of cholinergic cells, leading to the age-related cognitive decline and memory loss. Gradual deficit in cholinergic functions caused by dendritic, synaptic, and axonal degeneration as well as a decrease in the trophic support of these neurons are also observed in other dementing disorders, including Parkinson's disease (Rochester et al., 2012), Down-syndrome (Sweeney et al., 1989), progressive supranuclear palsy (Ruberg et al., 1985), Jakob–Creutzfeld disease (Kudo et al., 2013), Korsakoff's syndrome (Nardone et al., 2010) and traumatic brain injury (Hong et al., 2012).

1.5.3.1. Organization of cholinergic system with emphasis on basal forebrain BF

The cholinergic system plays number of important roles that include: control of cerebral blood flow (Sato et al., 2004), sleep-wake cycle (Lee et al., 2005), attention, arousal, motivation, executive functions, memory and conscious awareness (Woolf, 1997; Perry et al., 1999), behavioural state control, reward and plasticity (Semba, 2000). The integrity of cholinergic neurons is particularly important for cognitive processes and deterioration of their connections has been implicated in the pathophysiology of AD (Chapter 1.5.3.). In CNS, these neurons create the most rostral neuromodulatory system with the capacity to modulate information processing across the entire cortical mantle (Sarter et al., 2005). Anatomical organization and connectivity of cholinergic neurons have been extensively studied with use of immuno-cytochemical methods for detection of cholinergic markers (Mesulam and Hoesen 1976; Bigl et. al., 1982; Woolf and Butcher, 1991) and injections of various tracers into the rodent’s brain (Jones and Yang, 1985; Luiten et al., 1987; Härtig et al, 1998; Chandler et al., 2013; Bloem et al., 2014). A clear and phylogenetically conserved antero-posterior organization of cholinergic system is well known and reflected in the BF, located close to the medial and ventral surfaces of the cerebral hemispheres and innervating limbic and cortical brain areas. BF is subdivided from rostral to caudal order as illustrated in Figure 3: the medial septum (MS) (also designated as Ch1 cholinergic group by Mesulam et al.,1983), the nuclei of the diagonal band of Broca (DBB) with vertical and horizontal limbs (VDBB

(Ch2) or HDBB (Ch3) respectively), basal magnocellular complex (Ch4), which comprises cholinergic neurons of the ventral pallidum (VP), the magnocellular preoptic nucleus (MCPO), the substantia innominata (SI) and the magnocellular basal nucleus (MBN) (Semba, 2000), an area known as nucleus basalis of Meynert (NBM) in primates and human brain (Koelliker, 1986).

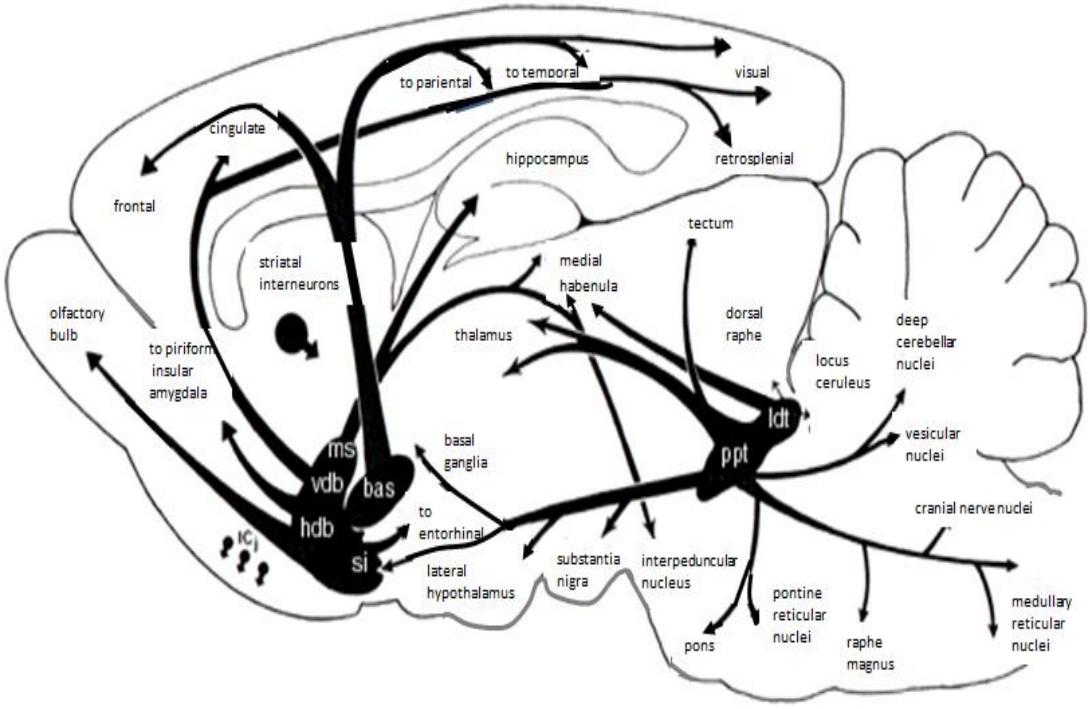

Figure 3. Schematic representation of BF cholinergic circuit (Woolf, 1991). Abbreviations: ms - medial septum, vdb-vertical diagonal band, hdb –horizontal diagonal band, bas-nucleus basalis, si - substantia innominata, ldt-laterodorsal tegmental nuclei, ppt- pedunculopontine tegmental nuclei

The contribution of projections of each BF subdivision varies within the telencephalic target area (Figure 3). The medial septal group of cholinergic neurons (ms, vdb) project to the hippocampus and para-hippocampal gyrus, while the nucleus basalis group (hdb, bas, si) innervate all parts of the neocortex, parts of limbic cortex and the amygdala. Loss of cholinergic neurons of medial septum and nucleus basalis of Meynert were mostly reported in the neurodegeneration of AD type (Whitehouse et al., 1981; Mesulam 2004; Mufson et al., 2007, Liu et al., 2015). The greatest loss of cholinergic activity is seen in the temporal lobe, which houses the hippocampus and entorhinal cortex. These structures play an important role in learning and memory, being also a primary target for neurodegeneration in AD. Significant shrinkage of these regions was noted on MRI scans of human diseased brains (Dickerson et al., 2001). The other group of central cholinergic nuclei – pedunculo-

pontine tegmental (PPT) and latero-dorsal nucleus (LDT,) act through thalamic intralaminar nuclei and provides only a minor innervation of the cortex (Schliebs and Arendt, 2006). Moreover, cholinergic projection neurons comprise also motor neurons in the spinal cord (cranial nerves 3-7 and 9-12) as well as cholinergic neurons in the sympathic and parasympathic nervous system (Martinez-Murillo and Rodrigo, 1995).

1.5.3.2. BF cholinergic neurons (BFCNs) – cells vulnerable in AD

Ontogenetically, cholinergic neurons differentiate from paraventricular neuronal precursor cells and arise first in the mouse basal forebrain circa embryonic day (E) 11, expressing cholinergic markers by E16 (Schnitzler et al., 2008). BFCNs extend their efferents toward hippocampal and cortical targets during the first postnatal weeks of development, when they critically depend on NGF supply and express neurotrophin receptors (TrkA and $p75^{NTR}$). Cholinergic neurons express also other receptors including adrenergic, glutamatergic, GABAergic (De Souza Silva et al., 2006; Gao et al., 1995; Zaborszky et al., 2004) as well as the receptors for estrogens and endocannabinoids (Harkany et al, 2003). Morphologically, these cells are the largest neurons in the forebrain and are classified into three types: multipolar, bipolar and triangular cells (Pongrac and Rylett, 1998). Trophic dependence on NGF remains important for the maintenance of their phenotypes and contents of neurotransmitters even in the mature and fully differentiated central nervous system (CNS) (Niewiadomska et al., 2002). It is worth to mention that NGF is not synthetized by BFCNs but it is supplied by target neurons and delivered to their cell body via uptake and retrograde axonal transport from cortical areas. Besides NGF, other peptides like pituitary adenylate cyclase-activating polypeptide (PACAP) were shown to promote survival of septal cholinergic neurons *in vitro* and *in vivo* after injury (Takei et al., 2000). Galanin, another peptide produced by cholinergic neurons, was reported to have trophic effect on BFCNs and can even compensate for lack of acetylcholine (ACh) in AD (O'Meara et al., 2000; Jhamandas et al., 2002).

The synthesis of ACh and its release from BFCNs is essential for normal learning, memory and attention (Winkler et al., 1995; Rasmusson 2000; Hasselmo, 2006). The ability to utilize acetyl-CoA for ACh synthesis is unique feature of BFCNs (Tucek, 1985). The acetyl CoA comes from pyruvate formed from glucose. Therefore,

cholinergic cells present higher demand for energy production and are more sensitive than other neurons to energy deprivation (Szutovicz, 2000). Choline is the second component critical for ACh biosynthesis and its uptake is considered as a rate limiting step in this process (Haga, 1971). The one-step reverse reaction is catalysed by choline acetyltransferase (ChAT) and the opposite process by acetylcholinesterase (AChE), which converts ACh into the inactive metabolites: choline and acetate. Once produced, ACh is packaged into synaptic vesicles via a vesicular ACh transporter (vAChT). Action potentials trigger the release of ACh into the synaptic cleft, where ACh binds to its receptors located on the post- and pre-synaptic membranes. Two types of acetylcholine receptors, muscarinic (mAChRs) and nicotinic (nAChRs), take part in this process (Nakayama et al., 1995; Rouse et al., 2000) (Figure 4). ACh may also spill out of synaptic contacts and produce volume transmission within the hippocampus via non-synaptic signalling (Yamasaki et al., 2010).

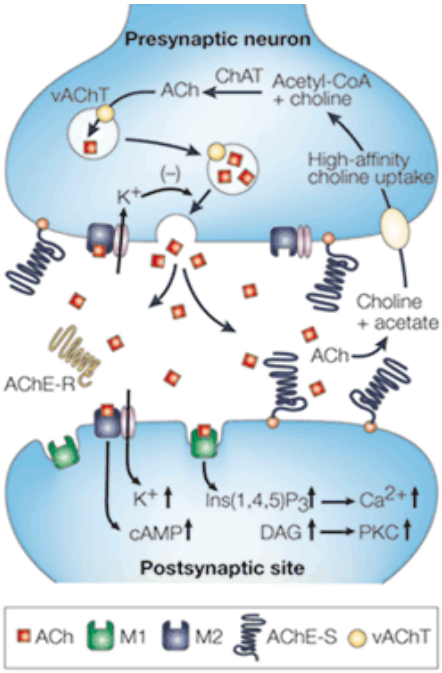

Figure 4. Schemat of acetylcholine synthesis and signalling (Soreq and Seidman, 2001).

The metabolism of ACh involves two enzymes: ChAT for synthesis this neurotransmitter from Acetyl-CoA and choline and acetylcholinesterase (AChE) for degradation. Vesicular ACh transporter (vAChT) package ACh into synaptic vesicles. Muscarinic M2 receptors (M2) on the presynaptic membrane regulate ACh release via a negative feedback response. At the postsynaptic site, M1 receptors transduce signals through a pathway involving diacylglycerol (DAG), inositol-1,4,5-trisphosphate (Ins(1,4,5)P3) and a Ca^{2+} -dependent protein kinase (PKC). ACh is hydrolysed in the synaptic cleft by AChE-S tetramers. AChE-R monomers would remain soluble within the synaptic cleft. A high-affinity choline-uptake mechanism returns choline to the presynaptic neuron.

Generally, nAChRs are ionotropic ACh - gated cation channels, while mAChRs are G protein – coupled receptors. Both families of these receptors regulate cognitive processes and are affected in AD (Bartus et al., 1982; Coyle et al., 1983; Whitehouse et al., 1986; Shimohama et al., 1986). Ionotropic nAChRs comprise of five subunits, each consisting of four transmembrane domains, that are arranged symmetrically around a hydrophilic central pore, mediating the flow of cations K^+, Na^+ and Ca^{2+}. In the human nervous system, there are eight α subunits (α2-α7, α9, α10) and three β

subunits (β2-β4) that assemble in different combinations to generate a variety of nAChR subtypes (Albuquerque et al., 2009, Gotti et al., 2006, Gotti et al., 2009). The α4β2 or α7 are the most abundant form of nAChRs in mammalian brain, with the latter reported to interact with Aβ (Wang et al., 2000; Liu et al., 2001), leading to the speculations that Aβ might be internalised with this receptor (Nagele et al., 2002), which however was not confirmed by the later studies (Small et al., 2007). Soluble Aβ(1-42) was reported to activate α4β2 and modulate postsynaptic transmission in septo-hippocampal neurons (Chin et al., 2007). However, other studies did not support this physiological action (Lilja et al., 2011). Recently new nAChRs subtype-α7β2 was found in rodent and human hippocampal interneurons and BFCNs, highly sensitive to functional inhibition by pathologically-relevant concentrations of oligomeric Aβ (Liu et al., 2009, Moretti et al., 2014).

In regards to metabotropic mAChRs, these are made up of seven transmembrane spanning regions bound to intracellular G proteins and activated when G protein alter the activity of one or more ion channels in the nerve cell membrane (Caulfield 1993; Brown et al., 1997). Five subtypes of mAChR (M1–M5) are widely distributed throughout the central nervous system and periphery (Levey, 1993). It has been shown the post-synaptic M1 receptor, which is expressed throughout the cortex and hippocampus plays a key role in regulating cognition and stimulates non-amyloidogenic APP processing (Nitsch et al., 1992; Anagnostaras et al., 2003), while M2 subtype inhibits sAPPα generation (Farber et al., 1995). M2 receptor knock-out mice show also deficits in behavioural flexibility, working memory, and hippocampal plasticity (Seeger et al., 2004). Range of nicotinic and muscarinic receptors agonists and antagonists were developed for AD treatment so far (Ren et al., 2007; Yang et al., 2012; Melancon et al., 2013; Gao et al., 2014; Fisher et al., 2016).

The activity of ChAT and consequently the synthesis of ACh is decreased in AD (Davies and Maloney, 1976; Perry et al., 1978). ACh is known to promote non-amyloidogenic APP processing and reduce tau phosphorylation (Hellström-Lindahl, 2000). In addition, the reduction of AchE was observed in AD brains (Bowen et al., 1976). However AChE inhibitors, which potentiate cholinergic function, have met with only limited success (Greig et al., 2013) and are further investigated (Rahim et al., 2015; Leong et al., 2016).

In addition to ACh, individual BFCNs also release glutamate (Allen et al., 2006). Glutamate excites BFCNs through NMDA receptors and can drive them into rhythmic burst discharge (Khateb et al., 1992), while normally these neurons exhibit a rather slow firing pattern (Duque et al., 2000). The highest firing rate of cholinergic neurons is observed in the wake state as compared to slow-wave sleep or rapid eye movement (REM) sleep. The discharge of cholinergic neurons is positively correlated with gamma activity (30-60 Hz) and negatively correlated with delta activity (1-3 Hz) during sleep-waking cycle (Hassani et al., 2009). Stimulation of cholinergic cells elicits an oscillatory theta rhythm in the hippocampus that occurs during periods of learning (McQuiston 2010). Additionally, 70 % of rostral BF cholinergic neurons in rat possess NADPH – diaphosphorase activity required for nitric oxide (NO) formation. The same neuronal population contains galanin; however, these substances are not present in higher primates and human. The human BF instead has been shown to contain large neurons expressing tyrosine hydrolase (TH) in 1.5 % of total magnocellular neurons (Semba, 2000).

1.5.3.2.1. Functional characteristics and dynamics of $p75^{NTR}$ in BFCNs

$P75^{NTR}$ (CD271) is a sixteenth member of the tumour necrosis factor receptor superfamily (TNFRSF), encompassing overall twenty five participants (Gruss, 1996). Genes for this receptor are located on chromosome 17 in humans and chromosome 11 in mice (Huebner et al., 1986). Like all members of TNFRSF, $p75^{NTR}$ contains an extracellular chain of cysteine rich domains (CRD) that have the ability to bind different ligands. They are attached to the cleavable "stalk" of 28 amino acids (aa). The single transmembrane region of $p75^{NTR}$ is highly conserved among the species and it is responsible for creating homodimers of this receptor. The juxtamembrane domain, called also "chopper domain" and the carboxy-terminal domain, called "death domain" are localized intracellulary. They contain multiple O-glycosylated (juxtamembrane domain), palmitoylated and phosphorylated sites ("death domain"), useful in the receptor signalling (Barker et a., 1994, Underwood et al., 2008). Although the "death domain" of $p75^{NTR}$ contains six-α helices typical for TNFRSF, it differs from the other members of this group, because it possess TNF receptor associated factor (TRAF)-interacting motifs and potential G-protein activation site, which classify it as Type-II death domain, allowing to multiple signal transduction

pathways (Dempsey et al., 2003). The schematic representation of $p75^{NTR}$ domains is illustrated on Figure 5 below.

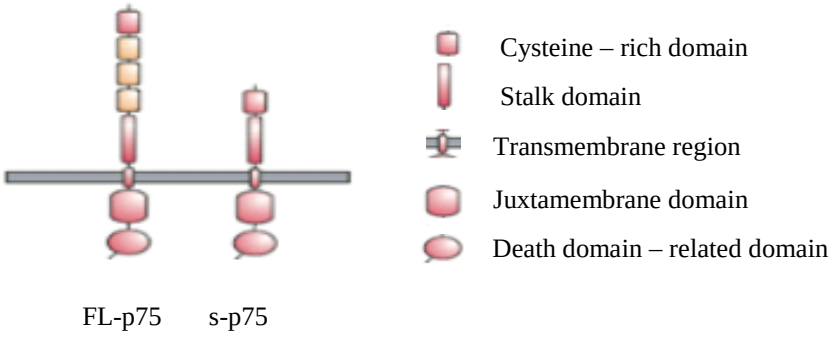

Figure 5. Schematic representation of $p75^{NTR}$ isoforms (Dechant and Barde, 2002).
FL-p75 -full length p75 neurotrophin receptor; s-p75 short isoform of p75 neurotrophin receptor

Figure 5 shows two naturally-occurring forms of $p75^{NTR}$: full length FL-$p75^{NTR}$and its short isoform s-$p75^{NTR}$ (Dechant and Barde, 1997). The shorter version results from alternative splicing or post-synthetic proteolysis and lacks three of four cysteine repeats in the extracellular ligand binding domain (Lee et al., 1992), which affects binding abilities of this receptor.

Homologs of $p75^{NTR}$ are highly conserved among the species. The receptor is found in fish, amphibians and birds [they are called neurotrophin receptor homolog 1 (NRH1)] as well as in mammals [variously called NRH2, 75-like apoptosis-inducing death domain protein (PLAIDD) or neurotrophic alike death domain protein (NRADD)] (Murray et al., 2004; Frankowski et al., 2002; Sasai et al., 2004; Wang et al., 2003). Mice lacking both FL-$p75^{NTR}$ and s-$p75^{NTR}$ show up to 40% lethality, presumably as a result of damage to the blood vessels, because p75 receptor is found in smooth muscle cells of blood veins. (von Schack et al., 2001). In brain, $p75^{NTR}$ is mainly expressed during neuronal development and in adult CNS it is restricted to a few neuronal populations (Richardson et al., 1986). Cholinergic neurons of BF, which are strongly affected by Alzheimer's disease express $p75^{NTR}$ throughout their lifetime (Kiss et al., 1988; Woolf et al., 1989). Additionally, re-expression of $p75^{NTR}$ occurs in hippocampus in conditions involving neuronal injury and in many neurodegenerative disorders including AD (Schor, 2005; Volosin et al., 2008). Although p75 receptor was first discovered as a receptor for nerve growth factor (NGF) (Herrup and Schooter, 1973), it is now established that it binds to all

neurotrophins (NTs): brain derived neurotrophic factor (BDNF), neurotrophin 3 (NT3), neurotrophin 4 (NT4) with similar nanomolar affinity (Kd = 10^{-9} M) (Bibel et al., 1999) (Figure 6).

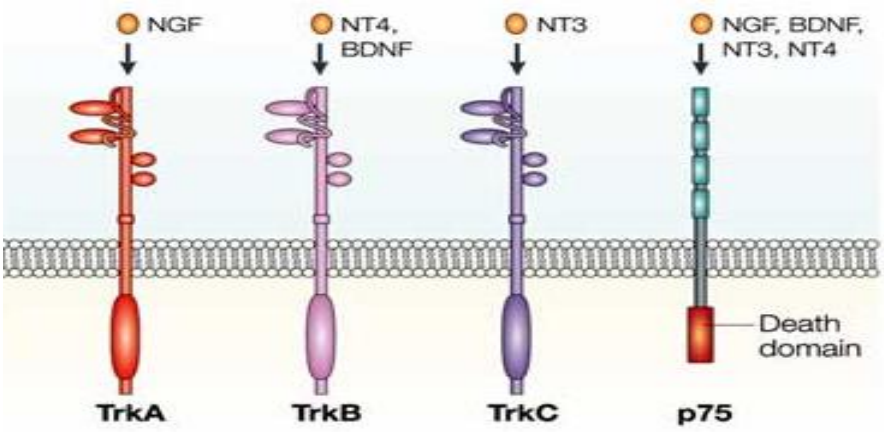

Figure 6. Schematic representation of neurotrophins binding to $p75^{NTR}$ (Chao, 2003). Abbreviations: NGF - nerve growth factor; BDNF - brain derived neurotrophic factor; NT3, 4 – neurotrophin 3,4; Trk A,B,C - tropomyosin-related tyrosine kinase A,B,C.

Released typically at synapses, these neurotrophins govern neuronal growth and survival as well as control the neuronal death during development (Kalb, 2005). Furthermore, like neurotransmitters, they can affect neuronal membrane permeability for sodium and potassium ions and excitability of neurons (Poo, 2001). Neurotrophins are synthesized in a precursor form as pro-neurotrophins, consisting of N-terminal prodomain and a C-terminal mature domain. They are cleaved to generate their mature form by furin or pro-convertases 1 and 2 (PC1 and PC2) at highly conserved sites (Seidah et al., 1996). Proteolytic processing of neurotrophins is believed to be crucially involved in neurodegenerative diseases (Peng et al., 2004) and their precursors have been reported to accumulate during AD (Fahnestock et al., 2001). Pro-neurotrophins bind to $p75^{NTR}$ with higher affinity (nanomolar range) than mature neurotrophins (e.g. pro-NGF has 5 times higher affinity for p75 receptor than the mature NGF) (Lee et al., 2001). The high affinity binding site of pro-neurotrophins is formed by complex of $p75^{NTR}$ with sortilin; the latter interacts with pro-domain while $p75^{NTR}$ binds to the mature portion of pro-neurotrophins (Nykjaer, et al., 2004).

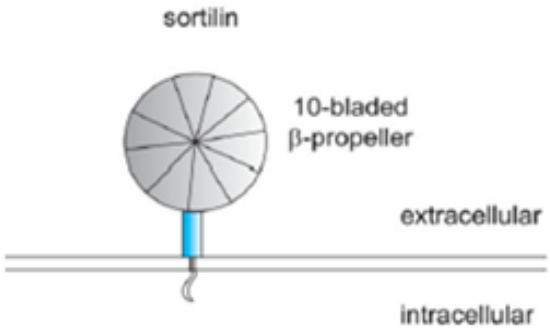

Figure 7. Schematic illustration of $p75^{NTR}$ co-receptor sortilin (Skeldal et al., 2011).

The schematic illustration of sortilin in Figure 7 (Skeldal et al., 2011) shows an unusual structure of this receptor, belonging to vacuolar protein sorting 10 protein (Vps10p) family. Sortilin possess the unique ligand binding domain forming 10-bladed β-propeller on the extracellular "stalk", that connects to the cytoplasmic tail through short transmembrane domain (Nykjaer and Willnow, 2012). In addition to binding of pro-neurotrophins, sortilin has been identified as a novel apolipoprotein E (APOE) receptor in neurons (Carlo et al., 2013). This is important because APOE has been regarded as the most important genetic risk factor for sporadic AD cases (Corder et al.,1993) (Chapter 1.2.). Recently, a role of sortilin has been implied in the clerance of Aβ peptides bound to APOE (Carlo et al., 2013).

$P75^{NTR}$ is often associated with other members of neurotrophin receptor family - tropomyosin-related tyrosine kinase (Trk) receptors, creating double-receptor complexes as illustrated in Figure 8 (Chao, 2003). In complex with TrkA, $p75^{NTR}$ forms high affinity binding sites (more than 100-fold higher than $p75^{NTR}$) for mature neurotrophins (Hempstead et al., 1991).

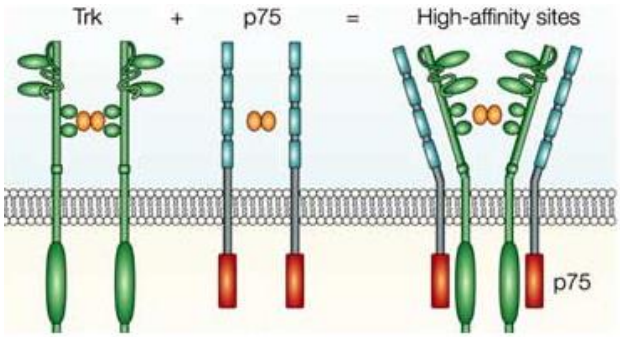

Figure 8. Schematic illustration of high affinity binding site created by $p75^{NTR}$ and Trk receptors (Chao, 2003).

So far, three members of Trk receptors family were identified: TrkA, TrkB and TrkC (Klein et al., 1991; Lamballe et al., 1991). Trk receptors family exhibits high ligand specificity: TrkA, TrkB and TrkC bind NGF, BDNF/NT4 and NT3, respectively (Figure 6). The extracellular domains of Trk receptors contain two cysteine-rich regions flanking a leucine-rich repeat, followed by two immunoglobulin (IgG)-like domains, the juxtamembrane region and tyrosine kinase domains as illustrated in Figure 9 (Dechant and Barde, 2002). Binding of neurotrophin homodimers causes Trk receptor dimerization and auto-phosphorylation of tyrosine residues (Figure 8). Phosphorylated tyrosines act as docking sites for signalling molecules which regulate cell growth and survival through Ras, phosphatidyloinositol 3-kinase (PI3-K) and phospholipase Cγ (PLCγ) pathways (Kaplan and Stephens, 1994).

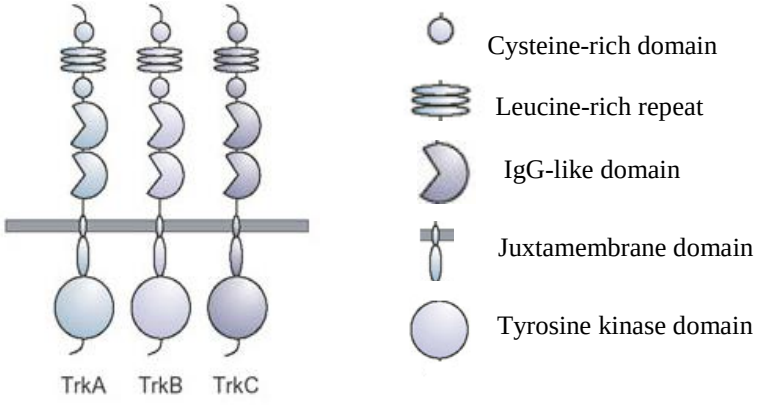

Figure 9. Schematic representation of Trk receptors family (Dechant and Barde, 2002). Trk A,B, C – tropomyosin-related tyrosine kinase A, B, C

Trk receptors display molecular diversity as some splice variants lack the intracellular tyrosine kinase domain (Middlemas et al., 1991). The truncated forms can have directed signalling activity influencing growth and survival of neurons e.g. truncated TrkB receptor can inhibit neurotrophin signaling by sequestering or trapping NTs, thus preventing their binding (Biffo et al., 1995); this may contribute to the deficits in BDNF/TrkB signaling and neuronal plasticity in schizophrenia (Wong et al., 2013). On the other hand elevated expression of TrkB-Shc (another isoform of TrkB) is found in hippocampus of AD patients suggesting its function as a compensatory response in neurons to promote their survival (Wong et al., 2012).

The ability of $p75^{NTR}$ to bind dimeric ligands like neurotrophins is an unusual feature of the tumour necrosis factor receptor subfamily TNFRSF; however, the most

interesting function of $p75^{NTR}$ is that it can directly or indirectly bind to non-neurotrophic ligands as exemplified in Figure 10.

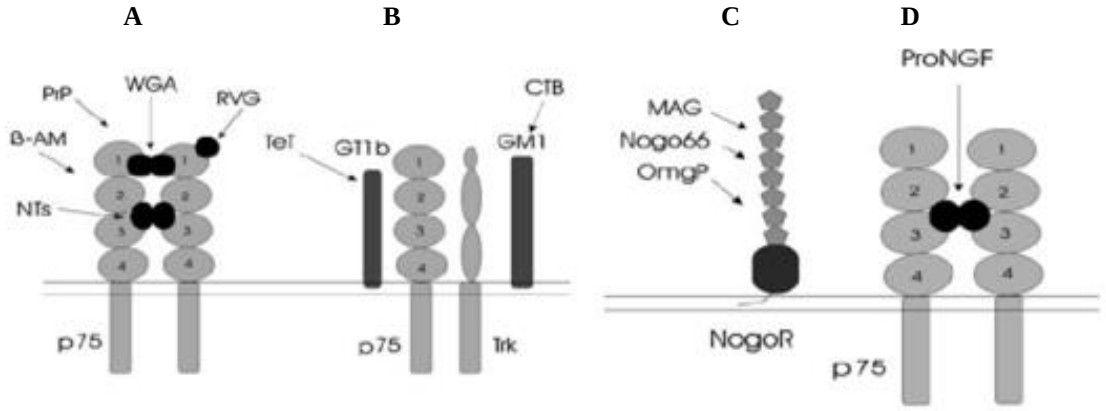

Figure 10. Schematic drawing of $p75^{NTR}$ binding to different non-neurotrophic ligands (Butowt and von Bartheld, 2003). A. B-AM – beta amyloid, NTs – neurotrophins, PrP – prion peptides, RVG – rabies virus glycoprotein, WGA - wheat germ agglutinin. B. CTB – cholera toxin binding, GT1b, GM1 – gangliosides, TeT – tetanus toxin, Trk – tropomyosin related kinase. C. MAG – myelin associated glycoprotein, NogoR – Neurite outgrowth inhibitor receptor, Nogo66 – ligands recognized by 66-amino acid fragment of Nogo, OMGP – oligodendrocyte – myelin glycoprotein, ProNGF – pro nerve growth factor

Pro-neurotrophins presumably bind to the same site at the second and third cysteine rich domain (CRD) on $p75^{NTR}$ as do the mature neurotrophins, while wheat germ agglutinin (WGA), commonly used neuronal tracers, binds to N-glycosylated site at the end of first CRD domain of $p75^{NTR}$, the same domain that binds also rabies virus glycoprotein (RVG). The sites for prion proteins (PrP) and Aβ peptides attaching to $p75^{NTR}$ remain unknown (Butowt and von Bartheld, 2003; Della-Bianca et al., 2011; Devarajan and Sharmila 2014). Some of the above ligands after internalization by $p75^{NTR}$ undergo axonal transport along microtubule tracts; e.g. NGF. In this case receptor-ligand complex is transported retrogradely and exerts its trophic effects upon arrival to the cell body (Johnson et al., 1987; Harrington et al., 2011; Marlin and Li, 2015). The pathways of many other $p75^{NTR}$ ligands are under investigation. Potential internalization of Aβ through $p75^{NTR}$ is of special relevance to Alzheimer's disease as this neurotoxic peptide is found in post-mortem brain tissues of AD patients in the form of amyloid plaques (Cummings annnd Cotman, 1995) as well as intracellulary (LaFerla et al., 2007). There is also literature suggesting direct role of

p75^{NTR} in the seeding of amyloid plaques (Zhou and Wang, 2011; Wang et al., 2011).

In regards to p75^{NTR} processing, the receptor undergoes two-step regulated intra-membrane proteolysis (RIP), schematically illustrated in Figure 11 (Chao, 2003). The first cut is catalysed by tumour necrosis factor α-converting protease (TACE/ADAM-17), which is a desintegrin metalloprotease and releases the ectodomain piece and C-terminal fragment (CTF), containing transmembrane and cytoplasmic domains (Kanning et al., 2003). The CTF fragment is further processed by a presenilin-dependent γ-secretase, liberating intracellular domain fragment (ICD). ICD is suspected to be involved in activation or repression of neurotrophin related genes (Frade, 2006) or be responsible for the role of p75^{NTR} in cell cycle regulation (Skeldal et al., 2011). These cleavages are strikingly similar to APP processing (Introduction Chapter 1.5.1.1.).

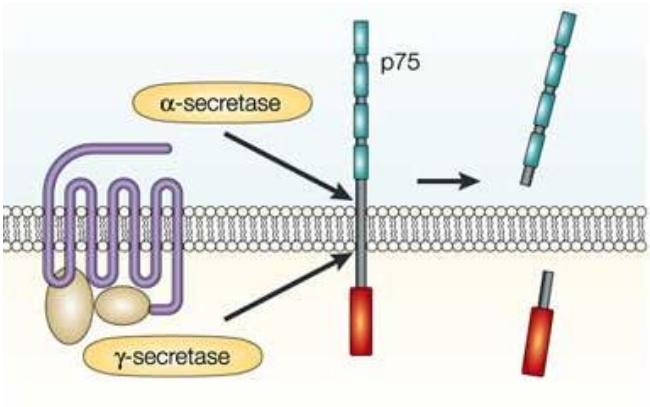

Figure 11. Schematic illustration of p75^{NTR} cleavage (Chao, 2003).

Cleavage of p75^{NTR} occurs mostly after ligand binding [it can also be induced by protein kinase C (PKC) activators such as e.g. the phorbol ester 12-myristate 13-acetate (PMA)]. In case of NTs, cleavage of p75^{NTR} requires Trk activity. It was shown that inhibition of TrkA completely abrogates both p75-CTF and p75-ICD production (Urra et al., 2007). Regulation of p75^{NTR} cleavage might be also dependent on the cell type, as different cells express different amounts of metalloproteases. Recent findings show that RIP of p75^{NTR} depends on dimerization of the receptor, influenced by transmembrane sequences and TrkA but not ligands binding (Sykes et al., 2012).

Generally, the functionality of p75^{NTR} mostly depends on ligand this receptor binds to, its co-receptors as well the cell type in which it is expressed (Skeldal et al., 2011).

The $p75^{NTR}$ is capable of activating multiple intracellular pathways, signalling cell survival or cell death. Typical effectors associated with apoptotic pathways are proteases of the caspase family, Jun N-terminal kinase (JNK) and p53 (Kenchappa et al., 2010). Other pathways involve neurotrophin receptor interacting factors (NIRF) and the production of ceramide (Dobrowsky et al., 1994). Anti-apoptotic signalling of $p75^{NTR}$ is mainly associated with binding of $p75^{NTR}$ to Trk receptors; however, pro-survival signalling of $p75^{NTR}$ independent of Trk is also possible. Main routes include PI3-K/Akt (Roux et al., 2001) or NF-κB activation (Yoon et al., 1998). All these life-death decisions are very complex in nature. They depend a lot on crosstalk between $p75^{NTR}$ and Trk receptors signalling which can modify $p75^{NTR}$ action.

In addition to promoting cell survival or directly enhancing cell death, p75 receptor modulates axonal elongation and plays a role in activity-dependent synaptic plasticity of neurons. The $p75^{NTR}$ influence axonal elongation positively by binding mature neurotrophins or inhibiting axonal elongation by activation of GTP-dependent Rho protein (Yamashita et al., 1999). A similar effect is caused by binding of $p75^{NTR}$ to myelin associated glycoprotein (MAG), indirectly through GT1b ganglioside. MAG activates Rho in $p75^{NTR}$-dependent fashion (Domeniconi et al., 2005). Also, Nogo receptor that associates with $p75^{NTR}$ can bind MAG and other myelin-associated inhibitors of axonal elongation (like: Nogo-66 and OmgP as shown on Figure 30), which results in growth inhibition of neuronal processes (Wang et al., 2002).

$p75^{NTR}$ was also found to co-localize with hyperphosphorylated tau protein in AD patients (Hu et al., 2002). There are even reports suggesting that phosphorylation of tau occurs in $p75^{NTR}$-dependent manner (Saez et al., 2006). Whether $p75^{NTR}$ is involved in the formation of neurofibrillary tangles, the other pathological hallmarks of AD, remains unknown and needs to be investigated in more detail.

1.5.4. Other BF neuronal populations that contribute to AD pathology

Although cholinergic system plays a number of physiological functions in brain, (Chapter 1.5.3.1) all these effects are exerted in cooperation with other systems of BF. In fact, cholinergic corticopoetal neurons in rodents represent only about 20% of the total BF cell population (Zaborsky, 2012). Other neuronal populations also

contribute to the cell loss during the AD (from the 30% decrease in the total number of neurons in aging only 11-15% are cholinergic) (Semba, 2000).

Apart from BFCNs, γ-amino butyric acid (GABA) neurons (GABAergic) and other peptide-containing neurons are present in BF (Semba, 2000). GABAergic neurons develop around E17 and they express glutamic acid decarboxylase (GAD) (Bender et al., 1996). Also, parvalbumin has been reported to be a selective marker of these cells in MS and DBB regions of rat (Freund, 1989). GABAergic neurons are usually distributed more laterally than cholinergic neurons e.g. in the horizontal limbs of the diagonal band of Brocca or magnocellular preoptic areas (Brashear et al., 1986). They are large multipolar cells in MS with a tendency to become much smaller caudally. Importantly, they do not show reduction during aging (Semba, 2000) and are resistant to ischemia and epilepsy (Brady and Mufson, 1997). GABAergic neurons in rat BF also express NGF mRNA, suggesting that they can provide local trophic support to BFCNs. GABAergic neurons possess Kv3.1 potassium channels that contribute to the fast spiking abilities of these cells (Henderson et al., 2010). Generally, they are inhibitory neurons with Ca^{2+} buffering properties that reduce Ca^{2+}-dependent K^{+} outward current.

Rodent GABAergic BF neurons receive glutamatergic inputs from cells which use glutamate as a fast excitatory neurotransmitter (Hur and Zaborszky, 2005). Because glutamate is precursor for GABA synthesis, it cannot serve as a definite marker for glutamatergic neurons. The only reliable markers for glutamatergic cells are vesicular glutamate transporters (Vglut 1 or 2) (Takamori, 2000). The glutamatergic neurons are present in BF as local inter-neurons (Hajszan et al., 2004) but a small proportion of them also projects to hippocampus. Dysfunction of glutamatergic neurons is proposed as another hypothesis of AD (Chapter 1.5.5). Also, alterations in both ionotropic (e.g. NMDA, AMPA) and metabotropic glutamate receptors (such as mGluRs 1 or 5) suggest that glutamatergic neurons play a central role in higher cognitive processes (Paula-Lima et al., 2013, Caraci et al., 2012).

In addition to cholinergic, GABAergic and glutamatergic neurons, peptide containing neurons co-exist in BF. For instance substance P and neurokinin B mRNA were detected in 26% of magnocellular BF neurons in humans (Semba, 2000). These neurons can be stained with calbindin in rodents. Both parvalbumin and calbindin as well as calretinin belong to a family of small acidic proteins with high affinity for Ca^{2+} binding. The major role of these Ca^{2+} binding proteins (CBPs) is the buffering

and transport of [Ca^{2+}] and the regulation of various Ca^{2+}-activated kinases. As cellular degeneration is often accompanied by impaired calcium homeosthasis (Chapter 1.5.1.2.), a protective role of CBPs has been postulated (Heizmann and Braun, 1992).

More recently, neuropeptide Y (NPY) has been described in projection neurons and interneurons of BF. NPY is often co-localized with GABA and acts as a potent inhibitory peptide with ability to inhibit cholinergic neurons via Y1 receptors (Gaykema et al., 1989). Recent reports suggest that NPY may be a neuroprotective agent against Aβ neurotoxicity (Corce et al., 2012).

Similarly somatostatin presynaptically inhibits both glutamate and GABA release onto BF neurons (Moiyama and Zaborszky, 2006). Neocortical neurons containing somatostatin decrease in AD, while those immuno-reactive for neuropeptide Y appear preserved (Dawbarn et al., 1986; Palop et al., 2011).

Likewise galanin is found in both septo-hippocampal cholinergic projections and non-cholinergic neurons (Melander et al., 1985), but it presence varies among the species and is not found in human cholinergic projections. In rodents, this peptide was found to inhibit synaptic transmission in the hippocampus and impair spatial memory (Elvander et al., 2004).

1.5.5. Glutamatergic theory of AD

The dysfunction of glutamatergic neurotransmission with resultant cytotoxic effects is also hypothesized to be involved in the etiology of AD. This is based largely on post-mortem evidence indicating reduced binding and uptake of D[3H]aspartate as well as loss of a number of other putative markers, such as phosphate-activated glutaminase activity, glutamate concentration and the number of pyramidal cell perikarya, correlating well with the severity of dementia (Palmer and Gershon, 1990). Over-stimulation of nerve cell by glutamate eventually causes cell apoptosis, disrupts synaptic plasticity [f.e long term potentiation (LTP)] and impairs learning and memory (Sheng and Ertürk, 2013; Park et al., 2015). Targeting the glutamatergic system, specifically NMDA receptors, offers a novel approach to treatment in view of the limited efficacy of the existing drugs targeting the cholinergic system (Molinuevo et al., 2005; Martinez-Coria et al., 2010) (Chapter 1.6).

1.5.6. Dysregulation in aminergic neurotransmitters systems in AD pathology

In addition to dysregulation of cholinergic system (mentioned in Chapter 1.5.3.1), aminergic neurotransmitter systems are reported also to be altered in AD. These include catecholamines, which are active amines containing catechol (active benzene with two hydroxyl side groups) with norepinephrine (NE), called also noradrenaline, epinephrine (Epi), known as adrenaline, with both produced largely by long range projection neurons of locus coeruleus (LoC) (Heneka et al., 2010). Alterations have also been reported in dopaminergic neurons (DA) of midbrain (Grace and Onn, 1989). Likewise, indolamines, synthetized from tryptophan are affected in AD. These include: serotonin (5-HT) from raphe nuclei (Anden et al., 1965) or melatonin mainly generated by pineal gland (Wu et al., 2003). Other neurotransmitters like orexin (recognized as hypocretin) and histamine from certain nuclei of hypothalamus also contribute to the disease (Brown et al., 2010, Panula et al., 1984).

The vigorous changes in noradrenergic and to lesser extend in adrenergic systems are documented in post mortem samples from AD patients (Mann, 1998), with progressive loss of LoC neurons reported in AD, which may contribute to the important non-cognitive behavioural impairments such as depression and wandering (Palmer et al., 1987, Mravec et al., 2014). The widespread projections of LoC neurons are involved in generation of stress responses, which become affected in AD. Several studies suggest that LoC system increases the ability to process relevant stimuli while suppressing responses to irrelevant stimuli (Berridge and Waterhouse, 2003). All this is important in the context of AD as LoC neurons degenerate at an even faster rate than cholinergic neurons of BF (Zarow et al., 2003).

Changes in dopaminergic system are mainly localized to the dopaminergic receptors rather than to dopaminergic innervation. The dopaminergic neurons project through the medial forebrain bundle to the dorsal striatum (nigrostriatal projection) and to the basal forebrain, ventral striatum and cortex (meso-limbocortical projection) (Ikemoto, 2007). DA produced mainly in two areas of brainstem - substantia nigra and ventral tegmental area (VTA) stimulates arousal and attention and supports locomotor and exploratory, reward-seeking behaviours during waking (Alcaro et al., 2007). The role of DA in sleep-wake regulation is less studied. Post-mortem concentrations of DA have been repeatedly found to be unaltered in the cerebral cortex of patients with AD (Palmer and DeKosky, 1993) but there is loss in D2

receptor binding in the areas that correlate with the appearance of traditional neuropathology (plaques and tangles) (Joyce et al., 1998).

More variable than the effects seen in adrenergic systems are serotonergic dysfunctions in AD (Bowen et al., 1983). The neurons of the midbrain raphe nuclei that give rise to ascending projections to the forebrain and cortex, release 5-HT. An autopsy studies has shown reduced concentrations of 5-HT and 5-HIAA, the principal metabolite of 5-HT as well as diminished 5-HT uptake in AD patients (Palmer et al., 1987). The decline of serotonergic transmission is paralleled by the reduction (30-40%) in number of 5-HT-positive neurons in the medial and dorsal raphe nuclei; however, the magnitude of this neuronal loss does not correlate with the density of NFTs (Chen et al., 2000).

The hypocretin/oxerin neurons of the posterior hypothalamus innervate the whole brain and spinal cord and send especially dense projections to the aminergic cell group e.g., the tuberomammillary nucleus (TMN), raphe nucleus, LoC and VTA (Peyron et al., 1998; Sakurai 2007). The interplay between orexins and catecholamines has implications for physiological regulation of behavioural state, plasticity and memory functions (Eriksson et al., 2010).

1.5.7. Default mode network hypothesis and spreading of AD pathology

The default mode network (DMN) is a task negative network, preferentially active at the awake rest of brain, when individual is not focused on the external environment. It is associated with episodic and autobiographical memory retrieval as well as with other internally driven processes such as mind wandering or future planning, when cognitive tasks that demand external stimuli are diminished (Greicius et al., 2003; Fox et al., 2005). The DMN is an evolutionarily old and conserved system present in humans and non-human primates (Mantini et al., 2011) and rodents (Upadhyay et al., 2011), with the appearance of last being currently debated. The DMN is anatomically defined and contains interconnected parts of the medial temporal lobe, part of the medial prefrontal cortex, the posterior cingulate and retrosplenial cortex along with the adjacent ventral precuneus and medial, lateral and inferior parietal cortexes (Gusnard and Raichle 2001; Greicius et al 2004). Dearangments of functional relationship between mentioned above brain areas of DMN occur in the early stages

of dementia as examined by functional magnetic resonance imaging (fMRI) (Sepulcre et al., 2013).

The most interesting is a striking overlap between areas of Aβ deposition and DMN (Buckner at al., 2005; Mormino et al., 2011). It is shown that AD pathology accumulates preferentially in DMN even before the symptoms emerge. Senile plaques deposition proceeds slowly begining in the neocortex through the allocortex and diencephalon to the striatum and BF cholinergic nuclei, followed by progression to the brainstem nuclei and finally to the cerebellum (Thal et al., 2002). This phenomenon is believed to relate to the metabolic properties or activity patterns of DMN. It has been demonstrated that Aβ level increase following stimulation of the brain (Cirrito et al., 2005, Selkoe 2006). Also, glycolysis (changing glucose into cell energy) correlates well with distribution of Aβ plaques (Mintun et al., 2006). According to this view, memory systems may be preferentially affected, because they play central role in resting brain activity as a part of DMN (Buckner et al., 2008). In the case of AD, resting-state activity may accelerate the formation of disease pathology. Also, neuron to neuron transfer of soluble Aβ oligomers was proved in several brain structures (Nath et al., 2012). According to this theory, neurotoxic Aβ accumulate in cells that show later beading of tubulin and endosomal leakage. The spread of NFTs is also known to occur via anatomical connections (Harris et al., 2010). NFTs progress in more hierarchical and fixed fashion, which begins from the enthorinal cortex and proceeds to medial temporal limbic areas, the hippocampus in particular and pariental lobe, to spread later to the selected regions of frontal cortex and cingulate gyrus (Braak and Braak 1991). Understanding these processes is the most important for deciphering the disease processes and designing therapeutics for clinical applications.

1.6. Current treatments of AD

Currently available therapies for AD are divided into pharmacological and non-pharmacological ones, with both methods providing only palliative and ameliorative treatments to slow the progression of the disease (Sugino et al., 2015).

At this point, AChEi remain the most effective and the first medications approved by FDA for AD therapy (Chapter 1.1.). Three commonly prescribed AChEi include: donepezil hydrochloride (Aricept; Eisai Inc, Woodcliff Lake, New Jersey or its

generics); rivastigmine tartrate (Exelon; Novartis Pharmaceuticals Corp, Basel, Switzerland or its generics) and galantamine hydrobromide (Razadyne [formerly Reminyl]; Janssen Pharmaceutica NV, Beerse, Belgium). All these drugs exert their therapeutic effects by slowing degradation of ACh in non-affected neurons, in which they irreversibly bind AChE, thus compensating for cholinergic neurons that are injured or lost as the illness progresses (Birks, 2006). These provide a considerable step forward over the first anti-cholinesterase based drug - tacrine hydrochloride (Cognex; Shionogi Inc, Florham Park, New Jersey) approved in 1993 and withdrawn subsequently from US market in 2012, due to complicated dosage schedule and adverse effects e.g. risk of hepatotoxicity. Current AChEIs are easer in dosage and have better safety profiles. They are most effective when applied early in the disease.

Another therapeutic - memantine hydrochloride (marketed under the brands Axura and Akatinol by Merz, Namenda by Forest Pharmaceutical, Ebixa and Abixa by Lundbeck and Memox by Unipharm) is the most recent FDA medication approved in 2003 for the treatment of patients with moderate to severe AD. Memantine is a non-competitive antagonist of the N-methyl-D-aspartate (NMDA) receptor (Lipton, 2005). It works by blocking NMDA receptor, thus providing neurons with time-limited protective mechanisms against excess of glutamate, which injured neurons release into the synaptic cleft, flooding the cell with calcium and causing cell damage and death (Budson and Solomon, 2012; Figure 12).

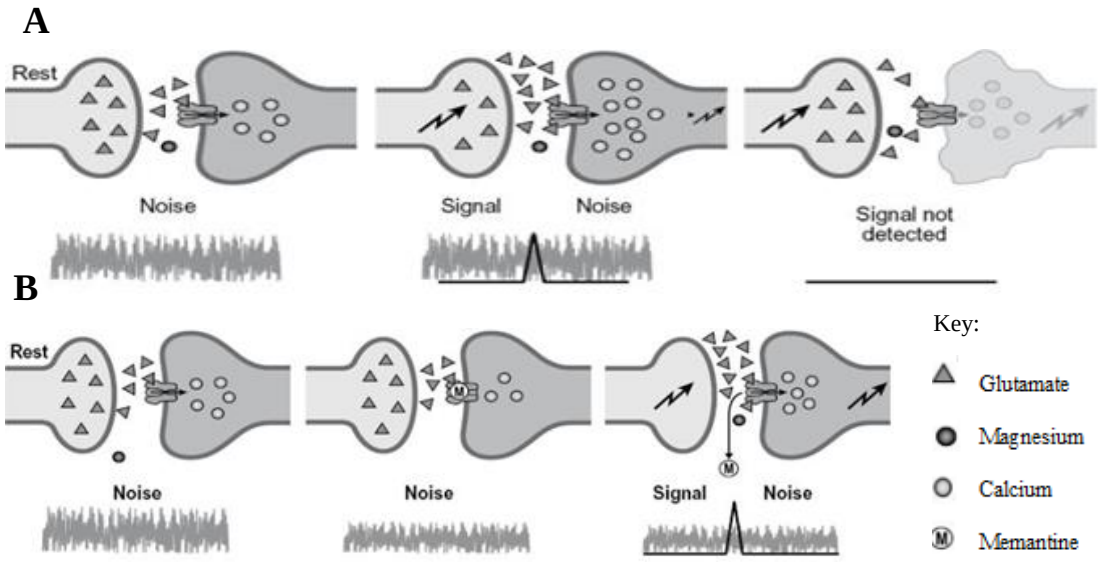

Figure 12. Schematic representation of memantine mechanism of action (Budson and Solomon, 2012). A – pathologically activation of NMDA receptors leading to excitotoxicity and chronic neurodegeneration; B – Action of memantine, which blocks NMDA receptor with a higher affinity than Mg^{2+} and inhibits the prolonged influx of Ca^{2+}.

Memantine can be prescribed in combination with cholinesterase inhibitors and it is a common strategy to initiate treatment with AChEi and to add memantine as the patient begins to show further decline in cognition (Matsunaga et al., 2014; Matsuzono et al., 2015). Memantine is generally well tolerated. The most common adverse effects include confusion, dizziness, drowsiness, headache, insomnia, agitation, and hallucinations. In addition to the effects on NMDA receptor, memantine acts a non-competitive antagonist at different neuronal nAChRs, especially α7 and serotonergic 5-HT3 receptors, with the clinical significance of these interactions remaining unknown. Moreover, memantine was also found to act as agonist at the dopamine D2 receptor; however, the mechanisms of such off-target effects are not entirely clear (Nakaya et al., 2011).

Another group of tested medications like statins tackle cardio-vascular dementia, which is often co-existing with AD and, therefore, believed to drive healthy brain towards AD type (Mendoza-Oliva et al., 2014). Also, non-steroidal anti-inflammatory drugs or hormone replacement therapies found their applications in Alzheimer's disease research and therapy (Lehrer, 2014).

Other approaches that have been utilized in clinical trials are designed to prevent aggregation of toxic Aβ species (anti-aggregants), as well as target amyloid plagues directly through active or passive immunization (Galimberti et al., 2013, Menting and Claassen, 2014; Wu et al., 2015). Recently developed embryonic stem cells and optimized induced pluripotent stem cells (iPSCs) technology provide a promising platform to create reliable models, not only for better understanding the etiopathological process of AD, but also for efficient anti-AD drugs screening and transplantation (Yang et al., 2016; Zhang et al., 2016, Bali et al., 2016). Trials with NGF-expressing autologous fibroblasts implanted to forebrain of AD patients brought encouraging outcome (Tuszynski et al., 2005). Likewise NGF gene therapy using ex vivo or in vivo gene transfer continuous worthy for AD treatment (Tuszynski et al., 2015).

Beside all of these pharmacological approaches, non-pharmacological interventions aim to improve the quality of life of AD affected patients or compensate memory loss are being developed. They range from improvements in care, counselling, education, physical and mental exercise, musical therapy to vitamins, herbs, Ginko Biloba and other diet supplements (Sun et al., 2007; Birks and Grimley Evans, 2009; Simmons-Stern et al., 2012; Hernández et al., 2014).

1.7. Objectives of the study

Functional disruption and loss of BFCNs are believed to contribute significantly to the pathogenesis and clinical manifestation of AD, characterized by a severe deficit of high integrative brain functions with impaired synaptic transmission and plasticity (Selkoe 2008; Walsh et al., 2002). However, the mechanism of progressive cognitive impairments and memory deficiencies responsible for the disease progression is not yet understood (Blennow et al., 2006). Dysregulation of $p75^{NTR}$, the receptor exclusively expressed in BFCNs (Härtig et al., 1998; Fombonne et al., 2009) have been suggested to determine the selective vulnerability of cholinergic system during early AD.

Based on these data, the primary objective of this study was to provide insights to the biology and function of $p75^{NTR}$ in basal forebrain cholinergic neurons, by looking at endo/exocytosis of this receptor and mechanism that govern its internalization and exit. The relevant research platform had to be developed.

Although neurotoxic Aβ is known to bind multiple targets (Verider and Penke, 2004), it is the interaction with $p75^{NTR}$ that mediates neuronal death (Sotthibundhu et al., 2008). Therefore second objective of this study was to investigate $p75^{NTR}$ and Aβ interaction with main impact on the study of the precise entry route of $p75^{NTR}$ and Aβ oligomers into BFCNs as well as detailed analysis of the parameters of their trafficking and co-localization in subcellular compartments of these cells.

Final goal of this work was to exploit $p75^{NTR}$ as a possible molecular target for delivery of potential therapeutics to BFCNs for AD treatment.

In addition, chemical induction of AD pathology in rats was proposed to create animal model for testing potential neurotherapeutics, that can protect BFCNs against Aβ damage.

Chapter II. Materials and Methods

All experiments that involve use of rodents were approved by the Research Ethics Committee at Dublin City University and licenced by the Department of Children and Health, Ireland.

2.1. Immuno-cytochemistry (IC)

Immuno-cytochemistry technique, commonly used in neuroscience, is based on antibody-antigen interaction with protein labelling. The work described throughout this study involved immunocytochemical staining procedures that were utilized in many experiments to visualize both cholinergic and non-cholinergic neurons as well as their projecting fibres or other structures of interest. Additionally Nissl method (Nissl, 1894) was used to highlight general structures of some parts of brain, which play a role in the processes involving modulatory influence of cholinergic innervations.

2.1.1. Preparation of tissues for IC

Brain extraction for IC has been undertaken under deep (lethal) anaesthesia of the animal with perfusion (Chapter 2.1.3), followed by slicing of the tissue. Therefore, all the buffers, surgery tools and perfusion pump had to be prepared in advance. Special care has been taken to remove the air bubbles from the tubing and perfusion pump to ensure easy flow of the solution before starting each experiment.

2.1.2. Sedation and anaesthesia of experimental animals

Deep (sub-lethal) anaesthesia of the rat was performed with intraperitoneal injection (i.p.) of sodium pentobarbital (Euthatal, Pfizer) at the dose of 200 mg/kg, preceded by subcutaneous (s.c.) injection of medetomidine (Domitor®, Pfizer) at the dose 0.4 mg/kg. The absence of tail pinch response was taken as an indicative of deep anaesthesia, prior to the perfusion. Only after complete loss of tail pinch response was the surgery performed.

2.1.3. Transcardial perfusion

Transcardial perfusions were necessary for removal of blood from brain tissue as blood can interfere with IC. The process entails perfusion of the cardiovascular system for delivery of fixative into the brain. Transcardial perfusions were performed prior to all immunocytochemical procedures (Materials and Methods Chapters 2.1.6.

– 2.1.8.). Briefly, under deep anaesthesia (according to anaesthesia procedure – Chapter 2.1.2.), rats were placed on operating platform and immobilized with the surgery tools. The skin and abdominal wall below the diaphragm were lifted with forceps and muscles cut using blunt scissors to avoid damage of the interior organs. An incision was made along the border of the diaphragm muscle to expose the heart. Then ¼ inch of the 25G needle was inserted into the left ventricle of the beating heart and the right atrium cut with sharp scissors. PBS, pH=7.4 (0.1~150 ml) was pumped slowly at 3ml/min rate until the blood was cleared. The solution was then changed for 4% paraformaldehyde (PFA) buffered with PBS (0.1 M), pH=7.4 with care to avoid air bubbles in the tubing; this fixative (100 ml) was also pumped slowly at 3 ml/min. The brain afterwards was removed from the skull and post-fixed in 4% PFA in 4°C overnight. In order to avoid freezing artefacts, the brains were cryo-protected by equilibration with 30 % sucrose (S7903, Sigma-Aldrich) solution in PBS in 4°C overnight to ensure that the tissue completely sunk in the Falcon tube.

2.1.4. Slicing of rodent brain

Cryo-protected brains were removed from sucrose after 24 h or more (when entire brain sunk in 30% sucrose in PBS) and glued on freezing stage of slicing microtome (Leica, CM3050 S) with Tissue-TeK O.C.T compound (4583, Sakura Finetek). Then sliced (usually 30 – 50 μm coronal sections) and immediately collected into PBS, pH 7.4. or PBS with 0.1 % sodium azide in case of longer storage in the cold room, at 4°C.

2.1.5. Direct immuno-chemical staining of BFCNs using fluorescent anti-p75^{NTR} antibodies and labelled Aβ

This procedure involved the use of flour labelled primary antibodies or proteins, which bind and label targeted antigen / acceptors. The method is quick as it utilizes only one molecule for an antigen detection and non-specific reaction are limited. In this work, I used 192-IgG-Cy3 or Cy3-labeled anti-murine NGFr IgG directed against low affinity p75 neurotrophin receptor (p75^{NTR}) in rats or mice, respectively; also, HiLyte Fluor β-amyloid (1-42) coupled with Alexa 488 (characterised in next section) and anti-p75^{NTR}-LentiGFP were used. These flour labelled proteins were

applied directly to BF in culture for *in vitro* work or injected icv into 21 days old rats for *in vivo* evaluation. Unilateral injections were made in experiments with 192-IgG-Cy3 (2 µl; 0.4 mg/ml) and anti-p75^{NTR}-LentiGFP (5 µl; 7.0x10^{6} IUs/ml), using stereotactic coordinates as follows: AP = -0.8 mm, ML = 1.2 mm, DV = 3 mm or bilateral for HiLyte Fluor β-amyloid (1-42) also to the ventricle (Levites et al., 2006; Zussy et al., 2013; Chen et al., 2015). For *in vitro* experiments, 4.7 nM of 192-IgG-Cy3; 0.3 µM HiLyte Fluor Aβ (both exposed for 2h) or 1 µl anti-p75-LentiGFP 7 x 10^{8} Lvs/ml (exposed 48h) were used (in 2 ml of medium).

2.1.5.1. Characteristics of anti-p75^{NTR} antibodies and labelled Aβ peptides used in direct fluorescence staining *in vitro* and *in vivo*

The anti-p75^{NTR} antibodies (FL-01 and FL-05, Advanced Targeting Systems) were used in the present study to monitor p75^{NTR} endocytosis in rat and mice primary BF tissue cultures as well as to characterise BFCNs *in vivo*. The Aβ labelled peptides (64572, AnaSpec) were utilized for intraventricular (icv) injections to follow the deposition of Aβ (1-42) in brain structures as well as they were applied to BF tissue culture model to track the trafficking process of Aβ (1-42) in live cells. Both: the anti-p75^{NTR} antibodies and Aβ peptides are available commercially (Table 1 and 2) and possess fluorochromes attached to them, that are excited at particular wavelengths 548 nm (Cy3) and 501 nm (HiLyteFluor^{TM} 488). They are able to emit signal at 561 nm (Cy3) and 527 nm (HiLyteFluor^{TM} 488) respectively.

Cat no., Company	Antibody name; (Isotype)	Host	Dilution used
FL-01, Advanced Targeting Systems	192-IgG-Cy3; (IgG1)	Mouse monoclonal	0,72 mg/ml (1:100) immuno-cytochemistry; 5 µl of 0.4 mg/ml for icv
FL-05, Advanced Targeting Systems	Cy3-labeled Anti-murine NGFr IgG	Rabbit polyclonal	25µg (1:100) Immuno-cytochemistry

Table 1. Characteristics of anti-p75^{NTR} antibodies used in direct fluorescence staining *in vitro* and *in vivo*.

Cat no., Company	Peptide name; molecular weight	Amino acid sequence of the peptide	Dilution used
64572, AnaSpec	B-Amyloid (1-42) HiLyte Fluor 488 labelled; MW=4775,1	Hilyte™ Fluor488 - Asp - Ala - Glu - Phe - Arg - His - Asp - Ser - Gly - Tyr - Glu - Val - His - His - Gln - Lys - Leu - Val - Phe - Phe - Ala - Glu - Asp - Val - Gly - Ser - Asn - Lys - Gly - Ala - Ile - Ile - Gly - Leu - Met - Val - Gly - Gly - Val - Val - Ile - Ala – OH	2-5 µl (1mg/ml)

Table 2. Characteristics of Aβ peptide used in direct fluorescent staining *in vitro* and *in vivo.*

2.1.6. Indirect immuno-chemical staining of neurons

Indirect immuno-chemical staining is two-step method that utilizes non-conjugated primary antibody that binds to the antigen of interest (first step) and a secondary antibody, coupled with fluorescent dye or an enzyme e.g. horseradish peroxidase (HRP) which gives a signal after contact with its substrate 3,3'-diaminobenzidine (DAB) (second step). This method is more versatile than direct staining because the variety of antibodies from the same species can be used with the same conjugated secondary antibody. This procedure is also more sensitive than direct method as several antibodies are likely to react with number of different epitopes of the primary antibody, thus amplifying the signal (more enzyme molecules are attached per each target site) (Boenish et al., 2001). In this study indirect immune-labelling was used to characterise BF brain slices or to visualise neurons and their connections or compartments in fixed neuronal cultures *in vitro*.

Briefly, free floating brain sections or culture dishes were washed in PBS, pH=7.4 and pre-incubated in 0.4% Triton X-100 (T9284, Sigma-Aldrich) diluted in PBS (0.1 M) for 1h. Then mixture of 5% BSA (A2153, Sigma-Aldrich) and 2% serum of the host in which secondary antibody was raised, blocked the non-specific binding sites (1h). The diluted primary antibody against the antigen of interest (Table 3.) was applied overnight at room temperature in the same blocking solution with 0.4%

Triton X-100 in PBS (0.1 M). Slices were then rinsed with 5 changes of PBS (5 min each) before incubation with secondary antibody labelled with fluorochrome at specified dilutions (Table 3.) for 1h at room temperature in the dark room.

Primary antibody cat no, Company	Primary IgG dilution	Secondary antibody cat no, Company	Secondary IgG dilution
goat anti-ChaT AB 144P, Millipore	1:100	Ab6737, Abcam (FITC) or Ab150136, Abcam	1:1000
mouse anti-calbindin ab9481, Abcam	1:200	A11004, Invitrogen (Alexa Fluor 568)	1:2500
mouse anti-parvalbumin P3088, Sigma-Aldrich	1:250	A11005, Invitrogen, (Alexa Fluor 594)	1:2500
rabbit anti-neurofilament 200, N4142, Sigma-Aldrich	1:300	A11034, Invitrogen (Alexa Fluor 488)	1:2500
rabbit anti-EE1 07-1820, Millipore	1:100	A11034, Invitrogen (Alexa Fluor 488)	1:1000
goat anti-Rab11 (C-19) sc-6565, Santa Cruz	1:100	A-11078, Invitrogen (Alexa Fluor 488)	1:1000
rabbit anti-Rab7 (H-50) sc-10767, Santa Cruz	1:100	A-11078, Invitrogen (Alexa Fluor 488)	1:1000
rabbit anti-Lamp1 SAB3500285, Sigma-Aldrich	1:100	A11034, Invitrogen (Alexa Fluor 488)	1:1000
Anti-streptavidin, Sc-52235, Santa Cruz	1:100	A-21121, Invitrogen (Alexa Fluor 488)	1:1000
Anti-amyloid (1-42), 55922, AnaSpec	1:200	A-11029,Invitrogen (Alexa Fluor 488)	1:1000

Table 3. Optimised dilutions of primary and secondary antibodies experimentally established for each type of neuronal labelling.

After this stage, sections were washed in PBS, pH=7.4 and mounted on charged glass slides, air-dried in the dark room and coverslipped with Vectashield mounting medium (H-1400 , Vector Lab.) before viewing.

In case of HRP staining, peroxidase blocking solution was added to the slices after staining with primary antibody. The slices were rinsed with 0.05% Tween 20 (P1379, Sigma) in PBS tree times by 2 min, before the addition of secondary antibody coupled with HRP for 1h. After rinsing in PBS, DAB kit containing HRP substrate (SK-4100, Vector Lab.) was applied. This step was followed by monitoring of slices under the light microscope until satisfied intensity of the staining was developed. Stained sections were mounted on glass slides and air-dried. Afterwards, they were dehydrated in 75% ethanol (EtOH) (E7023, Sigma) followed by 95% EtOH and 100% EtOH over few minutes each and cleared with Xylene (534056, Sigma) two times for 5 minutes. Finally they were coverslipped with DPX (06522, Sigma).

2.1.7. Indirect fluorescence double labelling

Double immuno-staining of cell cultures or tissue sections with use of unconjugated primary antibodies requires that those antibodies are raised in different species and that secondary antibodies recognize one of these species exclusively. This method utilizes the same principles as indirect IC staining (Chapter 2.1.6), but primary antibodies (for two different antigens) are added sequentially. When first immuno-chemical staining is finished, 10% serum (of the same host as the host of secondary antibody from the first staining) is applied to cover the effect of this visualisation. Second staining starts from the blocking step with Triton X-100 followed by the normal procedure as described in Chapter 2.1.6. f.e in case of ChAT/parvalbumin double labelling first IgG goat anti-ChaT (AB 144P, Millipore) (Table 3) was developed with FITC antibody (Ab6737, Abcam) and then blocked by 10% goat serum (G9023, Sigma-Aldrich) in PBS, pH=7,4 for half an hour. Secondly, mouse anti-parvalbumin IgG (P3088, Sigma-Aldrich) was applied and developed with Alexa Fluor 594 (A11005, Invitrogen) (Table 3) as described in Chapter 2.1.6.

2.1.8. Controls for immuno-cytochemistry

For the internal control of staining in each experiment the primary antibody step was omitted, while utilizing further the same staining protocol. In some experiments, cultured neurons from other brain areas than BF were used as controls (e.g.

hippocampal culture to establish the right dose of 192-IGg-Cy3 for experiments on BF).

2.1.9. Nissl staining protocol

Nissl staining was used to identify neuronal structures in brain, which are important for memory process. The staining was performed with use of Spraque-Dawley rats' brain after perfusion as described in Chapter 2.1.3. Coronal brain sections (50μm) were obtained and mounted on glass slides. After drying, the slides were de-waxed by immersion in Xylene (534056, Sigma-Aldrich) (2 or 3 changes of 3 min each) and re-hydrated in 100% EtOH (34935, Sigma-Aldrich), 3 min each. Then sections were submerged in freshly prepared Nissl stain solution containing 1% w/v of cresyl violet (C-1791, Sigma-Aldrich, 10g/L) and 1% v/v glacial acid (10ml/L) for 5-10 min. Next step involved rinsing slides with ddH_2O 2-5 times for few seconds. Staining in warmed cresyl violet solution (warm up in 37-50 ºC) was found to improve penetration and enhance staining, particulary of thicker (30 um) sections. Afterwards, slides were immersed in 50% EtOH for 5s and moved to 70% EtOH for a count of 5 before putting them to 95% EtOH solution.

Distaining of the slides was performed in 100% EtOH to a level determined under light microscope to the satisfactory visualization. The Nissl substance (rough endoplasmic reticulum) should appear in dark blue due to the staining of ribosomal RNA with aniline dye, giving the cytoplasm a mottled appearance. Individual granules of extra-nuclear RNA, named Nissl granules (ribosomes) and DNA present in the nucleus stains in a similar colour. Stained sections were then cleared in Xylene (2 times for 5 minutes), mounted in DPX (06522, Sigma-Aldrich) and left to dry.

2.2. Microscopy

Three types of microscopes were utilized in my research depending on the experimental purpose. Light microscope (Nikon Eclipse TS 100) was used to observe the development of BFCNs, HEK 293 or 293FT cells, hippocampal and mixed tissue cultures as well as to monitor HRP or Nissl staining. Fluorescent microscope Olympus IX71 allowed imaging with visualization of fluorescent stainings and documentation of the effectiveness of viral expression of GFP in BFCNs.

The best quality images were captured with a confocal laser scanning microscope LSM 710 Zeiss (Argon and Helium/Neon lasers) using 40x oil objective with suitable filter sets and excitation wavelengths. Separation of emission spectra was ensured with cut off filters e.g.: for Alexa 488 fluor green 505-550, for Cy3 fluor red 550–630 nm, for DAPI blue 405-480 nm. Emitted fluorescence signals were sampled at spatial resolution of 30 nm/pixels with 1.5 µs dwell time. LSM710 was also used to acquire stack images in Z- dimension for 0.5 µm thick optical sections. To ensure that identical data are obtained, the acquisition parameter were kept. Usually all microscope settings were saved and re-used. Time lapse imaging with LSM710 allowed monitoring of $p75^{NTR}$ (192-IgG-Cy3) and Aβ (Alexa 488) trafficking in live cells *in vitro*.

2.2.1. Measurement of co-localization of fluorescent markers

Co-localization of HiLyte fluor (Alexa 488) Aβ (1-42) and 192-IgG-Cy3 in BF cultures was assessed with laser scanning microscope (LSM 710, Carl Zeiss), which automatically measured and calculated the co-localization parameter and overlap coefficients (ZEN-2008 software), based on algorithm, which assesses the presence of two flours within the same pixel (Manders et al., 1993) (Figure 13).

$$M_1 = \frac{\sum_i R_{i,\,coloc}}{\sum_i R_i}$$

$$M_2 = \frac{\sum_i G_{i,\,coloc}}{\sum_i G_i}$$

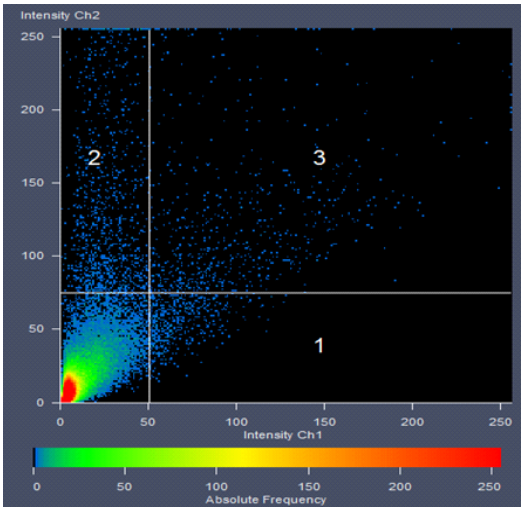

Figure 13. Measurement of co-localization coefficient by LSM710. Colocalization coefficients were measured for each channel (M1, M2). They were calculated by summing the pixels in the colocalized region (Quadrant 3) and then dividing by the sum of pixels either in Channel 1 (Quadrant 1 + Quandrant 3) or in Channel 2 (Quadrant 2 + Quadrant 3). Each pixel has a value of 1. The colocalization coefficient values ranged from 0 to 1. Single labelled control samples were imaged with the same microscope settings as the double label experimental samples. Exact (X,Y) coordinates on the scatter plot were determined by using the control samples and they were kept constant for the analysis of the double-label experimental samples.

The parameters, which influence the intensity of the image remain the same for all experiments. These include: objective (40X), the power of the laser, excitation wavelength and parameters of the detectors with appropriate cut-off filters (Chapter 2.2) as well as an acquisition speed settings. The type of mounting media was kept constant for all control and experimental samples as different types may exhibit varying levels of autofluorescence. Similarly, imaging through different types of material, such as glass coverslips versus a plastic bottom dishes was avoided, because it could influence the brightness and signal to noise ratio. Special dishes for LSM microscopy (81151, Ibidi) were utilized. Around 100 frames in total were analysed for each experiment. Values of fluorescence intensities were averaged off-line, using Excel; mean signal intensities and standard deviation from means with standard error were calculated.

2.2.2. Cells counting procedure

This study used a non-stereological, two dimensional quantification of neurons. Most often cells were counted manually with use of a counting tool from Photoshop CS4 programme vs.11. Cells counting was performed on equally thick sections (35µm), where neurons were visualised by indirect fluorescence or HRP labelling as described in Chapter 2.1.6. In case of cholinergic neurons, counts of FITC- and Cy3-stained cells were used versus all those visualised with DAPI. The results were verified by a randomly-chosen second researcher, blinded to the study. In some cases, Image G threshold macro was used to verify cell numbers. The data analysis was performed afterwards (Chapter 2.4.).

2. 3. Western blot (WB) analysis of cholinergic markers in BF

2.3.1. Dissection of rat brain for WB

The post experimental extraction of brain as well as control tissues were performed after decapitation of rodents under deep anaesthesia. An overdose of sodium pentobarbital (i.p.; 200 mg/kg) was used for sub-lethal anaesthesia. In some cases this was combined with medetomidine injection (s.c.; 0.4 mg/kg) in order to minimize the distress of the animal. The depth of anaesthesia was checked by the absence of tail pinch response. Then brains were removed from the cranial cavity and

placed on petri dish for dissection. For most of the experiments, BF, hippocampus (H) and prefrontal cortex (PC) areas were collected. The tissue was immediately placed on ice in buffer containing 0.5% Nonidet (74385, Sigma-Aldrich) and mix of protease inhibitors (Appendix 5.1). This detergent is powerful enough to study cytoplasmic and membrane–bound proteins without breaking the nuclear membrane. The tissues were then homogenised and kept 30 min on ice with vortexing every few minutes before centrifugation at (14Kxg) 10 min at 4ºC and stored in -20ºC. The supernatant was taken for further analysis and protein concentration was determined prior to the WB with standard Bradford (500-0006, BioRad) or PierceTM BCA (23227, Pierce) protein assay.

2.3.2. Development and analysis of WB

Protein extracts were mixed with loading buffer (10482055, Life Tech.) and heated 10 min at 95ºC. They were subsequently loaded on 12% NuPage Bis-Tris gel in known concentrations, previously defined with Bradford protein assay. Separation of proteins was carried out by applying 170 V in denaturing conditions (SDS-PAGE); polyacrylamide gels were then transferred (wet blot) approximately 4 h onto pVDF membrane (IPVH20200, Millipore) at 4°C with 40 mV current. The membrane was blocked for 0.5 hour with 5% milk (70166, Sigma) in TBST (Appendix 5.1). Then the relevant secondary antibody was applied overnight at room temperature. Depending on secondary antibody, the DAB Impact kit (SK-4105, Vector Labs.) was used (for secondary antibodies coupled with HRP) or combination of nitroblue tetrazolium chloride (NBT) (N6876, Sigma) and 5-bromo-4-chloro-3-indolyl phosphate (BCIP) (B6149, Sigma) in AP buffer (Appendix 7.1.), pH= 9.5 (in case of secondary antibodies coupled with alkaline phosphatase). The detected bands were then analysed in G:BOX from SynGene with the use of GeneTools programme. Semi-log plot tool was used to assign correct size of the bands. The plots were obtained from data normalized versus the same area of interest.

2.4. Data analysis

Different analytical approaches were utilized depending on experimental purpose and the techniques used. The experimental measurements were expressed as mean ± SE

with statistical significance assessed using paired or unpaired Student's *t*-test. The difference between samples was defined as significant if p value was less than 0.05. In experiments involving multiple repeated comparisons, one way ANOVA was applied for the assessment of significance.

2.5. Primary BF neuronal cultures

2.5.1. Coating of cell culture dishes

Depending on experimental purpose, culture dishes made of different materials were used e.g. glass bottom dishes for DIC microscopy or polystyrene dishes for culturing cells aimed for WB procedures (81158 Ibidi, 734-0005, BD Falcon). For confocal microscopy, specific Ibidi dishes (cat no 81151) were utilized. All dishes were coated with 0.01% poly-L-lysine (100μg/ml, Sigma, P4832) to promote adhesion of the cells. Poly-L-lysine was applied to the surface of each dish for 1 h and then washed away. Dishes were left to dry at room temperature and subsequently rinsed with sterile H_2O after that. Plating medium (2 ml) dependent on the tissue culture type (see below) was applied into each dish and the dishes were pre-incubated at 5% CO_2 in 37°C before applying neuronal cells.

2.5.2. Isolation of BF from embryonic or postnatal rodents brain

Primary BF tissue cultures were obtained from embryonic C57/BL6 or CD-1 mice or (E18) or postnatal Sprague-Dawley rats (p0) according to previously established protocols, optimized for our conditions (Nakajima et al., 1985; Pongrac and Rylett, 1988; Schnitzler et al., 2008, Banker and Gosslin, 1998).

For embryonic mice, the surgery was carried out under deep, ketamine-induced anaesthesia with use of Velatar, PfizerTM (i.p., 120 mg/kg) (Figure 14B). To avoid distress of the mice, animals were sedated with isofluran prior to i.p injection (5% isofluran, 1L/min oxygen) (Figure 14A). The depth of anaesthesia was verified by checking of the tail pinch response (Figure 14C). A longitudinal incision through the skin first and then through the abdominal muscle of the animal was performed (Figure 14D). When opened, the uterus was removed from abdominal cavity on the sterile dish (Figure 14E, 14F). Than embryos were dissected and placed in cold sterile Hank's Balanced Salt Solution (HBSS) (14170, Life Tech.) supplemented

with 10 mM HEPES buffer (H4034, Sigma) and 1% penicillin/streptomycin (15140-122, Life Tech) (Figure 14 G). The dam was euthanized by rapid decapitation under ketamine anaesthesia. Embryonic heads were isolated (Figure 14H, 14I) and brains dissected out (Fig. 14J – N). The BF was isolated in sterile conditions and kept on ice in dissecting media enriched with 25 mM of glucose (49163, Sigma). Removal of meninges was critical step during the whole procedure. The media was exchanged for 0.05% trypsin/EDTA (25300054, Life Tech.), pH=7.4-6, 270-310 mOsm/kg and incubated with extracted brain tissue around 10 min at 37°C to allow dissociation of the cells. Afterwards benzonease (E1014, Sigma) was added for 5 min and then all material centrifuged (5 min, 180g). The pellet was re-suspended with plating medium containing 1:1 [mixture of Dulbecco's modified Eagle's medium (DMEM) (D6429, Sigma) : F12 (N6658, Sigma); (1:1)] and dissecting medium supplemented with 5% foetal bovine serum (FBS) (F2442, Sigma). The dissociation of cells was facilitated by brief, gentle trituration (around 12-15 times) with glass fire-polished Pasteur pipette before another centrifugation for 5 min (180 g). The medium was then refreshed and cells plated at a density of 0.5–1.0 x 10^5 cells/cm^2 onto 35 mm glass dishes coated with poly-L-lysine. Standard tryptan blue method for cell counting was used to establish proper plating density.

Cells were cultured in serum-supplemented medium for 1 h to facilitate the initial attachment of neurons to the substratum and to inactivate proteolytic enzymes released from damaged cells during trituration (FBS contains protease inhibitors, such as α1-antitrypsin and α2-macroglobulin, which inhibit the trypsinization process). The medium and unattached cells were removed and replaced by serum free medium containing (1:1) DMEM: Neurobasal (21103-049, Life Tech.) with 2% B27 supplement (17504-044, Life Tech.), 50 ng/ml NGF (mouse, 2.5S; N6009, Sigma) and 1% penicillin/streptomycin. The dishes with cells were placed in humidified incubator at 5% CO_2, 37°C. Quick dissection time and using proper cell surface adhesion materials were very important for success of this procedure . The best cells adhesion was observed with Ibidi dishes coated with 0.01% poly L-lysine (Chapter 2.5.1.). After 48 hours of incubation, cytosine β-D-arabinofuranoside hydrochloride (C1768, Sigma) was added to inhibit the growth of other non-neuronal and glial cells. Culture media was refreshed every 5 days, each time only half of the medium was replaced. All media were previously sterilised by passing through 0.22μm syringe filter.

In regards to new-born rats, postanatal (P0) rat brains were isolated into the dissecting medium (already mentioned above) and minced with the use of sterile medical needles before changing of dissecting medium to the plating one (same as for embryonic cultures). Then the same protocol for BF cultures was applied.

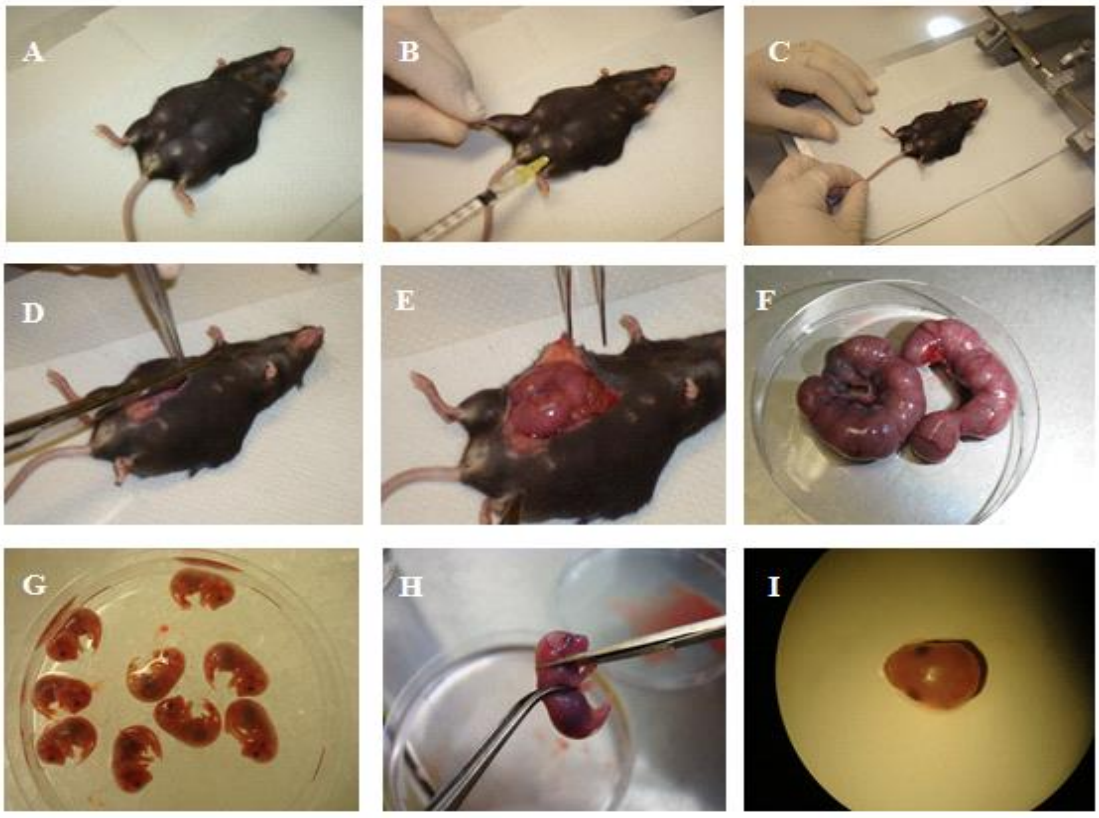

Figure 14. Isolation of brain from mice embryo. A. Mouse anaesthetised with isofluran. B. i.p. injection of ketamine. C. Pinch tail response check. D. Abdominal incision. E. Uterine with embryos inside the mouse. F. Uterine removed on sterile Petri dish. G. Separated embryos on ice. H. Isolation of embryo head. I. Embryo head under dissection microscope ready for brain isolation.

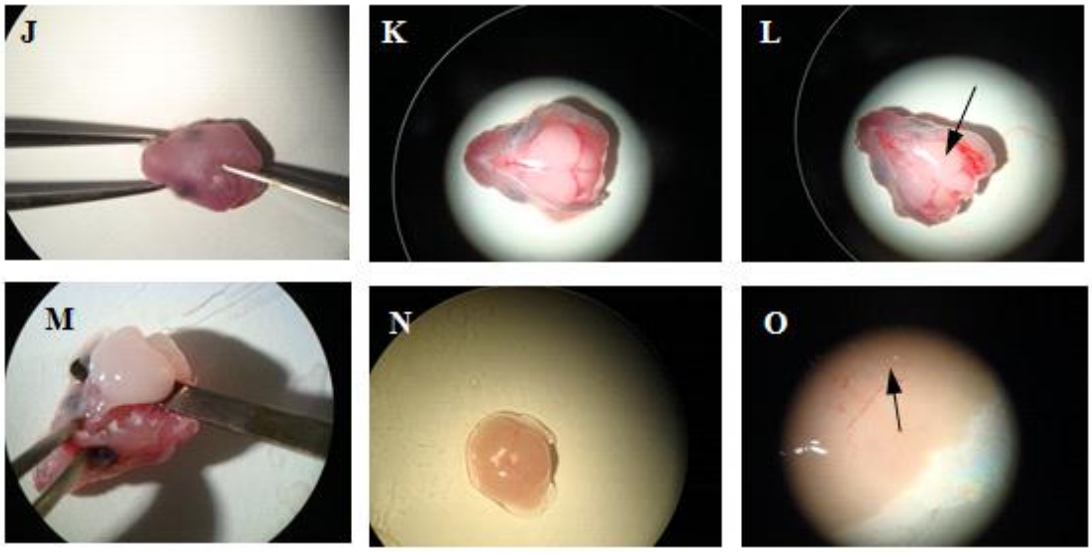

Figure 15. Isolation of BF from rodent brain. J. Incision of the head's skin. K. Embryo brain visible after skin removal. L. Half of the meninges removed (right side). M. Removal of the brain . N. Mouse brain ready for dissection. O. Opened hemispheres. Arrow points to the septum area.

2.6. Production of lentiviral particles

2.6.1. Transformation of competent cells

DH5α competent cells derived from *E.Coli* (18265-017, Life Tech.) were taken from -80°C freezer on ice to thaw. They were aliquoted (10 µl) into 4 sterile 1.5 ml eppendorfs and transformed with pMD-2G, pWPT-GFP (or modified pWPI) and pCMV plasmids (7271, 1 2225, 15785, Addgene). PUC 19 control DNA (15364-011, Life Technologies) was used to verify the efficiency of this transformation. Briefly, each plasmid (1 µl) was added to DH5α cells, incubated on ice for 30 min and then shocked by heating the vials for 20 seconds to 42°C and immediate transfer to ice for additional 2 minutes.

2.6.2. Growing of DH5α colonies

S.O.C (2% tryptone, 0.5% yeast extract, 10 mM NaCl, 2.5 mM KCl, 10 mM $MgCl_2$, 10 mM $MgSO_4$, and 20 mM glucose.) medium (950µl) (15544034, Life Tech.) with 50 mg/ml ampicillin (or other rich broth like LB - L7658, Sigma) was added to transformed DH5α cells and incubated for 1h in 37^{o}C with shaking at 225 rpm. Then two different amounts of colonies (20 - 200 µl) were added to previously-prepared pre-warmed selective plates and spread. DH5α cells (not transformed) were used as control. All plates were further incubated in 37°C overnight.

2.6.3. Selection of plasmid-positive colonies

Antibiotic resistance was used to select the colonies that have acquired the plasmids of interest during cells growth. All selective plates were freshly prepared with 50 µg/ml ampicillin in LB agar (L2897, Sigma) on sterile Petri dishes. Only the cells transformed with plasmids that confer the gene for ampicillin resistance were able to grow.

2.6.4. Amplification of DH5α colonies

Amplification of plasmid-positive DH5α colonies was performed in two steps. First one colony from each agar plate was inoculated into sterile Falcon tubes with 10 ml

of LB or 450 µl S.O.C media, each containing 50 mg/ml ampicillin. The tubes were placed on shaker for 5 h at 225 rpm, 37°C. Content of each tube was then poured into bigger 1L flask of LB medium containing 50 mg/ml ampicillin. The amplification was continued overnight (16 h altogether) in 37^{o}C with shaking at 225 rpm. Absorbency at 600 nm was measured to estimate the phase of cell growth. Incubation for more than 16 h was not recommended because the cells began to lyse and plasmid yields could be reduced.

2.6.5. Extraction of plasmids' DNA

Extraction of plasmids' DNA was performed with QIAfilter Plasmid Midi Kit (12243, Qiagen). All buffers and solutions used for this procedure are described in Appendix 7.3. Briefly, LB culture was harvested by centrifugation for 15 min in 4°C (6000 g) and the supernatant removed. The remaining bacterial pellet was homogeneously resuspended in 25 ml of buffer P1, containing 100 µg/ml RNAse A. Then 4 ml of lysis buffer (P2) was added and the tubes, vigorously inverted 4-6 times before incubation for 5 min. at the room temperature. During this time QIAfilter Midi Cartridge was prepared and the tip equilibrated by applying 4 ml of equilibration buffer (QBT) for gravity flow through the column. Then, 4 ml of neutralization buffer (P3) chilled to 4 °C was added to the tubes and thoroughly mixed. Bacterial lysate was poured into Falcon tubes and centrifuged 10 min at 1620 g before applying it into the cartridge. It was left there for 10 min and filtered into the Qiagen-tip for further binding, washing and eluting procedure. Gravity flow of the lysate through the column was allowed and the tip was then washed twice with 10 ml of wash buffer (QC). DNA was eluted with 5 ml of elution buffer (QF) into the sterile tube. Precipitation of plasmids' DNA was achieved by adding 3.5 ml of isopropanol at the room temperature and centrifugation of the mixture at 15000 g for 0.5 h at 4°C. After removing the supernatant, the DNA pellet was washed with 2 ml of 70% EtOH and centrifuged at 15000g for 10 min. To finish this procedure, the supernatant was carefully discarded and the tubes air-dried. After that DNA was dissolved in TE buffer which is routinely used to solubilize DNA or RNA to protect them from degradation.

2.6.6. Quality check of plasmids' DNA

Concentration of DNA was measured and purity assessed by 260/280 nm and 260/230 nm ratios using NanoDrop 1000 with 1.8 value reflecting pure DNA in first measurement and 2-2.2 ratio corresponding to pure DNA in the second measurement. Three readings of the same sample were averaged before calculation of DNA concentration.

The plasmids' DNA size was verified after restriction-digest reactions, designed with the enzymes specific for each plasmid and represented on the plasmid restriction maps attached (Appendix 7.4). The following restriction enzymes: BamH1 for pWPT-GFP plasmid, Pst1 for pMD-2G and EcoR1 with XhoR1 for pCMV [R0136, R0140, R0101 and R0146, respectively; all from New England (NE) BioLabs] were utilized. The reaction mixture contained 10 µl of plasmid DNA, 0.1 – 0.2 µl of appropriate enzyme, 0.1 – 0.2 µl of NE compatible buffer, 7.6 – 7.8 µl of H_2O and 0.2µl of BSA (B9000, NE BioLabs). Restriction-digest was carried out in 37°C for 2 h continuously or sequentially in case of two enzymes for the one plasmid. The size of each plasmid after digestion was checked on 1% agarose gel with ethidium bromide (E7637, Sigma) in TAE buffer (Apendix 7.4.) against molecular ladder (N3232S, New England BioLabs) and non-digested version of each plasmid.

2.6.7. Preparation of human embryonic kidney (HEK) 293FT cells

HEK 293FT cells were retrieved from liquid nitrogen, thawed and quickly transferred to T-25 sterile flask containing growth medium [DMEM (D6429, Sigma), 10% FBS (F9665, Sigma) and 1% penicillin/streptomycin/antimycotic (15240, Life Tech.]. After few hours, when most of the cells were attached to the bottom of the flask, the rest of DMSO from cryo-protecting medium (DMEM; 14.5 g/L glucose, 10% FBS, 8% DMSO) was removed and replaced with fresh, pre-warm growth medium. HEK 293FT cells were kept in optimum growth conditions (37°C, 5% CO_2) and split every 2- 4 days when reaching 80 – 90 % confluence. Splitting the cells involved removing of the old medium, washing cells twice with PBS, PH=7.4, detaching cells from plastic with trypsin-EDTA solution (25300104, Life Tech) (1-3 min in 37°C) and transferring the desired number of cells to a bigger flask with growth medium. HEK 293FT were usually reseed at 2×10^4 cells/cm^2 density

2.6.8. Safety precautions for lentivirus handling

Production and handling of the LVs demanded special care. Open tubes were handled inside class II cabinet in level 2 containment laboratory and taken out only when closed and sprayed with 75% EtOH. The infected cells were kept in incubator designated for viral work. All solid waste and plastics were discarded in biological safety yellow bags and autoclaved thereafter. Liquids were aspirated into a liquid waste bottle containing fresh bleach and spilt into the sink after neutralization. The Biosafety Committee at Dublin City University approved the procedures for the production and handling of LVs; an emergency response plan was written and submitted to the above Committee.

2.6.9. Transient transfection of HEK 293FT cells and lentivirus collection

One the day before transfection HEK 293FT cells were seeded at the density 1-3 $x10^6$ cells/Petri dish in RPMI-Glutamax medium (61870036, Life Tech.) with 10% FBS and 1% antibiotic. On transfection day (when HEK cells reached 80 % confluence), the above medium was removed and replaced with 9 ml of the same medium but without serum and antibiotic for each Petri dish. Transfecting solution was prepared separately in Falcon tubes with 1.2 ml of RPMI-Glutamax medium calculated per plate. In total DNA plasmids (9 µg) was added to this tube in ratio 4:3:1 for the following plasmids pWPT-GFP, pCMV-, pMD-2G. The mixture was combined with 45 µl of PEI (23966, Polyscience) per dish and vortexed immediately. After 15 min of incubation at room temperature, it was added to the HEK 293FT cells dropwise and spread over the dish gently. Transfected cells were incubated 2 h in 37°C and the medium was then enriched with 20% FBS and incubated for additional 2 days in 37°C, 5% CO_2. After that time, the medium was collected and centrifuged for 15 min at 1620 g. The supernatant was carefully transferred to glass tubes and ultracentrifuged for 2 h at 70409 g. The pellet was resuspended in 50-100 µl of PBS and stored in -80°C freezer.

2.6.10. Confirmation of lentiviral titter with p24 assay

The titter of lentiviral vectors was confirmed with p24 assay. This assay is based on

two sided sandwich ELISA in which p24 antigen (from the virus capsid) is captured from detergent lysate of virions by polyclonal antibodies, adsorbed to a solid phase. The method was previously described by Moore and McKeating (1990). Bound p24 antigen is detected by alkaline phosphatase, conjugated anti-p24 monoclonal antibody and chemiluminescent detection system. Briefly, each experimental and control well of 96-well microtiter plate were coated in duplicates with 100 µl mixture of sheep polyclonal antibodies (D7320, Aalto Bio Reagents) (5 µg/ml), which react with p24 gag structural protein of HIV-1. The plate was incubated overnight at room temperature and washed twice with TBS (200µl per well). Then 100µl/well of 2% milk in TBS, pH=7.5 was applied for 1 h at room temperature to block non-specific binding sites. In some cases, plates prepared in such way were frozen in -20°C and stored for several week to be thawed directly before use. The milk containing buffer was discarded and wells washed with TBS, pH=7.5 and tapped dry. Then 100 µl/well of p24 standards (AG 6054, Aalto Bio Reagents) was applied in duplicates as well as controls and supernatant of interest in the same amounts. Recombinant HIV-1 p24 antigen (p24 standard) was diluted in 1% FCS (4781, Sigma) in TBS to 100 µg/ml and then 1:1000 with 0.1% Empigen (45165, Sigma) prior to use. The assay involved few 1:3 dilutions down of this mixture also with 0.1% Empigen. Experimental samples were treated with 1% Empigen prior to assaying to inactivate the virus and linearize the proteins. Blank wells filled with 0.1% TBS served as controls. The incubated assay was leaved for 3 h at room temperature. The plate was then washed twice with TBS and tapped dry. Then 100µ/well of conjugate consisting of 1:1000 secondary monoclonal anti-HIV-1-p24 antibody coupled to alkaline phosphatase (BC 1071-AP, Aalto Bio Reagents), 20% sheep serum (S-7773, Sigma) and 0.05% TBST was incubated at room temperature for 1 h. The wells were washed 4 times with 0.1% Tween 20 (P9416, Sigma) in PBS, tapped dry and then washed 2 times with TROPIX wash buffer (EL100CX, Aalto Bio Reagents) and dried again. For detection, the chemiluminescent substrate for alkaline phosphatase (CSPD with Sapphire-II) (50 µl/well) was added and incubated for 0.5 h in dark at room temperature before reading the plate. The absorbance was measured at 450 nm against 690 nm wavelength using dual mode BioTek Synergy HT multifunction reader equipped with Gene 5 software programme. The experimental and control samples were read in duplicates and the plate background was subtracted from these readings. Quantification of p24 antigen was measured by endpoint evaluation and

form a standard curve. The viral titter was calculated from this curve (Figure 65A) according to the equation below.

Titter in IU/mL = (cells at starting time) x (dilution factor) x (percent infection)/(vol virus solution added expressed in mls); f.e ($4x10^5$ cells/ml) x (100 times dilution) x (5.0%/100)/(0.0025ml) = 8.0×10^8 IU/ml

2.7. Construction of anti-$p75^{NTR}$-LentiGFP vector

2.7.1. Biotinylation of LentiGFP

Sulfosuccinimidyl-2-[biotinamido]ethyl-1,3-dithiopropionate (sulfo-NHS-SS-Biotin) (21328, Thermo Scientific), a thiol-cleavable amine-reactive reagent was used for biotinylation of the LVs produced earlier. The conditions for this reaction were optimized and biotinylation was carried out for 2 h on ice with an excess of biotin or overnight in 4°C with an extensive mixing of the LVs and the biotinylation reagent. Non-reacted Sulfo-NHS-SS-Biotin was removed later by dialysis. The membrane for dialysis utilized 12-14 kDa MWCO, that was cleaned by heating in 2% $NaHCO_3$ and 1 mM EDTA at 80°C for 30 min. The tubing was then rinsed thoroughly in distilled water. Biotinylated LVs were introduced into the tube membrane and clipped at both ends. Then tube membrane was fixed to the edge of the flask containing PBS, pH=7.4. for dialysis, performed with gentle mixing at 4°C overnight.

The amount of biotin incorporation to the LVs was estimated with 2-(4'-hydroxyazobenzene)-2-carboxylic acid (HABA)/Avidin reagent (H2153, Sigma). The assay was based on binding of HABA dye to avidin and the ability of biotin to displace this dye in stoichiometric proportions. In principle, the maximal absorption of HABA/Avidin complex at 500 nm decreases when biotynylated molecule is added to the solution. The change in absorbance relates to the amount of biotin in the sample. Readings for blank wells were deducted from the assay and a dilution factor for HABA/Avidin calculated upon an addition of the sample or control (without biotin) (http://www.piercenet.com/haba/habacalcmp.cfm) (Green et al., 1970).

2.7.2. Conjugation of streptavidin to anti-p75 IgG

Lightning-LinkTM conjugation kit (708-0015, Innova Biosciences) was used to

conjugate streptavidin to anti-p75 antibody (07-476, Millipore). The antibody was prepared first as the previous dialysis steps might interrupt the traditional protein conjugation procedure. Therefore, 1µl of LL-Modifier was added for each 10µl of anti-p75 IgG and the mixture was kept for 3 h at room temperature or overnight in the cold room, 4°C. After this time 1µl of LL-Quencher reagent was applied for every 10 µl of anti-p75 IgG and left for additional 30 min on ice. Equal amounts of such prepared anti-p75 IgG and Lightning-LinkTM mix containing LL-Streptavidin were combined. There was no need to purify the conjugate because the chemicals used in Lightning-LinkTM are deactivated by the quencher as well as other by-products and do not need to be removed.

2.8. Stereotactic intra-ventricular (icv) injections into the rodent brain

2.8.1. Practice and quality control of icv injections

Icv injection is a skilful procedure which demands appropriate training; it involves animal handling, stereotactic surgery and post-operational care. The experiments should be carry out only if necessary and if they cannot be replaced with other methods. In this study icv injections were utilized for delivery of 192-IgG-Cy3 (5µl 0.4 mg/ml) to label cholinergic neurons *in vivo* (Chapter 3.3.), 192-IgG-SAP (2.5 µg/ml) to achieve cholinergic cell loss (Chapter 3.5.6.) and lentiviral vectors for targeting of $p75^{NTR}$ (5 µl, 7.0 x 10^7 IUs/ml) (Chapter 5.4.2.) into the rodents brain. Stereotactic icv injections of Aβ or saline were applied to mimic the excessive Aβ load and chemically-induce AD model in rats (Chapters 3.5.2. – 3.5.4.). Due to the use of expensive reagents and also to minimize failure during the experiments three, 21 days old rats were injected with Coomassie blue dye for the training purpose (Chapter 3.3.).

2.8.2. Preparation for the surgery

Adequate preparation is important step for the success of the whole surgery: researcher, instruments and animals needs to be prepared correctly prior to the each procedure.

I was trained to carry out the surgery and performed *in vivo* experiments when confident with the procedure, which minimized the distress to the animal.

I autoclaved the surgical tools prior to the surgery and decontaminated thereafter and during the procedure with ethanol if necessary. S Hamilton syringe was washed several times in PBS to ensure easy flow of the reagents. Adequate chemicals and active ingredients were prepared prior to injections and kept close to the surgery site. In case of using viral aliquots, they were spun down before use and loaded into a Hamilton syringe in Class II microbiological safety cabinet.

Each rat was tail-marked and weighted prior to the surgery. While taking the animal from the cage it was important to leave the other rodents together with full access to food and water. To minimize distress, some rats were injected with medetomidine (Domitor®, Pfizer) 0.4mg/kg (s.c.) prior to anaesthesia. For easier access to the animal's skull, the fur on the head was gently trimmed and skin (the surgical field) cleaned with Betadine® (Santa Cruz Biotech.). Once taken from the cage the animal was monitored until full recovery from the sedative.

2.8.3. Anaesthesia for icv injections

The experiments were conducted under general anaesthesia (ketamine, Velatar ™, Pfizer) (50 mg/kg, i.p.). 5-7 minutes after injection, rats were checked for the absence of tail pinch response prior to the surgery. The depth of anaesthesia was also monitored in the course of the surgery. In some cases (e.g. to close the re-opened wound after surgery) anaesthesia was induced with 5% isofluran vaporizer in oxygen 1L/min, connected to the glass chamber and maintained at 3% through the tubing. The recovery of the animal was quick after removal of the isofluran mask.

2.8.4. Stereotactic surgery

During surgery, rats were placed on a warm pad and body temperature was maintained at 37°C throughout the procedure. The rostrum of the animal was fixed within stereotactic frame (Stoelting, Leica Vernier stereotaxic apparatus) in the horizontal position with head supported by the ear bars. When immobilized, 2-3 subcutaneous injections of 10 µl local anaesthetic (5mg/ml, Bupivacaine, Antigen Pharmaceuticals) were given to the skin of rat's head, to the place where small longitudinal incision was made later (after 2-5 minutes) in order to gain access to the bregma of the skull. Using bregma as a reference point, the coordinates for various

brain structures were determined, according to the rat's brain atlas (Paxinos and Watson, 1998). A Hamilton syringe, equipped with 33 gauge needle was fixed to the stereotactic frame and positioned accordingly. The place for injection was marked and a hole made in the skull with dental drill. 28 G needle was then utilized to puncture the dura. Icv injections of the desired material were slowly performed (1μl/min). The needle was removed very gently to avoid reflux along the needle track and wound sutured after injection, using absorbable vicryl. Additional antibiotic (Betamox LA, Norbrock) was applied over the closed wound to prevent the infection.

2.8.5. Post-operative care

Animals after surgery were kept on 24 light/dark cycles in properly labelled cages with easy access to food and water. Often the cages were kept warm with absorbent paper. The animal was continuously monitored until it recovered from the sedative. The researcher, responsible for post-operative care, monitored the animals health and wellbeing regularly, on the daily basis (according to monitoring check list pro-forma attached to each cage). Any signs of pain or distress of animal were immediately reported to Biological Research Unit stuff and alleviated. In case of re-opening the wound, isofluran anaesthesia (Materials and Methods, Chapter 2.8.3.) was applied to suture the wound.

Chapter III. Chemically-induced rat model of AD revealed involvement of cholinergic neurons in Aβ clearance – results with discussion

3.1. Review of AD animal models with reference to Aβ-induced models

One of the main obstacles in AD therapy is complexity of the disease (Chapter 1.5). The available animal models are useful for studying some but not all aspects of AD and are used for mimicking and preclinical evaluation of the treatments directed at Aβ or tau. Different scientific questions demand creating specific animal models that allow addressing particular problems. In other words no engineered animal model has yet reproduced the full spectrum of AD phenotypes in a manner closely similar to the human disease, despite the significant effort that has been made to create such models. However, partial reproduction of AD neuropathological phenotype with cognitive deficit has been achieved with genetic and pharmacological approaches.

In regards to transgenic animals, modelling of AD has been most heavily pursued in mice within the framework of amyloid cascade hypothesis. Genetic modification techniques have taken advantage mostly of mutations in APP and PSEN (Sawamura et al., 2000; Ashe, 2001; van Groen et al., 2006; Elder et al., 2010). Nevertheless, rat AD transgenic models have also been made and tested (Folkesson et al., 2007; Flood et al., 2009). These models exhibit age-dependent deposition of Aβ plaques in the hippocampus and neocortex and present extensive axonal dystrophies with inflammatory responses.

Neuronal loss and formation of NFTs is not evident in all models (Takeuchi et al., 2000; Richardson and Burns, 2002), however, models reflecting tau pathology have been also successfully made. These are often double transgenic mice that express both mutant human APP and tau (Lewis et al., 2001; Boutajangout et al., 2004), but single transgenic mice overexpressing tau do also exist (Adams et al., 2009). Such models allow to study mechanisms of Aβ and tau accumulation and enable studies of the relationship between these two key pathogenic proteins.

Non-transgenic animal models provide a complementary alternative to transgenic ones. They involve administration of exogenous Aβ through icv injections or chronic Aβ infusions. Most Aβ introductions were performed using synthetic Aβ (1-40) or Aβ (1-42) peptides, which are found in abnormally high level in neuritic plaques. The effects of such attempts are variable due to numerous reasons e.g. differences in brain structures targeted, concentration and aggregation state of Aβ peptides delivered, animal strain and handling procedures (Table 4).

Injected brain region	Type of injection, concentration of Aβ and its form/ organism	Time of effects	Main results/(reference)
Retrosplenial granular cortex	single unilateral micro-injection of 2 μg/μl Aβ (1-40) fibrilliar /female Wistar albino rat	10 days	Significant loss of cholinergic and glutamate-immunoreactive neurons in MSDB complex. Reduction in fibers and terminals immunoreactive for substance P, neurotensin and glutamate (Gonzalo-Ruiz and Sanz, 2002).
cingulate cortex, particularly the retrosplenial cortex	single unilateral micro-injection of 2 μg/μl Aβ (1-42) oligomers/ female Wistar rat	24h and 72h	IC analysis revealed an intense Aβ immunoreactivity in cortical cells, particularly in frontal and temporal cortices at 24 h, hippocampus and other cortical areas, increasing at 72 h. Activation of astrocytes was also observed in a time-dependent manner (Perez et al., 2010)
Hippocampus	bilateral injections of 10μg/2μl Aβ (1-42)/ male Wistar albino rat	10 days	Glutathione levels were significantly increased in temporal cortex and BF while malondialdehyde and NO levels were increased in temporal cortex and BF but without statistical significance (Cetin and Dincer, 2007).
dorsal Hippocampus	6-8 days of bilateral injections of 200pM Aβ(1-42)/Avertin mouse	4 days	Picomolar concentrations of Aβ (1-42) enhance LTP, whereas high nanomolar concentrations reduce hippocampal-dependent memory (Puzzo et al., 2008)
Medial Septum	Single injection 2 μg/μl Aβ (1-40) oligomers/ male Sprague Dawley rat	7 days	57% decrease in cholinergic and 53% drop in glutamatergic neurons were reported with 49% reduction in hippocampal theta rhythm (Colm et al., 2010)
Cerebral ventricle	Continuous 3 days infusion of Aβ (1–42) 10, 20 μg/ male Fischer rat.	3 days	Dose-dependent and a time-dependent impairment in spatial working memory and spatial reference memory as well as in non-spatial long-term memory. The reduction in ChAT activity up to 85 days was observed in hippocampus and striatum (Nakamura et al., 2001).

Table 4. Chemically- induced AD model - successful attempts of Aβ injections into the rodents' brain

However, lack of significant differences between the Aβ peptide and the vehicle control injections were also reported in rodents' brain (Games et al., 1992; Stein-Behrens et al., 1992) with conclusions that simple intraparenchymal injection of Aβ is not an appropriate model of AD-related neurotoxicity. Similar negative results were also found in adult rhesus monkeys (Podlisny et al., 1993).

Other pharmacological approaches have also been utilized in creating animal models, which reflect AD pathology. The mostly known is scopolamine-induced amnesia (Ebert and Kirch, 1998), which increased knowledge about the role of cholinergic system in cognition. Scopolamine is a tropane alkaloid drug with muscarinic antagonist effects (Rush, 1988), but blocking of both muscarinic and nicotinic receptors has given even better results (Levin et al., 1990).

A number of lesion models for studying AD pathology have also been developed. These lesions are performed in different brain structures, depending on the objective of the study (Gray and McNaughton, 1983; Glenn et al., 2003; Sloan et al., 2006; Castañé et al., 2010). They include quinolic, kainic, N-methyl-D-aspartic, ibotenic and quisqualic acids lesions (Page et al., 1993; Morimoto et al., 1998; Guillemin and Brew, 2002; Zheng et al., 2011; Toledana and Alvarez, 2010). The immunotoxins like cholinotoxin AF64 (Männistö et al., 1994), and the immunotoxin 192 IgG-saporin (192 IgG-SAP) have been also used with the latter ribosome-inactivating and specific for cells expressing $p75^{NTR}$ (Schliebs et al., 1996). Intraventricular injection of 192-IgG-SAP results in almost complete elimination of $p75^{NTR}$-positive cells in MSDB, nucleus basalis of Meynert, and Purkinje neurons of the cerebellum in rat (Wiley et al., 1991 and 2001). It provides researchers with a powerful tool - more specific and effective than chemical, surgical or electrolytic lesions. 192-IgG-SAP eliminates cholinergic cells, while sparing neighbouring neurons. The damage is not only selective but also permanent, what makes it an important animal model for study the plasticity, behavior, neuronal loss and other systems' responses. It is also important for replacement therapy and drug effects preclinical testing. Some other chemically-induced AD models utilize endotoxins, like lipopolysaccharide (Hauss-Wegrzyniak et al., 1998) or proinflammatory cytokines (Wenk et al., 2003) to study brain inflammation or other specific pathophysiological pathways e.g. glucose metabolism in neurodegeneration.

The aim of this chapter was to create AD model in rat useful for testing potential neurotherapeutics protecting BFCNs against damage of Aβ during the disease.

3.2. Brain structures involved in learning and memory – a Nissl staining study in the rat brain

Brain structures involved in learning and memory and affected by AD (Introduction, Chapter 1.4.) were visualised with Nissl staining of coronal sections (50 μM) from rat brain with cresyl violet acetate (Materials and Methods, Chapter 2.1.9.). The MS area of BF with vertical and horizontal limbs of diagonal bands of Broca (HDB and VBD) were labelled (Figure 16A). Additionally, the myelin rich structures such as anterior commissures (AC) were strongly stained (Figure 16A). The single neurons of BF were visible together with Nissl granules (negatively charged RNA in blue) on enlarged photos of HDB area (Figure 16B).

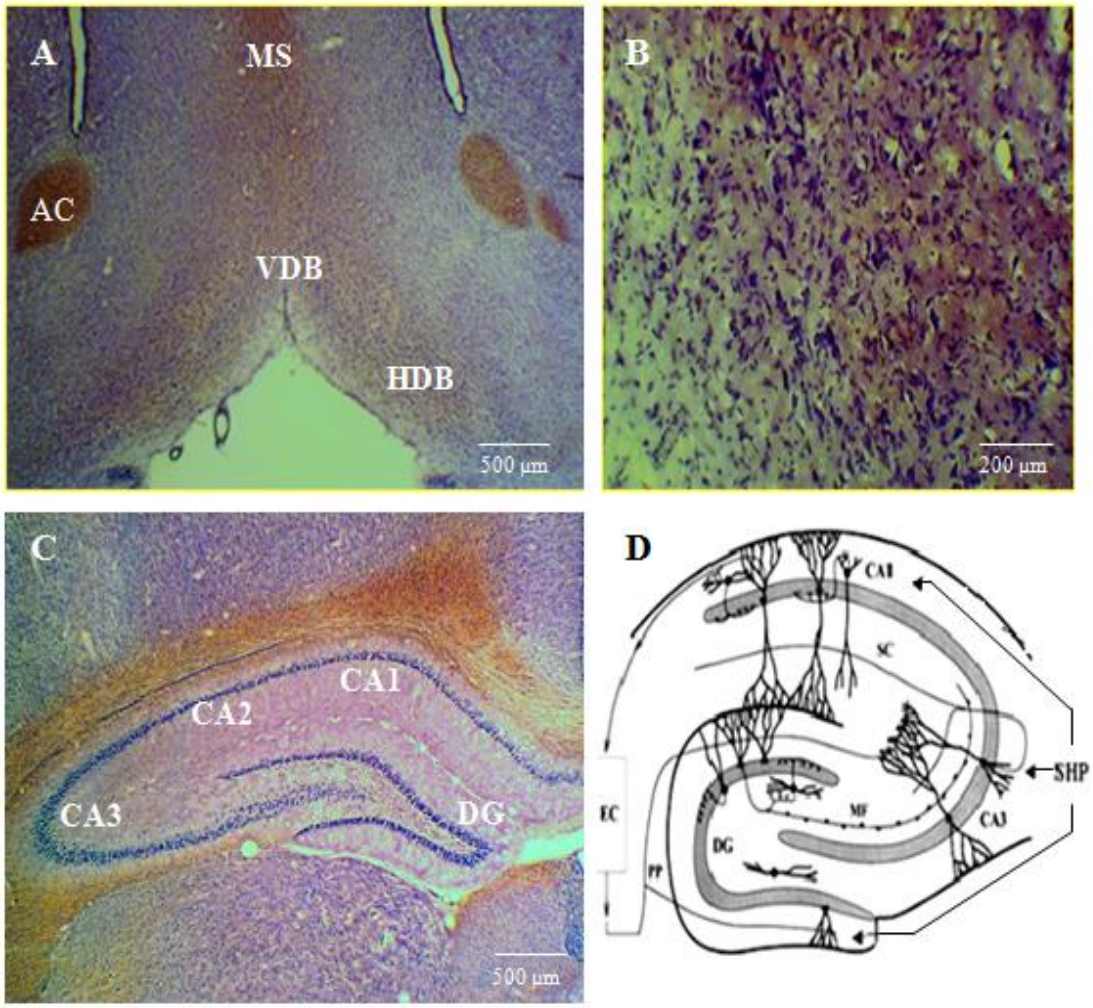

Figure16. Nissl staining of rat brain areas involved in learning and memory. A. BF coronal section; AC - anterior comissure; MS – medial septum; HDB – horizontal limbs of Broca; VDB – vertical limbs of Broca. B. Enlarged HDB area with visible Nissl granules. C. Hippocampal formation: DG – dentate gyrus; CA1, CA2, CA3 – Cornu Ammonis areas 1,2,3. D. Schematic representation of connections between parts involved in learning and memory (Schultz et al., 1998). EC – enthorinal cortex; CA1, CA3 areas; DG – dentate gyrus; MF – mossy fibres; PP – prefrontal fibres; SC – Schaffer collaterals; SHP – septo-hippocampal pathway

Structural parts of the hippocampus, which play a role in the formation and storage of new memories (Scoville and Milner, 1957; Bliss and Collingridge, 1993) were also distinguished and marked on the Figure 16C. The pronounced hippocampal atrophy occurs in AD (Pennanen, 2004; Lazarow, 2010). CA1 and CA3 pyramidal neurons are more vulnerable in the disease than dentate gyrus granule neurons. This differential neuronal vulnerability might be explained, in part, by the fact that dentate granule neurons express high concentrations of the neuroprotective Ca^{2+} binding protein - calbindin, whereas pyramidal neurons contain little or none (Mattson et al., 1991).

Additional schematic shown on Figure 16D (Schultz et al., 1998) explains the connections of these areas. Briefly, the entorhinal cortex (EC) serves as a gateway for all neocortical inputs to the hippocampus and sends perforant pathway fibres (PP) to the dentate gyrus (DG) and CA3 hippocampal areas, from where DG granule mossy fibres (MF) project to CA3 pyramidal cells that develop axons to CA3 and to CA1 areas through the Schaffer collaterals (SC). CA1 pyramidal cells project back to layer V of EC and to the subicular complex (not depicted on this Figure). The septum and the hippocampus are heavily interconnected through the fimbria-fornix and are functionally coupled (Bland and Colom, 1993), with projections connecting these key limbic structures referred further in this work as the septo-hippocampal pathway (SHP). Principal cells of DG, CA3 and CA1 receive cholinergic input via the SHP. This pathway is the main source of ACh important for memory encoding, retrieval and consolidation (Introduction, Chapter 1.5.3.2.). Other connections (not depicted in the Figure 16D) can enhance memory consolidation e.g. amygdala in relation to stress and emotionality associated with experience (Hadad-Ophir, 2014).

Obviously, the anatomy of the above connections does not fully explain the complexity of signals influencing learning and memory. Aminergic neurotransmitters with diffuse neuromodulatory system (Introduction, Chapters 1.5.6.) should be taken into account while considering memory processes and AD pathology.

3.2.1. BFCNs distinguished from non-cholinergic neurons

BFCNs were visualised on coronal sections containing BF area and distinguished from non-cholinergic neurons (Figure 17) with use of specific markers described in Introduction Chapters 1.5.3.2. and 1.5.4.

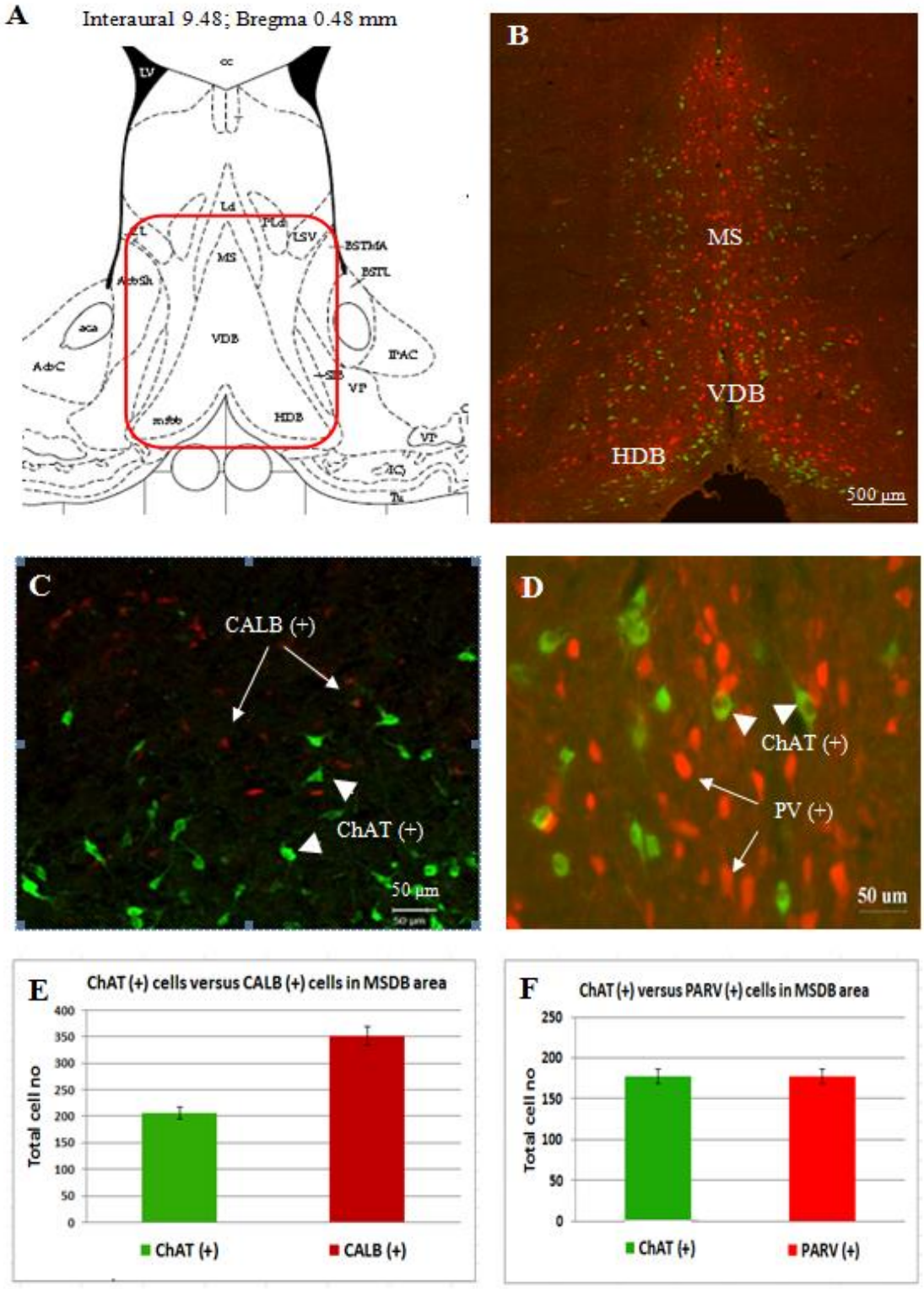

Figure 17. Characterisation of BF population with reference to BFCNs. A. Fragment of coronal section from Paxinos and Watson rat brain atlas (1998). BF area is highlighted within the red square. MS – medial septum; HDB - horizontal limbs of diagonal bands of Broca; VDB - vertical limbs of diagonal bands of Broca, LSV – lateral septal nucleus. B. MSDB area double labelled with anti-ChAT IgG (green) and anti-parvalbumin IgG (red). C. Double labelling of the same area with anti-ChaT IgG (green) and anti-calbindin IgG (red). Arrows point to calbindin positive cells – CALB (+) and arrow heads to ChAT positive cells – ChAT (+). D. Enlarged region from picture B showing lack of co-localization for ChAT and parvalbumin expressing cells. Arrows point to parvalbumin positive cells - PV (+) and arrow heads to ChAT positive cells - ChAT (+). E. Counts of cholinergic neurons versus non-cholinergic cells stained with calbindin (E) and parvalbumin (F).

Double stainings with anti-ChAT and anti-parvalbumin or anti-calbindin antibodies were utilized in these experiments (Materials and Methods, Chapter 2.1.6 and 2.1.7). ChAT and calbindin positive cells were counted in MSDB area (Figure 17A) on slices taken from brains of 21 days old Sprague-Dawley rats (n=3), also parvalbumin cells were counted in the same area on slices from 21 days old rats of the same strain (n=3) (Figure 17B). Double fluorescence labelling with ChAT/calbindin or ChAT/parvalbumin is shown on the enlarged areas Figure 17C and 17D. It has revealed that parvalbumin- or calbindin- containing non-cholinergic neurons do not co-localize with ChAT positive cells in MSDB area and follow different distribution patterns. They were usually detected more laterally than cholinergic neurons and had tendency to become smaller caudally. From analysis of cell number almost equal amount of ChAT and parvalbumin positive neurons were counted (Figure 17F) (7 slices) (n=177 and n=178), which is in the agreement with previously reported data (Gritti et al., 2006). Calbindin-positive cells were much smaller than parvalbumin containing neurons and their number much exceeded the amount of ChAT positive cells (Figure 17E) (5 slices) (n= 352 and n=206 respectively). Calcium binding proteins are known for their protective role in BF (Lacopino et al., 1994). Loss of their Ca^{2+} buffering properties were postulated to leave the neurons vulnerable to damage in neurodegenerative disorders (Geula et al., 2003) and these findings were recently confirmed for calbindin (Kook et al., 2014). Selective loss of this protein from BF or DG was earlier reported in the aged and AD brains (Wu and Geula 1997, Palop et al., 2003). Also depletion of parvalbumin from EC and certain hippocampal regions (CA1, CA2, DG) is known while other hippocampal subfields (CA3) remain less sensitive (Brady and Mufson, 1997). In contrast to calbindin, parvalbumin immunoreactive cells are reduced only after substantial loss of projection neurons in AD diseased brain (Solodkin et al., 1996).

3.3. BFCNs revealed strong enrichment with $p75^{NTR}$ (+) cells in MSDB region

Pre-labelling of BFCNs was performed by unilateral icv injection of 192-IgG-Cy3 (5 µl of 0.4 mg/ml) (Materials and Methods, Chapter 2.1.5.1.) of 21 days old rats (n=3), according to the stereotactic coordinates as follows: AP = -0.8 mm, ML = 1.2 mm, DV = 3 mm. The injection coordinates were optimised using Coomassie blue dye as shown on Figure 18A and B.

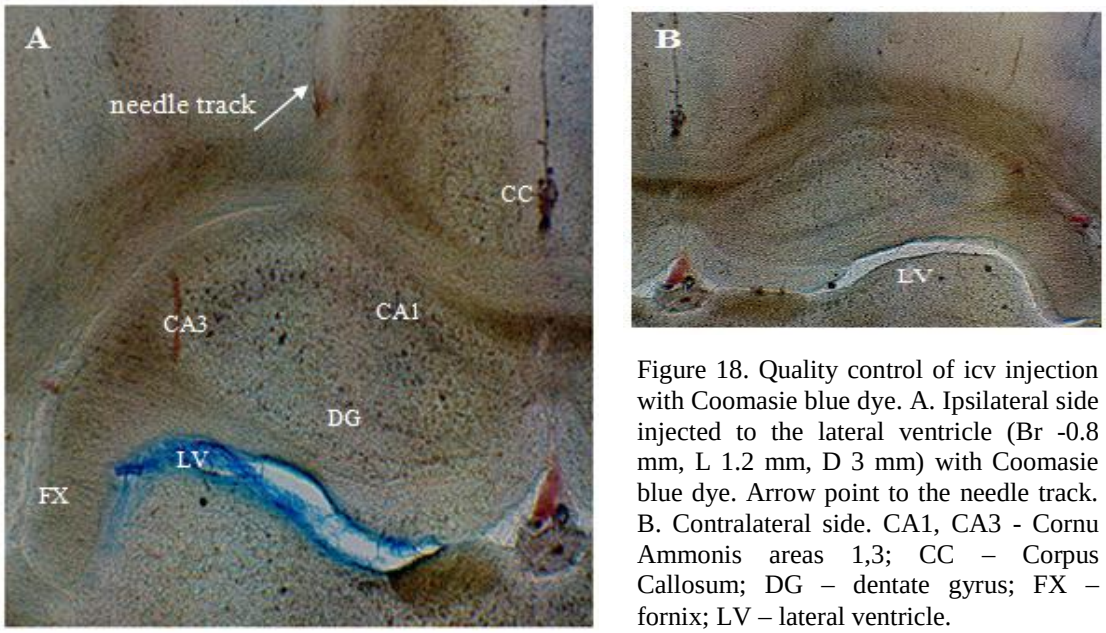

Figure 18. Quality control of icv injection with Coomasie blue dye. A. Ipsilateral side injected to the lateral ventricle (Br -0.8 mm, L 1.2 mm, D 3 mm) with Coomasie blue dye. Arrow point to the needle track. B. Contralateral side. CA1, CA3 - Cornu Ammonis areas 1,3; CC – Corpus Callosum; DG – dentate gyrus; FX – fornix; LV – lateral ventricle.

48-72h after injections, rats were perfused (Materials and Methods, Chapter 2.1.3.) and coronal sections (35 μm), containing BF nuclei were cut according to the rat brain atlas (Paxinos and Watson, 1998). The slices were kept in PBS pH 7.4 in darkness, mounted, air dried and coverslipped for viewing. Robust staining was visible in MSDB areas of the injected and contralateral sides (Figure 19A). The higher magnification revealed punctate pattern in the cell bodies (Figure 19B) and processes (Figure 19C), which is in agreement with the uptake and accumulation of 192-IgG-Cy3 within endosomes (Härtig et al., 1998; Kacza et al., 2000).

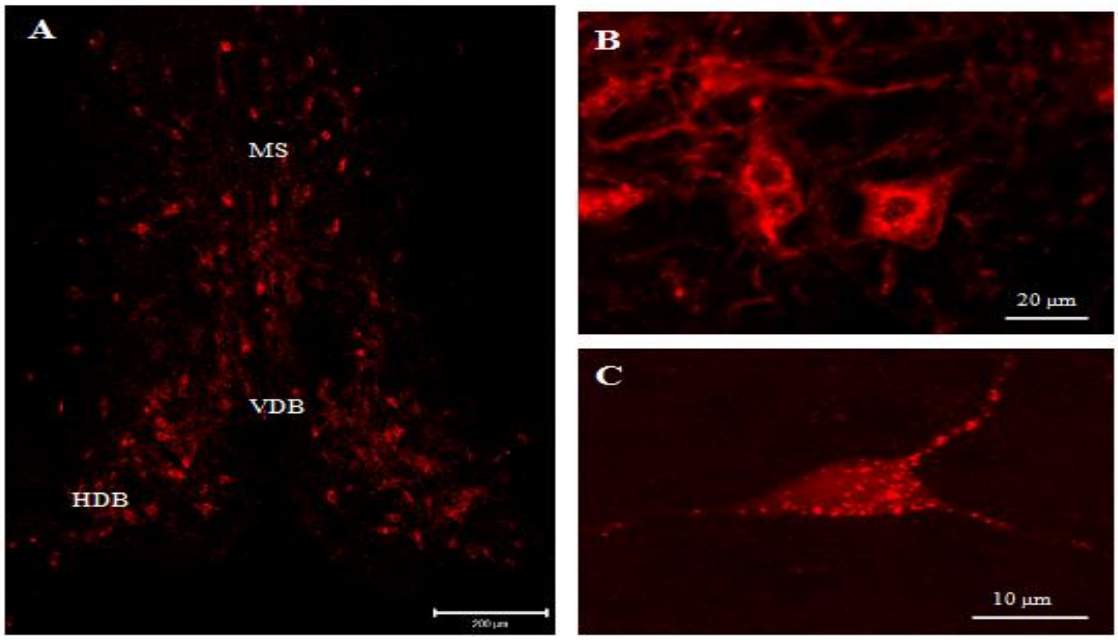

Figure 19. Cholinergic neurons of MSDB area pre-labelled with 192-IgG-Cy3. A. Enlarged area of DBB area stained with 192-IgG-Cy3. C. Single cholinergic cell – punctate staining observed in cell bodies and neurites after 192-IgG-Cy3 icv injection.

The same slices were then also stained for ChAT (Figure 20), according to the protocol (Materials and Methods, Chapters 2.1.6.and 2.1.7.) and the number of cells that co-localize both markers was counted (Materials and Methods, Chapter 2.2.2.)

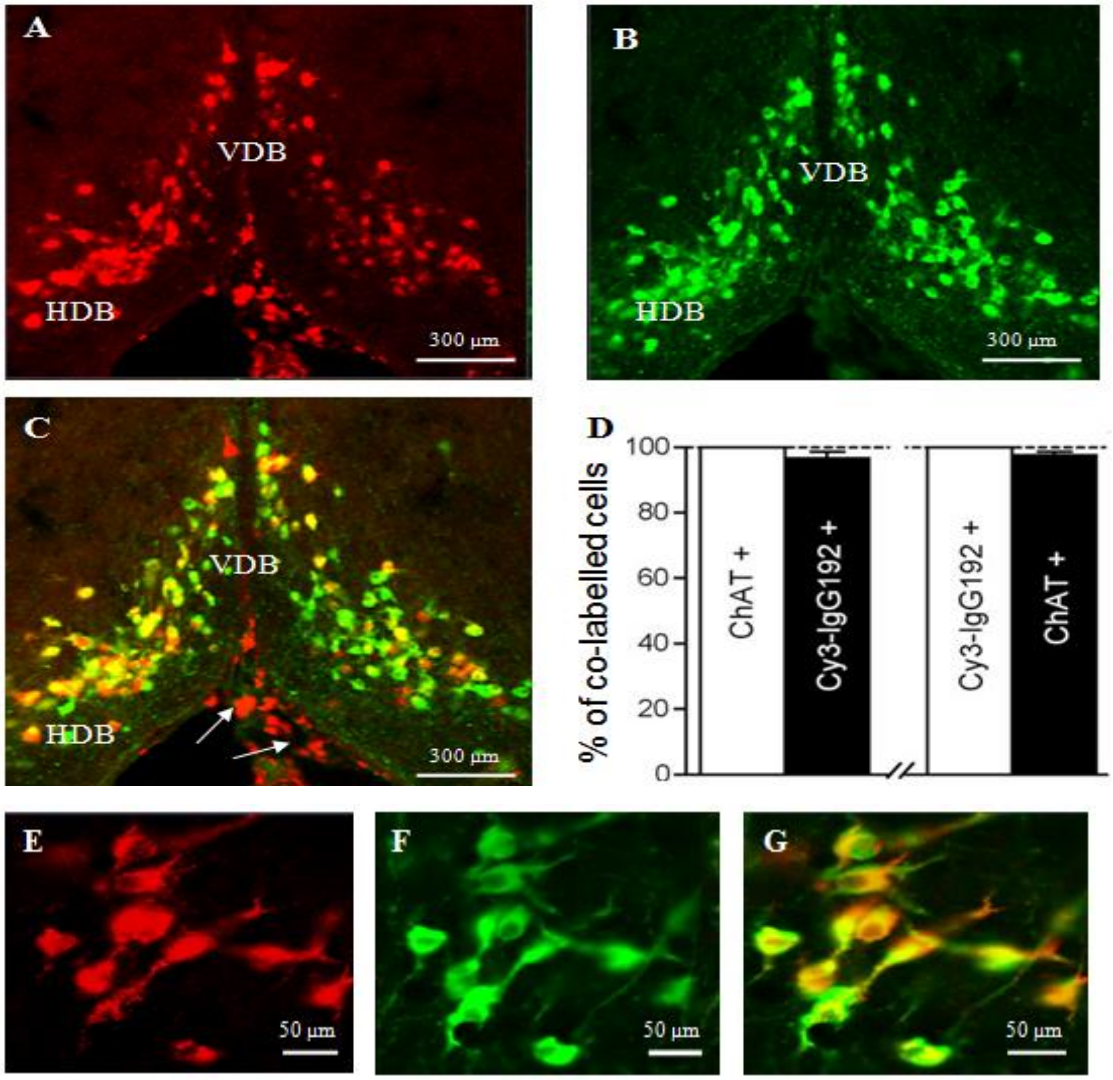

Figure 20. Double labelling of BFCNs with reference to $p75^{NTR}$. A. Cholinergic neurons of DBB area pre-labelled with 192-IgG-Cy3 i*n vivo*. B. Same field co-stained for ChAT. C. Merged image - double labelling in DBB area with exception of vascular elements stained with 192-IgG-Cy3only (arrows). D. Plots indicating the percentage of co-labelled ChAT positive cells with 192-IgG-Cy3 and vice versa [The total population of cells (n=297) is taken as 100% (white bars)]. E. Enlarged view of MS area - cholinergic cells pre stained *in vivo* with 192-IgG-Cy3 (E) and co-stained with ChAT (F) as shown in the merged area (G).

Double immuno-staining of ChAT positive neurons with 192-IgG-Cy3 confirmed the exclusive expression of $p75^{NTR}$ in the cholinergic population. The vast majority of ChAT positive neurons in MSDB were labelled with 192-IgG-Cy3 (97.4±1.9%) and vice versa, almost all 192-Cy3 cells were labelled for ChAT (98.7±1.1%). The results mean that with no exception, all 192-IgG-Cy3 (+) cells were immuno-reactive for ChAT but small fraction of ChAT (+) cells did not show 192-IgG-Cy3 labelling.

3.4. BF cholinergic markers profile quantified by WB

Cholinergic neuronal markers of BF are connected to the production, metabolism and transport of ACh (Introduction, Chapter 1.5.3.2.) and the level of these markers is significantly decreased during the course of AD (Quirion, 1993). Controversy persists over the changes in specific marker for cholinergic neurons – $p75^{NTR}$ with some research indicating increase of its level during aging and AD (Hu et al., 2002; Mufson and Kordower, 1992), while others suggesting its significant reduction (Salehi, 2000) or no difference in expression of $p75^{NTR}$ in the diseased brain (Ginsberg et al., 2006). I isolated rats' brains (Materials and Methods, Chapter 2.3.1.) and optimized antibodies dilution and protein load for the detection of ChAT, AChE, VaChT, $p75^{NTR}$ in BF area as well as [Beta III tubulin, CNPase (myelin associated enzyme), Snap25] that served as internal WB controls (Figure 21).

A

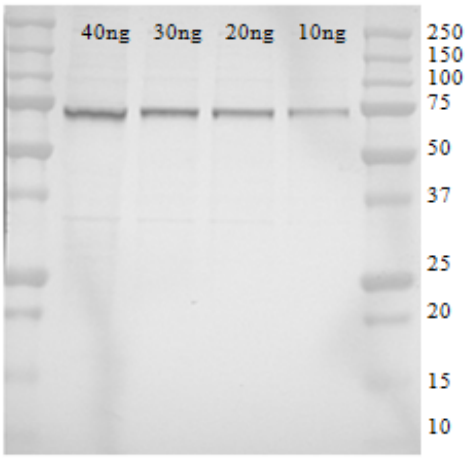

B

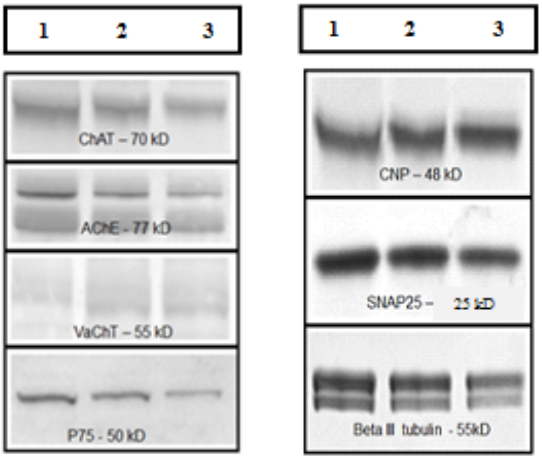

C

Cholinergic markers		
Cat no, Company	IgG name	Optimised dillution
AB144P, Millipore	Anti-ChAT	1:300
AB1588, Millipore	Anti-VaChT	1:1000
Sc-6432, Santa Cruz	Anti-AchE	1:300
07-476, Millipore	Anti-P75	1:500

D

Internal control proteins		
Cat no, Company	IgG name	Optimised dillution
C5922, Sigma	Anti-CNPase	1:1000
S9684, Sigma	Anti-SNAP-25	1:5000
T2200, Sigma	Anti-β III tubulin	1:3000

Figure 21. Optimized detection of cholinergic markers from rat brain. A. Example of ChAT detection from BF. Different protein loads are indicated. Molecular marker values (in kDa) are shown on the right side of WB. B. Detected bands for other proteins specific for BFCNs and internal controls. Lanes 1, 2, 3 reflect various protein loading (30, 20, 10 ng, respectively). C. Optimised antibodies dilution for the detection of cholinergic markers in BF by WB. D. Optimised antibodies dilution for detection of internal control proteins.

Molecular weights of these proteins were assigned using semi log plot (Gene Tool programme from SynGene) that compares sizes of the detected bands to the molecular marker (161-0373, BioRad) and automatically measures the intensity. These data were then exported to Excel for further analysis (Figure 22B).

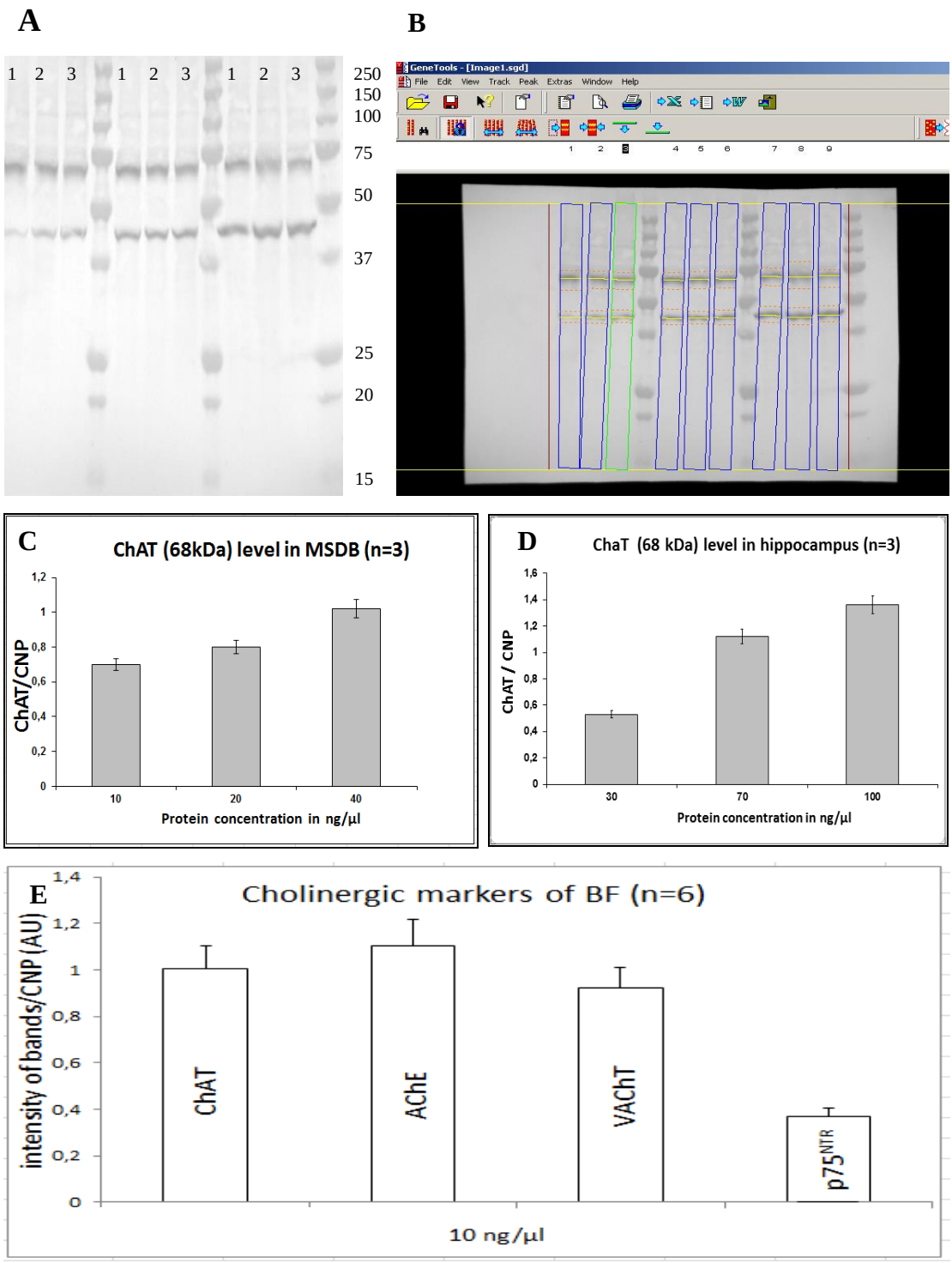

Figure 22. Quantitative analysis of cholinergic markers in BF. A. WB for ChAT/CNP. Lanes 1,2,3 show same protein load (20 ng) from BF of 3 rats. B. Example of semi log plot measurement in Gene Tool programme (Syn Gene). C. Quantification of ChAT level in MSDB. D. Quantification of ChAT level in hippocampus. E. Proportions of cholinergic markers in BF.

3.5. Chemical induction of AD in a rat model

Since Aβ is known to be neuro-toxic *in vitro*, it has been also applied *in vivo* by icv injections or local injections into defined brain structures (Chapter 2.8.). While the first approach has been used to study general effects, the second was utilized to determine Aβ effects on specific neuronal populations. Since the primary goal of this study was to obtain research platform to study AD, chemically-induced rat model was proposed. Local injections of oAβ preparation (Chapter 3.5.1.) to MS and its projecting areas: hippocampus (H) and prefrontal cortex (PC) were performed. The experiments were conducted according to the following plan (Table 5).

Place of injection	Concentration of oAβ (1-42) preparation (Chapter 3.4)	Number of rats	processing
Medial Septum	3 nmol	5	IC and WB
Hippocampus	3 nmol	3	WB
Lateral ventricle	3 nmol	3	WB
Lateral ventricle	6 nmol	5	IC and WB

Table 5. Experimental plan of Aβ chemical induction for rat model of AD.

All samples were analysed 2 weeks after icv injections. In all cases WB for ChAT versus control protein were performed (example Figure 23A and B) and analysed as previously described in (Materials and Methods, Chapter 2.3.2.). Bradford protein assay was conducted before loading of samples on polyacrylamide gel.

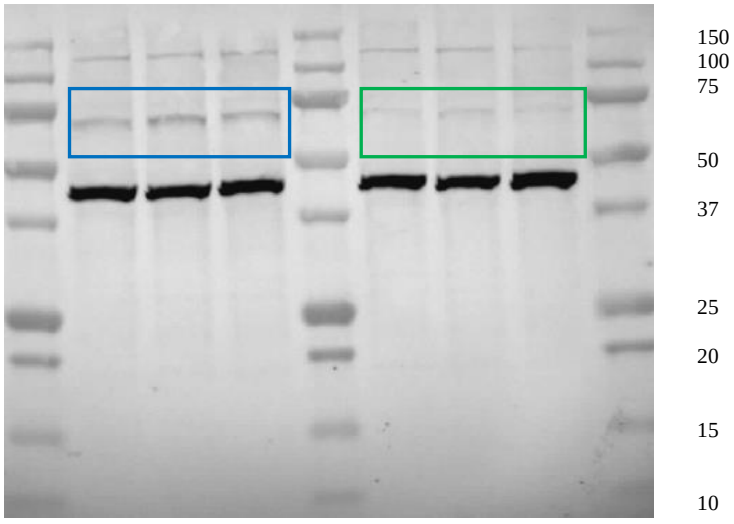

Figure 23. WB analysis of Aβ induced rat model of AD. Blue frame contains ChAT bands for saline injected rats while green frame include much weaker ChaT bands after oAβ injection. CNP (48 kDa) serves as internal WB control. Molecular weight of protein marker are given on the right side.

3.5.1. Preparation and analysis of Aβ oligomers for induction of AD in rat

Aβ oligomers (oAβ) were prepared from Aβ (1-42) peptide (73537, AnaSpec) according to the previously described methods (Dahlgren et al., 2002). Standard quality control analysis was performed with every new lot of this peptide. Samples were diluted in NuPage sample buffer and separated by SDS-PAGE on a 12% NuPage Bis-Tris gel (NP0342PK2 , Life Tech). Coomasie blue staining was used to visualize Aβ oligomers on the gels, which were scanned using imaging and analysis system G: BOX from SynGene and GeneTool programme (Figure 24).

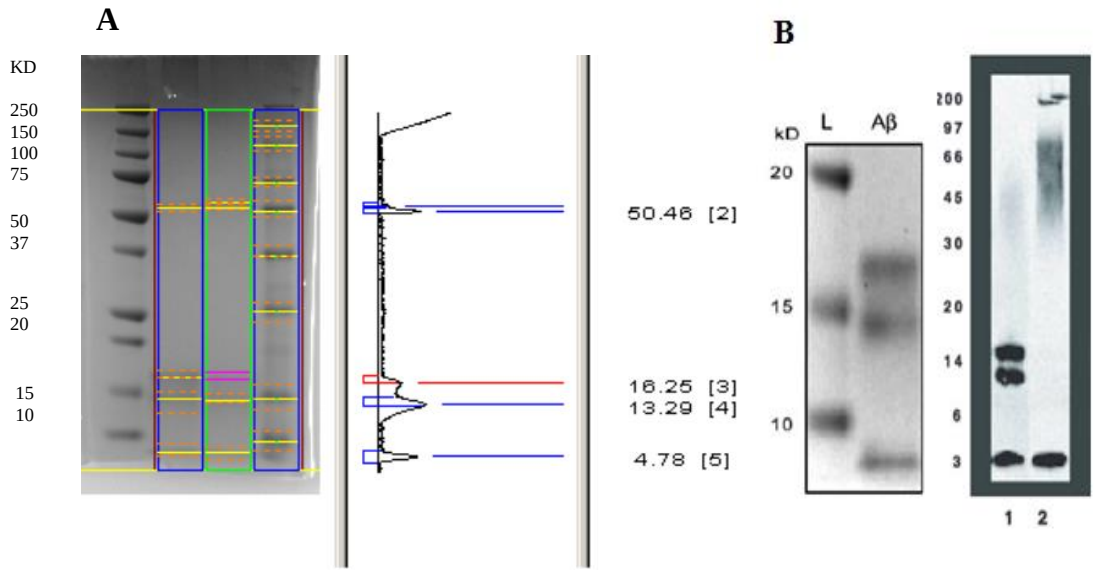

Figure 24. Quality control analysis of the created Aβ oligomers. A. Sizes of individual bands are assigned by semi-log plot in Gene Tool programme from SynGene compared to protein standard (Bio Rad). B. Enlarged area from picture A (left side), L-fragment of protein standard (BioRad), Aβ - oligomers experimentally achieved. The gel is compared to WB reported by Dahlgren et al., 2002 (right side) where lane 1 – shows Aβ oligomers, lane 2 -. Aβ fibrils separated by SDS-PAGE on a 12% NuPage Bis-Tris gel and probed with monoclonal antibody 6E10.

In this way, mix of Aβ peptides comparable to Aβ oligomers previously reported in literature has been achieved (Dahlgren et al., 2002). The aggregation state of Aβ peptides was crucial for further experiments in which these proteins were injected into the rat's brain or applied to primary BF cultures *in vitro.* Aβ oligomers are most neurotoxic variants (Walsh and Selkoe, 2007) correlating highly with hallmarks of AD (McLean et al., 1999). However, Aβ preparations may differ in stability, enrichment of different sized oligomers and most importantly reproducibility, despite using the consistent protocol. Therefore, each new batch of oAβ aggregates should be tested before an experimental application.

3.5.2. Reduction of cholinergic markers in septo-hippocampal pathway (SHP) and prefrontal cortex (PC) after injections of oAβ

Local icv injections of oAβ (prepared as in Chapter 3.5.1.) to MS and hippocampus (H) of wild type rats revealed reductions in ChAT protein level in all areas of cholinergic innervation that were subject to the study as compared to saline injected control rats (Figure 25A-F).

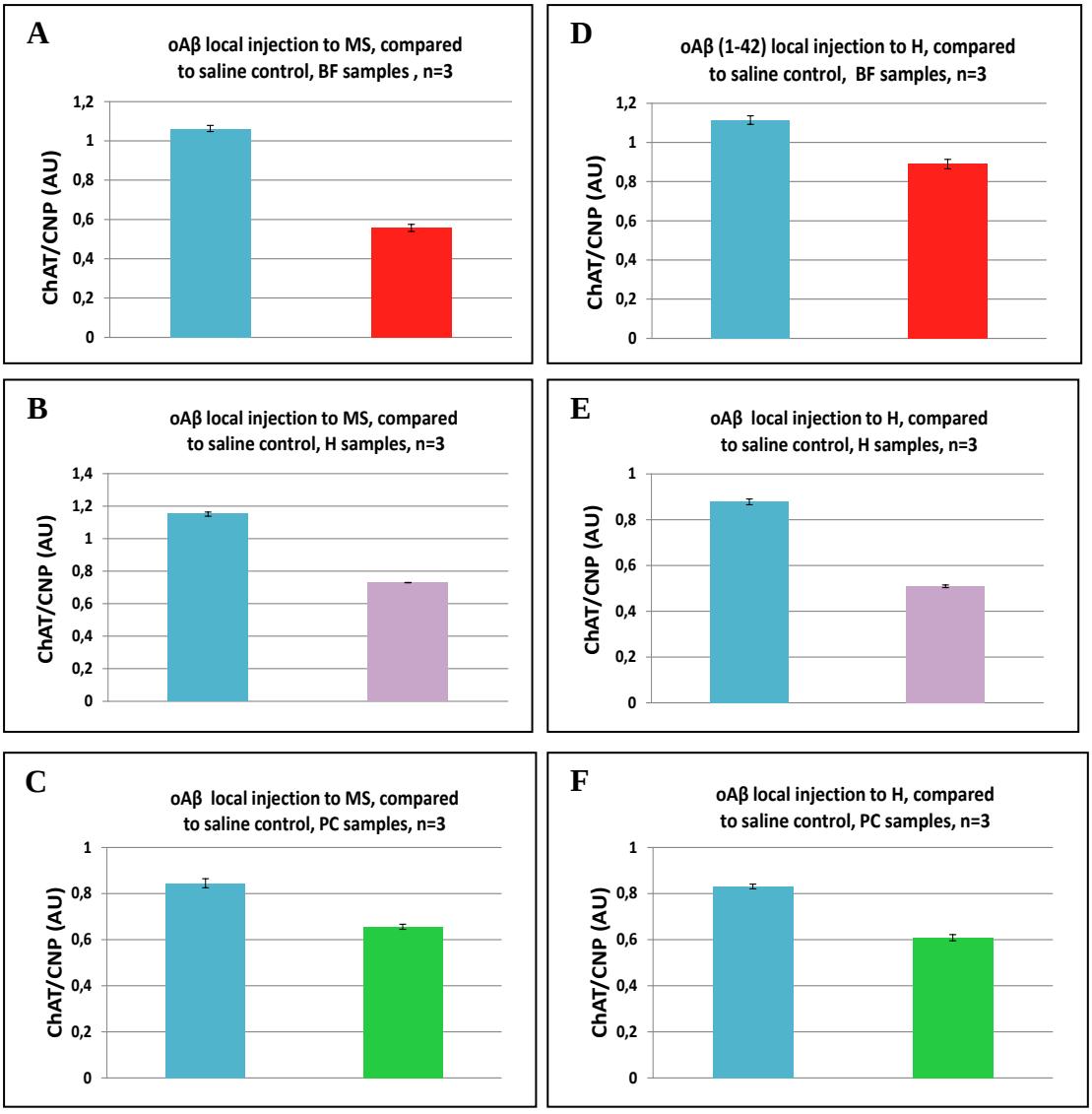

Figure 25. Reduction of ChAT level in SHP and PC after oAβ local injections (3 nmol) to MS and hippocampus as compared to saline injected controls. CNP serves as internal control of WB. Colour code: saline injected controls (blue), MS samples (red), H samples (violet), PC samples (green).

Local injection of oAβ mix to MS (3 µl, 0.1 mg/ml) show 47.58 % decrease of ChAT in BF samples (p=0.003) (Figure 25A), lowering ChAT up to 36.58 % and 22.38 % in hippocampus and prefrontal cortex (PC) areas (p=0.0008; p=0.02) (Figure 25B and C) as compared to controls. Same amount of oAβ mix injected to the

hippocampus revealed largest 42.04 % decline of ChAT in H samples (p=0.0006) (Figure 25E) while MS and PC tissue show smaller decrease of ChAT (20.16 % and 26.74 % respectively, p=0.04 and p=0.0004) (Figure 25D and F, respectively). The reductions of ChAT were also observed in MS, H and PC areas after injections of oAβ mix (3 µl, 0.1 mg/ml) into the lateral ventricle as compared to saline injected control rats (Figure 26A-C) with even bigger drop of ChAT achieved with repeated injections of oAβ mix to lateral ventricle (6 nmol in total) (Figure 26D-F).

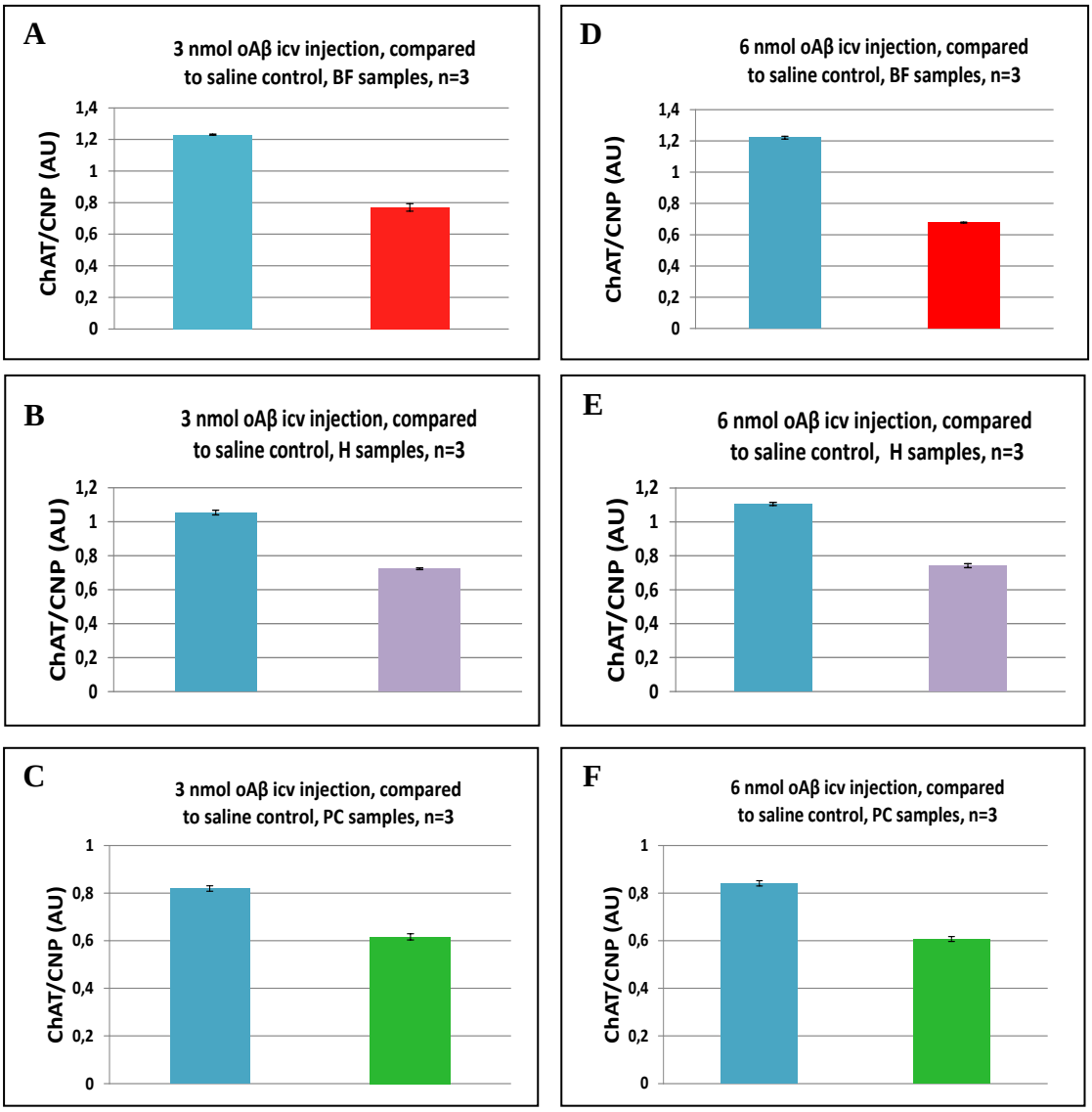

Figure 26. Reduction of ChAT level in SHP and PC after oAβ icv injections (3 nmol and 6 nmol) as compared to saline injected controls. CNP serves as internal control of WB. Colour code: saline injected control rats (blue), MS samples (red), H samples (violet), PC samples (green).

As illustrated in histograms significant loss of ChAT has occurred in BF tissue as compared to saline injected controls: 37.49 % (p=0.003) (Figure 26A), 31.36 % (p=0.0007) in hippocampus (Figure 26B) and 24.79 % (p=0.004) in PC (Figure 26 C). Loss of ChAT was increased with second injection of the same oAβ amount of (6

nmol in total) and caused 44.48% drop of ChAT in BF (p=0.0003) (Figure 26D); 36.56% fall in hippocampus (p=0.0006) (Figure 26E) and diminish ChAT protein in PC up to 27.83% (p=0.0004) (Figure 26F). Summary of the reduction in ChAT level induced by local and icv injections of oAβ mix are shown in the Table 6.

Injection place	BF samples	H samples	PC samples
local to MS	47.58 ± 0.93%	36.58 ± 0.58%	22.38 ± 0.5%
local to H	20.16 ± 0.59%	42.02 ± 0.15%	26.74 ±0.74%
Lateral ventricle	37.49 ± 1.75%	31.36 ± 0.4%	24.79 ± 0.56%
Lateral ventricle	44.48 ± 0.18%	36.56 ± 1.16%	27.83 ±0.23%

Table 6. Summary effect of local and icv injections of oAβ in different brain areas. The table include results shown as % drop in ChAT level versus saline injected controls.

Overall, these results suggest that rats, subjected to oAβ injections suffered from progressive cholinergic dysfunction making this model useful for evaluating the effects of the integrity of cholinergic innervations under the deposition of Aβ in AD.

3.5.3. Non significant cholinergic cell loss in oAβ induced AD model

Despite the considerable reductions in ChAT level throughout the brain, the number of cholinergic neurons in MSDB area did not change significantly (p=0.97), 2 weeks post oAβ icv injections (Figure 27B) as compared to saline injected control rats (Figure 27A) (n=3 rats for each group). However, the decrease in cell number was observed as damage of 13.5% of cholinergic neuronal population (stained with anti-ChAT IgG) while sparing GABAergic neuronal population (labelled with anti-parvalbumin IgG). Saline control injections has confirmed that cholinergic cell loss was specific to oAβ not to the transitory injuries.

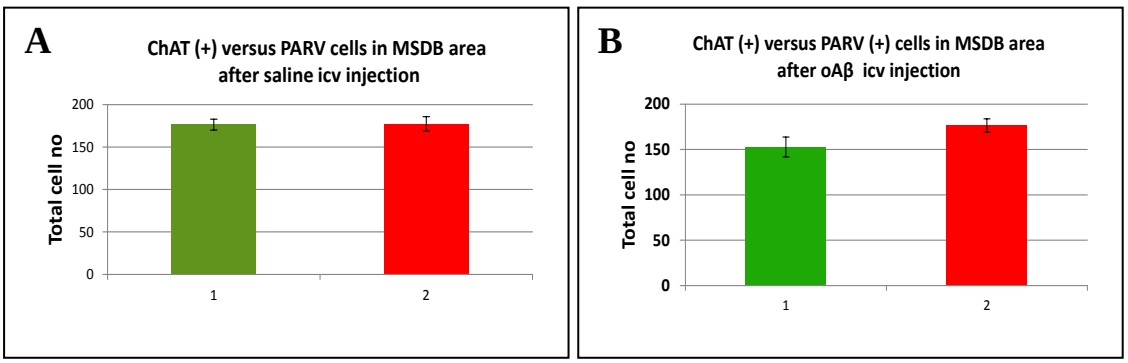

Figure 27. Loss of cholinergic neurons in MSDB area in chemically-induced rat AD model. A. Number of ChAT (green bars) and parvalbumin (red bars) positive cells after saline icv injection that served as control for this experiment. B. ChAT and parvalbumin cell number after oAβ icv (3 nmol).

3.5.4. Oligomeric Aβ damaged cholinergic synapses in the rat AD model

Synaptic plasticity is crucial for the process of learning and memory formation, with synaptotoxicity involved in the early stages of AD. The number of damaged synapses correlates better with the level of memory impairment in AD patients as compared to the number of senile plaques or NFTs (Introduction Chapter, 1.4). Therefore, the density of cholinergic synapse was estimated in brain slices of Aβ-induced AD model (Chapter 3.5.3.) with use of vesicular acetylcholine transporter (VAChT) immunostaining (Figure 28A and B). VAChT is a transmembrane protein associated with synaptic vesicles in the cholinergic nerve terminals and responsible for the refilling of ACh in synaptic vesicles, making it available for synaptic release. This process is driven by proton exchange mechanism whereby 2 protons (transported into the vesicle from the cytoplasm by vacuolar ATPase) are exchanged for one molecule of acetylcholine and it is coupled to VAChT mediated transport of ACh into the synaptic vesicles located in the terminals (Roghani et al., 1994). In the present study the density of cholinergic terminals was measured in CA1, CA3 and DG of hippocampus and compared to saline injected controls (n=3 rats per each group).

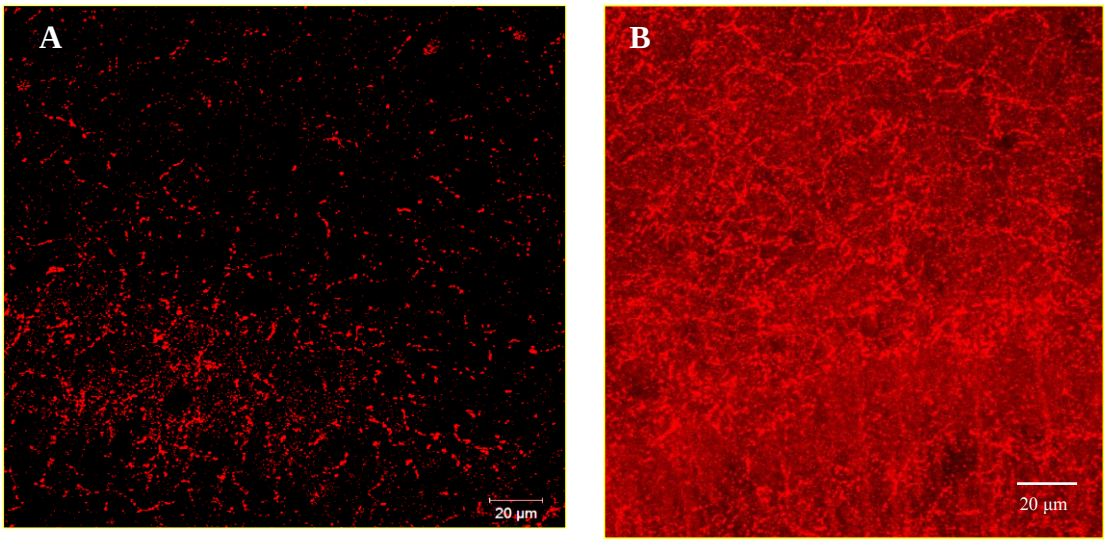

Figure 28. VAChT immunocytochemistry on hippocampal slices (example). A. Punctate staining of cholinergic synapses visualised with anti-VAChT IgG (AB1588 Millipore, 1:500) and developed with goat anti guinea pig Alexa 594 IgG (A-11076, LifeTech.1:1000). B 3D image of staining hippocampal slice with VAChT.

The highest density of VaChT positive fibers was found in CA3/DG of controlled rats, which is in line with literature (Aznavour et al., 2002). The effect of 3 nmol Aβ icv injection on VaChT fibers in various hippocampal regions is illustrated below (Figure 29) .

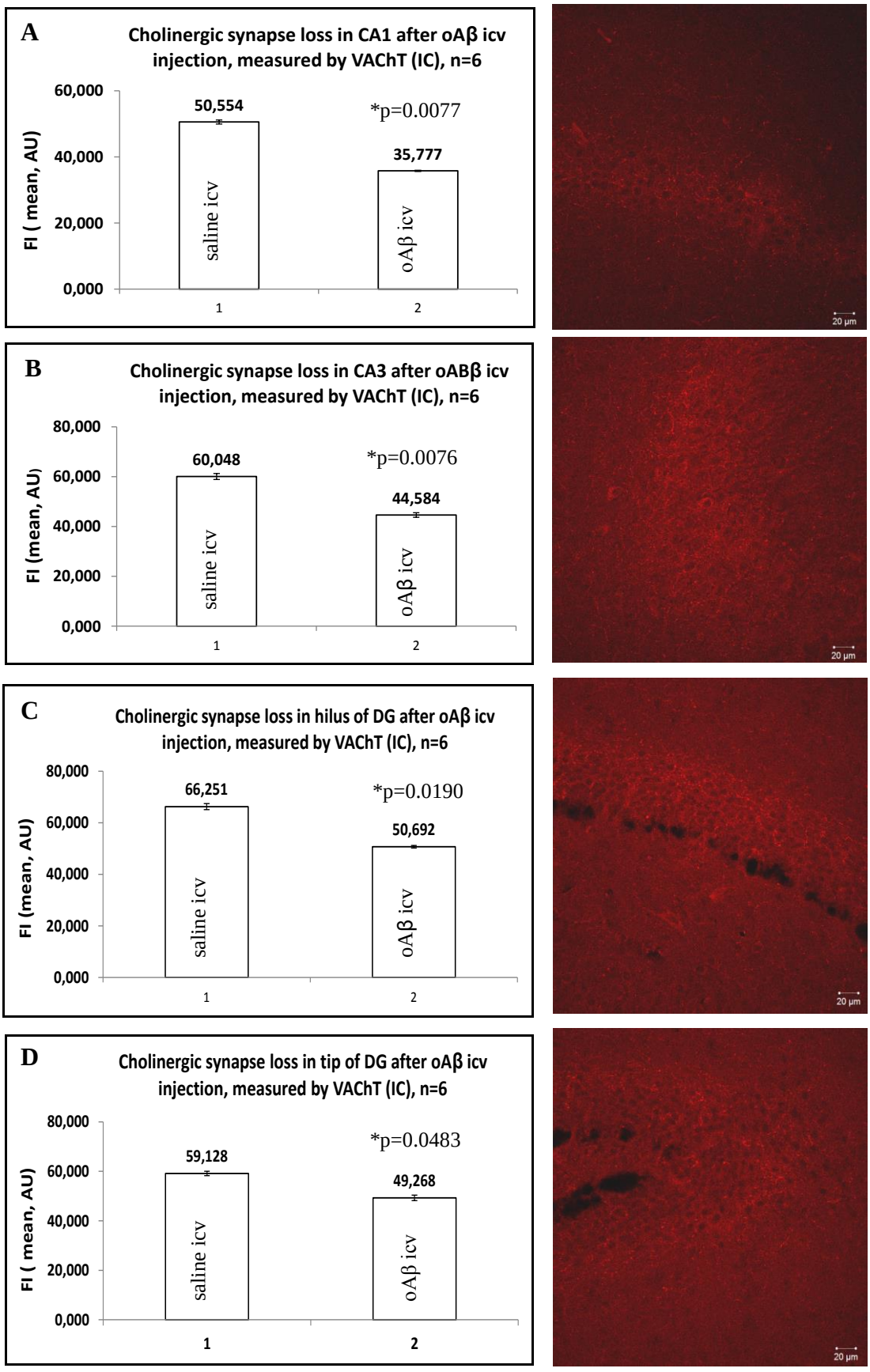

Figure 29. Quantification of cholinergic synapse loss in hippocampal formation after oAβ icv injection. A. 29.23 % loss of cholinergic fibers in CA1 area. B. 25.75% drop in cholinergic fibers density of CA3 area. C. 25.75% damage of cholinergic innervation in hilus of DG. D.16.68 % fall of VAChT staining in the tip of DG. All values are compared to saline injected rats. (n=6 represent number of brain slices in which the synapse density was measured, averaged from 3 different rats)

The loss of cholinergic synapse was significant already after 3 nmol of oAβ icv injection as revealed by VAChT immuno-cytochemistry with comparable p values = 0.008 in CA1 and CA3 areas giving 29.23 % and 25.75 % of cholinergic fibers loss (Figures 29A, B) respectively. The other significant values were achieved in hillus and tip of DG (p=0.02; p=0.05, respectively), corresponding to 25.75% and 16.68% loss of cholinergic fibers in these areas (Figures 29C, D).

3.5.5. Distribution of HiLyte Fluor 488 labelled Aβ (1-42) signal in the forebrain after icv injections

Aβ (1-42) is known to be the most toxic fragment of peptides generated from APP cleavage (Introduction Chapter, 1.5.1.1.). I monitored the spread of HiLyte Fluor 488 labelled Aβ (1-42) (Materials and Methods, 2.1.5.1.) after bilateral icv injections of 2-5 µl (1mg/ml) into the rat brain.

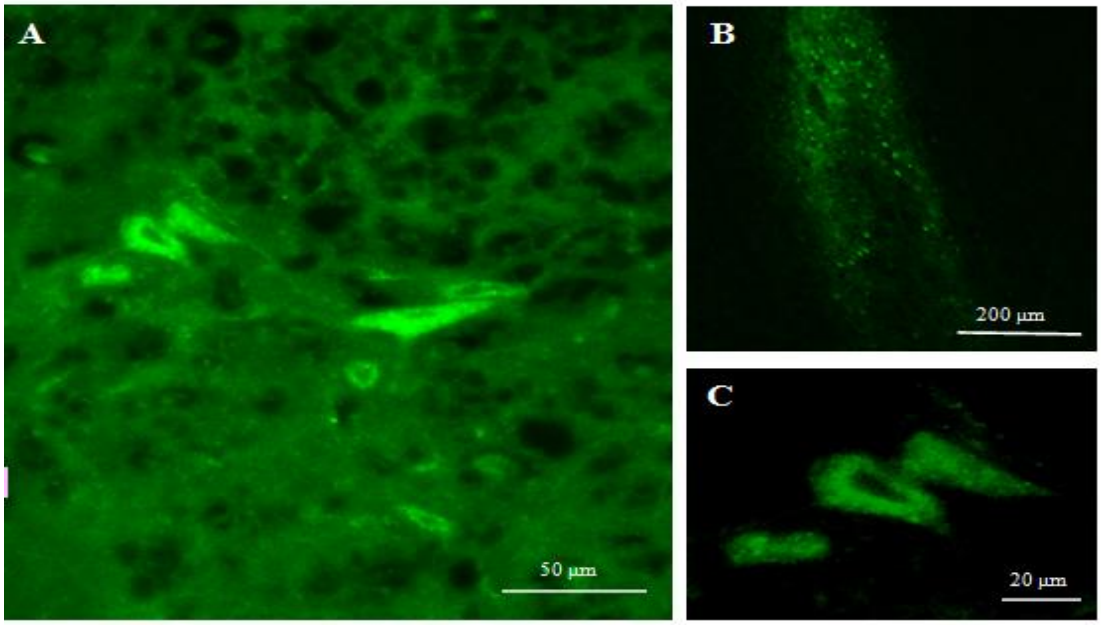

Figure 30. The effect of bilateral Alexa 488 Aβ (1-42) icv injection. A. Signal observed in ventral pallidum. B. Needle track. C. enlarged image of cell stained with Aβ (1-42) labelled with Alexa 488.

The bulk of the signal was observed in the ventral pallidum that lies within the substantia innominata of BF (Introduction Chapter, 1.5.3.1.) and receives efferent connections from the ventral striatum (the nucleus accumbens and the olfactory tubercle). It projects to the dorso-medial nucleus of the dorsal thalamus, which, in turn, projects to the prefrontal cortex. It also projects to the pedunculopontine nucleus and tegmental motor areas.

3.5.6. Selective loss of MSDB neurons after lesion with 192-IgG-SAP

192-IgG-SAP provided more specific cholinergic lesions in BF than oAβ. This immunotoxin consists of the monoclonal antibody 192 IgG coupled through disulphide-bond to saporine, the ribosome-inactivating protein derived from the plant *Saponaria officinalis*. The antibody component is directed against rat low-affinity $p75^{NTR}$, which ensures the specificity of this toxin to cholinergic cells (Book et al., 1994; Schliebs et al., 1996). Following receptor binding and internalization, saporin enzymatically inactivates the large ribosomal subunit, blocking protein synthesis and ultimately resulting in cell death. The irreversible neurodegenerative process can be considered as completed in about 2 weeks. Therefore I injected 2.5 µg /ml of 192-IgG-SAP into the lateral ventricle of 21 days old rats (stereotactic coordinates: AP = -0.8 mm, ML = 1.0 mm, DV = 2.5 mm) and perfused them 2 weeks post-injection. The brains were processed with anti-ChAT-HRP staining (Materials and Methods Chapter 2.1.6.) and cell number counted versus age-matched controls (Figure 31).

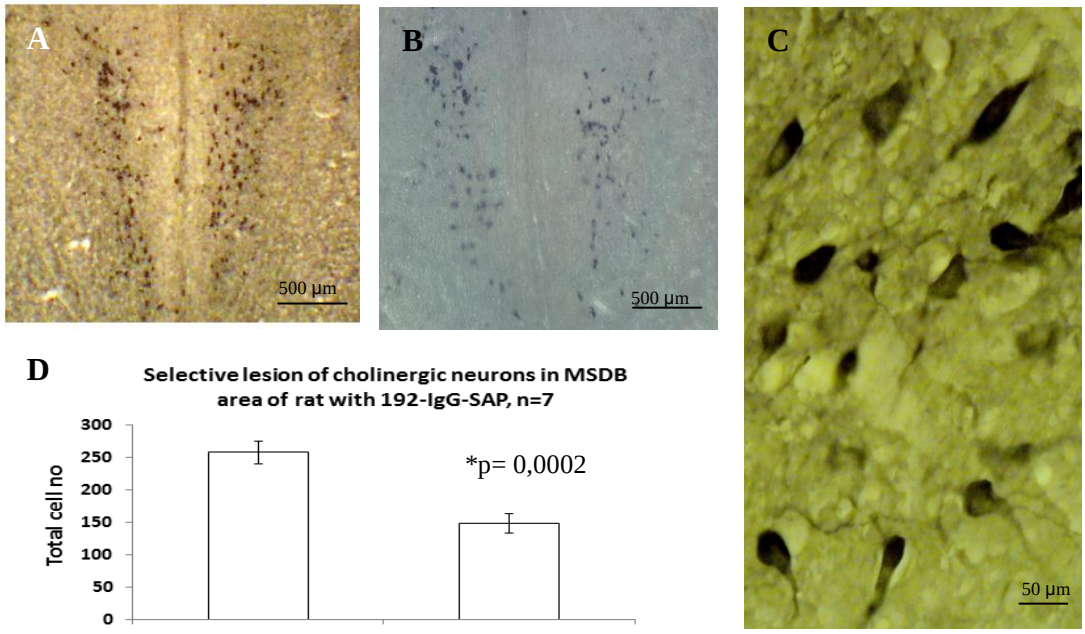

Figure 31. The effect of 192-IgG-SAP lesion on BFCNs in MSDB area. A. MS area of BF stained with anti-ChAT IgG developed with HRP (control rat). B. Same area after 2 weeks from 192-IgG-SAP injection. C. Enlarged cholinergic cells stained with ChAT-HRP. D. Plot of cholinergic cell number neurons before and after icv injection of 192-IgG-SAP.

Significant loss of cholinergic cells expressing $p75^{NTR}$ ($p=0.0002$) corresponding to 57.78% was observed in MSDB area in rat. This is in agreement with previously reported data (Schliebs et al., 1996; Szigeti et al., 2013), thus providing very robust and reproducible rat model of AD that is quite quick to achieve.

3.5.6.1. 192-IgG-SAP lesion of cholinergic neurons increases Aβ (1-42) load in cortex and hippocampus

Lesion of cholinergic neurons was performed with 192-IgG-SAP as previously described in Chapter 3.5.6. Two weeks after the injection, the experimental and control samples (from saline injected rats) were collected and checked for the presence of cholinergic cells in MSDB area with anti-ChAT staining Materials and Methods, Chapter 2.1.6.) (Figure 32A and B). Same slices were then stained with anti-Aβ IgG (55922, AnaSpec), which is able to label core of amyloid plaques and diffused Aβ (1-42). The results show presence of astrocyte-shaped cells in the cortex (Figure 32D) as compared with saline injected controls (Figure 32C).

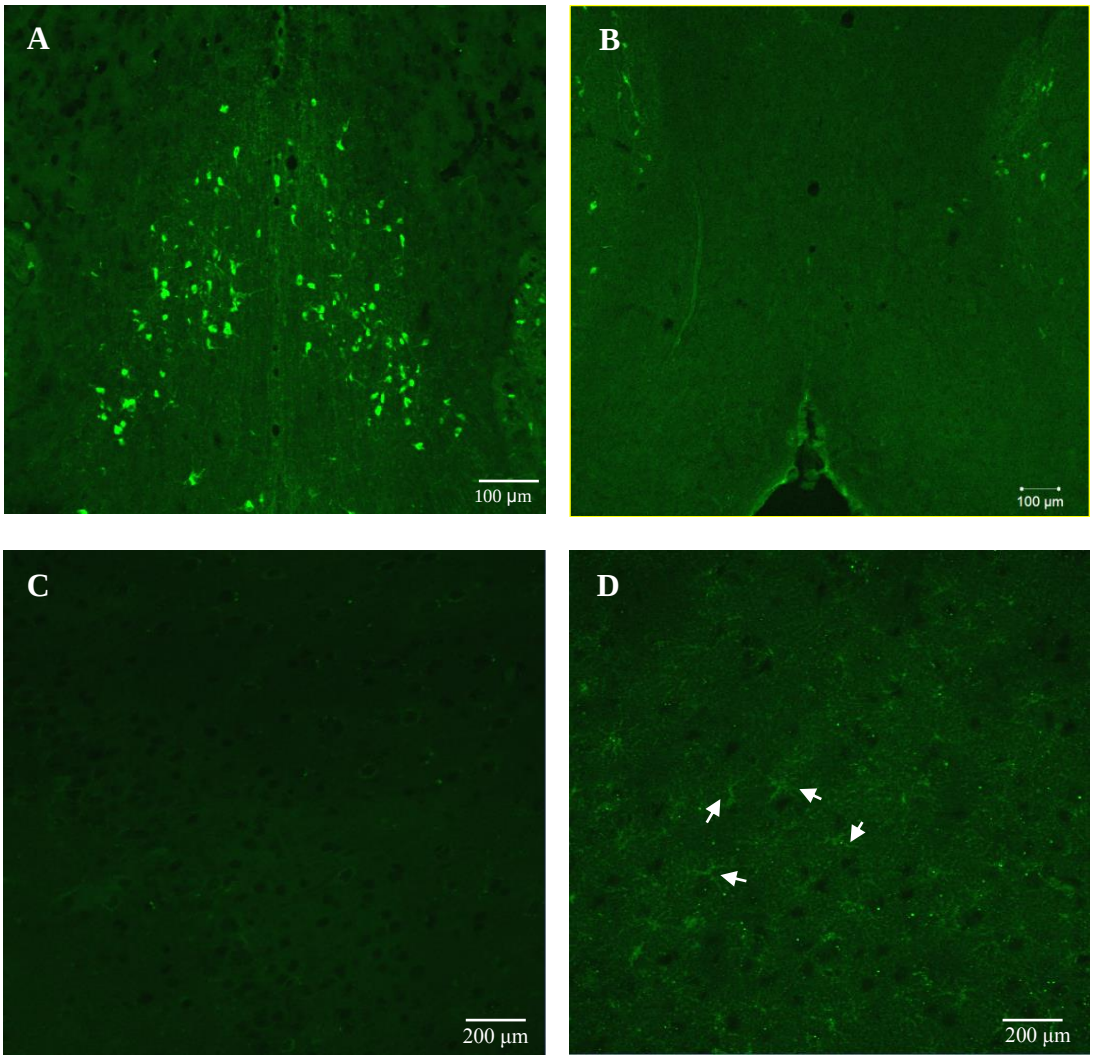

Figure 32. Lesion of cholinergic neurons increase Aβ (1-42) load in cerebral cortex. A. MSDB area of BF with cholinergic cell bodies labeled with ChAT (control rat). B. ChAT staining of MSDB area 2 weeks after 192-IgG-SAP icv injection. C. Immuno-histochemistry for Aβ (1-42) in the cortex 2 weeks after saline icv injections. D. The effect of 192-IgG-SAP icv injections on Aβ (1-42) load after 2 weeks. Arrow heads point to astrocyte-shaped cells.

Similar changes were observed 2 weeks after 192-IgG-SAP icv injections (2.5 μg/μl) in all hippocampal regions (Figure 33B, D) as compared to saline icv injected control rats (Figure 33A, C). Interestingly, on enlarged photos of hippocampal areas, Aβ (1-42) staining was visible in neurons of saline injected rats (Figure 33E) or astrocyte-shaped cells of 192-IgG-SAP injected rats (Figure 33F).

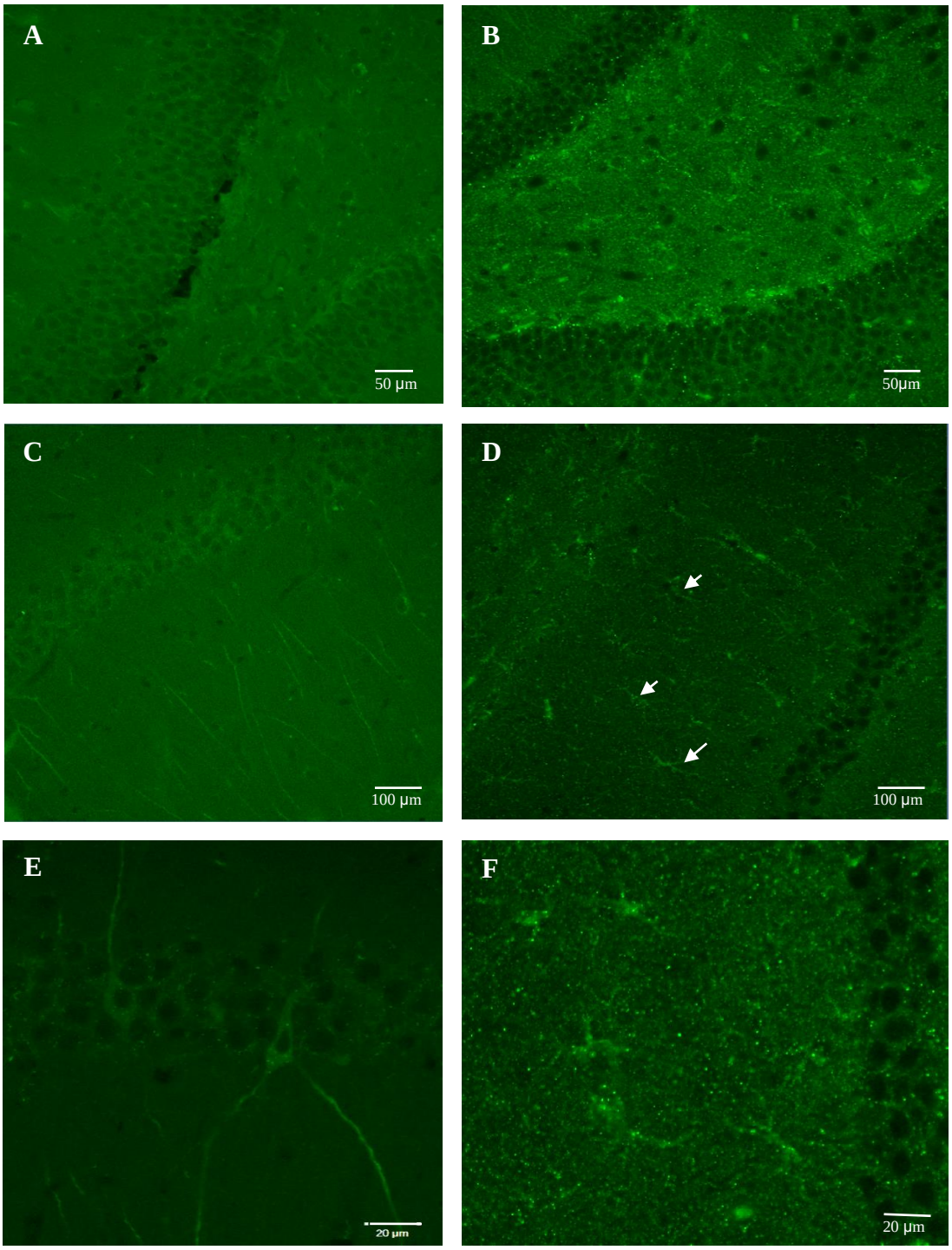

Figure 33. Lesion of cholinergic neurons increase Aβ (1-42) load in hippocampus. A. Aβ (1-42) IC of DG (saline injected rats). B. Aβ (1-42) IC of DG (192-IgG-SAP injected rats). C. CA1 stained with Aβ (1-42) in saline injected rats compared to same area in 192-IgG-SAP injected rats in D. Arrows point to astrocyte-shaped cells. E. Closer view on neurons (CA2) in control samples versus astrocyte –shaped cells in experimental samples F.

3.6. Discussion of the results achieved with AD rat models

The cholinergic system of rat BF was used as a model for the homologous region in humans. The structures involved in learning and memory were distinguished (Chapter 3.2.) and stayed in agreement with previously published literature. This part of the brain is highly susceptible to neuropathological changes occurring in AD (reviewed in Chapter 1.4.). Immuno-histochemical techniques were implemented in the first part of this study to visualize and count neurons of rat BF. BFCNs were marked with anti-ChAT antibodies and coronal forebrain sections containing MS and DBB were imaged. In line with published literature ChAT positive cells occupied lateral areas of MS, while in DBB resided predominantly in the medioventral portions. Labelling of cholinergic neurons was confirmed with 192-IgG-Cy3 antibody characterised in Chapter 2.1.5.1. However, not all cholinergic cells were stained for both markers (ChAT and $p75^{NTR}$). 192-IgG-Cy3 did not label all ChAT positive profiles in caudal nuclei of BF due to the fact that not all cholinergic neurons there express $p75^{NTR}$, which agrees with the previous data (Ferreira et al., 2001). To distinguish cholinergic from non-cholinergic cells, the latter were stained with calbidin or anti-parvalbumin antibody and show similar profiles to the already reported in literature. Results of these stainings were acknowledge in publication (Ovsepian et al., 2012). Cholinergic and non-cholinergic neurons were counted in healthy rats. The aim of these experiments were to establish a reference point of cholinergic cell loss for further induction of AD model in rats. Cholinergic cells are susceptible to damage during neuropathological changes occurring in AD (reviewed in Chapter 1.4. and 1.5.3.), while non-cholinergic neurons remain more resistant to the disease processes (Solodkin, 1996). Similarly, the level of key cholinergic markers was measured (Chapter 3.4). Same experiments were conducted for rats icv injected with Aβ oligomers (prepared as in Chapter 3.5.1.) in chemically-induced AD rat model. Aβ is believed to be a primary factor in the pathogenic pathway leading to AD, according to the amyloid cascade hypothesis (reviewed in Chapter 1.5.1.). Decrease in ChAT-protein in septo-hippocampal pathway as well as in prefrontal cortex was confirmed in this model (Chapter 3.5.2.). However, the reduction of ChAT protein was not reflected by the cholinergic cell bodies loss in MSDB areas. These data although seem to be conflicting, remain in agreement with previous research suggesting that senile impairment of the cholinergic system in rats manifests

in decrease of ChAT-protein expression (perhaps due to loss of cholinergic synapses and axons in the cerebral cortex) rather than an acute degeneration of neuronal cell bodies (Niewiadomska et al., 2000). This also confirm that loss of neurons happens in later stages of the disease, which is in line with the previous literature (Glimor et al., 1999; Schliebs and Arendt, 2006). Thus injections of oAβ into the lateral ventricle confirmed the induction of early AD model in rats as they caused significant cholinergic synapse loss in BF, prefrontal cortex and hippocampus, visualised by VAChT immuno-histochemistry of hippocampal area (Chapter 3.5.4.). Cholinergic synapse loss is known to correlate best with the severity of dementia (DeKosky and Scheff, 1990) thus making this model highly valuable for further applications.

In regards to the local injections of oAβ to MS and hippocampus these resulted in more profound decline in ChAT protein level in the injected areas, with the diffusing effect along nerve terminals. These seem to be similar to the effects of oAβ seeding and spread of misfolded protein (Harper and Lansbury, 1997; Kane et al., 2000; Riddley et al., 2006; Rosen et al., 2012). However, although very interesting, this results were not exploited in further details in terms of cell or synapse counts in the affected structures, due to time limitation.

Cholinergic cell bodies were completely abolished within 2 weeks post injection of 192-IgG-SAP directed specifically towards $p75^{NTR}$, selectively expressed by BFCNs (Chapter 3.5.6.). Interestingly, this model stained with anti-Aβ (1-42) IgG showed an increase in the deposition of Aβ (1-42) in cortex and hippocampal areas, with Aβ staining seen mainly in astrocyte-shaped cells (Chapter 3.5.6.1.). Interestingly, the increased number of astrocytes and microglia was also observed in demented individuals with AD as compared to controls (Perez-Nievas et al., 2013), however, whether or not astrocyte activation substantially contributes to structural damage and impaired cognition in AD remains unknown. This result however stays in agreement with recent *in vivo* work on transgenic mice, similarly lysed with cholinergic immunotoxin mu-p75-saporin. These show the increase in number of amyloid plaque load in hippocampus and prefrontal cortex as well as elevated levels of tau and phospho-tau (Laursen et al., 2013; Härtig et al., 2014). Deposition of Aβ around cerebral blood vessels after lesion of cholinergic neurons with anti-p75 IgG conjugated with saporin was also found in the earlier studies in rabbits (Roher et al., 2000). In humans, AD brain autopsies also support topographic overlap between the

areas undergoing extensive loss of cholinergic projections and those with Aβ load (Davies and Maloney, 1976; Geula et al., 1998).

The depositions of Aβ after cholinergic cells loss suggest a new role of BF cholinergic system in Aβ clerance, beyond normal function of BFCNs for ACh supply to the targeted brain areas (reviewed in Chapter 1.5.3.2.). This idea was also discussed I the recent publication (Ovsepian et al., 2016).

Additional icv injections of HiLyte Fluor Alexa 488 Aβ (1-42) were performed to verify this process (Chapter 3.5.5.). Quite unexpectedly the injected amount of HiLyte Fluor Alexa 488 Aβ (1-42) did not show labelling of MSDB area (Chapter 3.5.5.). The signal was visible instead in other BF regions e.g. ventral pallidum. This result can be interpreted in favour of the above hypothesis suggesting the preferential role of neurons in Ch1-Ch3 areas for Aβ clearance (Chapter 1.5.3.1.). These cells are known to be enriched in $p75^{NTR}$. However, binding of Aβ (1-42) can also possibly occur by other multiple receptors suggested by the literature e.g. metabotropic glutamate, nicotinic, muscarinic, insulin growth factor receptors (Patel and Jhamandas, 2012). Therefore further research is needed to decipher the mechanisms that underlie possible Aβ clearance by BF cholinergic cells. These mechanism may also explain high vulnerability of cholinergic system to deleterious Aβ effects in AD.

Mu p75-saporin Tg2576 mice model was recently proposed as a new tool to study the interrelations between cholinergic deficits and Aβ burden (Gil-Bea et al., 2012, Laursen et al., 2014). However this model still does not allow to find out the role of $p75^{NTR}$ in possible Aβ clearance by BFCNs as saporin damage completely cholinergic cells through their ribosomal inactivation. Therefore other models with partial or complete knock-down of $p75^{NTR}$ are needed to decipher the involvement of this receptor in Aβ clearance. Such models were already used to show changes in the number of cholinergic neurons not Aβ load (Naumann et al., 2002). Later studies with use of APPSwe/PS1dE9/$p75^{NTR/ExonIII-/-}$ mice implicated $p75^{NTR}$ in the regulation of Aβ deposition by increased production and inhibited aggregation of this peptide by $p75^{NTR}$ extracellular domain (Wang et al., 2011). This study is the most supportive so far for establishing the new role of $p75^{NTR}$ in Aβ clearance from brain. Interestingly, although these triple transgenic mice revealed the extensive Aβ depositions in the hippocampus and cerebral cortex they did not show memory deficits, which supports dissociation of cognitive functions from amyloid load.

Chapter IV. New role of P75^{NTR} in homeostasis and clearance of Aβ - results with discussion

4.1. The p75^{NTR} system in AD

The role of mature p75^{NTR} in adult brain remains controversial especially in BF that is one of the region most vulnerable to AD (McKinney and Jacksonville, 2005). As mentioned in introduction (Chapter 1.5.3.2.1.) p75^{NTR} has number of functions, depending on ligands it binds to. Except that, studies of p75^{NTR} knock-out mice with the truncated insertion in the exon 3 or 4 of p75^{NTR,} coding extracellular domain of this receptor, revealed an increase in number of ChAT positive neurons including septo-hippocampal pathway (Naumann et al., 2002), suggesting apoptotic role of p75^{NTR} in basal forebrain. However, recent studies implicate that p75^{NTR} has broad non-apoptotic anti-neurotrophic actions in BF that are more extensive than induction of apoptosis and do not support apoptotic role of p75^{NTR} (Greferath et al., 2011). The role of p75^{NTR} in AD remains unexplored despite many therapies boosting cholinergic system of BF (Chapter 1.6.).

Binding of Aβ to p75^{NTR} is believed to be the most relevant feature of p75^{NTR} to AD. High affinity binding of Aβ to p75^{NTR} was initially reported by Yaar (Yaar et al., 1997) in immuno-precipitation experiments using cortical neurons and NIH-3T3 cell line, stably expressing p75^{NTR}. Subsequent studies suggested a role of p75^{NTR} in Aβ-induced neurodegeneration in human neuroblastoma cells (Kuner et al., 1998) and hippocampal neurons (Sotthibundhu et al., 2008). However, how exactly Aβ causes degeneration of neurons and if it directly inhibits neurotransmission or indirectly alters synaptic activity remains unknown (Coulson et al., 2006).

P75^{NTR} is widely expressed during development and gradually switched off in adulthood. However, upon several types of injury and cellular stress, including AD, p75^{NTR} is thought to be re-expressed. Quantitative analysis revealed unchanged level of p75^{NTR} during early and moderate stages of AD (Ginsberg et al., 2006) while reduction in the expression of TrkA and down regulation of TrkB and TrkC were significant. The level of p75^{NTR} increases whereas TrkA decreases in aging (Costantini et al., 2005). This elevated expression of p75^{NTR} increases the binding of Aβ to p75^{NTR}. Currently research of P75^{NTR} and Aβ interaction and accumulation of toxic species are key interest in the field (Jian et al., 2016).

The aim of this chapter is to analyse the mechanisms that govern the endocytosis and transport of IgG-Cy3 labelled p75^{NTR} as well as internalization of this receptor with Alexa 488 labelled Aβ 1-42 in cholinergic neurons of primary BF cultures.

4.2.3. Characteristics of BF cultured cells

The quality of neuronal cultures was assessed by light microscopy (Nikon Eclipse TS 100) utilizing the differential interference contrast (DIC) optics (Figure 34A and B) and also with the use of laser scanning microscope LSM 710, Carl Zeiss.

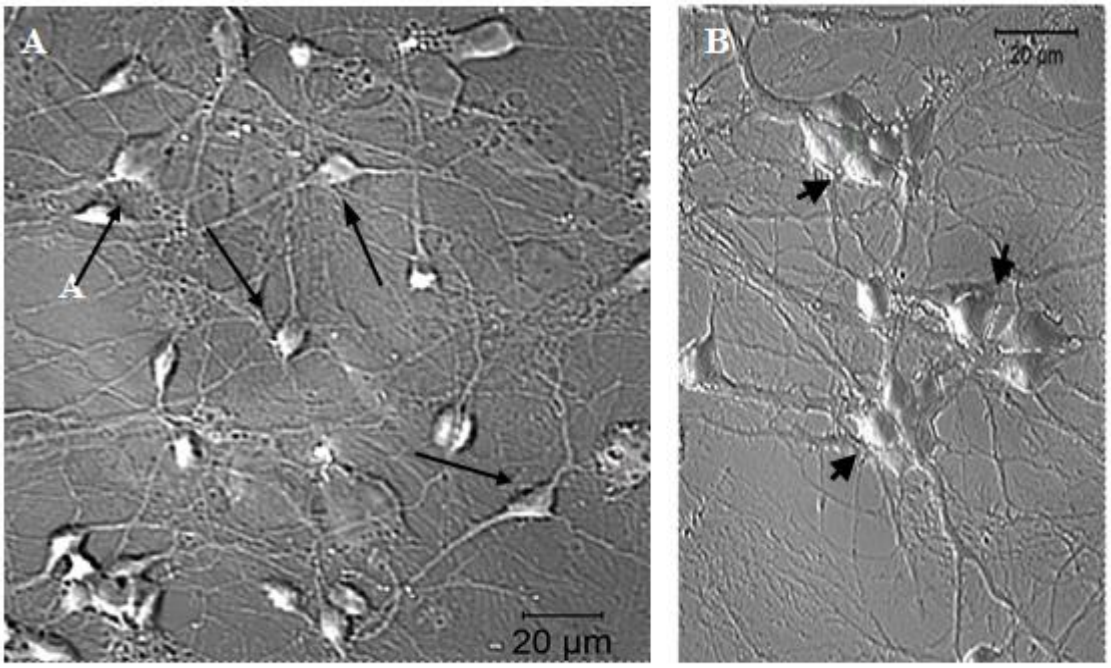

Figure 34. DIC of 6 day old BF culture. A. Arrows point to BF neurons (culture density 0.7 x 10^6 over 35 mm dish). B. Arrow heads point to cells clusters (culture density 1.2 x 10^6 over 35 mm dish).

Healthy growth of BF neurons was critically dependent on cell density and the absence of non-neuronal cells. Therefore, each time before plating the number of live neurons was counted with tryptan blue in a haemocytometer. Optimal growth of BF cells was achieved with 0.5 – 1x10^6 plating density (9.62 cm^2/35 mm dish) (Figure 34A). Cell clusters negatively-influenced longevity of the BF culture [e.g. clusters, 1.2 x 10^6 plating density (9.62 cm^2/35 mm dish)] (Figure 34B).

Relatively pure cultures of BF neurons were obtained with the inclusion of 10 µM (final concentration) cytosine-β-D-arabinofuranoside (AraC) - applied to the cultures on the second day after plating; this reduced proliferation of non-neuronal cell types such as glia and macrophages (Figure 35B), facilitating more direct influence of experimental compounds on neurons. Serum-free medium provided precisely-defined experimental conditions eliminating unknown components which are usually introduced through FBS.

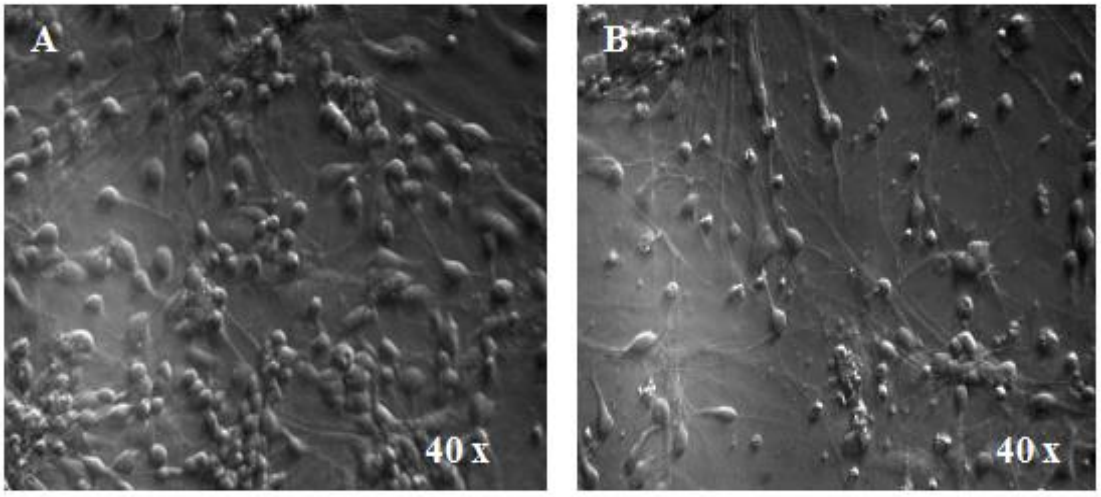

Figure 35. The effect of AraC treatment on cultured BF neurons. A. BF culture 48h after plating whithout AraC. B. Same culture 72 h post plating – after AraC treatment.

The development of neuronal cultures was regularly monitored and half of the growth medium was changed every 3-5 days to maintain the neuronal health and overall good culture quality (Figure 36). Maintenance of BF cultures was dependent on vitamins and supplements. The presence of NGF was crucial for the growth and differentiation of cholinergic cells. The concentrations of NGF were optimized 50 and 200 ng/ml for 2.5S and 7S units, respectively.

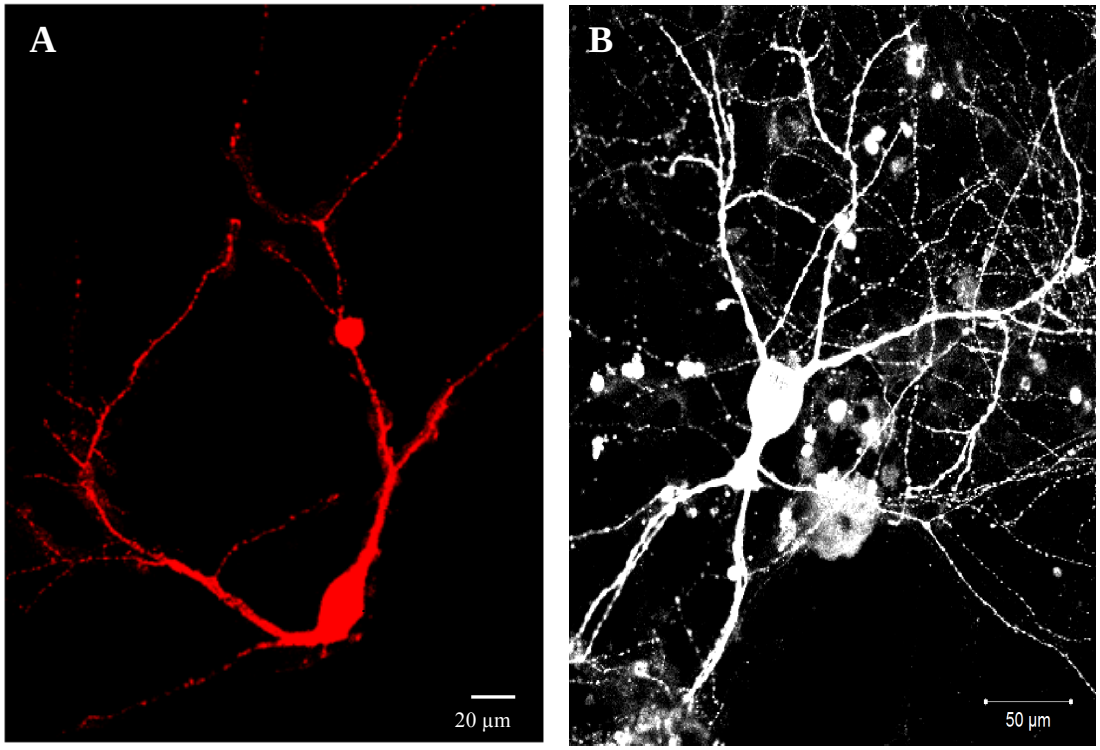

Figure 36. Development of cholinergic phenotype in BF culture. A. Cholinergic neuron p14 stained with 9.4 nM 192-IgG-Cy3 (red). B. DIC image of cholinergic neuron p21.

4.2.4. Viability of primary BF cultures

The viability assay was performed on BF cultures with use of Nuclear-ID™ Blue/Green cell viability reagent (53004-C100, Enzo Life Sciences). This compound is a mixture of blue and green fluorescent nucleic acid dye suitable for staining live and dead cells, respectively. The amount of cell-permeable (blue) and cell-impermeable (green) signals were counted with use of use of Photoshop CS4 v11 at 24h, 48h, p7 and p14 time points and analysed with Excel software (Figure 37A, B).

.

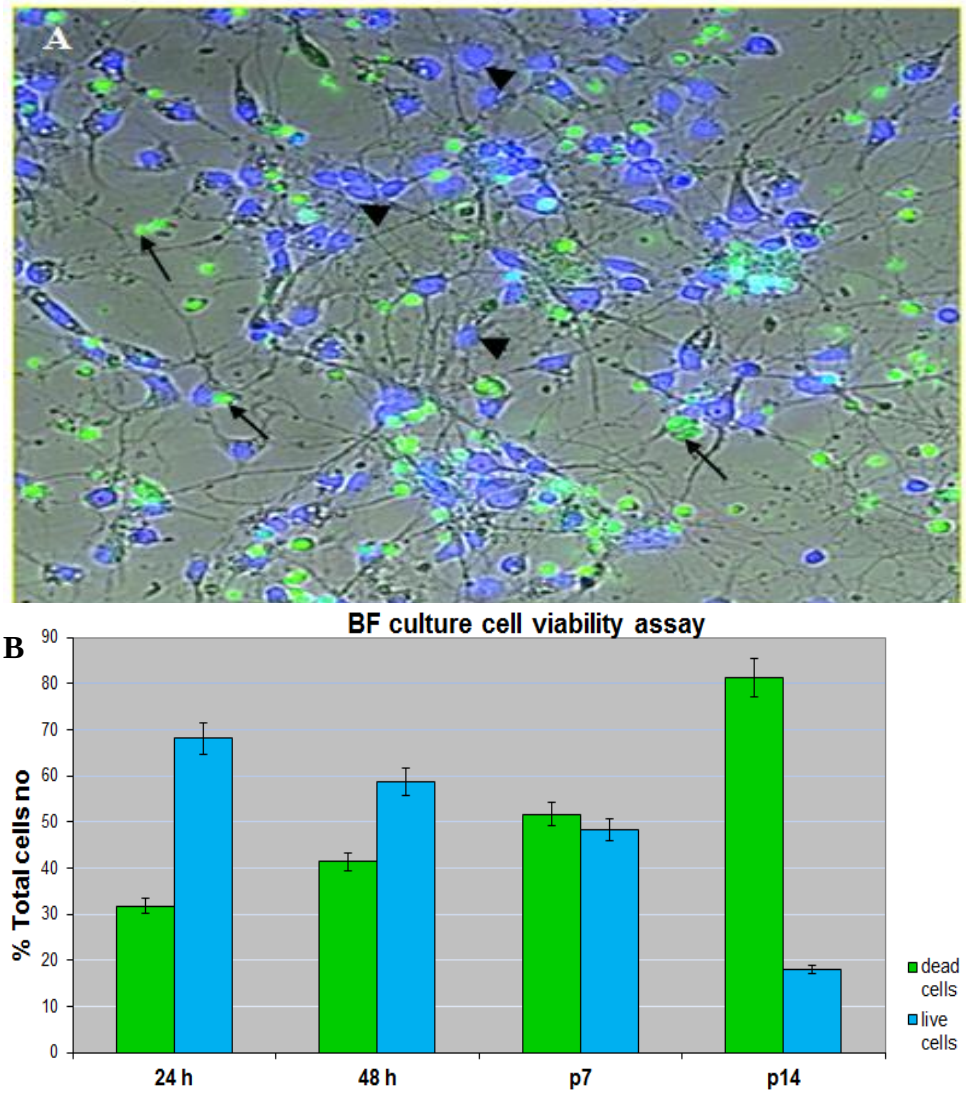

Figure 37. A. BF culture viability assay. DIC/fluorescent image of BF culture stained with Nuclear – ID™ Blue/Green cell viability reagent. Black arrow heads point to live cells (blue) while arrows point to dead cells (green). The image shows viability assay at 48h. B. Analysis of cell viability in BF culture. Plot of cell numbers expressed as percentage of live versus dead cells at different time points - 24h, 48h, p7, p14.

Due to progressive increase of dead neurons in cultures, I limited my experimental analysis to the young cultures (p5-p7).

4.2.5. Primary BF cultures retain high level of $p75^{NTR}$

Anti-$p75^{NTR}$ IgGs (FL-01 or FL-05, ATS) were used to identify cholinergic neurons in primary rat or mice BF cultures; these antibodies (4.7 nM or 3 nM, respectively) were applied to 2 ml of BF cultures for 2h and 24 h (Figure 38) to yield the best signal. The medium was removed after that time and cells were fixed with 4% PFA, pH=7.4 for half an hour in darkness and then washed a few times in phosphate buffered saline (PBS), pH=7.4. Labelled BF culture dishes were further processed for ChAT immuno-cytochemistry (Materials and Methods, Chapter 2.1.6 and 2.1.7).
Cholinergic phenotype of neurons in rat and mice primary BF cultures was identified on the basis of ChAT and $p75^{NTR}$ expression in the same cell as shown in Figure 38 and 40, co-stained with a nuclear marker - DAPI.

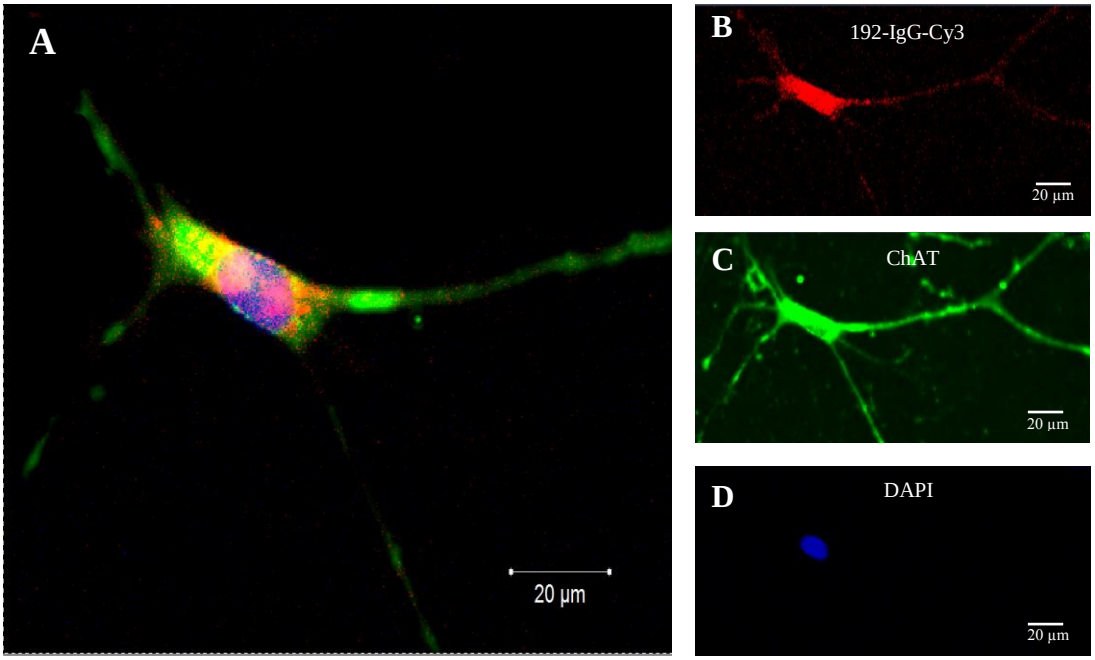

Figure 38. Characteristic of cholinergic phenotype. Image of cholinergic neuron from p7 rat BF culture co-labelled with 192-IgG-Cy3 (red) and anti-ChAT (green), fixed and mounted with DAPI (blue). Detailed explanation of different colours in various areas – B, C, D.

In regards to primary rat BF culture cholinergic neurons, these were counted with Photoshop CS4 v.11 as described in Materials and Methods, Chapter 2.2.2 (Figure 39). Counting of double-labelled neurons revealed that only 40 % of cholinergic cells were positive for both markers (ChAT and 192-IgG-Cy3). Similarly to brain slices, all 192-IgG-Cy3 positive neurons were immuno-reactive for ChAT, but ~25 % of ChAT positive cells were not labelled with 192-IgG-Cy3.

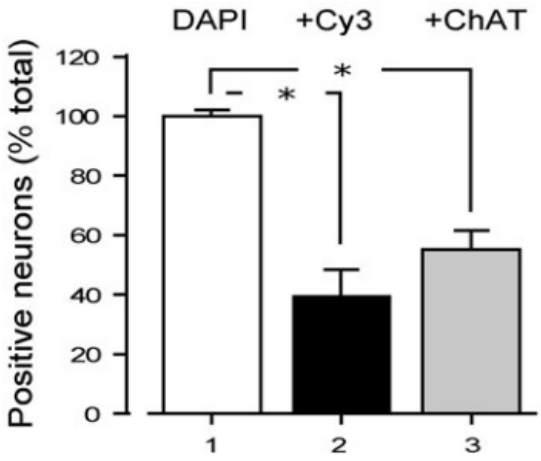

Figure 39. The proportion of cholinergic neurons in rat BF culture. Histogram is based on counting 400 neurons from 3 BF culture dishes. Cy3(+) - cells positive for 192-IgG-Cy3, ChAT(+) - cells positive for ChAT. DAPI - all cells.

Similar results were achieved with Cy3-labeled anti-murine NGFr IgG (Chapter 2.1.5.1.) for BF cultures from C57/BL6 and CD1 mice strains (Figure 40).

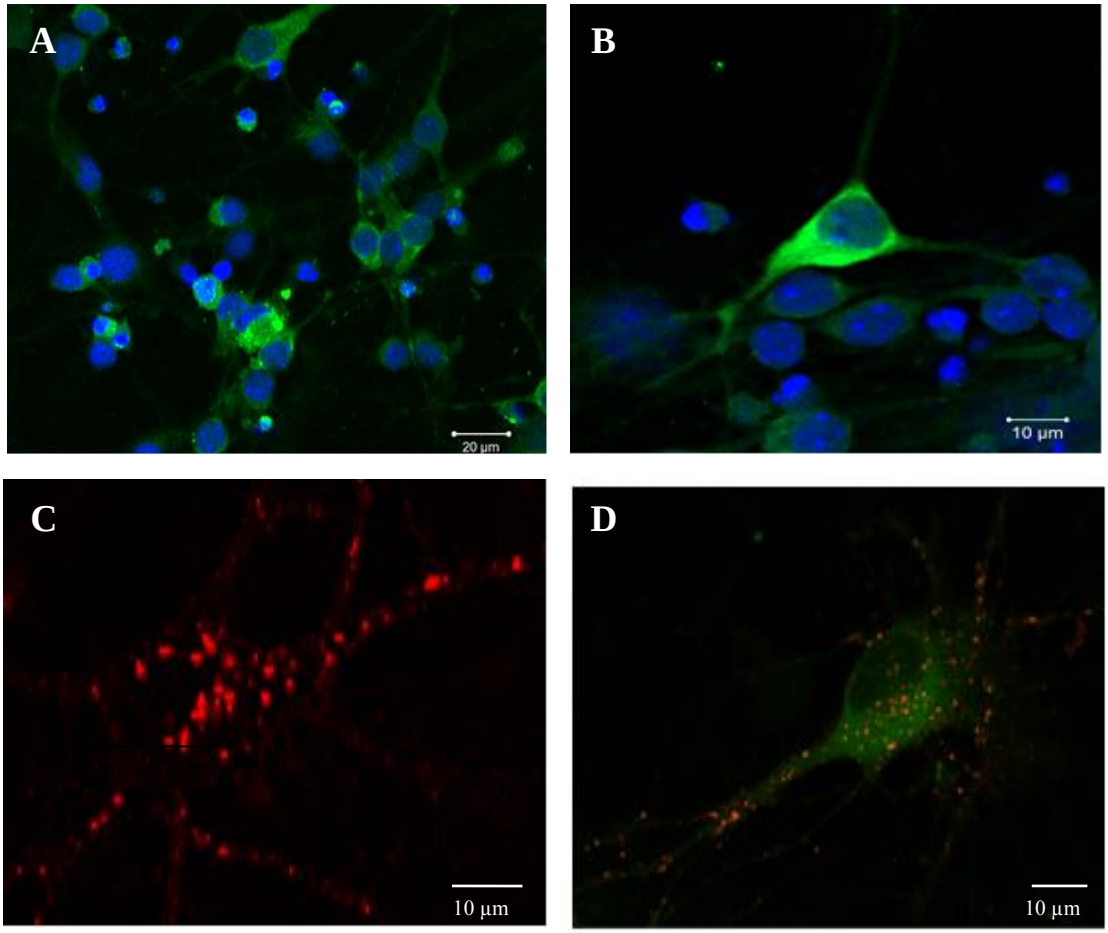

Figure 40. Identification of cholinergic neurons in BF of C57/BL6 mice. A. ChAT/DAPI staining of p7 BF culture. B. Representative cholinergic neuron stained with ChAT/DAPI.C. Cholinergic neuron stained with Cy3-labeled anti-murine NGFr IgG. D. Cholinergic neuron stained with ChAT(green) and Cy3-labeled anti-murine NGFr IgG.

4.2.6. p75^{NTR} uptake and trafficking in cholinergic neurons

Both primary BF rat and mice cultures displayed robust uptake of anti-p75^{NTR} antibodies (FL-01 and FL-05, 4.7 nM and 3 nM in 2 ml of BF culture, respectively) within first 2 h and did not show significant increase in the uptake of these antibodies by neuronal cells up to 24 h (example Figure 41), therefore limiting further experimental analysis to this time frame.

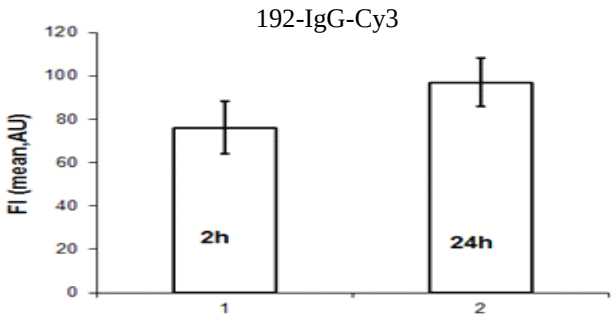

Figure 41. Time course of anti-p75^{NTR} IgG uptake in BFCNs. The histogram show uptake of 192-IgG-Cy3 by rat BFCNs in time. The bulk of this antibody - 78.1% was internalised within 2h of exposure and this number did not change significantly within 24h (p=0,23)

Trafficking of p75^{NTR}-192-IgG-Cy3 vesicles was observed in cholinergic cells with use of live confocal microscopy (LSM 710, Zeiss) (Figure 42). BF cell cultures were washed to remove excess of anti-p75^{NTR} IgG by re-freshing culture medium before viewing.

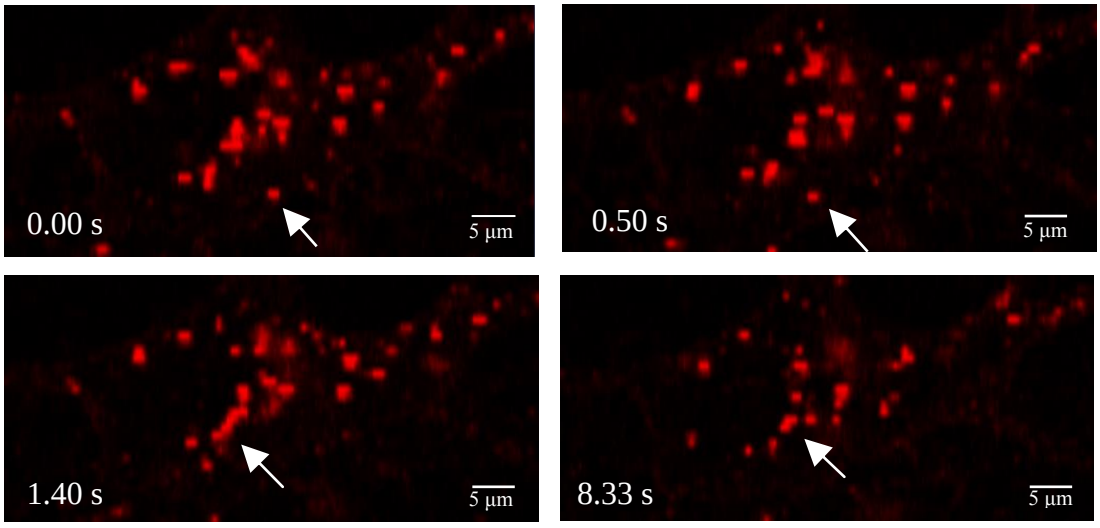

Figure 42. Trafficking of p75^{NTR}-192-IgG-Cy3 in rat BFCNs. Arrows point to the moving vesicles (example).

The observed punctate Cy3 signal in soma and neurites reflected vesicles, moving bi-directionally with various speed. The details of their size and velocity are described in Chapter 4.3.2.

4.3. Co-localization of $p75^{NTR}$ and Aβ in cholinergic neurons

HiLyte fluor 488 Aβ (1-42) (78673, AnaSpec) (0.1- 0.3 μM) were co-applied with 192-IgG-Cy3 (4.7 nM) of to 2ml of p7 BF culture for 24 h incubation at 37°C, 5% CO_2. After that time, cells were fixed in 4% PFA, buffered in PBS, pH=7.4 for half an hour and then washed with 0.1 M PBS, pH=7.4, before viewing. Co-localization of $p75^{NTR}$ and Aβ(1-42) was defined by the presence of two fluorescent labels within the same pixel in digitally acquired images by LSM710, Zeiss (Figure 43A). Co-localization co-efficients were automatically calculated with ZEN software, that estimated the degree of co-localization within the selected region of interest using a co-localization algorithm (Chapter 2.2.1) (Figure 43B).

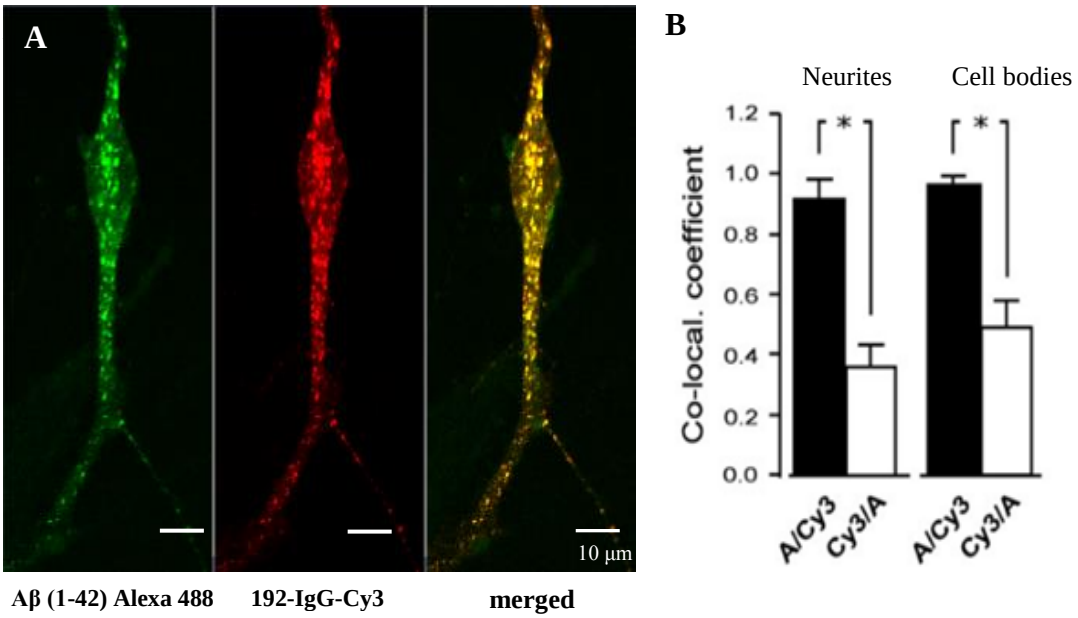

Figure 43. Co-localization study of $p75^{NTR}$ and Aβ (1-42) in cholinergic cell. A. representative cholinergic neuron showing co-localization of Aβ (1-42) Alexa 488 (left) and 192-IgG-Cy3 (middle) merged on the right panel. B. Plots of Aβ-Alexa488/192-IgG-Cy3 (and vice versa) co-localization in bar pairs from soma and neurites.

Analysis of randomly-defined regions revealed strong co-localization of HiLyte Fluor 488 Aβ (1-42) and 192-IgG-Cy3 in perykarion and neurites, with closely matching co-efficients (0.91±0.07 versus 0.96±0.1, neurites versus soma). Reversed assessment of 192-IgG-Cy3 and HiLyte Fluor 488 Aβ (1-42) showed significantly lower co-efficients (0.36±0.05 versus 0.48 ±0.08, neurites and cell bodies, respectively), suggesting the crucial role of $p75^{NTR}$ for the uptake of Aβ by BFCNs.

4.3.1. Compartmented cultures of superior cervical ganglionic neurons (SCGNs) confirmed retrograde trafficking of Aβ (1-42) and $p75^{NTR}$

The above findings were also confirmed in peripheral nervous system, where examined by looking at superior cervical ganglion neurons (SCGNs) in compartmented neuronal culture. Isolation of SCGNs from neonatal rat pups, enzymatic dissociation of the neurons and their maintenance in culture were performed as described before (Mahanthappa and Patterson, 1998; Banker and Goslin, 1998). Neurones were seeded into compartmented cultures following published procedures (Campenot, 1982) and using chambers supplied by the Tyler Research Corporation (Alberta, Canada). HiLyte fluor 488 Aβ (1-42) (0.3 μM) and 192-IgG-Cy3 (4.7 nM) (Chapter 2.1.5.1.) were utilized in this experiment. Trafficking of both molecules was observed in live cells from distal to the central (cell bodies) compartment, using LSM 710, Zeiss (Figure 44).

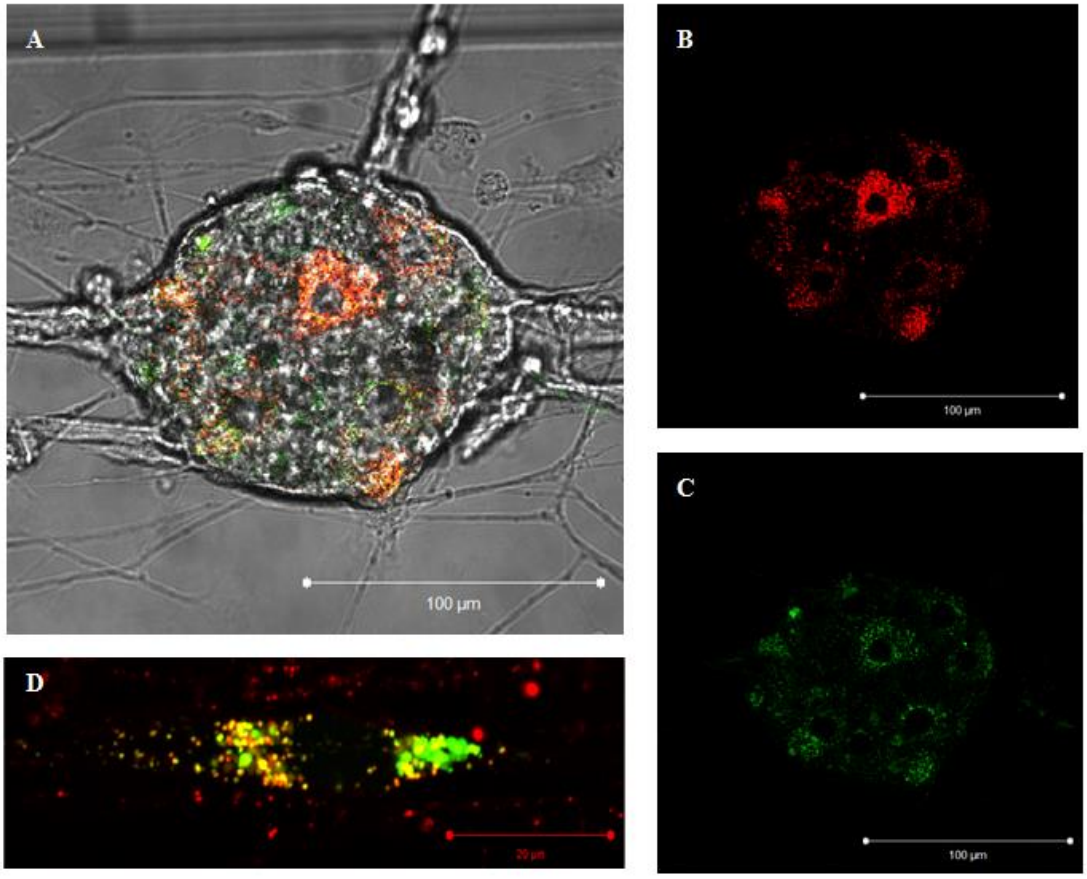

Figure 44. SCGNs traffic $p75^{NTR}$ to the cell body. A Cell body from central compartment of SCGNs culture containing co-localized vesicles of 192-IgG-Cy3 (red) and Alexa 488 labelled Aβ (1-42) (green), merged image of B and C. B. 192-IgG-Cy3 (red) in the central cell bodies compartment. C. Alexa 488 labelled Aβ (1-42) in central – cell bodies compartment. D. Distal compartment of SCGNs culture were both molecules (High Light Fluor Aβ (1-42) and 192-IgG-Cy3 were co-applied.

4.3.2. Parameters of trafficking Aβ (1-42) and p75^{NTR} loaded vesicles in BFCNs

Parameters of p75^{NTR} and Aβ (1-42) trafficking were assessed in BFCNs using live microscopy (Figure 45). The experiment was performed with 0.3 μM of HiLyte Fluor 488 Aβ (1-42) and 4.7 nM of 192-IgG-Cy3 co-applied for 2 h to 2 ml of rat BF cultures and delicately washed with re-feeding medium before viewing. The diameters of vesicles containing fluorescent Aβ (1-42) and 192-IgG-Cy3 within BFCNs were measured for about 200 vesicles (hundred for each channel) using ZEN software (Figure 46A). The speed of these vesicles was determined from time lapse live microscopy images for around 30 vesicles. The distance of migration of each vesicle was compared between the frames in a row, separately for vesicles containing HiLyte Fluor 488 Aβ (1-42) or 192-IgG-Cy3. The values were then averaged and analysed statistically (Figure 46B).

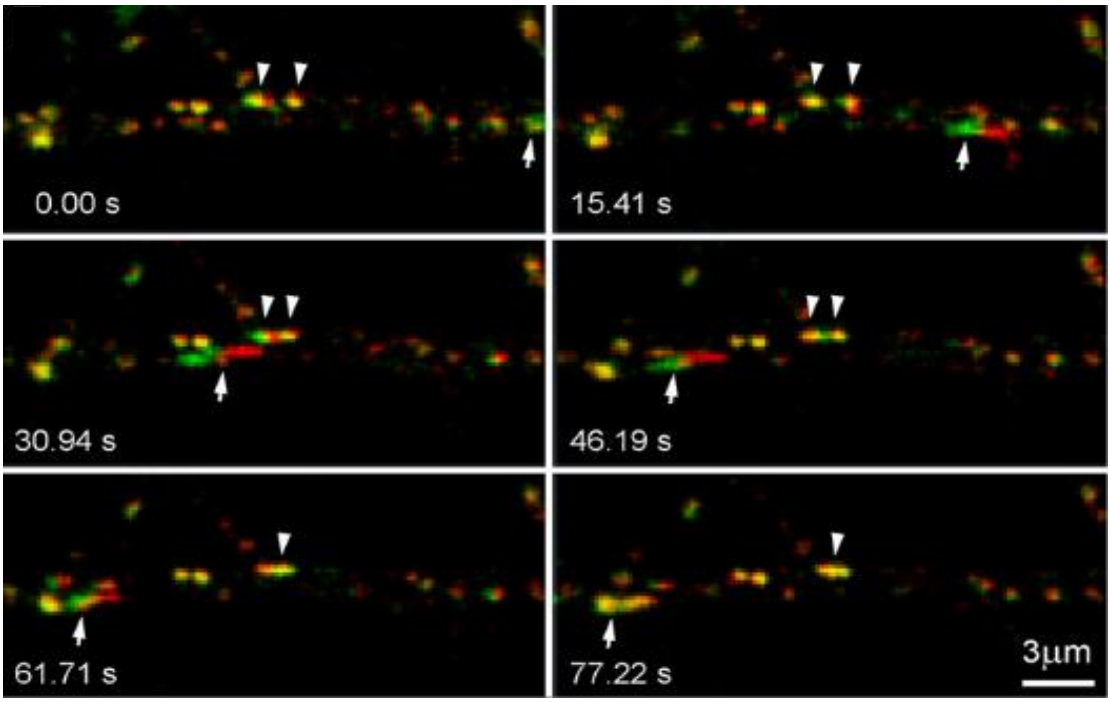

Figure 45. p75^{NTR} (labelled with 192-IgG-Cy3) and Aβ (1-42) (labelled with Alexa 488) traffics together in BFCN. Arrows point to the rapidly moving vesicles while arrowheads mark the slowly moving vesicles, in addition to the stationary or oscillating ones.

I observed double labelled round - slow and fast moving vesicles (0.05-4.2 μm/s) in both directions (somato-petal and somato-fugal) (Figure 45). Analysis of randomly defined images revealed closely matching average movement velocity of Cy3 and Alexa 488 labelled vesicles (3.18±0.7 μm vs. 2.81±0.8 μm, p=0.81). There were also stationary and oscillating double-labelled vesicles observed within both neurites and

perykarion. The average sizes of Cy3 and Alexa moving organelles were similar (0.8±0.06 versus 0.71±0.08 μm, respectively; p=0.34)

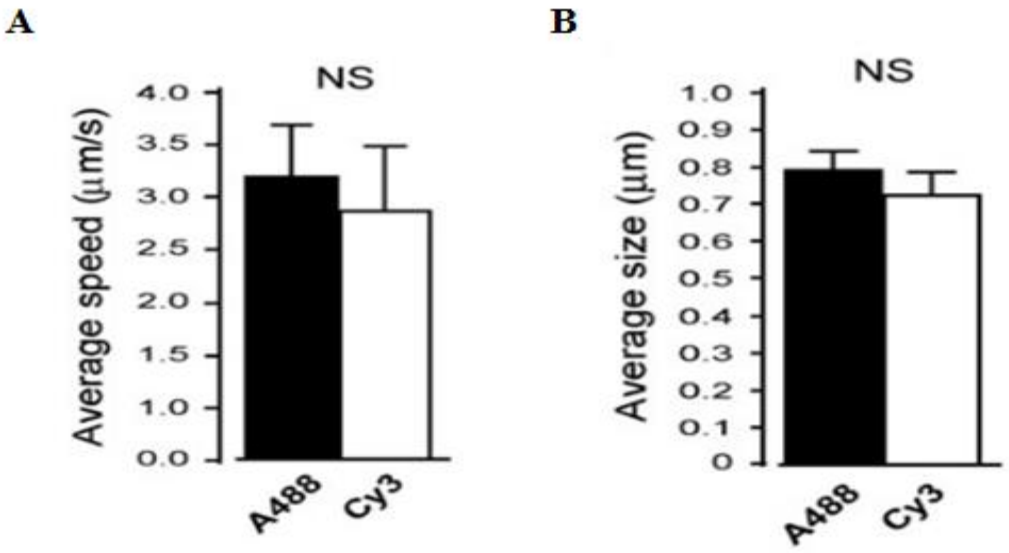

Figure 46. The average speed and size of vesicles loaded with 192-IgG-Cy3 and Aβ (1-42) –Alexa 488.

4.4. Mechanisms of Aβ and p75^{NTR} internalization by BFCNs

The uptake of Aβ by BFCNs can be important in the context of toxicity of these peptides in BF. Many receptors have been proposed to play role in Aβ internalization (Patel and Jhamandas, 2012) with some reviewed in Chapter 1.5.1. However, there is no detailed study of the internalization of p75^{NTR}, independent of TrkA. On the basis of microscopic observations from Chapter 4.3.2, we hypothesised that Aβ (1-42) may highjack the existing p75^{NTR} transport pathway for entering and propagation within BFCNs. Confirming this hypothesis as well as deciphering the mechanism of p75^{NTR} and Aβ uptake may be crucial for validation of p75^{NTR} as a molecular target for AD therapy. For this purpose the following experiments were undertaken.

4.4.1. p75^{NTR} uptake does not depend on regulated endocytosis

Firstly, rat BFCNs in culture were treated with 50 mM KCl (P9333, Sigma), 10 min at 37°C, 5% CO_2, prior to the addition of 4,7 nM 192-IgG-Cy3 to 2ml of same culture for 2 h and compared to not depolarised control (5.33 mM, K^+). Experimental and control samples were then washed in PBS, pH=7.4, fixed with 4% PFA for half

an hour and washed again with PBS, pH=7.4, before microscopic analysis. The result showed significant increase in the uptake of $p75^{NTR}$ in soma and neurites of BFCNs (89±18.2%, p=0.0071) as compared to non-stimulated controls (Figure 47).

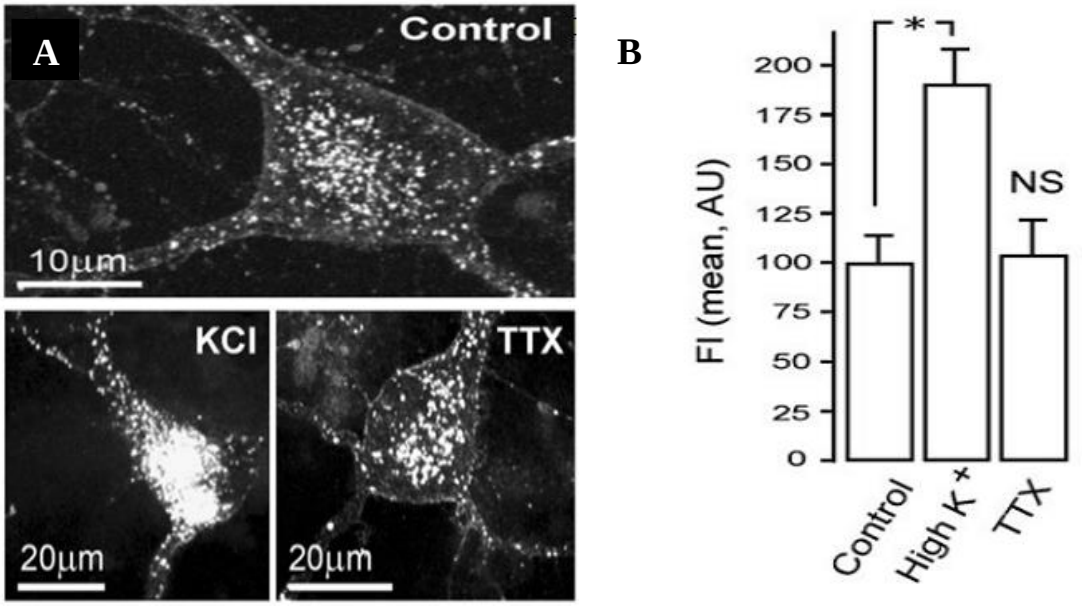

Figure 47. $P75^{NTR}$-192-IgG-Cy3 uptake by BFCNs is enhanced by depolarisation but the resting uptake is not susceptible to a Na^+ channel blocker. A. Representative images of BFCNs under high [K^+] or in the presence of tetrodoxin (TTX) compared to the control neuron in resting state. All neurons show uptake of 192-IgG-Cy3. B. Plots of fluorescence intensity signal generated by neurons under depolarisation and Na^+ channel blocking conditions versus BFCNs in resting state.

However, when Na^+ channels were blocked with tetrodoxin (TTX), (1069, Tocris Bioscience), in experiment where 500 nM of TTX was applied 10 min prior to the addition of 192-IgG-Cy3 (4.7 nM) to 2 ml of rat BF culture and incubated at 37°C, 5% CO_2 for 2 h, the effect was not significant (2.1±17.1%, p=0.24) as compared to the controls. Failure of TTX to alter the basal uptake of 192-IgG-Cy3 suggested independence of $p75^{NTR}$ from regulated synaptic activity.

To prove this directly, the effects of recombinant *Clostridial Botulinum* neurotoxins (BoNT/A and BoNT/B), expressed and purified in ICNT, DCU, on $p75^{NTR}$ endocytosis were examined. These neurotoxins were applied in concentrations that normally block SNARE-dependent exo/endocytosis BoNT/A (5 nM) or BoNT/B (10 nM) half an hour before addition of 192-IgG-Cy3 (4.7 nM) for 2h incubation in 37ºC, 5% CO_2. The addition BoNTs was omitted in control samples. Both experimental and control samples were washed after 2h of incubation in PBS, pH=7.4, fixed with 4% PFA for half an hour and washed again with PBS, pH=7.4, before microscopic analysis. As shown on Figure 48A and B loading of BFCNs with

192-IgG-Cy3 was not compromised with either BoNT/A or BoNT/B proteases 4.8±7.2% and 9.2±12% reduction, p=0.53 and p=0.16, respectively).

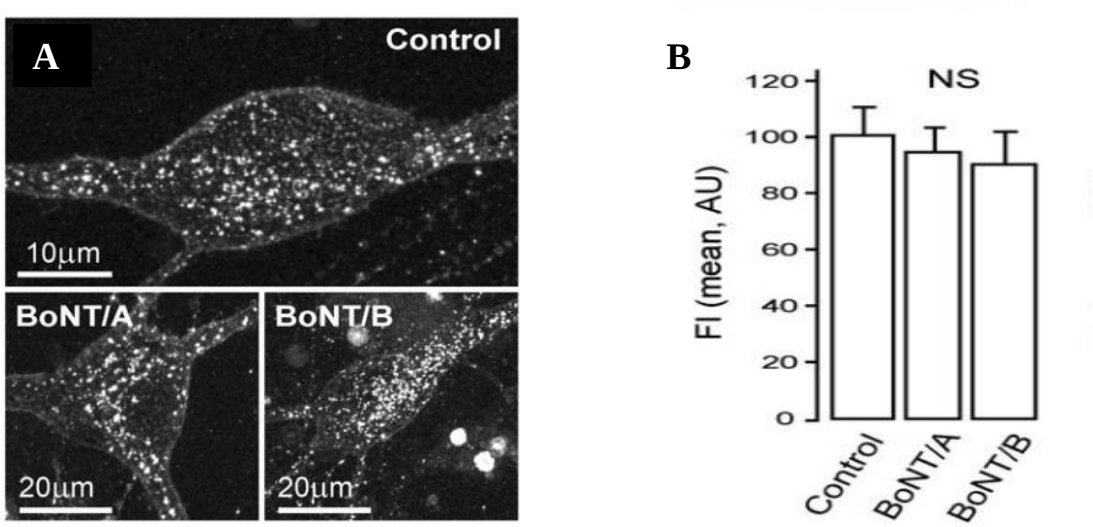

Figure 48. Basal internalization of $p75^{NTR}$-192-IgG-Cy3 by BFCNs is independent of SNARE-regulated exo/endocytosis. A. Representative images of BFCNs treated with BoNT/A or BoNT/B in concentrations that normally block vesicles turnover. B. Plots of fluorescence intensity signals generated in these cells during experiments with BoNTs versus control BFCNs.

4.4.2. Ca^{2+} homeostasis play major role in $p75^{NTR}$ internalization

Because Ca^{2+} homeostasis is altered in AD (Introduction, Chapter 1.5.1.2.) the effects of Ca^{2+} channel blockers and chelators on $p75^{NTR}$ endocytosis have been analysed. I assessed if 192-IgG-Cy3 internalization changes in the presence of broad spectrum of internal: cyclopiazonic acid (C1530, Sigma), thapsigargin (T9033, Sigma), and external: EGTA (E3889, Sigma), $CdCl_2$ (208299, Sigma), mibefradil (M5441, Sigma), nifedipine (N7634, Sigma) Ca^{2+} channel blockers (Tsien et al., 1998). These substances were incubated for half an hour at 37°C, 5% CO_2 with rat BFCNs, in subsequent experiments, prior to the addition of 192-IgG-Cy3 (4.7 nM) to 2 ml of same cultures, for the additional 2 h of incubation. Ca^{2+} blockers and chelators were omitted from control dishes to which 192-IgG-Cy3 only was applied. After incubation time, all samples were washed in PBS, pH=7.4 and fixed with 4% PFA for half an hour, before washing them in PBS, pH=7.4, prior to microscopic analysis.

Chelation of Ca^{2+} with EGTA (200 μM), strongly supressed basal endocytosis of $p75^{NTR}$ (61.2±2.1% decrease, p=0.0081) as compared to control samples. Indiscriminate blockade of high-voltage Ca^{2+} gated channels with $CdCl_2$ (50μM)

only marginally inhibited the loading of cholinergic neurons with 192-IgG-Cy3 (9.6±6.3% reduction, p=0.41) (Figure 49A). This contrasted with the effect of selective low-voltage T-type Ca^{2+} channel blocker – mibefradil (MIB), (10 μM), which significantly diminished the uptake of 192-IgG-Cy3 (75.4±3.1% reduction, p=0.004) as compared to the controls (Figure 49B).

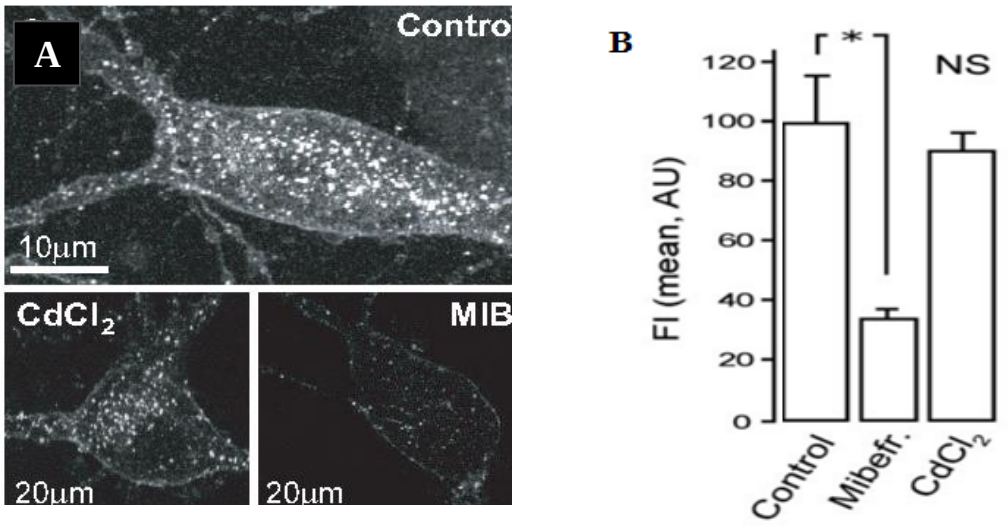

Figure 49. Internalization of $p75^{NTR}$-192-IgG-Cy3 by BFCNs depends on extracellular Ca^{2+}. A. Representative images of BFCN blocked with $CdCl_2$ and mebefradil (MIB) compared to control neuron in resting state. B. Plot of fluorescence intensity signals generated by 192-IgG-Cy3 in BFCN exposed to $CdCl_2$ or mibefradil versus control BFCNs.

Interestingly, high voltage, L-type Ca^{2+} channels were also found to significantly reduce $p75^{NTR}$ uptake (74.39±4,23%, p=0,0003) as shown by studies with nifedipine (10 μM) (Figure 50).

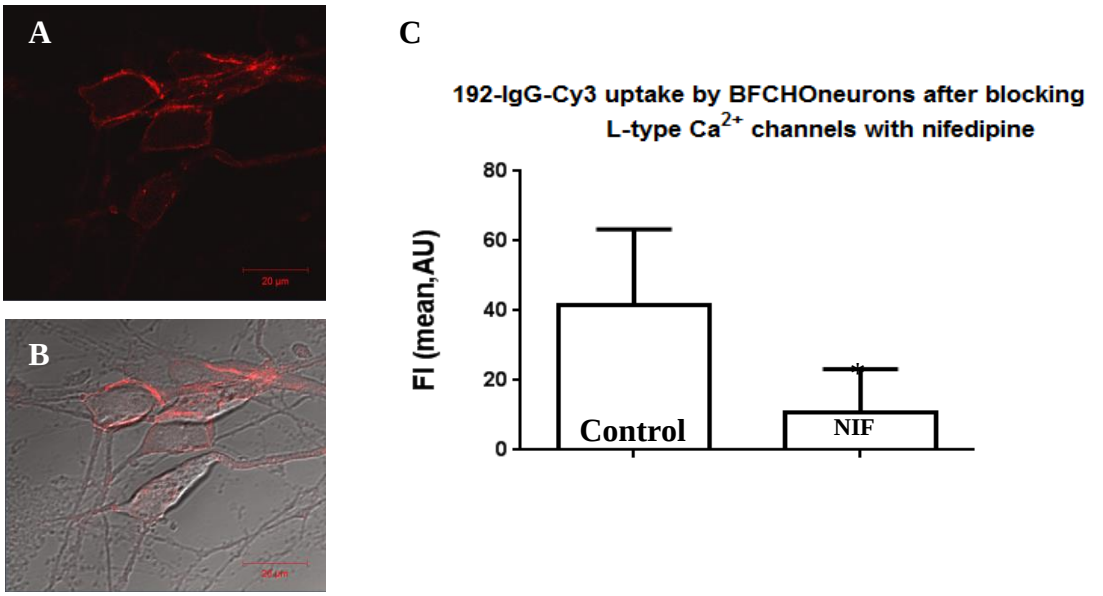

Figure 50. Contribution of L-type channels to endocytosis of $p75^{NTR}$-192-IgG-Cy3 by BFCNs. A. Z-stack of BFCNs cluster pre-treated with 10μM nifedipine. B. The same neuronal cluster imaged with DIC. C. Plot of fluorescence intensity signals generated by $p75^{NTR}$-192-IgG-Cy3 in BFCNs exposed to nifedipine versus control BFCNs.

Additionally, similar inhibitory effects of 192-IgG-Cy3 endocytosis were observed upon blockade of sarco-endoplasmic reticulum (SERCA) ATPase with cyclopiazonic acid (CPA), (10 μM), (51.2±6.4%, p=0.021) or thapsigargin (TG), (1 μM), (59.2±1.4%) as shown on Figure 51A and B as compared to the controls.

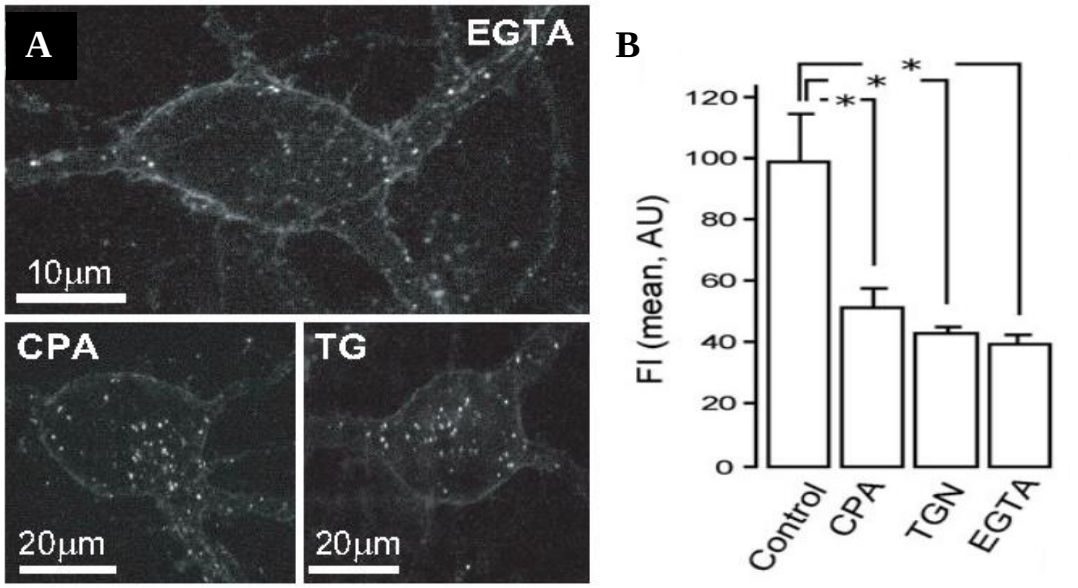

Figure 51. Internalization of p75^{NTR}-192-IgG-Cy3 by BFCNs relies on intracellular Ca^{2+}. A. Representative images of BFCNs treated with general Ca^{2+} chelator (EGTA) and SERCA ATPase pump inhibitors – CPA and TG. D. Summary of the average fluorescence intensities (FI) pooled from experimental groups imaged on picture C versus the control BFCNs.

4.5. Aβ oligomers compete with 192-IgG-Cy3 for binding to p75^{NTR}

Binding of Aβ oligomers to p75^{NTR} was assessed in compartmented SCGN cultures described in Chapter 4.3.1. for neurons: somata localised in the central compartment and neurites developing in distal compartment. Aβ oligomers, prepared as in Chapter 3.5.1 (1.2 μM) and 192-IgG-Cy3 (4.7 μM) were sequentially applied for 1h each at 4°C to the experimental samples. The addition of oAβ was omitted from control samples. Then experimental and control samples were processed in the same way. SCGNs from central compartment were washed carefully three times by exchange of the culture medium with PBS, pH=7.4. They were lysed in NuPage LDS sample buffer (NP0007, Life Tech.) afterwards and separated by SDS-PAGE on a 12% NuPage Bis-Tris gel. Samples were taken from two distal compartments with a small amount of ddH_2O (20 μl) and ultracentrifuged in 4 °C at 180 000 g for 15 minutes before heating them in loading buffer for 5 min to 95ºC and resolving on a SDS-PAGE 12% NuPage Bis-Tris gel. The gels were imaged using Fujifilm laser scanner

(FLA-5100) and analysed with advanced image data analyser (AIDA) programme (Figure 51B). WB was also performed to confirm this result (Figure 52C).

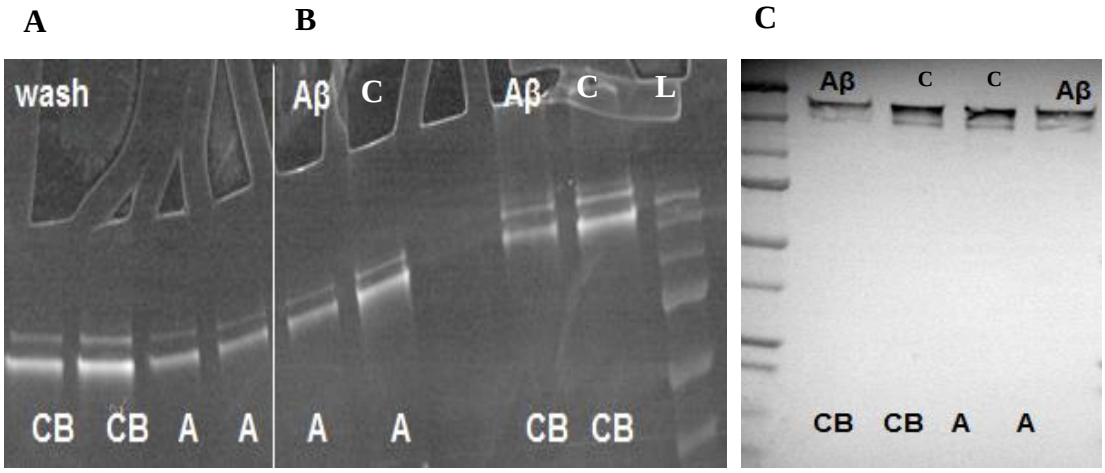

Figure 52. Aβ oligomers compete with 192-IgG-Cy3 for binding to $p75^{NTR}$. A. internal control of 12% NuPage Bis-Tris gel imaged by FLA-5100 – samples from the wash. Abbreviation: A – axonal distal compartment, CB – cell bodies (central compartment). B. diminished 192-IgG-Cy3 signal in Aβ samples as compared to the controls (without Aβ).Abbreviations Aβ – samples with preliminary Aβ binding, C – samples with omission of Aβ (192-IgG-Cy3 only), L – molecular size marker. C. WB of same experiment. The previous abbreviations applied.

The above experiment indicate that Aβ oligomers compete with 192-IgG-Cy3 for binding to $p75^{NTR}$. Image J analysis of the above gels show 47.13% and 33.3% (axons and cell bodies, respectively) of signal reduction in 192-IgG-Cy3 binding to $p75^{NTR}$, for samples where oAβ (1-42) was added prior to their exposure to fluorescent antibody (192-IgG-Cy3). This was confirmed by WB analysis, which detected 49.41% decrease in 192-IgG-Cy3 bands intensity of SCGNs somata (central compartments) and 46.84% reduction in 192-IgG-Cy3 bands intensity of SCGNs neuritis (distal compartments), where oAβ were added.

4.5.1. Oligomeric Aβ inhibits endocytosis of $p75^{NTR}$

Aβ oligomers previously prepared as in Chapter 3.5.1. were applied in subcytotoxic concentrations (6 nM – 630 nM) to postnatal (P5) rat BF cultures and pre-incubated for 24 h in humidified incubator at 37°C in 5% CO_2 before the addition of 192-IgG-Cy3 (4.7 nM) to 2ml of cultures for 2 h. Cells were then fixed with 4% PFA in PBS, pH=7.4 for half an hour and then washed few times with PBS, pH=7.4, before microscopic analysis.

Pre-exposure of cultures to oAβ significantly diminished the basal uptake of $p75^{NTR}$-192-IgG-Cy3 as compared to controls. This effect was concentration dependent. Figure 53 shows, significant decrease in the basal $p75^{NTR}$ uptake observed for 60 and 600 nM of oAβ ($p=0.004$ and $p=0.008$, respectively).

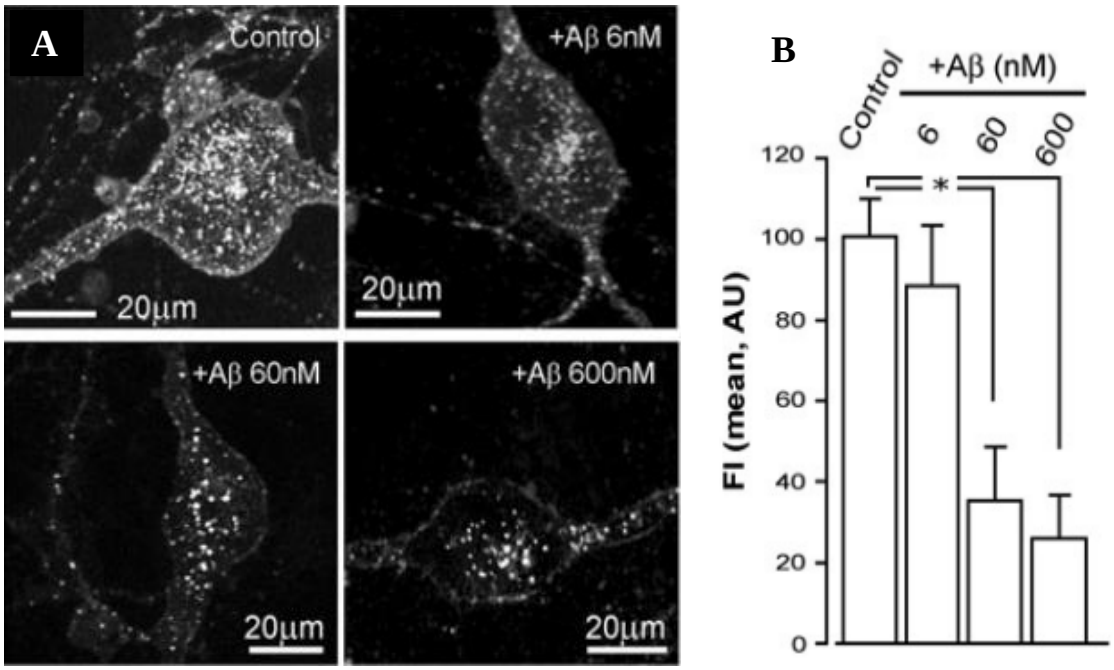

Figure 53. Oligomeric Aβ diminishes $p75^{NTR}$-192-IgG-Cy3 uptake by BFCNs. A. Representative images of BFCNs in the presence of different amounts of Aβ oligomers as compared to the control. B. Histogram showing fluorescence intensity signals of 192-IgG-Cy3 in BFCNs in the presence of different concentrations of Aβ oligomers versus control.

The uptake of $p75^{NTR}$-192-IgG-Cy3 was inversely proportional to the amount of oAβ applied, suggesting the existence of negative feedback loop in Aβ uptake by BFCNs but also homeostatic role of $p75^{NTR}$ in regulating Aβ level in BF as well as in the areas to which BFCNs project (Chapter 1.5.3.1.). This phenomenon may be important for Aβ clearance process, which is disrupted in AD (Chapter 1.5.1.1.).

4.6. $p75^{NTR}$ co-localizes with Cs-HC-TeTx in BF culture

Normally TeTx toxin (TeTx) shows tropism to peripheral nerve ending at neuromuscular junction and its retrogradely transported to the spinal cord and brain stem, with $p75^{NTR}$ implicated in this process (Lalli and Schiavo, 2002; Ovsepian et al., 2015).

TeTx composed of heavy chain (HC), responsible for binding and translocation of the toxin and protease domain, both linked by a disulphide bond (Pellizari, 1999); was re-engineered using recombinant technology and site-directed mutagenesis (O'Leary et al., 2013). HC of TeTx was fused to core streptavidin (CS)-generating Cs-H_C-Tetx molecule (Figure 54A).

High (19.4 nM) and low (9.7 nM) amounts of Cs-Hc TeTx were added to 2ml of (P6) BF rat primary culture together with 192-IgG (9.5 pM) and incubated for 2h at 37°C, 5% CO_2. In control dishes, Cs-Hc-TeTx was omitted. The cultures were fixed in 4% PFA in PBS, pH=7.4 and immuno-cytochemistry with anti-streptavidin mouse monoclonal IgG was performed, as described in Materials and Methods, Chapter 2.1.6. High degree of co-localization was observed for both molecules (Cs-Hc-Tet and 192-IgG-Cy3) (Figure 54).

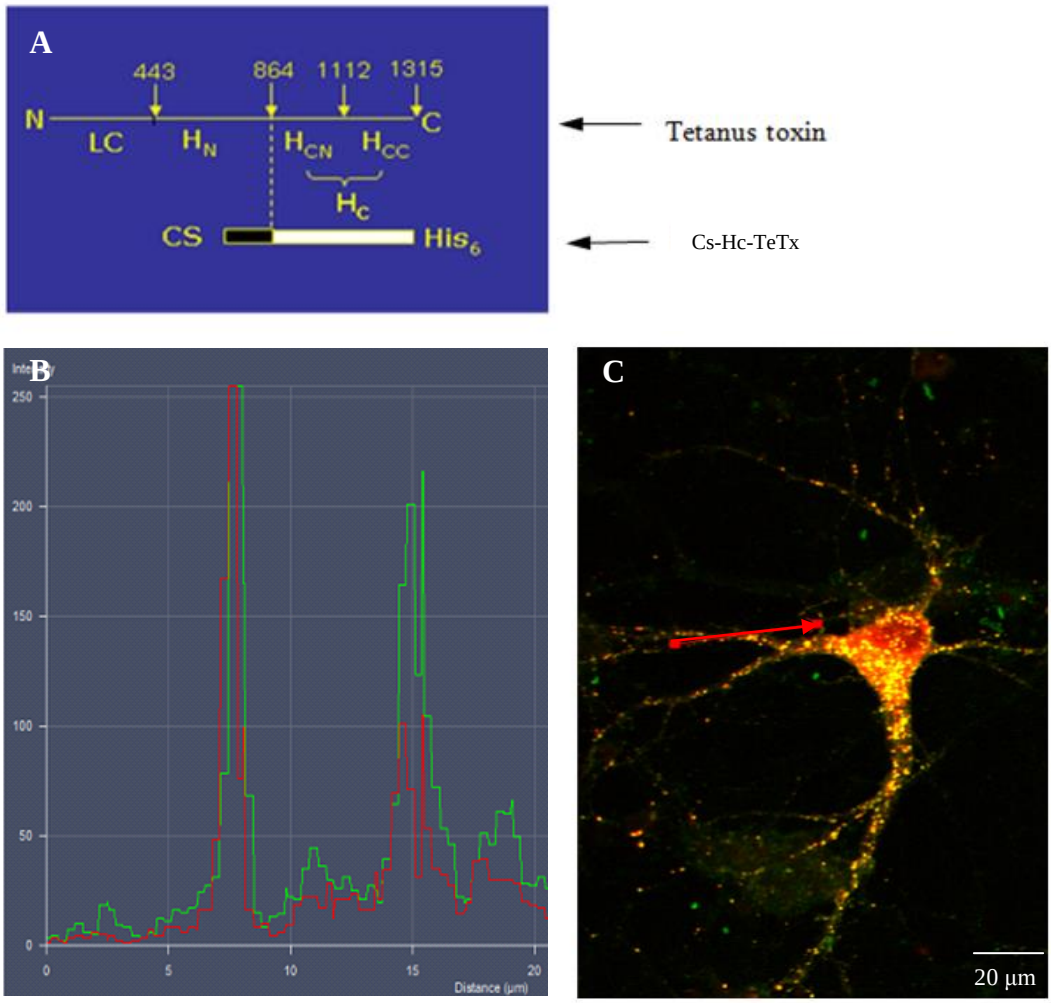

Figure 54. Colocalization of Cs-Hc TeTx with 192 ɔn protein Cs-Hc-TeTx. B. Fluorescence intensity n o-localization of Cs-Hc-TeTx with $p75^{NTR}$-192-IgG-Cy3 in vesicle crossed by arrow in C. C. Colocalization of Cs-Hc- TeTx (green) with 192-IgG-Cy3 (red). Red arrow crosses the vesicle which co-localizes both molecules.

4.7. Aβ oligomers are sorted for lysosomal degradation in BFCNs

Immunocytochemistry for early (EE1), recycling (Rab 11) and late (Rab7) endosomal proteins as well as lysosomes (Lamp1) were performed on BFCNs pre-labelled for 2 h with 192-IgG-Cy3 (4.7 nM), added to 2ml of (P7) rat cultured BF cells. The cultures stained for Rab7, Rab11 and Lamp1 were incubated with those IgGs overnight, while cultures stained with EE1 were incubated for 2 h at 37°C, 5% CO_2. All dilutions of primary and secondary antibodies were previously tested and described in Materials and Methods, Chapter 2.1.6. These cultures were fixed in 0.4% PFA in PBS, pH=7.4 for half an hour and washed with 0.1M PBS before microscopic analysis.

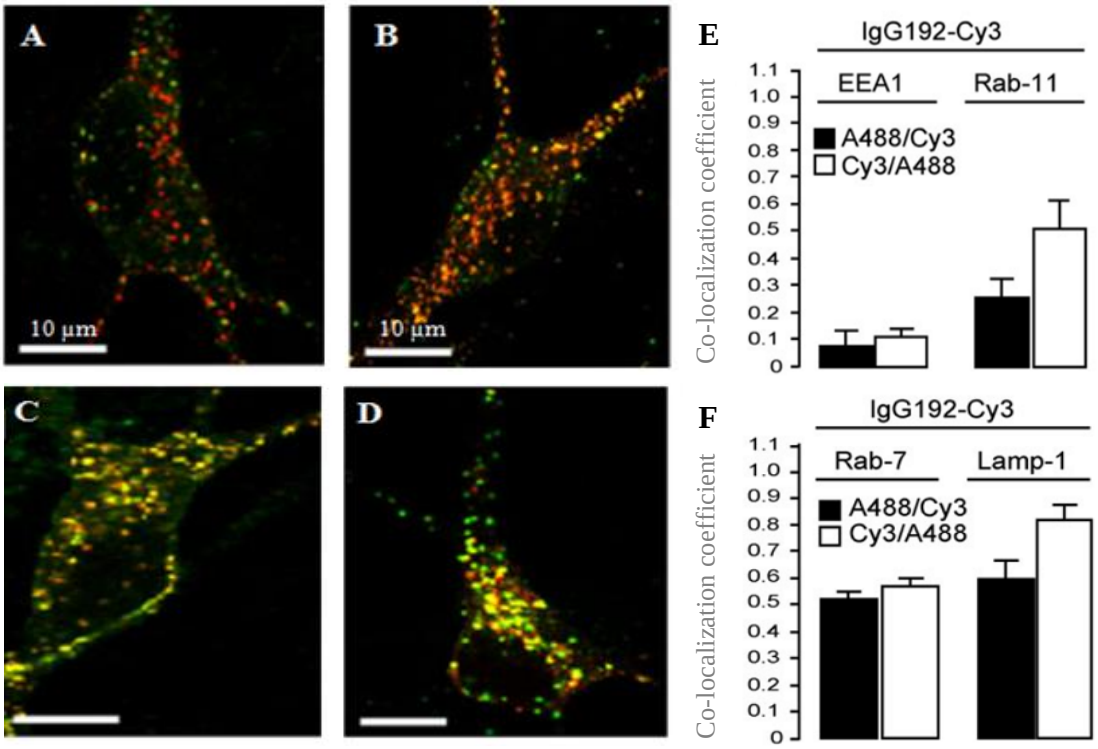

Figure 55. Location of $p75^{NTR}$-192-IgG-Cy3 in intracellular compartments of BFCNs. Representative images of double labelling in various endosomal/lysosomal compartments in BFCNs with 192-IgG-Cy3 and early endosomal marker - EE1 (A), recycling endosomal marker - Rab11 (B), late endosomal marker - Rab 7 (C), lysosomal protein - Lamp1 (D). E. Summary plots showing the average co-localization coefficients of 192-IgG-Cy3 with EE1 and Rab11. F. Similar plots for Rab 7 and Lamp1.

The double labelling revealed that only small fraction of 192-IgG-Cy3 was present in early endosomes (7.7±6.7%) and higher - 25.1±11% were positive for 192-IgG-Cy3 and Rab 11. This suggests that a substantial fraction of 192-IgG-Cy3-$p75^{NTR}$ carrying endosomes are sorted to trans-Golgi network and recycled. Strong labelling of 192-IgG-Cy3 with late endosome (Rab7) or lysosome protein (Lamp1)

(56.1±3.2% and 82.1±5.9%, respectively) suggested that the bulk of $p75^{NTR}$ with its cargo is guided for degradation in BFCNs (Figure 55).

4.8. Exocytosis of $p75^{NTR}$

Not only the uptake but the release of amyloidogenic peptides is a matter of great interest especially in light of their trans-neuronal spread of AD pathology.

In previous chapters, I demonstrated that $p75^{NTR}$ can mediate the uptake of Aβ and sort it for degradation by BFCNs but it was also found that some of the $p75^{NTR}$ carriers get sorted into the recycling pool of vesicles. Therefore, there is the possibility that recycling vesicles can get fuse back with the membrane and release their content to the extracellular space. These investigations of Aβ exocytosis may lead to the discovery of the mechanisms by which Aβ spreads during the course of the disease, if hijacking the existing $p75^{NTR}$ endocytic pathways.

The initial experiments were conducted in postnatal CD-1 mice BF cultures with Cy3 labelled anti-murine NGFr (Chapter 2.1.5.1.) (3 nM) added to 2ml of cultures for 2 h and kept in humidified incubator 37ºC, CO_2. The samples were then washed with medium and imaged live by LSM710. Then they were incubated for additional period of time: 2; 5,5; 29h. At each time point BFCNs were imaged again. Images from 49 cells (368 frames) were analysed. The data were normalized versus the same area. The results are shown in Figure 56.

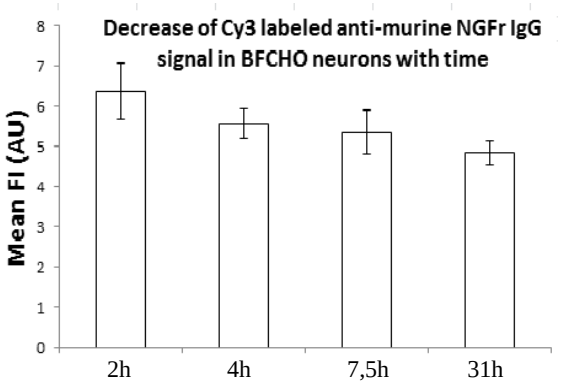

Figure 56. Trend in $p75^{NTR}$-cargo decrease. The data show analysis of Cy3 labelled anti-NGFr antibody in CD-1 postnatal mice BF culture.

A declining trend in Cy3 labelled anti-NGFr IgG intensity was observed within the first 31h; however, these changes were not significant (p=0,2). Further experiments are required to establish the time point at which the signal significantly drops down and to answer what are the mechanism of $p75^{NTR}$ cargo release.

4.9. Discussion of p75^{NTR} internalization by BFCNs in the context of AD

p75^{NTR}, expressed exclusively by BFCNs throughout the adulthood was investigated in rat and mice primary BF cultures, which retain high level of this receptor (Chapter 4.2.5.). Development of BFCNs in these cultures was strictly dependent on exogenous supply of NGF as in agreement with previously reported data (Banker and Goslin, 1998). Such trophic support did not clash with further analysis of p75^{NTR} because NGF and 192-IgG-Cy3 (main monitoring ligand used in this study) bind to different extracellular epitopes (Taniuchi and Jonson, 1985), giving the opportunity to observe p75^{NTR} in various experimental conditions.

Although much is known about release of p75^{NTR} cargo as e.g. neurotrophins (Hartmann et al., 2001; Dean et al., 2009), only little studies focus on their uptake (Campenot, 2009, Wong et al., 2015). These studies mostly consider TrkA co-operation with p75^{NTR}. However, it is known that p75^{NTR} can act independently from Trk signaling. This unique receptor lack enzymatic activity and exerts its function depending on ligands it binds to as reviewed in Chapter 1.5.3.2.1. This is particulary interesting in case of non-neurotrophic ligands binding, especially Aβ binding in regards to AD, as this peptide is known from its deleterious effects on cholinergic cells during the course of this disease (reviewed in Chapter 1.5.1.1.). Therefore I focused my studies on p75^{NTR} endocytosis independent on TrkA.

Using primary BF cultures I demonstrated for the first time with live confocal microscopy data, rapid and robust internalization of Aβ (1-42) together with p75^{NTR} as revealed with use of HiLyte fluor tagged peptide and labelled antibodies (192-IgG-Cy3) (Chapter 4.3). The retrograde trafficking of both molecules was also confirmed in different neuronal setting e.g. with use of SCGNs compartmentalized cultures (Chapter 4.3.1.). The analysis of trafficking Aβ (1-42) and p75^{NTR} loaded vesicles in BFCNs revealed their movement in both directions with some stationary oscillating vesicles in neurites and perykarion (Chapter 4.3.2). The endocytosis of p75^{NTR} was further analysed (Chapter 4.4). While active at rest conditions this process was significantly accelerated under K^+ induced depolarisation. Interestingly, same vesicles turnover was insensitive to inhibitors of regulated synaptic activity such as TTX. To demonstrate this directly the effects of potent inhibitors of synaptic exocytosis - *Clostridial Botulinum* neurotoxins (BoNT/A and /B) were examined (Chapter 4.4.1.). Loading of vesicles with 192-IgG-Cy3 was not compromised by

these proteases, suggesting segregation between the processes governing the uptake of $p75^{NTR}$ ligands including Aβ from those contributing to the membrane recovery.

Because Ca^{2+} is ubiquitous regulator of membrane turnover at both axonal terminals and dendrites (Ovsepian and Dolly, 2011) I assessed if the uptake of 192-IgG-Cy3 relies on the increase of the intracellular Ca^{2+}. BFCNs are known to express a range of voltage-gated Ca^{2+} channels (Griffith et al., 1994) and undergo increased calcium buffering during aging (Murchison and Griffith, 1998). In my experiments the indiscriminate blockade of high-voltage gated Ca^{2+} channels with cadmium ($CdCl_2$, 50μl) (Tsien et al., 1988) only marginally inhibited the loading of BFCNs with 192-IgG-Cy3. This contrasted with blockade of low and high-voltage activated Ca^{2+} influx by mibefradil and nifedipine, respectively which significantly decreased the basal endocytosis of $p75^{NTR}$ (Chapter 4.4.2.). Similar results were evident under global chelation of BFCNs with EDTA. The involvement of internal calcium stores into $p75^{NTR}$ uptake was also examined. The smooth endoplasmic reticulum (SER) was investigated with the SER ATPase Ca^{2+} uptake blockers - thapsigargin and cyclopiazonic acid. The depletion of internal Ca^{2+} stores by inhibitors of the SERCA pump suggests the involvement of these structures in endocytosis of $p75^{NTR}$. In conclusion all the above experiments confirmed the important role of Ca^{2+} in $p75^{NTR}$ correct functioning what has a meaning particulary in aging and AD, where calcium homeostasis is altered (reviewed in Chapter 1.5.1.2.).

Because amyloid hypothesis implicates Aβ as the main culprit of pathogenic events leading to AD, I examined influence of this peptide on $p75^{NTR}$ endocytosis in various sub-cytotoxic concentrations. In these experiments monomeric and oligomeric mixture of Aβ (1-42) reduced basal uptake of $p75^{NTR}$ in dose dependent manner as revealed in Chapter 4.5.2. This occurs by yet unidentified mechanisms, suggesting however, the new homeostatic role of $p75^{NTR}$ in Aβ uptake. In other words BFCNs may keep check on Aβ level in BF and through their diffuse ascending projections in the cerebral cortex and hippocampus (Chapter 1.5.3.1.). Overloading of this system with excess of Aβ during AD may cause disruption of degradation mechanisms and cause preferential deposition of Aβ peptides in the areas of cholinergic projections. Such hypothesis would also explain preferential vulnerability of BFCNs in the pathological processes of AD (Ovsepian and Herms, 2013). On the other hand oAβ was found to compete with 192-IgG-Cy3 for binding to $p75^{NTR}$ (Chapter 4.5.1.), conflicting the previous result. Therefore further experiments e.g. with truncated

forms of p75^{NTR} or its silencing are needed to confirm the hypothesis of Aβ clearance by p75^{NTR}. *In vivo* experiments with knock-down parts of p75^{NTR} or the whole receptor would be also beneficial. However, due to limitation of time and resources I did not conducted those experiments. In the analysis of p75^{NTR} trafficking I found however the lysosomes as a primary destination of p75^{NTR} cargo (Chapter 4.7.) what suggests it degradation by BFCNs. Interestingly, in set of those experiments p75^{NTR} was found not to co-localize with early endosomal marker (EE1), which is in agreement with previous literature data, showing Aβ (1-42) apart from EE1 marker and caveolin (Saavedra et al., 2007).

Although Aβ entry to BFCNs remains elusive there is no doubt that this neurotoxic peptides hijack p75^{NTR} pathway for trafficking within cholinergic cells. P75^{NTR} particulary enriched in axons of these neurons are definitely sorting this deleterious peptide for degradation in lysosomes, what happens in addition to other processes known for Aβ clearance (reviewed in Chapter 1.5.1.1.). This observation is in agreement with the reports viewing disruption of lysosomal system as the main cause of neurological disorders including AD (LaFerla et al., 2007; Nixon et al., 2008).

It should be of notion, that pool of p75^{NTR} was found in the recycling vesicles (Chapter 4.7.). These vesicles may get fuse back to the membrane and release their neurotoxic cargo outside the cell. This is especially interesting in the context of spreading Aβ pathology and should be important aspect to consider for further studies. Possible exocytosis of Aβ or other escape routes from lysosomal degradation should be the matter of further research as explained in more details in Chapter 4.8. The possible p75^{NTR} trafficking with its cargo is illustrated in Figure 57.

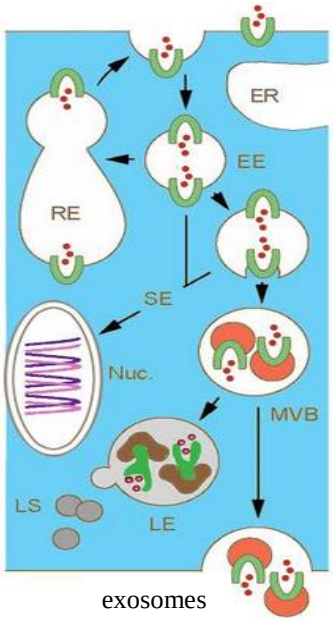

After internalization of p75^{NTR} with its cargo to the early endosomes (EE), the fraction of loaded vesicles is recycled back to the plasma membrane (recycling endosomes - RE), while the rest is sorted to the signalling endosomes (SE). Other fraction get fused with multivesicular bodies (MVB), which maturate to late endosomes (LE) and within lysosomes (LS) degrade most of the content. It is possible however that not all material is degraded and can escape lysosomal route of degradation. In this case p75^{NTR} with its cargo e.g, Aβ can be released outside the cell through exososmes. Other abbreviations: ER – endoplasmic reticulum, Nuc - nucleus

P75^{NTR} with its cargo e.g Aβ

Figure 57. Possible routes of p75^{NTR} trafficking with its cargo.

Chapter V. Targeted lentivirus transduce BFCNs *in vivo* - results with discussion

5.1. Targeting of neuronal cells by lentiviral vectors

Lentiviral vectors (LVs) have been widely used in fundamental biological research, functional genomics and gene therapy (Dugal and Choudhary, 2012). They are important tools for gene transfer because of possessing the ability to transduce a number of cell types without the need for host cells to be dividing (Blömer et al., 1997; Ausubel et al., 2012). The biggest advantage of LVs over other viral delivery systems is their large capacity. Lentiviruses can integrate up to 8 kb of transgene into the host genome (Davidson and Breakefield, 2003). Moreover, innate immune responses are not very problematic for LVs as only minimal and asymptomatic inflammation has been observed in animal models after their administration (Kordower et al., 2000). Generation of recombinant LVs targeting BFCNs through recognition and binding of $p75^{NTR}$ was undertaken in this study with intention to clarify if $p75^{NTR}$ can provide novel therapeutic target for AD therapy. To achieve that, I used second generation hybrid viral vector system (Tiscorniaet al., 2006) made from the core proteins and enzymes of human immunodeficiency virus type I (HIV-1), pseudotyped with vesicular stomatitis glycoprotein (VSV-G). An infectious retroviral particle of this virus comprised RNA genome that carries cis-acting sequences necessary for packaging, nuclear translocation and transcription as well as trans-acting sequences, encoding viral structural proteins (gag end env genes) and the enzymatic product of pol gene (schematic drawing Figure 57) (Rohll et al., 2002, Delenda 2004). Due to the separation of cis and trans acting elements, this lentivirus has a high biological safety profile and is replication deficient. The chances of crossing this lentivirus with eventual native HIV viruses are reduced by replacement of native lentiviral envelope protein with VSV-G envelope protein. Deletion of native HIV promoters in the packaging construct and their replacement by a heterologous constitutive promoter (resulting in the presence of only 3 of the original HIV proteins) further lowers the biohazard level (Biosafety level 2). The resulting LVs are also self–inactivating because of the U3 region being deleted from long terminal repeats (LTR), which are duplicated when the virus infects the host cell. The duplication of this deletion results in transcriptional inactivation of the virus (Zufferey et al., 1998).

The production of LVs was achieved by simultaneous transfection of HEK293 cells with three different plasmids: pMD-2G, pCMV and pWPI or pWPT-GFP (Figure 58)

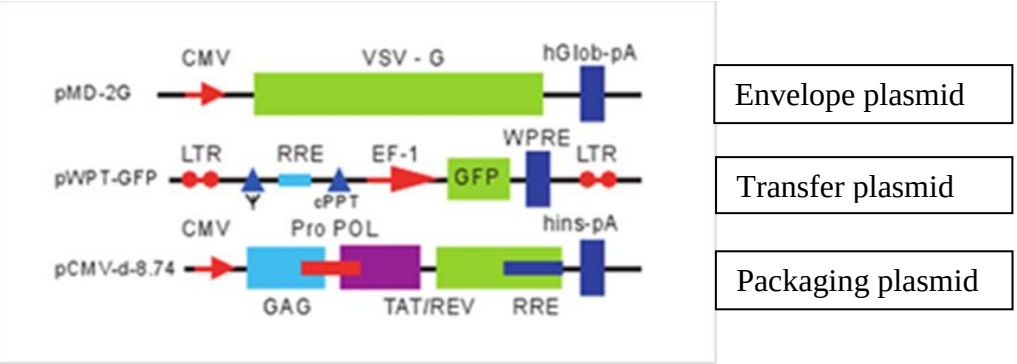

Figure 58. Schematic representation of pMD-2G, pWPT-GFP and pCMV plasmids. DNA sequences encode the following proteins: CMV – cytomegalovirus promoter, VSV-G – vesicular stomatitis virus glycoprotein, hGlob-pA – human globin poly- adenylation site, LTR – long terminal repeats, ψ – encapsidation signal, RRE – rev responsive element, cPPT – central polypurine tract, EF-1 – elongation factor 1, GFP – green fluorescence protein, WPRE – woodchuck post-translational regulatory element, GAG – group specific antigen, TAT/REV – reverse transcriptase. hins-pA – human insulin polyadenylation sequence (Raghunath et al., 2008).

The recipient cells incorporated into their genome the sequences encoded by these plasmids and maintained stable expression of the gene of interest thanks to very efficient eukaryotic promoter – elongation factor 1 (EF-1) (found in the transfer plasmid), while other cytomegalovirus promoters (CMV) of envelope and packaging plasmid underwent gradual silencing (Radhakrishnan et al., 2008).

In the transfer plasmid (pWPT-GFP) internal ribosome entry site (IRES) for co-expression of GFP, a reporter of viral genes expression or the gene of interest was flanked with post-translational regulatory element (WPRE), that promotes an effective polyadenylation of the transcript and can increase the total amount of the required product (Li et al, 2012). The plasmid contained also rev responsive element (RRE) – regulatory protein essential for post-transcriptional transport of the unspliced and incompletely spliced viral mRNAs from nuclei to cytoplasm (Lesnik et al., 2002), flanked with highly conserved ψ – encapsidation signal and sequences for central polypurine tract (cPPT), protecting lentiviruses from editing by cytidine deaminases (Wurtzer et al., 2006).

The envelope plasmid (pMD2G) encoded vesicular stomatitis virus glycoprotein (VSV-G) that increased the viral tropism for neurons and ended with human globin poly-adenylation site (hGlob-pa) which affects stability, translation and efficiency of viral transfection/transduction (Beaudoing et al., 2000).

Integration of viral elements was possible due to the pol sequence (incorporated into the pCMV plasmid) that encodes reverse transcriptase (REV), integrase and RNAase H activity (Samlon and Trono, 2006). Reverse transcription followed sequential steps, during which first (minus) strand of DNA uses genomic viral RNA as a

template and is initiated by a tRNA primer that defines the 3′ boundary of the U5 region of the long terminal repeat (LTR). The second (plus) strand of DNA uses minus-strand DNA as a template (Smith et al., 1984). pCMV plasmid contained also gag gene, which is a codon for optimum efficiency of viral matrix proteins, RNA genome binding proteins and other proteins comprising the nucleoprotein core particle (Raghunath et al., 2008). In addition, TAT protein acts as a transcriptional factor and RRE is required for expression of unspliced, packageable transcripts. The structure of packaging plasmid ended with human insulin polyadenylation sequence (hins-pA), playing role in the effective transfection/transduction of this construct (Levy et al., 1995). As mentioned before, the end sequence, coding the surface glycoprotein is completely deleted from this plasmid to reduce the virus pathogenicity and making this system very safe and efficient tool that to transduce neurons *in vivo* in rodents (Galimi and Verma, 2002; Azzouz et al., 2004, O'Leary et al., 2013).

The novel experimental strategy was adapted to re-direct the tropism of lentiviruses to BFCNs (Figure 59). Briefly, biotynylated LentiGFP was combined through streptavidin to anti-p75^{NTR} IgG, conjugated to streptavidin. The reaction of biotin with streptavidin occurs within seconds and is one of the strongest non-covalent interactions known in nature, which enabled to prepare anti-p75^{NTR}-LentiGFP vector. This vector was tested on BFCNs *in vitro* and *in vivo* to verify p75^{NTR} as a molecular target for gene therapy of BFCNs in AD.

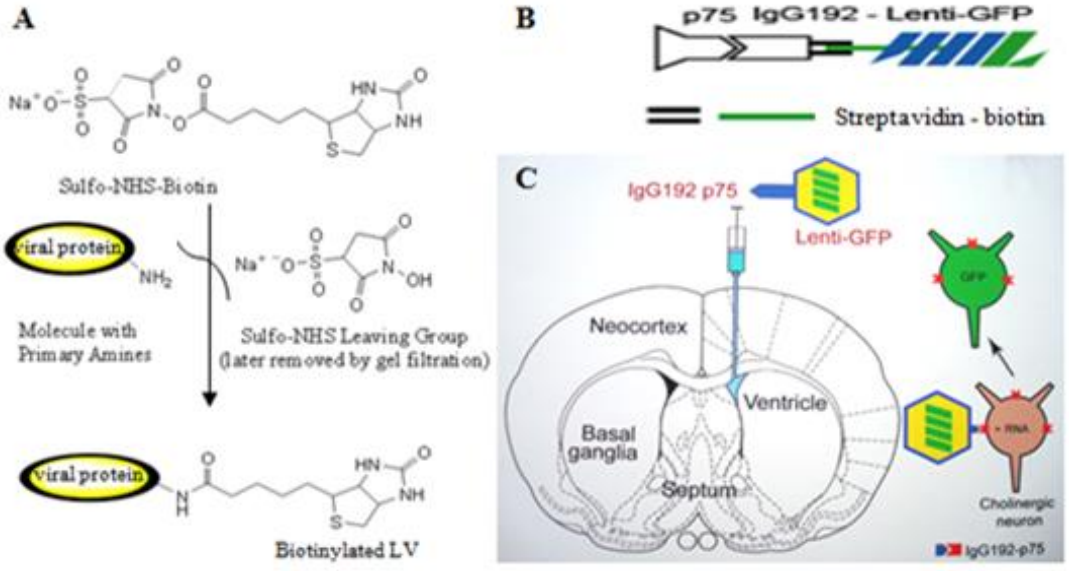

Figure 59. Strategy for LVs delivery of GFP into BF cholinergic neurons. A. Principle of LVs biotinylation. NHS ester group on this regent reacts with amine or lysine residues of protein to produce a stable product. B. Schematic of conjugating biotynylated LVs to anti-p75IgG through streptavidin. C. Illustration of icv injection of 192IgG-LentiGFP particles into ventricle of rodents' brain.

5.2. Optimization of lentiviral vectors titter

Lentiviral particles were produced according to procedures described in Chapter 2.6. Pure DNA proved to be critical for production of high number of lentiviral vectors. DNA quality was justified as described in Chapter 2.6.6., example Figure 60.

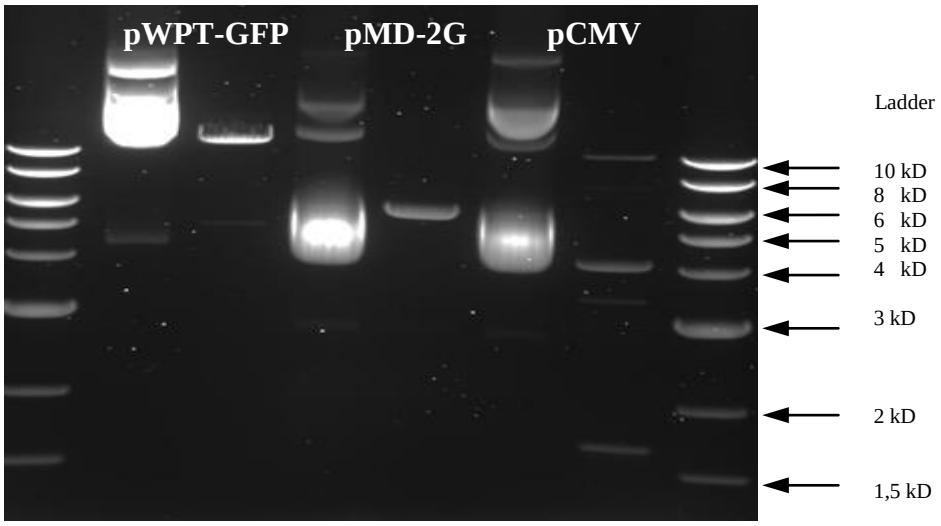

Figure 60. Quality check of lentiviral plasmid DNA before cells transfection. DNA sizes of pWPT-GFP (9495bp), pMD-2G (5824bp), and pCMV (11921bp) plasmids (lanes 1) confirmed with restriction-digest reactions with Bam H1 (lane 2), Pst I (lane 4) and EcoR1, with XhoR1 (lane 6) compared to DNA ladder marker.

In result of using high quality material I doubled the number of LentiGFP viral vectors produced initially (Figure 61C).

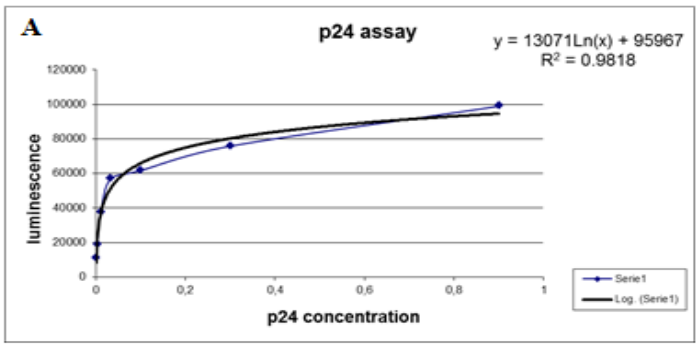

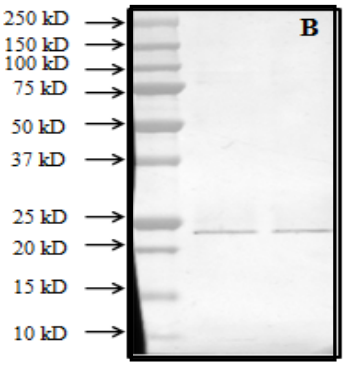

C

Batch no	ng/ml	No. of Lentiviral particles (Lvs)/ml	No. of infectious units (IUs)/ml
1	44	$44x10^8$ LVs/ml	$4.4x10^6$ IUs/ml
2	70	$70 x 10^8$ Lvs/ml	$7.0 x10^6$ IUs/ml
3	90	$90 x10^8$ LVs/ml	$9.0 x 10^6$IUs/ml

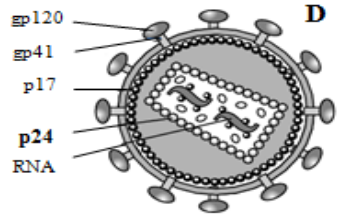

Figure 61. Optimization of LVs titter. A. Standard curve typical for chemiluminescent reading of p24 antigen standards with CSPD substrate for alkaline phosphatase. B. Detection of p24 lentiviral protein on WB of 12% polyacrylamide gel. C. Lentiviral titters improved across the production of different batches. D. Schematic of HIV-1with p24 core protein highlighted.

5.2.1. The viability of LentiGFP virus in HEK 293FT cells

The viability of LentiGFP virus was checked with HEK 293FT cells, prepared as in Chapter 2.6.7., which were infected with different dilutions of freshly made LentiGFP viruses. The presence of GFP was assessed by fluorescent microscopy after 24 and 48h (Figure 62A and B).

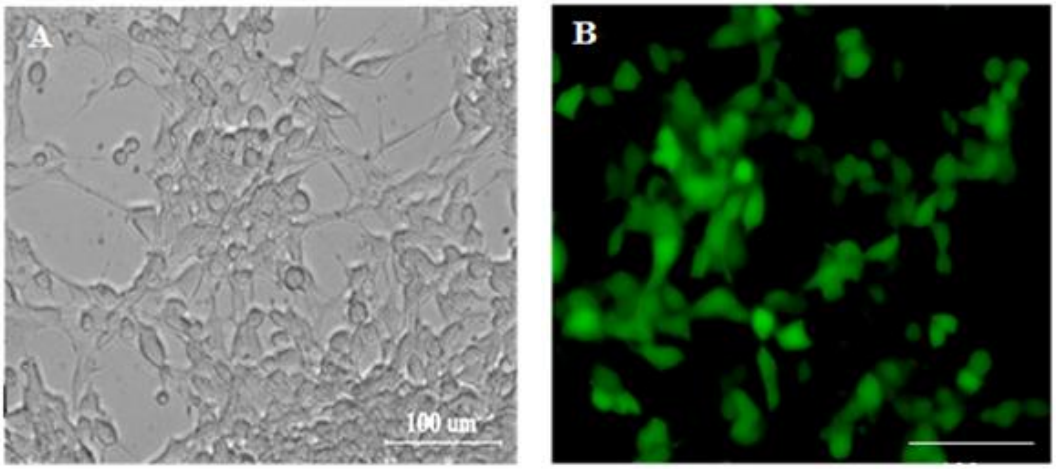

Figure 62. Transient transfection of HEK 293FT cells with lentivirus expressing GFP. A. HEK293FT cells in culture. B. Fluorescent image of HEK293FT cells 48 h after transfection with LentiGFP viruses (7.0 x 10^6 IUs/ml).

The viability of LentiGFP viruses was also checked on neuronal cells in BF cultures. 2 µl of 9.0 x 10^6 IUs/ml LentiGFP vectors was kept up to 48 h on culture dishes. Then medium was removed and cells were stained with 4',6-diamidino-2-phenylindole (DAPI) and fixed with 4% PFA in PBS for 30 min. After this step, dishes were washed and coverslipped (Figure 63A and B)

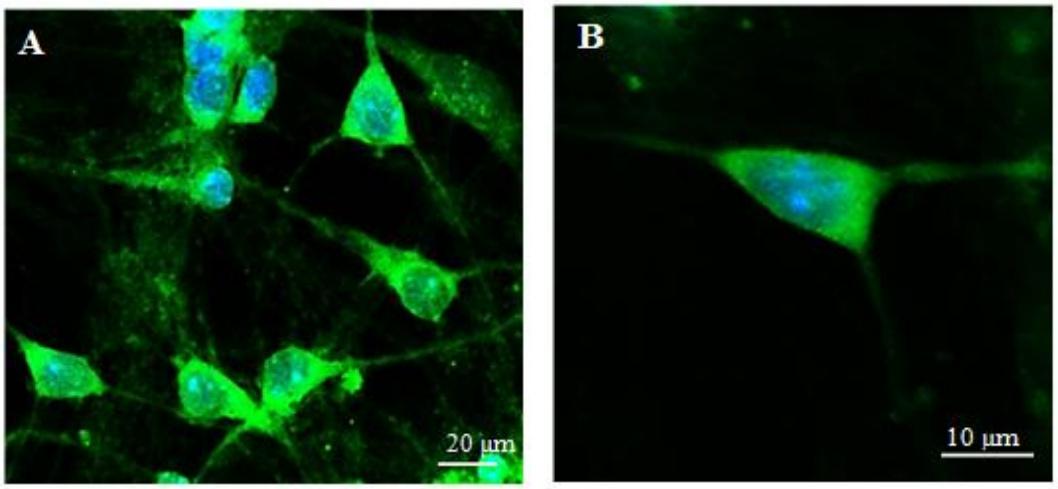

Figure 63. Viability of Lentiviral vector in p7 BF culture. Mouse BF culture infected with 2µl of LentiGFP (9.0 x 10^6 IUs/ml), co-stained with DAPI. B. Enlarged view of a neuron infected with lentivirus expressing GFP and stained with DAPI.

5.2.2. Efficiency of viral infection

The extent of HEK 293FT cells infection was measured after 48 h by flow cytometry (BD FACS Aria I), which sorted cells expressing green fluorescence protein (GFP), encoded by the lentiviral vector from the ones that did not get infected (Figure 64). For this experiment, infected and control HEK 293FT cells were transferred to FACS solution containing 10% FBS in PBS, pH=7, 4.

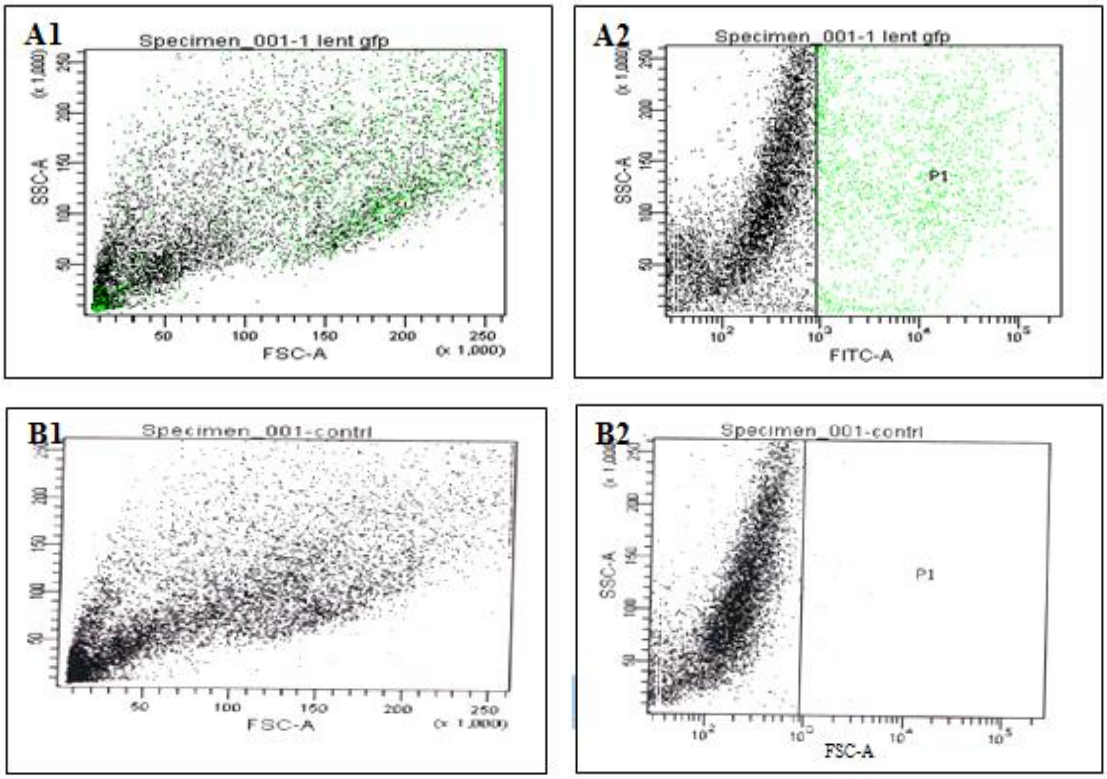

Figure 64. Extent of infection by LentiGFP checked by fluorescence activated cell sorting (FACS). A1. Dot plot showing HEK293FT cells infected with 1 µl of LentiGFP (7.0x 10^6 IUs/ml) after 48h compared to the control in B1 [A2, B2 – forward scatter (FSC) threshold gate].

1µl LentiGFP

Population	#Events	%Parent	SSC-A Mean	FITC-A Mean
All Events	10,000	####	125,840	6,823
P1	2,887	28.9	187,693	22,957

0.1 µl LentiGFP

Population	#Events	%Parent	SSC-A Mean	FITC-A Mean
All Events	10,000	####	118,727	1,236
P1	1,071	10.7	215,870	9,584

control

Population	#Events	%Parent	SSC-A Mean	FITC-A Mean
All Events	10,000	####	91,720	207
P1	201	2.0	238,364	1,733

Table 7. FACS data from LentiGFP infection of HEK293FT cells. Abbreviations: FITC – fluorescein isothiocyanate, P1 – infected cells, SSC – side scatter.

Lentivirus (1 µl) (7.0 x 10^6 IUs/ml) was able to transduce 28.9 % cells as shown in Table 7 versus total cells (all events) sorted.

5.3. Optimization of anti-p75^{NTR}-LentiGFP viral production

Anti-p75^{NTR}-LentiGFP viral vectors were produced according to the procedures described in Chapters 2.7. However to get high quality, effective particles these procedures were optimized. The critical steps involved using high quality material verified by biochemical assays (HABA) and WBs (Figures 65 A-D). Purification of biotynylated LVs by dialysis was also critical.

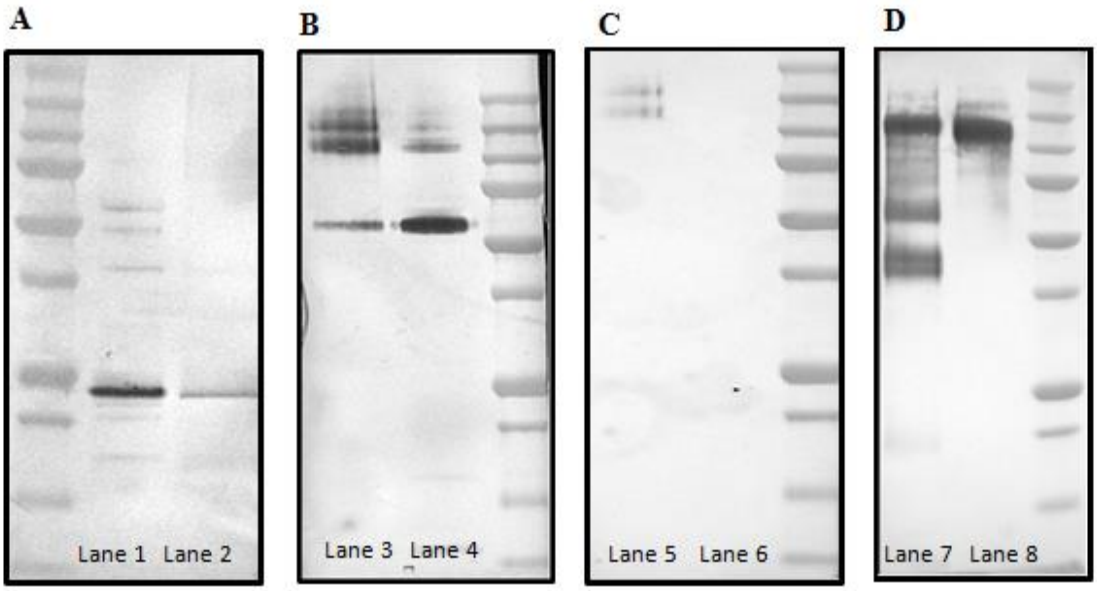

Figure 65. Construction of anti-p75^{NTR}-LentiGFP vector targeting cholinergic neurons of BF. A. p24 antigen (MW=24kD) detected in the sample with raw lentivirus (Lane 1) and biotynylated lentiGFP vector (Lane 2). B. VSV-G protein (MW=57kD) detected with anti-VSV-G IgG in raw (Lane 4) and biotynylated (Lane 3) lentiGFP vector. C. Backbone (fragment of 2 heavy and 2 light IgG chains) of p75IgG detected with anti-p75IgG in anti-p75^{NTR}-LentiGFP construct (Lane 5) against raw lentiGFP particles (Lane 6). D. Original anti-p75IgG from Millipore (Lane 7) run against streptavidin conjugated one (Lane 8). All WBs were run on 12% polyacrylamide gels along with standard molecular marker (Materials and Methods)

During this process, the titter of original lentivirus dropped as shown in Figure 65A, lane 2. The biotynylation of envelope proteins were additionally confirmed with anti-VSV-G antibody as indicated on Figure 65B, lane 3. Full anti-p75^{NTR}-LentiGFP construct was run on the gel shown on Figure 65C, lane 5 and compared with non targeted vector. However, because only the fragment of p75^{NTR} IgG was detected in targeted construct, the original anti-p75^{NTR} IgG from Millipore was shown on Figure 65D before and after streptavidin conjugation process. Full verification of constructed anti-p75^{NTR}-LentiGFP vectors included their viability testing in BF cultures and *in vivo*.

5.4. Transduction of anti-p75^{NTR}-LentiGFP vectors in BFCNs *in vitro*

The anti-p75^{NTR}-LentiGFP vectors produced earlier were tested onto cholinergic cells in rat primary BF culture. Anti-p75^{NTR}-LentiGFP (2 µl) (9.0 x 10^6 IUs/ml) were added for 48 h to primary rat BF cultures [2ml volume (0.7 x 10^6 plating density (9.62 cm^2/35 mm dish)]. After that time, dishes were fixed with 4% PFA, pH=7,4 for 30 min and washed with PBS, pH=7,4 before viewing. These vectors were able to transduce BFCNs as confirmed by double staining of BFCNs with 192-IgG-Cy3 (4.7 nM) added for 2h to the culture dishes before fixing them as usual (Figure 66).

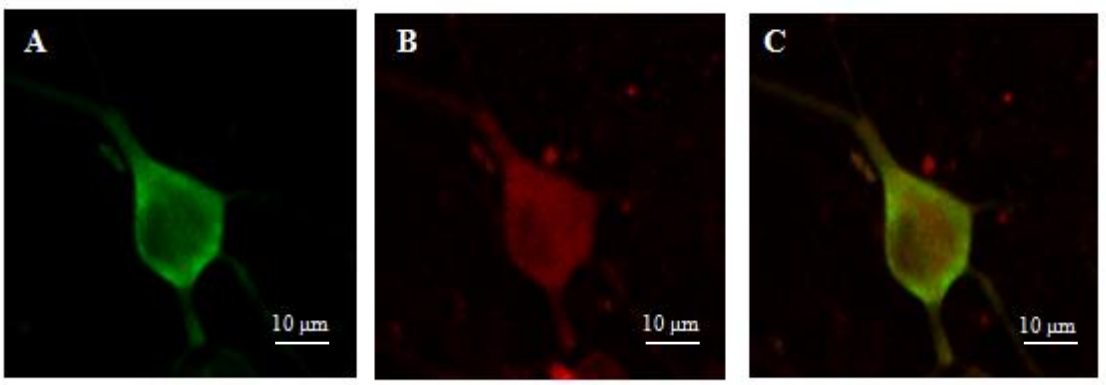

Figure 66. Enlarged view of BFCN transduced by anti-p75^{NTR}-LentiGFP vector in rat primary BF cultures. A. Neuron from p7 rat BF culture infected with anti-p75^{NTR}-LentiGFP (9.0 x 10^6 IUs/ml). B. Same cell fixed with 4%PFA and stained with 192-IgG-Cy3. C. Merged image of A and B.

5.5. Anti-p75^{NTR}-LentiGFP vectors transduce cholinergic neurons *in vivo*

All surgical procedures were conducted in accordance to SOPs written for ICNT on basis of the literature available (Cetin at al., 2006.) and approved by the Research Ethics and Biosafety Committees of DCU. The experiments were licensed by the Department of Children and Health, Ireland and based on pilot data (Figure 67).

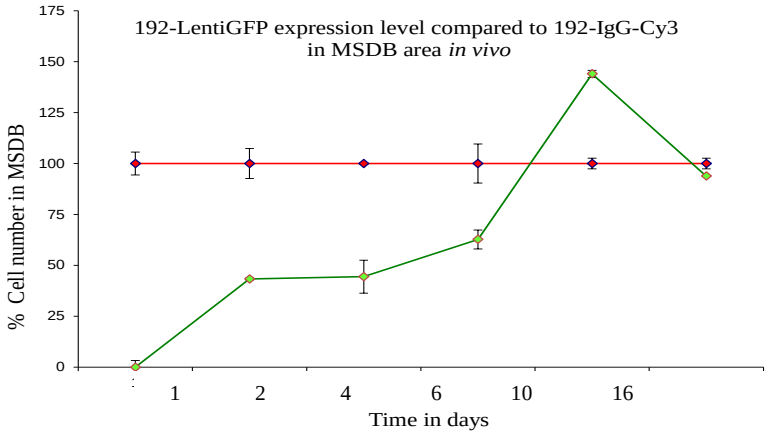

Figure 67. Trend in anti-p75^{NTR}-LentiGFP expression level compared to 192-IgG-Cy3 based on cell counting in MSDB area.

The constructed anti-p75^{NTR}-lentiGFP vector (5 µl, 7.0 x 10^7 IUs/µl) was unilaterally injected (0.2 µl/min) into 21 days old Spraque Dawley rats (3 groups, n=5) according to stereotactic coordinates: AP = -0.8 mm; ML=1.2 mm; DV = 3 from Paxinos and Walsh rat brain atlas (1998) and left for recovery time (2, 4, 6 weeks). A group of the same animals (n=3) received also icv injections of 192-IgG-Cy3 (5µl) a week later (Materials and Methods, Chapter 2.5.). This time point was concluded from preliminary experiment illustrated in Figure 67. Control experimental group was injected with saline (0,9% NaCl) and non-targeted LentiGFP (5 µl, 7.0 x 10^7 IUs/µl) (n=3 for each group). The animals were perfused at the time point (2, 4 and 6 weeks post initial injection) (Materials and Methods, Chapter 2.1.3.) and coronal sections of their brains cut (30 µm) before mounting and viewing (Figure 68).

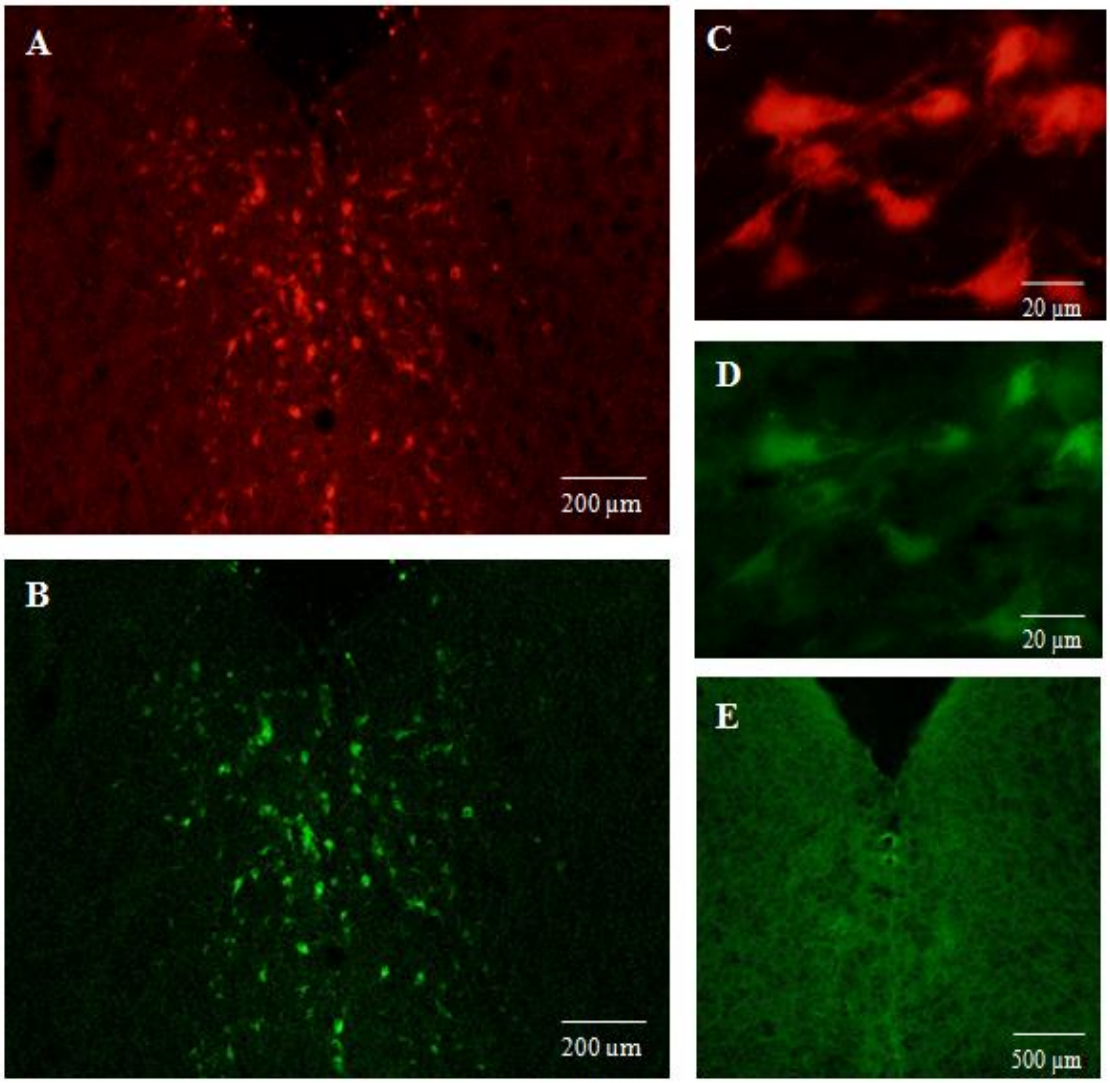

Figure 68. Transduction of BFCNs by anti-p75^{NTR}-LentiGFP *in vivo*. A. Control injection of 192-IgG-Cy3 marking BFCNs. B. Anti-p75^{NTR}-LentiGFP signal in cholinergic cells of MSDB. C. Enlarged view of BFCNs labelled with 192-IgG-Cy3. D. BFCNs transduced by anti-p75^{NTR}-LentiGFP vector (5 µl, 7.0 x 10^7 IUs/µl) – enlarged area (same area) as in C. E. Control MSDB area without any injections.

The signal for anti-p75^{NTR}-LentiGFP vector was detected in medial septum (MS) and the nuclei of the diagonal band of Broca (DBB) with vertical and horizontal limbs areas (VDBB (Ch2) or HDBB (Ch3), respectively. GFP–positive and p75^{NTR} positive cells were counted at experimental time points 2, 4 and 6 weeks. (Figure 69).

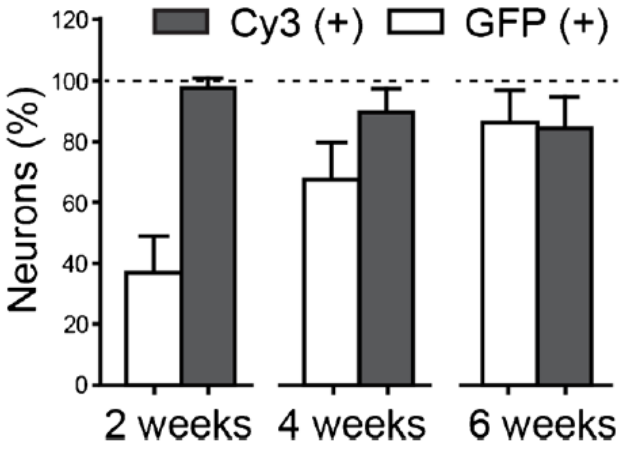

Figure 69. Quantification of neurons labelled with anti-p75^{NTR}-LentiGFP and 192-IgG-Cy3. Strong co-labelling of Cy3-positive neurons with GFP reporter at later time points (4 and 6 weeks).

Counting of cholinergic neurons revealed that all GFP-positive neurons in BF were also labelled for 192-IgG-Cy3. These neurons exhibited enhanced GFP labelling over time (Figure 69). GFP labelling was also visible along the injection track through the motor cortex (M2) with the green signal present within ventral corpus callosum and ventricular wall and few green neurons scattered within the dorsal septum, ventral areas of pallidum and caudate areas (Figure 70).

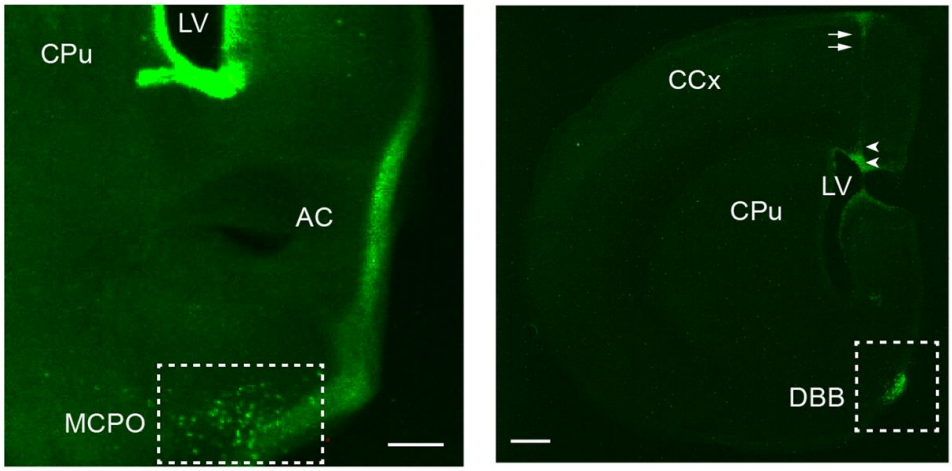

Figure 70. GFP-fluorescence along the injection track and adjacent areas. BF regions in dashed boxes. Arrow heads point to lateral ventricle while arrows show ventral corpus collosum in higher magnification image. Abbreviations: LV- lateral ventricle, CpU – caudate putamen, AC nucleus accumbens, MCPO – magnocellular preoptic area, CCx – cerebral cortex, DBB – diagonal bands of Brocca

In controls intraventricular injections of non-targeted LentiGFP also caused pronounced labelling of cells of ventricular wall and underlying glia with sparse GFP-positive neurons visible in adjacent dorsolateral and medial part of caudate nucleus. In regards to MS and DBB, GFP-labelled cells constituted around 5% and 0.4% of cholinergic cell population respectively (n=3, 6 weeks post injection) as revealed by ChAT-staining (figure 71).

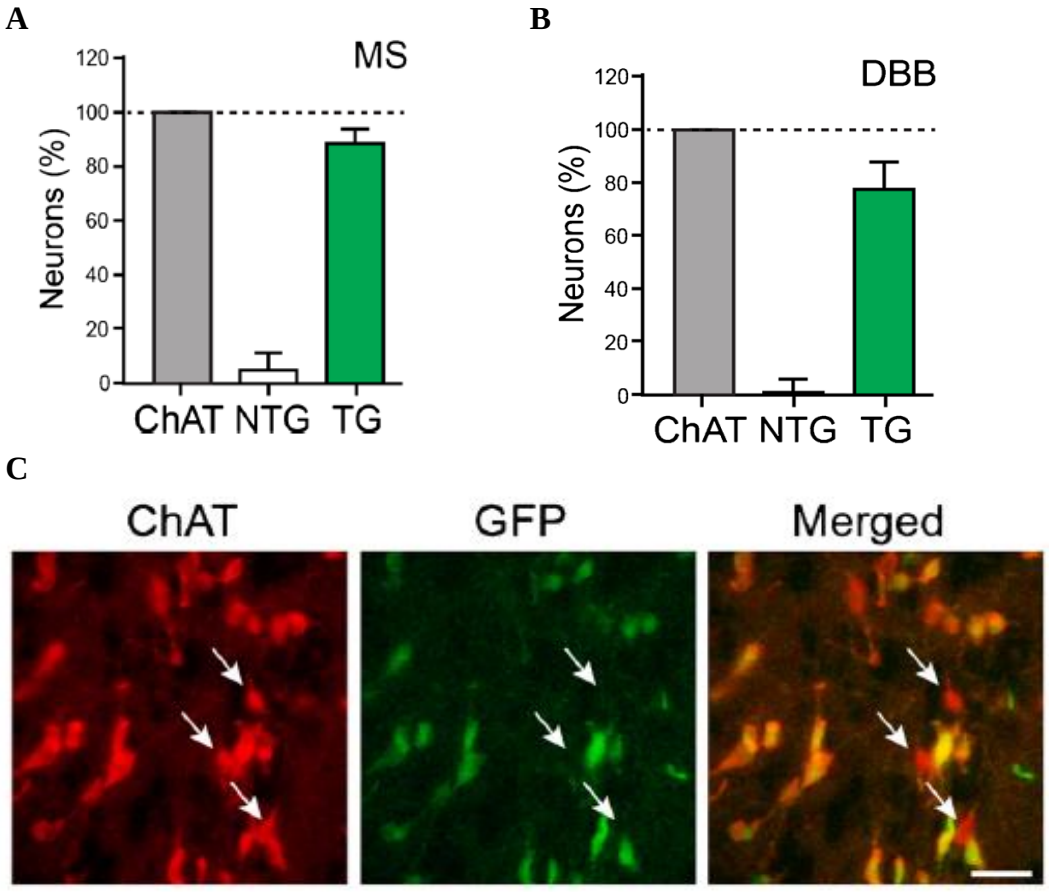

Figure 71. Double labelling of cholinergic neurons transduced with targeted (TG) versus non targeted (NTG) LentiGFP vectors revealed by ChAT staining. A. MS area of BF. B. DBB area of BF. C. Example of double immunohistochemistry for ChAT and GFP protein in the above areas. Arrows point to non-targeted cholinergic cells.

Altogether these data demonstrate that $p75^{NTR}$ can robustly facilitate transduction of viral vectors to BFCNs. The increase of GFP signal in transduced neurons over time was most probably caused by gradual accumulation of GFP protein in BFCNs. This finding is significant for AD gene therapy, which so far struggle with targeting therapeutics into BF. Best treatment for AD is up to now achieved with NGF (reviewed in Chapter 1.6), however this molecule binds not only $p75^{NTR}$ but also other TrkA receptors elsewhere and may lose its binding abilities when biotynylated as was already reported (Rosenberg et al., 1986).

5.6. Discussion on the role of lentiviral vectors in AD therapy

In this chapter, replication-deficient LVs pseudotyped with VSVG were successfully constructed from three independent plasmids: pMD-2 G, pWPT-GFP or modified pWPI and pCMV as already reported (Tiscorniaet al., 2006). The high titter of these viruses enable robust transduction of HEK 293FT cells and neurons in primary BF cultures. The best effects were achieved within 24 - 48 hours expression of the LentiGFP viruses.

Same viruses was targeted to cholinergic neurons of BF. For this purpose I utilized unique biological feature of BFCNs – the expression of $p75^{NTR}$ (reviewed in Chapter 1.5.3.2.1.). I modified lentiviral particles to target this receptor. This was achieved through biotynylation of lentivirus containing the reporter protein GFP and combining it with anti-$p75^{NTR}$ antibody through biotin – streptavidin covalent bond. Conjugation of anti-$p75^{NTR}$ with streptavidin antibody had proceeded this step. Effective conjugates of small fluorescent probes and active proteins to anti-$p75^{NTR}$ 192 IgG were shown earlier, confirming the stability of this approach (Wiley et al., 1991; Rossner et al., 1995; Hartig et al., 1998). Streptavidin-biotin conjugates have been also successfully applied before for targeting vectors in various experimental models (Lesch et al., 2010; Waehler et al., 2007). The virus after the biotynylation was purified using dialysis to achieve high quality of vectors targeting BFCNs. These vectors successfully transduced cholinergic neurons of BF in rat primary culture prior to *in vivo* verification.

To find out if $p75^{NTR}$ can facilitate transduction of viral vectors to BFCNs *in vivo* I injected the anti-$p75^{NTR}$-LentiGFP construct and naive LentiGFP vectors into lateral ventricle of the rats' brains. The receptor-antibody-virus complex get internalized by cholinergic terminals and underwent retrograde trafficking to the cell bodies where it yield robust expression of GFP in MSDB areas, seen best 7 days after the injection and monitored up to 6 weeks post injection. Non targeted vectors caused pronounced labelling of cells of ventricular wall with some cells scattered in dorsolateral and medial direction. Thus the proof of principle was obtained for the effective and selective targeted transduction BFCNs through $p75^{NTR}$ *in vivo*.

This is a very promising result for further research of AD and eventual gene therapy to AD. Thanks to large capacity of lentiviral viruses (reviewed in Chapter 5.1) further genes can be introduced along with GFP reporter protein to counteract

deleterious effects of Aβ, tau hyperphosphorylation, modulate AChE activity or enhance lysosomal or mitochondrial function.

The protection of BFCNs from harmful Aβ effects could be achieved for instance by introduction of Fe65 genes while using the above strategy. Fe65 belongs to family of adaptor, scaffolding proteins acting downstream APP signalling, which are reported to reduce the risk of development late onset of AD (Hu et al., 2002; Lambert et al., 2000) if associated with the expression of full-length variant of Fe65 protein (Wang et al., 2004). The Fe65 family consists of three members: Fe65, Fe65-like 1 (Fe65L1) and Fe65L2 (Bressler et al., 1996; Blanco et al., 1998) from which Fe65 is expressed exclusively in brain (Hu et al., 1999; Kesavapany et al., 2002) while Fe65L1 or Fe65L2 are more widely distributed. Fe65 protein has a multi-domain structure as illustrated on Figure 72.

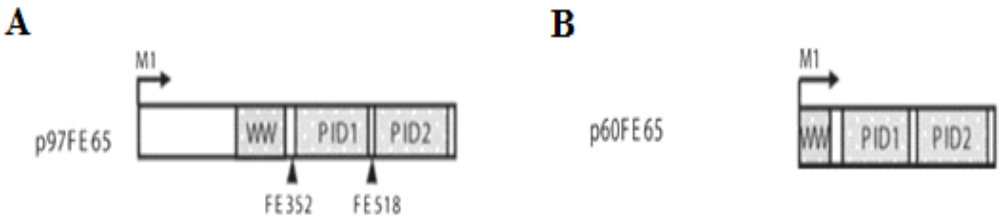

Figure 72. Schematic illustration of Fe65 isoforms. A) The full length Fe65 (p97Fe65) contains three domains: WW important for Fe65 transcriptional function (Cao and Sudhof 2001; Minopoli et.al., 2001) and two C-terminal phosphotyrosine interaction domains (PID1 and PID2) important for AICID binding ability B. Fe65short isoform (p60Fe65) that lacks WW.

Fe65 forms complexes with a variety of binding partners to exert a number of functions in the brain that may include modulation of APP processing (Sabo et. al., 1999; Pietrzik et al., 2004; Hu et al., 2005) plasma membrane dynamics (including neurite outgrowth and neuronal positioning) (Sabo et. al., 2001 and 2003; Guenette et. al., 2006; Ikin et al., 2007) and transcriptional activation (Cao and Sudhof, 2001; Yang et. al., 2006). The functional significance of these interactions require additional research and especially roles of Fe65 isoforms in learning and memory needs to be determined.

By this occasion it is important to discuss the feasibility of using viral vector gene delivery as a treatment for AD in the clinic. Generally it offers unique advantages over the traditional therapeutic methods as it theoretically permits generation of active drugs at the sites where they are mostly needed. The attempts have been made

so far to deliver NGF using adeno-associated viruses (Mandel et al., 1999) and lentiviruses (Blesch et al., 2005) or improved tetracycline-dependent lentiviral vectors, regulating transgene expression *in vivo* (Vigna et al., 2005). However, all these systems lack of adequate efficacy. In some cases they brought unexpected and undesirable side effects. In general, the magnitude and consistency of their clinical benefits were disappointing. By far the most consistently proposed reason for their side effects and poor efficacy has been inadequate dosing and delivery. The creation of CERE-110 (AAV2-NGF) vector system for dose dependent delivery of NGF has been reported (Bishop et al., 2008). Recently AAV2-NGF vectors were stereotaticly injected to nucleus basalis of Meynert in clinical trial Phase 1 clinical study to AD (Rafii et al., 2014). However these vectors still have broad tropism to the neuronal cells. Given very complex nature of the BF region they may cause not favourable side effects in the longer term. Therefore the method presented in this thesis offers better choice for targeting BFCNs, due to the unique expression of $p75^{NTR}$. Moreover, LVs can efficiently deliver genes of interest due to their large capacity. They are also able to maintain long-term expression. What is important, these vectors can be easy generated in high titters, and do not give immunological complications. This means they can be safely produced for clinical applications. By far many animal studies have demonstrated the effectiveness of LVs to deliver therapeutic genes into the nervous system, as well as to model human diseases (Shaughnessy et al., 2005; Nanou and Azzouz, 2009). Certain limitations of LVs can be even beneficial e.g. they limited intra-axonal mobility. Only few GFP-positive cells were found scattered in this study after LentiGFP icv. The lack of retroaxonal transport already proved to be beneficial in other applications of these vectors (O'Leary et al., 2013; Ovsepian et al., 2015). More and more human gene therapy clinical trials are underway using LVs in a wide range of human diseases (Escors and Breckpot, 2010; Kumar and Woon-Khiong, 2011). Lentiviral vectors applications proved to be beneficial especially in those trials where other method were difficult to apply (Kantor et al., 2014). Moreover, these vectors can be used to reprogram cells, generate iPSCs and silence genes by combination with siRNA and microRNA-based technologies what is putting them at forefront of gene delivery systems for research and clinical applications (Rubinson et al., 2003; Nethercott et al., 2011). Therefore the use of proposed targeted LVs for potential delivery of therapeutic genes into BFCNs becomes fully justified, given high complexity of cholinergic system of BF.

Chapter IV. Summary and Final Conclusions

There is no doubt that AD is one of the most complex illnesses known of the aged human brain. It is characterised by specific neuropathological changes in certain brain regions, (reviewed in Chapter 1.4.) but a cascade of molecular events leading to these alterations remains elusive, despite many years of scientific investigations. Last century brought numerous hypothesis of AD (reviewed in Chapter 1.5.) with amyloid cascade hypothesis prevailing in this area of research (Chapter 1.5.1). Although this hypothesis is based on the solid data it does not explain why Aβ is preferentially deposited in the certain sections of brain, while sparing the others. Similarly cholinergic hypothesis (reviewed in Chapter 1.5.3.) is not fully able to explain this phenomenon. Likewise, it does not clarify why cholinergic projections not the others are vulnerable to the disease process. Moreover, it is of note that Aβ plaques does not always correlate with severity of cognitive decline. Importantly also the cholinergic drugs (e.g. AchE inhibitors reviewed in Chapter 1.6.) meet only with partial success in the treatment of AD. Even more challenging are the reports doubting the selective loss of cholinergic neurons as well as the causal relationship between the degeneration of cholinergic projections with plaque- or tangle-related pathology. Recent theories undertake these challenges and are viewing the basal high metabolic activity of certain areas of brain as main cause of region-specific Aβ depositions (e.g. DMN hypothesis reviewed in Chapter 1.5.7.), which is supported by previous research suggesting the causal relationship between synaptic activity and Aβ production (Cirrito et al., 2005). This hypothesis however does not explain why sporadic AD strikes some individuals not the others. There is also poor overlap between DMN hypothesis and cholinergic one, particulary in regards to the susceptibility of cholinergic neurons to AD. In summary further research is needed to decipher still unknown mechanisms of AD. There is great scope for investigations of novel molecular targets and designing new therapeutics to fight with this devastating disorder.

In this research I focused on $p75^{NTR}$ because this receptor is unique for cholinergic neurons and it is expressed not only during brain development but also throughout adulthood by these cells. The level of $p75^{NTR}$ is significantly elevated with aging and further activated by Aβ in AD brain, with the meaning of this appearance remaining unclear (Zeng et al., 2011). $P75^{NTR}$ has a number of functions in the BF which include neuronal apoptosis, cell survival and differentiation, neurite outgrowth and others (reviewed in Chapter 1.5.3.2.1.) that depend on ligands it binds to. NGF gene

therapy is currently viewed as very promising approach for the treatment of AD in the clinic (Tuszynski et al., 2015), which is pointing further to the relevance of $p75^{NTR}$ as an important molecular target. $P75^{NTR}$ biology is unique for TNFRSF as this receptor interacts with non-neurotrophic ligands including Aβ – main culprit of AD. Interestingly Aβ binds to $p75^{NTR}$ with even higher nanomolar affinity than NGF (Kd=12nM for Aβ; Kd=7nM for NGF), stressing further the importance of $p75^{NTR}$ to neurodegenerative processes in AD. All these facts made $p75^{NTR}$ worth investigation, despite the existence of others multiple receptors implicated in AD pathology.

Surprisingly, not much research was done up to date for $p75^{NTR}$ internalization, especially its uptake apart from TrkA co-receptors that mediate neuronal survival. Therefore this thesis constitute valuable asset to the knowledge of $p75^{NTR}$ biology and function. My experiments confirmed that Ca^{2+} influx through T-type and L-type channels with mobilization of intracellular Ca^{2+} stores are needed for triggering the endo/exocytosis of $p75^{NTR}$. Indeed, the specific calcium channels blockers (mibefradil and nifedipine for T and L type Ca^{2+} channels, respectively) significantly decreased $p75^{NTR}$ uptake by BFCNs in culture (Chapter 4.4.2.). Likewise, the inhibitors of SERCA pump ATPase – thapsigargin or cyclopiazonic acid, brought similar effects. Chelating extracellular Ca^{2+} in cultured medium with EGTA also inhibited the endocytosis of $p75^{NTR}$. These findings are important as they are linking $p75^{NTR}$ biology to the Ca^{2+} homeostasis, that is known to be altered during AD (reviewed in Chapter 1.5.1.2.).

Other experiments supported basal constitutive endo/exocytosis of $p75^{NTR}$ that is increased by K^{+} depolarization but seems to be independent from regulated synaptic activity as found by tests with potassium channel blocker – TTX (Chapter 4.4.1.) and confirmed later with *Clostridial Botulinum* neurotoxins BoNT/A and BoNT/ B - the potent inhibitors of the membrane turnover.

Because Aβ, the product of endogenous cleavage of APP (process reviewed in Chapter 1.5.1) is a culprit of neuronal death I investigated the influence of oligomeric forms of Aβ on the endocytosis of $p75^{NTR}$. These forms of Aβ are known to be the most neurotoxic and have higher affinity for $p75^{NTR}$ than soluble amyloids. The experiments were design carefully with sub-cytotoxic concentrations of aggregated Aβ not to cause BFCNs death. In these experiments I found out that oligomeric forms of Aβ inhibit $p75^{NTR}$ uptake in a dose dependent manner (Chapter 4.5.1.).

P75^{NTR} trafficking together with Aβ (1-42) was also followed by confocal microscopy in live BFCNs and SCGNs with parameters of this movement established (Chapter 4.3.1. and 4.3.2.). Although p75^{NTR} entry to these cells remains elusive, with no doubt p75^{NTR} is directing its cargo for degradation in lysosomal compartments of BFCNs as shown by investigation of p75^{NTR} immobilization in different endosomes (Chapter 4.7). This is in agreement with previous literature suggesting that phosphorylation of p75^{NTR} is a sorting signal for delayed degradation of neurotrophins after retrograde axonal transport (Butowt and Bartheld, 2009). This finding was also confirmed in chemically induced animal model with 192-IgG-SAP, resulting in the increased deposition of Aβ (1-42) in hippocampal and cortex formation after deletion of cholinergic neurons through their ribosomal inactivation (Chapter 3.5.6.1.) and discussed in Chapter 3.6.

In summary these results suggest possible Aβ clearance by cholinergic neurons and together with *in vitro* results showing p75^{NTR} uptake dependent on the amount of Aβ oligomers, they suggest a new role of p75^{NTR} in maintaining Aβ homeostasis in the brain through the diffuse cholinergic projections. This challenge the traditional view of cholinergic system, seen so far as neuromodulatory arrangement coordinating ACh supply to the targeted brain areas (reviewed in Chapter 1.5.3.1. and 1.5.3.2.). Thus the new role of cholinergic system beyond the cholinergic transmission is proposed and described in the recent publication (Ovsepian et al., 2016). Cholinergic fibers enriched with p75^{NTR} and lacking post-synaptic specifications seem to be ideally suitable for maintaining physiological concentrations of Aβ in brain. Such view could also explain high selective vulnerability of BFCNs to Aβ damage during AD. The disrupted calcium homeostasis in aging could put the whole system of Aβ clearance into overdrive, causing disturbance of the clearance mechanisms and high vulnerability of cholinergic neurons to damage in AD in consequence. However further research is warranted to confirm these hypothesis.

In the light of the recent reports and clinical trials (Chapter 1.6.) p75^{NTR} become the valuable target for gene therapy to BF. By combining streptavidin biotin technology with modifications of lentivirus and anti-p75^{NTR} antibodies, I proposed designing of LVs targeting BFCNs (Chapter 5.1). These vectors effectively transduced BFCNs in culture (Chapter 5.4.1.) as well as *in vivo* (Chapter 5.4.2.) proving usefulness of this strategy for targeting LVs into BF, discussed in Chapter 5.5. Further research is currently ongoing on p75^{NTR} as a new molecular target (Tanaka et al., 2016).

Chapter VII. Appendix

7.1. Acknowledgments

I want to acknowledge funding bodies, thanks to whom this work was possible. The above experiments were supported by the Program for Research in Third Level Institutions Cycle 4 grant from Irish Higher Education Authority for the Neuroscience section of "Targeted-driven Therapeutics and Theranostics".

Thank you very much to Prof. Oliver Dolly for the opportunity of doing this work in International Centre for Neurotherapeutics (ICNT) at Dublin City University. Thank you to Prof. Jochen Herms from German Centre for Neurodegenerative Diseases, Munich, Germany for possibility of work in the laboratories there.

Thank you to Dr. Saak Ovsepian for supervising this project in both places.

Special thanks to Dr. Gary Lawrence for supervising me during laboratory rotation in ICNT and his many practical advice. Thanks also to Dr.Valerie O'Leary for help in viral part of this project; Dr. Arman Rahman for training in flow cytometry, and Dr. Saak Ovsepian for training and help in confocal microscopy, primary cultures and stereotaxic surgeries. Thank you to Liam Ryan for expressing and purifying BoNT/A and BoNT/ B, Carolyn Wilson for help in animal facility and all ICNT members.

Finally I would like to thank my parents and friends for their support during my study.

7.2. Bibliography

1. Abraham C.R., Selkoe D.J., Potter H. Immunochemical identification of the serine protease inhibitor alpha 1-antichymotrypsin in the brain amyloid deposits of Alzheimer's disease. Cell. 1988, 52(4), 487-501

2. Akama K.T., Van Eldik L.J. Beta-amyloid stimulation of inducible nitric-oxide synthase in astrocytes is interleukin-1beta- and tumor necrosis factor-alpha (TNF alpha)-dependent, and involves a TNF alpha receptor-associated factor- and NF kappa B-inducing kinase-dependent signaling mechanism. J Biol Chem. 2000, 275(11), 7918-24.

3. Alberdi E., Sánchez-Gómez M.V., Cavaliere F., Pérez-Samartín A., Zugaza J.L., Trullas R., Domercq M., Matute C. Amyloid beta oligomers induce Ca^{2+} dysregulation and neuronal death through activation of ionotropic glutamate receptors. Cell Calcium. 2010, 47(3), 264-72.

4. Albuquerque E.X., Pereira E.F., Alkondon M., Rogers S.W. Mammalian nicotinic acetylcholine receptors: from structure to function. Physiol Rev. 2009, 89(1), 73-120

5. Alcaro A., Huber R., Panksepp J. Behavioral functions of the mesolimbic dopaminergic system: an affective neuroethological perspective. Brain Res Rev. 2007, 56(2), 283-321.

6. Allen T.G., Abogadie F.C, Brown D.A. Simultaneous release of glutamate and acetylcholine from single magnocellular "cholinergic" basal forebrain neurons. J Neurosci. 2006, 26(5), 1588-95.

7. Alvarez A., Alarcón R., Opazo C., Campos E.O., Muñoz F.J., Calderón F.H., Dajas F., Gentry M.K., Doctor B.P., De Mello F.G., Inestrosa N.C. Stable complexes involving AChE and amyloid-beta peptide change the biochemical properties of the enzyme and increase the neurotoxicity of Alzheimer's fibrils. J Neurosci. 1998, 18(9), 3213-23.

8. Alvarez A., Opazo C., Alarcon R., Grrido J., Inestrosa N.C. Acetylcholinesterase promotes the aggregation of amyloid-beta-peptide fragments by forming a complex with the growing fibrils. J Mol Biol. 1997, 272(3), 348-61

9. Amadoro G., Corsetti V., Ciotti M.T., Florenazo F., Capsoni S., Amato G., Calissano P. Endogenous Aβ causes cell death via early tau hyperphosphorylation. Neurobiol Aging. 2011, 32(6), 969-90.

10. Anagnostaras S.G., Murphy G.G., Hamilton S.E., Mitchell S.L., Rahnama N.P., Nathanson N.M., Silva A.J. Selective cognitive dysfunction in acetylcholine M1 muscarinic receptor mutant mice. Nat Neurosci. 2003, 6(1), 51-8.

11. Anden, N.E., Dahlstrom, A., Fuxe, K., and Larsson, K. Mapping out of catecholamine and 5-hydroxytryptamine neurons innervating the telencephalon and diencephalon. Life Sci. 1965, 4, 1275-79.

12. Araujo D.M., Lapchak P.A., Robitaille Y., Gauthier S., Quirion R. Differential alteration of various cholinergic markers in cortical and subcortical regions of human brain in Alzheimer's disease. J Neurochem. 1988, 50(6), 1914-23.

13. Arendt T. Synaptic degeneration in Alzheimer's disease. Acta Neuropathol. 2009, 118(1), 167-79.

14. Archana M., Ramakrishnan S. Detection of Alzheimer disease in MR images using structure tensor. Conf Proc IEEE Eng Med Biol Soc. 2014, 1043-46

15. Ashe K.H. Learning and memory in transgenic mice modeling Alzheimer's disease. Learn Mem. 2001, 8(6), 301-8.

16. Ausubel L.J., Hall C., Sharma A., Shakeley R., Lopez P., Quezada V., Couture S., Laderman K., McMahon R., Huang P., Hsu D., Couture L. Production of CGMP-Grade Lentiviral Vectors. Bioprocess Int. 2012, 10(2), 32-43.

17. Aznavour N., Mechawar N., Descarries L. Comparative analysis of cholinergic innervation in the dorsal hippocampus of adult mouse and rat: a quantitative immunocytochemical study. Hippocampus. 2002, 12(2), 206-17.

18. Bali P., Lahiri D.K., Banik A., Nehru B., Anand A. Potential for Stem Cells Therapy in Alzheimer's Disease: Do Neurotrophic Factors Play Critical Role? Curr Alzheimer Res. 2016 [Epub ahead of print]

19. Banker D., Goslin K. Culturing nerve cells. 2nd ed. Cambridge, MA: MIT Press, 1998.

20. Barker P.A., Barbee G., Misko T.P., Shooter E.M. The low affinity neurotrophin receptor, p75LNTR, is palmitoylated by thioester formation through cysteine 279. J Biol Chem. 1994, 269(48), 30645-50.

21. Bartus R.T., Dean R.L. 3rd, Beer B., Lippa A.S. The cholinergic hypothesis of geriatric memory dysfunction. Science. 1982, 217(4558), 408-14.

22. Beaudoing E., Freier S., Wyatt J.R., Claverie J.M., Gautheret D. Patterns of variant polyadenylation signal usage in human genes. Genome Res. 2000, 10(7), 1001-10.

23. Becker J.T., Morris, R.G. Working Memory. Brain and Cognition 1999, 41, 1-8

24. Bender R., Plaschke M., Naumann T., Wahle P., Frotscher M. Development of cholinergic and GABAergic neurons in the rat medial septum: different onset of choline acetyltransferase and glutamate decarboxylase mRNA expression. J Comp Neurol. 1996, 372(2), 204-14.

25. Bennett B.D., Babu-Khan S., Loeloff .R, Louis J.C., Curran E., Citron M., Vassar R. Expression analysis of BACE2 in brain and peripheral tissues. J Biol Chem. 2000, 275(27), 20647-51.

26. Berger Z., Roder H., Hanna A., Carlson A., Rangachari V., Yue M., Wszolek Z., Ashe K., Knight J., Dickson D., Andorfer C., Rosenberry T.L., Lewis J., Hutton M., Janus C. Accumulation of pathological tau species and memory loss in a conditional model of tauopathy. J Neurosci. 2007, 27(14), 3650-62.

27. Berridge, C.W., Waterhouse, B.D. The locus coeruleus-noradrenergic system: modulation of behavioral state and state-dependent cognitive processes. Brain Res. Brain Res. Rev. 2003, 42, 33–84.

28. Bibel M., Hoppe E., Barde Y.A. Biochemical and functional interactions between the neurotrophin receptors trk and p75 NTR. EMBO J. 1999, 18(3), 616-22

29. Bierer L.M., Haroutunian V., Gabriel S., Knott P.J., Carlin L.S., Purohit D.P., Perl D.P., Schmeidler J., Kanof P., Davis K.L. Neurochemical correlates of dementia severity in Alzheimer's disease: relative importance of the cholinergic deficits. J Neurochem. 1995, 64(2), 749-60.

30. Biffo S., Offenhäuser N., Carter B.D., Barde Y.A. Selective binding and internalisation by truncated receptors restrict the availability of BDNF during development. Development. 1995, 121(8), 2461-70.

31. Bigl V., Woolf N.J., Butcher L.L. Cholinergic projections from the basal forebrain to frontal, parietal, temporal, occipital, and cingulate cortices: a combined fluorescent tracer and acetylcholinesterase analysis. Brain Res. 1982, 8, 727-49.

32. Billings L.M., Oddo S., Green K.N., McGaugh J.L., LaFerla F.M. Intraneuronal Abeta causes the onset of early Alzheimer's disease-related cognitive deficits in transgenic mice. Neuron. 2005, 45(5), 675-88.

33. Birks J. Cholinesterase inhibitors for Alzheimer's disease. Cochrane Database Syst Rev. 2006, (1), CD005593.

34. Birks J., Grimley Evans J. Ginkgo biloba for cognitive impairment and dementia. Cochrane Database Syst Rev. 2009, (1), CD003120.

34. Bishop K.M., Hofer E.K., Mehta A., Ramirez A., Sun L., Tuszynski M., Bartus R.T. Therapeutic potential of CERE-110 (AAV2-NGF): targeted, stable, and sustained NGF delivery and trophic activity on rodent basal forebrain cholinergic neurons. Exp Neurol. 2008, 211(2), 574-84.

35. Blanco G., Irving N.G., Brown S.D., Miller C.C., McLoughlin D.M. Mapping of the human and murine X11-like genes (APBA2 and apba2), the murine Fe65 gene (Apbb1), and the human Fe65-like gene (APBB2): genes encoding phosphotyrosine-binding domain proteins that interact with the Alzheimer's disease amyloid precursor protein. Mamm Genome. 1998, 9(6), 473-75.

36. Bland B.H., Colom L.V. Extrinsic and intrinsic properties underlying oscillation and synchrony in limbic cortex. Prog Neurobiol. 1993, 41(2), 157-208.

37. Blennow K., de Leon M.J., Zetterberg H. Alzheimer's disease. Lancet. 2006, 368(9533), 387-403.

38. Blesch A., Conner J., Pfeifer A., Gasmi M., Ramirez A., Britton W., Alfa R., Verma I., Tuszynski M.H. Regulated lentiviral NGF gene transfer controls rescue of medial septal cholinergic neurons. Mol Ther. 2005, 11(6), 916-25.

39. Bliss T.V., Collingridge G.L. A synaptic model of memory: long-term potentiation in the hippocampus. Nature. 1993, 361(6407), 31-39.

40. Bloem B., Schoppink L., Rotaru D.C., Faiz A., Hendriks P., Mansvelder H.D., van de Berg W.D., Wouterlood F.G. Topographic mapping between basal forebrain cholinergic neurons and the medial prefrontal cortex in mice. J Neurosci. 2014, 34(49), 16234-46

41. Blömer U., Naldini L., Kafri T., Trono D., Verma I.M., Gage F.H. Highly efficient and sustained gene transfer in adult neurons with a lentivirus vector. J Virol. 1997, 71(9), 6641-49.

42. Bloom G.S. Amyloid-β and tau: the trigger and bullet in Alzheimer disease pathogenesis. JAMA Neurol. 2014, 71(4), 505-8.

43. Boenisch T., Farmilo A.J., Stead R., Key M., Welcher R., Harvey R., Atwood K.N. Immunochemical Staining Methods. Copyright Dako Corporation, 2001

44. Book A.A., Wiley R.G., Schweitzer J.B. 192 IgG-saporin: I. Specific lethality for cholinergic neurons in the basal forebrain of the rat. J Neuropathol Exp Neurol. 1994, 53(1), 95-102.

45. Borlongan C.V. Recent preclinical evidence advancing cell therapy for Alzheimer's disease. Exp Neurol. 2012, 237(1), 142-46.

46. Borson S., Scanlan J.M., Watanabe J., Tu S.P., Lessig M. Simplifying detection of cognitive impairment: comparison of the Mini-Cog and Mini-Mental State Examination in a multiethnic sample. J Am Geriatr Soc. 2005, 53(5), 871-74.

47. Bosch M., Hayashi Y. Structural plasticity of dendritic spines. Curr Opin Neurobiol. 2012, 22(3), 383-88.

48. Boutajangout A., Authelet M., Blanchard V., Touchet N., Tremp G., Pradier L., Brion J.P. Characterisation of cytoskeletal abnormalities in mice transgenic for wild-type human tau and familial Alzheimer's disease mutants of APP and presenilin-1. Neurobiol Dis. 2004, 15(1), 47-60.

49. Bowen D.M., Smith C.B., White P., Davison A.N., 1976. Neurotransmitter-related enzymes and indices of hypoxia in senile dementia and other abiotrophies. Brain 1976, 99, 459–96.

50. Braak H., Braak E. Neuropathological staging of Alzheimer-related changes. Acta Neuropathol. 1991, 82(4), 239-59

51. Braak H., Braak E. The human entorhinal cortex: normal morphology and lamina-specific pathology in various diseases. Neurosci Res. 1992, 15(1-2), 6-31.

52. Brady D.R., Mufson E. Parvalbumin-immunoreactive neurons in the hippocampal formation of Alzheimer's diseased brain. Neuroscience. 1997, 80(4), 1113-25.

53. Brashear H.R., Zaborszky L., Heimer L. Distribution of GABAergic and cholinergic neurons in the rat diagonal band. Neuroscience. 1986, 17(2), 439-51.

54. Bressler S.L., Gray M.D., Sopher B.L., Hu Q., Hearn M.G., Pham D.G., Dinulos M.B., Fukuchi K., Sisodia S.S., Miller M.A., Disteche C.M., Martin G.M. cDNA cloning and chromosome mapping of the human Fe65 gene: interaction of the conserved cytoplasmic domains of the human beta-amyloid precursor protein and its homologues with the mouse Fe65 protein. Hum Mol Genet. 1996, 5(10), 1589-98.

55. Brown D.A., Abogadie F.C., Allen T.G., Buckley N.J., Caulfield M.P., Delmas P., Haley J.E., Lamas J.A., Selyanko A.A. Muscarinic mechanisms in nerve cells. Life Sci. 1997, 60(13-14), 1137-44.

56. Brown, R.E., Sergeeva, O., Eriksson, K.S., and Haas, H.L. Orexin A excites serotonergic neurons in the dorsal raphe nucleus of the rat. Neuropharmacology 2001, 40, 457–59.

57. Buckner R.L., Andrews-Hanna J.R., Schacter D.L. The brain's default network: anatomy, function, and relevance to disease. Ann N Y Acad Sci. 2008, 1124, 1-38

58. Buckner R.L., Snyder A.Z., Shannon B.J., LaRossa G., Sachs R., Fotenos A.F., Sheline Y.I., Klunk W.E., Mathis C.A., Morris J.C., Mintun M.A. Molecular, structural, and functional characterization of Alzheimer's disease: evidence for a relationship between default activity, amyloid, and memory. J Neurosci. 2005 Aug 24, 25(34), 7709-17.

59. Budson A.E., Solomon P.R. New diagnostic criteria for Alzheimer's disease and mild cognitive impairment for the practical neurologist. Pract Neurol. 2012, 12(2), 88-96

60. Butowt R., von Bartheld C.S. Connecting the dots: trafficking of neurotrophins, lectins and diverse pathogens by binding to the neurotrophin receptor p75NTR. Eur J Neurosci. 2003, 17(4), 673-80.

61. Butowt R., von Bartheld C.S. Fates of neurotrophins after retrograde axonal transport: phosphorylation of p75NTR is a sorting signal for delayed degradation. J Neurosci. 2009, 29(34), 10715-29.

62. Butterfield D.A. Amyloid beta-peptide (1-42)-induced oxidative stress and neurotoxicity: implications for neurodegeneration in Alzheimer's disease brain. Free Radic Res. 2002, 36(12), 1307-13.

63. Calvo A.C., Oliván S., Manzano R., Zaragoza P., Aguilera J., Osta R. Fragment C of tetanus toxin: new insights into its neuronal signaling pathway. Int J Mol Sci., 2012, 13(6), 6883-901.

64. Campenot R.B. Development of sympathetic neurons in compartmentalized cultures. II. Local control of neurite survival by nerve growth factor. Dev Biol. 1982, 93(1), 13-21.

65. Campenot R.B. NGF uptake and retrograde signaling mechanisms in sympathetic neurons in compartmented cultures. Results Probl Cell Differ. 2009, 48, 141-58.

66. Cao X., Südhof T.C. A transcriptionally active complex of APP with Fe65 and histone acetyltransferase Tip60. Science. 2001, 293(5527), 115-20.

67. Capell A., Steiner H., Willem M., Kaiser H., Meyer C., Walter J., Lammich S., Multhaup G., Haass C. Maturation and pro-peptide cleavage of beta-secretase. J Biol Chem. 2000, 275(40), 30849-54.

68. Caraci F., Battaglia G., Sortino M.A., Spampinato S., Molinaro G., Copani A., Nicoletti F., Bruno V. Metabotropic glutamate receptors in neurodegeneration/neuroprotection: still a hot topic? Neurochem Int. 2012, 61(4), 559-65.

69. Carlo A.S., Gustafsen C., Mastrobuoni G., Nielsen M.S., Burgert T., Hartl D., Rohe M., Nykjaer A., Herz J., Heeren J., Kempa S., Petersen C.M., Willnow T.E. The pro-neurotrophin receptor sortilin is a major neuronal apolipoprotein E receptor for catabolism of amyloid-β peptide in the brain. J Neurosci. 2013, 33(1), 358-70.

70. Caspersen C., Wang N., Yao J., Sosunov A., Chen X., Lustbader J.W., Xu H.W., Stern D., McKhann G., Yan S.D. Mitochondrial Abeta: a potential focal point for neuronal metabolic dysfunction in Alzheimer's disease. FASEB J. 2005, 19(14), 2040-41

71. Castañé A., Theobald D.E., Robbins T.W. Selective lesions of the dorsomedial striatum impair serial spatial reversal learning in rats. Behav Brain Res. 2010, 210(1), 74-83.

72. Caulfield M.P. Muscarinic receptors--characterization, coupling and function. Pharmacol Ther. 1993, 58(3), 319-79.

73. Cavallucci V., Berretta N., Nobili A., Nisticò R., Mercuri N.B., D'Amelio M. Calcineurin inhibition rescues early synaptic plasticity deficits in a mouse model of Alzheimer's disease. Neuromolecular Med. 2013, 15(3), 541-48.

74. Cetin A., Komai S., Eliava M., Seeburg P.H., Osten P. Stereotaxic gene delivery in the rodent brain. Nat Protoc. 2006, 1(6), 3166-73

75. Cetin F., Dincer S. The effect of intrahippocampal beta amyloid (1-42) peptide injection on oxidant and antioxidant status in rat brain. Ann N Y Acad Sci. 2007, 1100, 510-17.

76. Chandler D.J., Lamperski C.S., Waterhouse B.D. Identification and distribution of projections from monoaminergic and cholinergic nuclei to functionally differentiated subregions of prefrontal cortex. Brain Res. 2013, 1522, 38-58

77. Chao M.V. Neurotrophins and their receptors: a convergence point for many signalling pathways. Nat Rev Neurosci. 2003, 4(4), 299-309.

78. Chen G., Chen K.S., Knox J., Inglis J., Bernard A., Martin S.J., Justice A., McConlogue L., Games D., Freedman S.B., Morris R.G. A learning deficit related to age and beta-amyloid plaques in a mouse model of Alzheimer's disease. Nature. 2000, 408(6815), 975-79.

79. Chen J.H., Ke K.F., Lu J.H., Qiu Y.H., Peng Y.P. Protection of TGF-β1 against Neuroinflammation and Neurodegeneration in Aβ1-42-Induced Alzheimer's Disease Model Rats. PLoS One. 2015, 10(2), 0116549.

80. Chen Y., Zeng J., Cen L., Chen Y., Wang X., Yao G., Wang W., Qi W., Kong K. Multiple roles of the p75 neurotrophin receptor in the nervous system. J Int Med Res. 2009, 37(2), 281-88.

81. Cheung K.H., Mei L., Mak D.O., Hayashi I., Iwatsubo T., Kang D.E., Foskett J.K. Gain-of-function enhancement of IP3 receptor modal gating by familial Alzheimer's disease-linked presenilin mutants in human cells and mouse neurons. Sci Signal. 2010, 3(114), 22

82. Chin J.H., Ma L., MacTavish D., Jhamandas J.H. Amyloid beta protein modulates glutamate-mediated neurotransmission in the rat basal forebrain: involvement of presynaptic neuronal nicotinic acetylcholine and metabotropic glutamate receptors. J Neurosci. 2007, 27(35), 9262-69.

83. Choi S., Friedman W.J. Inflammatory cytokines IL-1β and TNF-α regulate p75NTR expression in CNS neurons and astrocytes by distinct cell-type-specific signalling mechanisms. ASN Neuro. 2009, 1(2).

84. Cirrito J.R., Kang J.E., Lee J., Stewart F.R., Verges D.K., Silverio L.M., Bu G., Mennerick S., Holtzman D.M. Endocytosis is required for synaptic activity-dependent release of amyloid-beta in vivo. Neuron. 2008, 58(1), 42-51.

85. Cirrito J.R., Yamada K.A., Finn M.B., Sloviter R.S., Bales K.R., May P.C., Schoepp D.D., Paul S.M., Mennerick S., Holtzman D.M. Synaptic activity regulates interstitial fluid amyloid-beta levels in vivo. Neuron. 2005 Dec, 48(6), 913-22.

86. Colton C.A., Chernyshev O.N., Gilbert D.L., Vitek M.P. Microglial contribution to oxidative stress in Alzheimer's disease. Ann N Y Acad Sci. 2000, 899, 292-307.

87. Corder E.H., Saunders A.M., Strittmatter W.J., Schmechel D.E., Gaskell P.C., Small G.W., Roses A.D., Haines J.L., Pericak-Vance M.A. Gene dose of apolipoprotein E type 4 allele and the risk of Alzheimer's disease in late onset families. Science. 1993, 261(5123), 921-23.

88. Corona C., Pensalfini A., Frazzini V., Sensi S.L. New therapeutic targets in Alzheimer's disease: brain deregulation of calcium and zinc. Cell Death Dis. 2011, 2, 176

89. Costantini C., Weindruch R., Della Valle G., Puglielli L. A TrkA-to-p75NTR molecular switch activates amyloid beta-peptide generation during aging. Biochem J. 2005, 391(1), 59-67.

90. Coulson E.J. Does the p75 neurotrophin receptor mediate Abeta-induced toxicity in Alzheimer's disease? J Neurochem. 2006, 98(3), 654-60.

91. Covaceuszach S., Capsoni S., Ugolini G., Spirito F., Vignone D., Cattaneo A. Development of a non-invasive NGF-based therapy for Alzheimer's disease. Curr Alzheimer Res. 2009, 6(2), 158-70.

92. Coyle J.T., Price D.L., DeLong M.R. Alzheimer's disease: a disorder of cortical cholinergic innervation. Science. 1983, 219(4589), 1184-90.

93. Cras P., Kawai M., Lowery D., Gonzalez-Dewhitt P., Greenberg B., Perry G. Senile plaque neurites in Alzheimer disease accumulate amyloid precursor protein. Procl Natl Acad Sci USA. 1991, 88(17), 7552-56

94. Croce N., Ciotti M.T., Gelfo F., Cortelli S., Federici G., Caltagirone C., Bernardini S., Angelucci F. Neuropeptide Y protects rat cortical neurons against β-amyloid toxicity and re-establishes synthesis and release of nerve growth factor. ACS Chem Neurosci. 2012, 3(4), 312-18.

95. Cruts M., Van Broeckhoven C. Presenilin mutations in Alzheimer's disease. Hum Mutat. 1998, 11(3), 183-90.

96. Cummings B.J., Cotman C.W. Image analysis of beta-amyloid load in Alzheimer's disease and relation to dementia severity. Lancet. 1995, 346(8989), 1524-28.

97 . Dahlgren K.N., Manelli A/M., Stine W.B.. Jr., Baker L.K., Krafft G.A., LaDu M.J. Oligomeric and fibrilliar species of amyloid-beta peptides differentially affect neuronal viability. J Biol Chem. 2002, 277(35), 32046-63.

98. Davidson B.L., Breakefield X.O. Viral vectors for gene delivery to the nervous system. Nat Rev Neurosci. 2003, 4(5), 353-64.

99. Davies P., Maloney A.J. Selective loss of central cholinergic neurons in Alzheimer's disease. Lancet 1976, 2(8000), 1403.

100. Dawbarn D., Rossor M.N., Mountjoy C.Q., Roth M., Emson P.C. Decreased somatostatin immunoreactivity but not neuropeptide Y immunoreactivity in cerebral cortex in senile dementia of Alzheimer type. Neurosci Lett. 1986, 70(1), 154-59.

101. Dean C., Liu H., Dunning F.M., Chang P.Y., Jackson M.B., Chapman E.R. Synaptotagmin-IV modulates synaptic function and long-term potentiation by regulating BDNF release. Nat Neurosci. 2009, 12(6), 767-76.

102. Dechant, G., Brade, Y.A. Signaling through the neurotrophin receptor p75NTR. Current Opinion in Neurobiology. 1997, 7, 413-18.

103. Dechant G., Barde Y.A. The neurotrophin receptor p75(NTR): novel functions and implications for diseases of the nervous system. Nat Neurosci. 2002, 5(11), 1131-36.

104. Decker H., Lo K.Y., Unger S.M., Ferreira S.T., Silverman M.A. Amyloid-beta peptide oligomers disrupt axonal transport through an NMDA receptor-dependent mechanism that is mediated by glycogen synthase kinase 3beta in primary cultured hippocampal neurons. J Neurosci. 2010, 30(27), 9166-71.

105. DeKosky S.T., Scheff S.W. Synapse loss in frontal cortex biopsies in Alzheimer's disease: correlation with cognitive severity. Ann Neurol. 1990, 27, 457-64

106. Delenda C. Lentiviral vectors: optimization of packaging, transduction and gene expression. J Gene Med 6 Suppl. 2004, (1), 25-138.

107. Della-Bianca V., Rossi F., Armato U., Dal-Pra I., Costantini C., Perini G., Politi V., Della Valle G. Neurotrophin p75 receptor is involved in neuronal damage by prion peptide-(106-126). J Biol Chem. 2001, 276(42), 38929-33

108. Dempsey P.W., Doyle S.E., He J.Q., Cheng G. The signaling adaptors and pathways activated by TNF superfamily. Cytokine Growth Factor Rev. 2003, 14(3-4), 193-209.

109. Demuro A., Parker I., Stutzmann G.E. Calcium signaling and amyloid toxicity in Alzheimer disease. J Biol Chem. 2010, 285(17), 12463-68.

110. De Souza Silva M.A., Dolga A., Pieri I., Marchetti L, Eisel U.L., Huston J.P., Dere E. Cholinergic cells in the nucleus basalis of mice express the N-methyl-D-aspartate-receptor subunit NR2C and its replacement by the NR2B subunit enhances frontal and amygdaloid acetylcholine levels. Genes Brain Behav. 2006, 5(7), 552-60.

111. Deutsch J.A. The cholinergic synapse and the site of memory. Science. 1971, 174(4011), 788-94.

112. Devarajan S., Sharmila J.S. Computational Studies of Beta Amyloid (Aβ42) with p75NTR Receptor: A Novel Therapeutic Target in Alzheimer's Disease. Adv Bioinformatics. 2014, 736378.

113. Dickerson B.C., Goncharova I., Sullivan M.P., Forchetti C., Wilson R.S., Bennett D.A., Beckett L.A., deToledo-Morrell L. MRI-derived entorhinal and hippocampal atrophy in incipient and very mild Alzheimer's disease. Neurobiol Aging. 2001, 22(5), 747-54.

114. Dinamarca M.C., Ríos J.A., Inestrosa N.C. Postsynaptic Receptors for Amyloid-β Oligomers as Mediators of Neuronal Damage in Alzheimer's Disease. Front Physiol. 2012, 3, 464.

115. Dineley K.T., Westerman M., Bui D., Bell K., Ashe K.H., Sweatt J.D. Beta-amyloid activates the mitogen-activated protein kinase cascade via hippocampal alpha7 nicotinic acetylcholine receptors: In vitro and in vivo mechanisms related to Alzheimer's disease. J Neurosci. 2001, 21(12), 4125-33.

116. Dobrowsky R.T., Jenkins G.M., Hannun Y.A. Neurotrophins induce sphingomyelin hydrolysis. Modulation by co-expression of p75NTR with Trk receptors. J Biol Chem. 1995, 270(38), 22135-42.

117. Domeniconi M., Zampieri N., Spencer T., Hilaire M., Mellado W., Chao M.V., Filbin M.T. MAG induces regulated intramembrane proteolysis of the p75 neurotrophin receptor to inhibit neurite outgrowth. Neuron. 2005, 46(6), 849-55.

118. Dubois B., Feldman H.H., Jacova C., Cummings J.L., Dekosky S.T, Barberger-Gateau P., Delacourte A., Frisoni G., Fox N.C., Galasko D., Gauthier S., Hampel H., Jicha G.A., Meguro K., O'Brien J., Pasquier F., Robert P., Rossor M., Salloway S., Sarazin M., de Souza L.C., Stern Y., Visser P.J., Scheltens P. Revising the definition of Alzheimer's disease: a new lexicon. Lancet Neurol. 2010, 9(11), 1118-27.

119. Dugal S., Choudhary A. Lentiviral Mediated Correction of Genetic Disorders. J Adv Sci Res, 2012, 3(4), 04-14.

120. Duque A., Balatoni B., Detari L., Zaborszky L. EEG correlation of the discharge properties of identified neurons in the basal forebrain. J Neurophysiol. 2000, 84(3), 1627-35.

121. Durazzo T.C., Mattsson N., Weiner M.W.; Alzheimer's Disease Neuroimaging Initiative. Smoking and increased Alzheimer's disease risk: A review of potential mechanisms. Alzheimers Dement. 2014, 10(3), 122-45.

122. Ebert U., Kirch W. Scopolamine model of dementia: electroencephalogram findings and cognitive performance. Eur J Clin Invest. 1998, 28(11), 944-9.

123. Eckert A., Nisbet R., Grimm A., Götz J. March separate, strike together--role of phosphorylated TAU in mitochondrial dysfunction in Alzheimer's disease. Biochim Biophys Acta. 2014, 1842(8), 1258-66.

124. Elder G.A., Gama Sosa M.A., De Gasperi R. Transgenic mouse models of Alzheimer's disease. Mt Sinai J Med. 2010, 77(1), 69-81.

125. Elvander E., Schött P.A., Sandin J., Bjelke B., Kehr J., Yoshitake T., Ogren S.O. Intraseptal muscarinic ligands and galanin: influence on hippocampal acetylcholine and cognition. Neuroscience. 2004, 126(3), 541-57.

126. Eriksson K.S., Sergeeva O.A., Haas H.L., Selbach O. Orexins/hypocretins and aminergic systems. Acta Physiol (Oxf). 2010, 198(3), 263-75

127. Escors D., Breckpot K. Lentiviral vectors in gene therapy: their current status and future potential. Arch Immunol Ther Exp (Warsz). 2010, 58(2), 107-19.

128. Evinger C., Erichsen J.T. Transsynaptic retrograde transport of fragment C of tetanus toxin demonstrated by immunohistochemical localization. Brain Res. 1986, 380(2), 383-88.

129. Fahnestock, M., Michalski, B., Xu, B., Coughlin, M.D. The precursor pro-nerve growth factor is the predominant form of nerve growth factor in brain and is increased in Alzheimer's disease. Molecular and Cellular Neuroscience. 2001, 18, 210-20.

130. Fargo K. Alzheimer's Association Report: 2014 Alzheimers disease facts and figures. Alzheimers Dement. 2014, 10(2), 47-92.

131. Ferreira G., Meurisse M., Tillet Y., Lévy F. Distribution and co-localization of choline acetyltransferase and p75 neurotrophin receptors in the sheep basal forebrain: implications for the use of a specific cholinergic immunotoxin. Neuroscience. 2001, 104(2), 419-39.

132. Fisher A., Bezprozvanny I., Wu L., Ryskamp D.A., Bar-Ner N., Natan N., Brandeis R., Elkon H., Nahum V., Gershonov E., LaFerla F.M., Medeiros R. AF710B, a Novel M1/σ1 Agonist with Therapeutic Efficacy in Animal Models of Alzheimer's Disease. Neurodegener Dis. 2016, 16(1-2), 95-110.

133. Flood D.G., Lin Y.G., Lang D.M., Trusko S.P., Hirsch J.D., Savage M.J., Scott R.W., Howland D.S. A transgenic rat model of Alzheimer's disease with extracellular Abeta deposition. Neurobiol Aging. 2009, 30(7), 1078-90.

134. Folkesson R., Malkiewicz K., Kloskowska E., Nilsson T., Popova E., Bogdanovic N., Ganten U., Ganten D., Bader M., Winblad B., Benedikz E. A transgenic rat expressing human APP with the Swedish Alzheimer's disease mutation. Biochem Biophys Res Commun. 2007, 358(3), 777-82.

135. Fombonne J., Rabizadeh S., Banwait S., Mehlen P., Bredesen D.E. Selective vulnerability in Alzheimer's disease: amyloid precursor protein and p75(NTR) interaction. Ann Neurol. 2009, 65(3), 294-303.

136. Fox M.D., Snyder A.Z., Vincent J.L., Corbetta M., Van Essen D.C., Raichle M.E. The human brain is intrinsically organized into dynamic, anticorrelated functional networks. Proc Natl Acad Sci U S A. 2005, 102(27), 9673-78

137. Fraering P.C. Structural and Functional Determinants of gamma-Secretase, an Intramembrane Protease Implicated in Alzheimer's Disease. Curr Genomics. 2007, 8(8), 531-49.

138. Frankowski H., Castro-Obregon S., del Rio G., Rao R.V., Bredesen D.E. PLAIDD, a type II death domain protein that interacts with p75 neurotrophin receptor. Neuromolecular Med. 2002, 1(3), 153-70.

139. Freund T.F. GABAergic septohippocampal neurons contain parvalbumin. Brain Res. 1989, 478(2), 375-81.

140. Fukuchi K., Hart M., Li L. Alzheimer's disease and heparin sulphate proteoglycan. Front Biosci. 1998, 3, 327-37

141. Galimberti D., Ghezzi L., Scarpini E. Immunotherapy against amyloid pathology in Alzheimer's disease. J Neurol Sci. 2013, 333(1-2), 50-54.

142. Galimi F., Verma I.M. Opportunities for the use of lentiviral vectors in human gene therapy. Curr Top Microbiol Immunol 2000, 261, 245-54.

143. Games D., Khan K.M., Soriano F.G., Keim P.S., Davis D.L., Bryant K., Lieberburg I. Lack of Alzheimer pathology after beta-amyloid protein injections in rat brain. Neurobiol Aging. 1992, 13(5), 569-76.

144. Gao B., Hornung J.P., Fritschy J.M. Identification of distinct GABAA-receptor subtypes in cholinergic and parvalbumin-positive neurons of the rat and marmoset medial septum-diagonal band complex. Neuroscience. 1995, 65(1), 101-17.

145. Gao J., Adam B.L., Terry A.V. Jr. Evaluation of nicotine and cotinine analogs as potential neuroprotective agents for Alzheimer's disease. Bioorg Med Chem Lett. 2014, 24(6), 1472-8.

146. Garibotto V., Borroni B., Kalbe E., Herholz K., Salmon E., Holtoff V., Sorbi S., Cappa S.F., Padovani A., Fazio F., Perani D. Education and occupation as proxies for reserve in a MCI converters and AD: FDG-PET evidence. Neurology. 2008, 71(17), 1342-49.

147. Garibotto V., Tettamanti M., Marcone A., Florea I., Panzacchi A., Moresco R., Virta J.R., Rinne J., Cappa S.F., Perani D.. Cholinergic activity correlates with reserve proxies in Alzheimer's disease. Neurobiol Aging. 2013, 34(11), 2694

148. Gaykema R.P., Compaan J.C., Nyakas C., Horvath E., Luiten P.G. Long-term effects of cholinergic basal forebrain lesions on neuropeptide Y and somatostatin immunoreactivity in rat neocortex. Brain Res. 1989, 489(2), 392-96.

149. Geula C., Bu J., Nagykery N., Scinto L.F., Chan J., Joseph J., Parker R., Wu C.K. Loss of calbindin-D28k from aging human cholinergic basal forebrain: relation to neuronal loss. J Comp Neurol. 2003, 455(2), 249-59.

150. Geula C., Mesulam M.M., Saroff D.M., Wu C.K. Relationship between plaques, tangles, and loss of cortical cholinergic fibers in Alzheimer disease. J Neuropathol Exp Neurol. 1998, 57(1), 63-75.

151. Giacobini E., Becker R.E. One hundred years after the discovery of Alzheimer's disease. A turning point for therapy? J Alzheimers Dis. 2007, 12(1), 37-52.

152. Giannakopoulos P., Herrmann F.R., Bussière T., Bouras C., Kövari E., Perl D.P., Morrison J.H., Gold G., Hof P.R. Tangle and neuron numbers, but not amyloid

load, predict cognitive status in Alzheimer's disease. Neurology. 2003, 13, 60(9), 1495-500.

153. Gil-Bea F.J., Gerenu G., Aisa B., Kirazov L.P., Schliebs R., Ramírez M.J. Cholinergic denervation exacerbates amyloid pathology and induces hippocampal atrophy in Tg2576 mice. Neurobiol Dis. 2012, 48(3), 439-46

154. Gilmor M.L., Erickson J.D., Varoqui H., Hersh L.B., Bennett D.A., Cochran E.J., Mufson E.J., Levey A.I. Preservation of nucleus basalis neurons containing choline acetyltransferase and the vesicular acetylcholine transporter in the elderly with mild cognitive impairment and early Alzheimer's disease. J Comp Neurol. 1999, 411(4), 693-704.

155. Ginsberg S.D., Che S., Wuu J., Counts S.E., Mufson E.J. Down regulation of trk but not p75NTR gene expression in single cholinergic basal forebrain neurons mark the progression of Alzheimer's disease. J Neurochem. 2006, 97(2), 475-87.

156. Giuffrida M.L., Caraci F., Pignataro B., Cataldo S., De Bona P., Bruno V., Molinaro G., Pappalarado G., Messina A., Palmigiano A., Garozzo D., Nicoletti F., Rizzarelli E., Copani A. Beta-amyloid monomers are neuroprotective. J Neurosci. 2009, 29(34), 10582-87.

157. Glabe C.G. Structural classification of toxic amyloid oligomers. J Biol Chem. 2008, 283(44), 29639-43.

158. Glenner G.G., Wong C.W. Alzheimer’s disease: initial report of the purification and characterisation of a novel cerebrovascular amyloid protein 1984. Biochem Biophys Res Commun. 2012, 425 (3),534-39

159. Glenner G.G., Wong C.W., Quaranta V., Eanes E.D. The amyloid deposits in Alzheimer’s disease: their nature and pathogenesis. Appl Pathol. 1984, 2(6), 357-69

160. Glenn M.J., Nesbitt C., Mumby D.G. Perirhinal cortex lesions produce variable patterns of retrograde amnesia in rats. Behav Brain Res. 2003, 141(2), 183-93.

161. Golde T.E., Janus C. Homing in on intracellular Abeta? Neuron. 2005, 45(5), 639-42.

162. Gonzalo-Ruiz A., Sanz J.M. Alteration of cholinergic, excitatory amino acid and neuropeptide markers in the septum-diagonal band complex following injections of fibrillar β-amyloid protein into the retrosplenial granular cortex of the rat. Eur J Anat, 2002, 6 (2), 95-107

163. Gotti C., Clementi F., Fornari A., Gaimarri A., Guiducci S., Manfredi I., Moretti M., Pedrazzi P., Pucci L., Zoli M. Structural and functional diversity of native brain neuronal nicotinic receptors. Biochem Pharmacol. 2009, 78(7), 703-11

164. Gotti C., Zoli M., Clementi F. Brain nicotinic acetylcholine receptors: native subtypes and their relevance. Trends Pharmacol Sci. 2006, 27(9), 482-91.

165. Gozes I. Neuroprotective peptide drug delivery and development: potential new therapeutics. Trends Neurosci.2001, 24(12), 700-5.

166. Grace, A.A., Onn, S.P. Morphology and electrophysiological properties of immunocytochemically identified rat dopamine neurons recorded in vitro. J. Neurosci. 1989, 9, 3463–81.

167. Gray J.A., McNaughton N. Comparison between the behavioural effects of septal and hippocampal lesions: a review. Neurosci Biobehav Rev. 1983, 7(2), 119-88.

168. Green K.N., LaFerla F.M. Linking calcium to Abeta and Alzheimer's disease. Neuron. 2008, 59(2), 190-94

169. Green K.N., Smith I.F., LaFerla F.M. Role of calcium in the pathogenesis of Alzheimer's disease and transgenic models. Subcell Biochem. 2007, 45, 507-21.

170. Green N.M., Toms E.J. Purification and crystallization of avidin. Biochem J. 1970, 118(1), 67-70.

171. Greferath U., Bennie A., Kourakis A., Bartlett P.F., Murphy M., Barrett G.L. Enlarged cholinergic forebrain neurons and improved spatial learning in p75 knockout mice. Eur J Neurosci. 2000, 12(3), 885-93.

172. Greferath U., Trieu J., Barrett G.L. The p75 neurotrophin receptor has nonapoptotic antineurotrophic actions in the basal forebrain. J Neurosci Res. 2012, 90(1), 278-87.

173. Greicius M.D., Krasnow B., Reiss A.L., Menon V. Functional connectivity in the resting brain: a network analysis of the default mode hypothesis. Proc Natl Acad Sci U S A. 2003, 100(1), 253-58

174. Greicius M.D., Srivastava G., Reiss A.L., Menon V. Default-mode network activity distinguishes Alzheimer’s disease from healthy aging: evidence from functional MRI. Proc Natl Acad Sci USA. 2004, 101(13), 4637-42

175. Greig N.H., Reale M., Tata A.M. New Pharmacological Approaches to the Cholinergic System: An Overview on Muscarinic Receptor Ligands and Cholinesterase Inhibitors. Recent Pat CNS Drug Discov. 2013, 8(2), 123-41.

176. Griffith W.H., Taylor L., Davis M.J. Whole-cell and single-channel calcium currents in guinea pig basal forebrain neurons. J Neurophysiol. 1994, 71(6), 2359-76.

177. Grimmer T., Henriksen G., Wester H.J., Förstl H., Klunk W.E., Mathis C.A., Kurz A., Drzezga A. Clinical severity of Alzheimer's disease is associated with PIB uptake in PET. Neurobiol Aging. 2009, 30(12), 1902-9.

178. Gritti I., Henny P., Galloni F., Mainville L., Mariotti M., Jones B.E. Stereological estimates of the basal forebrain cell population in the rat, including neurons containing choline acetyltransferase, glutamic acid decarboxylase or

phosphate-activated glutaminase and colocalizing vesicular glutamate transporters. Neuroscience. 2006, 143(4), 1051-64.

179. Grundke-Iqbal I., Iqbal K., Tung Y.C., Quinlan M., Wisniewski H.M., Binder L.I. Abnormal phosphorylation of the microtubule-associated protein tau (tau) in Alzheimer cytoskeletal pathology. Proc Natl Acad Sci U S A. 1986, 83(13), 4913-17.

180. Gruss H.J. Molecular, structural and biological characteristics of the tumour necrosis factor ligand superfamily. Int J Clin Lab Res. 1996, 26(3), 143-59.

181. Grynspan F., Griffin W.R., Cataldo A., Katayama S., Nixon R.A. Active site-directed antibodies identify calpain II as an early-appearing and pervasive component of neurofibrillary pathology in Alzheimer's disease. Brain Res. 1997, 763(2), 145-58.

182. Guénette S., Chang Y., Hiesberger T., Richardson J.A., Eckman C.B., Eckman E.A., Hammer R.E., Herz J. Essential roles for the FE65 amyloid precursor protein-interacting proteins in brain development. EMBO J. 2006, 25(2), 420-31.

183. Guillemin G.J., Brew B.J. Implications of the kynurenine pathway and quinolinic acid in Alzheimer's disease. Redox Rep. 2002, 7(4), 199-206.

184. Gusnard D.A., Raichle M.E., Raichle M.E. Searching for a baseline: functional imaging and the resting human brain. Nat Rev Neurosci. 2001, 2(10), 685-94.

185. Haass C., Lemere C.A., Capell A., Citron M., Seubert P., Schenk D., Lannfelt L., Selkoe D.J. The Swedish mutation causes early- onset Alzheimer’s disease by beta-secretase cleavage within the secretory pathway. Nat Med. 1995, 1(12), 1291-96.

186. Hadad-Ophir O., Albrecht A., Stork O., Richter-Levin E. Amygdala activation and GABAergic gene expression in hippocampal sub-regions at the interplay of stress and spatial learning. Front Behav Neurosci. 2014, 8, 3.

187. Haga T. Synthesis and release of (14 C) acetylcholine in synaptosomes. J Neurochem. 1971, 18(6), 781-98.

188. Hajszan T., Alreja M., Leranth C. Intrinsic vesicular glutamate transporter 2-immunoreactive input to septohippocampal parvalbumin-containing neurons: novel glutamatergic local circuit cells. Hippocampus. 2004, 14(4), 499-509.

189. Han F., Shioda N., Moriguchi S., Qin Z.H., Fukunaga K. The vanadium (IV) compound rescues septo-hippocampal cholinergic neurons from neurodegeneration in olfactory bulbectomized mice. Neuroscience. 2008, 151(3), 671-79.

190. Hardy J., Selkoe D.J. The amyloid hypothesis of Alzheimer's disease: progress and problems on the road to therapeutics. Science. 2002, 297(5580), 353-56.

191. Harkany T., De Jong G.I., Soos K., Penke B., Luiten P.G., Gulya K. Beta-amyloid (1–42) affects cholinergic but not parvalbumin-containing neurons in the septal complex of the rat. Brain Res., 1995, (698), 270-74

192. Harkany T., Härtig W., Berghuis P., Dobszay M.B., Zilberter Y., Edwards R.H., Mackie K., Ernfors P. Complementary distribution of type 1 cannabinoid receptors and vesicular glutamate transporter 3 in basal forebrain suggests input-specific retrograde signalling by cholinergic neurons. Eur J Neurosci. 2003, 18(7), 1979-92.

193. Harrington A.W., St Hillaire C., Zweifel L.S., Glebova N.O., Philippidou P., Halegoua S., Ginty D.D. Recruitment of actin modifiers to TrkA endosomes governs retrograde NGF signaling and survival. Cell. 2011, 146(3), 421-34.

194. Harris J.A., Devidze N., Verret L., Ho K., Halabisky B., Thwin M.T., Kim D., Hamto P., Lo I., Yu G.Q., Palop J.J., Masliah E., Mucke L. Transsynaptic progression of amyloid-beta-induced neuronal dysfunction within the entorhinal-hippocampal network. Neuron 2010, 68, 428–41.

195. Härtig W., Bauer A., Brauer K., Grosche J., Hortobágyi T., Penke B., Schliebs R., Harkany T. Functional recovery of cholinergic basal forebrain neurons under disease conditions: old problems, new solutions? Rev Neurosci. 2002, 13(2), 95-165.

196. Härtig W., Saul A., Kacza J., Grosche J., Goldhammer S., Michalski D., Wirths O. Immunolesion-induced loss of cholinergic projection neurones promotes β-amyloidosis and tau hyperphosphorylation in the hippocampus of triple-transgenic mice. Neuropathol Appl Neurobiol. 2014, 40(2), 106-20.

197. Härtig W., Seeger J., Naumann T., Brauer K., Brückner G. Selective in vivo fluorescence labelling of cholinergic neurons containing p75(NTR) in the rat basal forebrain. Brain Res. 1998, 808(2), 155-65.

198. Hartmann T., Bieger S.C., Brühl B., Tienari P.J., Ida N., Allsop D., Roberts G.W., Masters C.L., Dotti C.G., Unsicker K., Beyreuther K. Distinct sites of intracellular production for Alzheimer's disease A beta40/42 amyloid peptides. Nat Med. 1997, 3(9), 1016-20.

199. Hartmann M., Heumann R., Lessmann V. Synaptic secretion of BDNF after high-frequency stimulation of glutamatergic synapses. EMBO J. 2001, 20(21), 5887-97.

200. Hassani O.K., Lee M.G., Henny P., Jones B.E. Discharge profiles of identified GABAergic in comparison to cholinergic and putative glutamatergic basal forebrain neurons across the sleep-wake cycle. J Neurosci. 2009, 29(38), 11828-40.

201. Hasselmo M.E. The role of acetylcholine in learning and memory. Curr Opin Neurobiol. 2006, 16(6), 710-5.

202. Hauss-Wegrzyniak B., Dobrzanski P., Stoehr J.D., Wenk G.L. Chronic neuroinflammation in rats reproduces components of the neurobiology of Alzheimer's disease. Brain Res. 1998, 780(2), 294-303.

203. Heizmann C.W., Braun K. Changes in Ca(2+)-binding proteins in human neurodegenerative disorders. Trends Neurosci. 1992, 15(7), 259-64.

204. Hellström-Lindahl E. Modulation of beta-amyloid precursor protein processing and tau phosphorylation by acetylcholine receptors. Eur J Pharmacol. 2000, 393(1-3), 255-63.

205. Hempstead B.L., Martin-Zanca D., Kaplan D.R., Parada L.F., Chao M.V. High-affinity NGF binding requires coexpression of the trk proto-oncogene and the low-affinity NGF receptor. Nature. 1991, 350(6320), 678-83.

206. Henderson Z., Lu C.B., Janzsó G., Matto N., McKinley C.E., Yanagawa Y., Halasy K. Distribution and role of Kv3.1b in neurons in the medial septum diagonal band complex. Neuroscience. 2010, 166(3), 952-69.

207. Heneka M.T., Nadrigny F., Regen T., Martinez-Hemandez A., Dumitrescu-Ozimek L., Terwel D., Jardanhazi-Kurutz D., Walter J., Kirchhoff F., Hanisch U.K., Kummer M.P. Locus ceruleus controls alzheimer's disease pathology by modulating microglial functions through norepinephrine. Proc Natl Acad Sci USA. 2010, 107(13), 6058-63

208. Hernández S.S., Sandreschi P.F., Silva F.C., Arancibia B.A., da Silva R., Gutierres P.J., Andrade A. What are the Benefits of Exercise for Alzheimer´s Disease? A Systematic Review of Past 10 Years. J Aging Phys Act. 2015, 23(4), 659-68.

209. Herrup K., Shooter E.M. Properties of the beta nerve growth factor receptor of avian dorsal root ganglia. Proc Natl Acad Sci U S A. 1973, 70(12), 3884-88.

210. Hirai K., Aliev G., Nunomura A., Fujioka H., Russell R.., Atwood C.S., Johnson A.B., Kress Y., Vinters H.V., Tabaton M., Shimohama S., Cash A.D., Siedlak S.L., Harris P.L., Jones P.K., Petersen R.B., Perry G., Smith M.A. Mitochondrial abnormalities in Alzheimer's disease. J Neurosci. 2001, 21(9), 3017-23.

211. Holtzman D.M., Kilbridge J., Li Y., Cunningham E.T.Jr., Lenn N.J., Clary D.O., Reichardt L.F., Mobley W.C. TrkA expression in the CNS: evidence for the existence of several novel NGF-responsive CNS neurons. J Neurosci. 1995, 15(2), 1567-76.

212. Hong J.H., Jang S.H., Kim O.L., Kim S.H., Ahn S.H., Byun W.M., Hong C.P., Lee D.H. Neuronal loss in the medial cholinergic pathway from the nucleus basalis of Meynert in patients with traumatic axonal injury: a preliminary diffusion tensor imaging study. J Head Trauma Rehabil. 2012, 27(3), 172-76.

213. Huebner, K., Isobe, M., Chao, M., Bothwell, M., Ross, A.H., Finan, J., Hoxie, J.A., Shegal, A., Buck, C.R., Lanahan, A. The nerve growth factor receptor gene is at human chromosome region 17q12-17q22, distal to the chromosome 17 breakpoint in acute leukemias. Proceedings of the National Academy of Sciences U.S.A. 1986, 83, 1403-7.

214. Hu Q., Cool B.H., Wang B., Hearn M.G., Martin G.M. A candidate molecular mechanism for the association of an intronic polymorphism of FE65 with resistance to very late onset dementia of the Alzheimer type. Hum Mol Genet. 2002, 11(4), 465-75.

215. Hu Q., Hearn M.G., Jin L.W., Bressler S.L., Martin G.M. Alternatively spliced isoforms of FE65 serve as neuron-specific and non-neuronal markers. J Neurosci Res. 1999, 58(5), 632-40.

216. Hu Q., Wang L., Yang Z., Cool B.H., Zitnik G., Martin G.M. Endoproteolytic cleavage of FE65 converts the adaptor protein to a potent suppressor of the sAPPalpha pathway in primates. J Biol Chem. 2005, 280(13), 12548-58.

217. Hu X.Y., Zhang H.Y., Qin S., Xu H., Swaab D.F., Zhou J.N. Increased p75(NTR) expression in hippocampal neurons containing hyperphosphorylated tau in Alzheimer's patients. Exp Neurol. 2002, 178(1), 104-11.

218. Hur E.E., Zaborszky L. Vglut2 afferents to the medial prefrontal and primary somatosensory cortices: a combined retrograde tracing in situ hybridization study. J Comp Neurol. 2005, 483(3), 351-73.

219. Iacopino, A.M., Quintero, E.M., Miller, K. Calbindin-D28k: a potential neuroprotective protein. Neurodegeneration 1994, 3, 1-20.

220. Iadecola C. Neurovascular regulation in the normal brain and in Alzheimer's disease. Nat Rev Neurosci. 2004, 5(5), 347-60

221. Ikemoto S. Dopamine reward circuitry: two projection systems from the ventral midbrain to the nucleus accumbens-olfactory tubercle complex. Brain Res Rev. 2007, 56(1), 27-78.

222. Ikin A.F., Sabo S.L., Lanier L.M., Buxbaum J.D. A macromolecular complex involving the amyloid precursor protein (APP) and the cytosolic adapter FE65 is a negative regulator of axon branching. Mol Cell Neurosci. 2007, 35(1), 57-63.

223. Ittner L.M., Götz J. Amyloid-β and tau--a toxic pas de deux in Alzheimer's disease. Nat Rev Neurosci. 2011, 12(2), 65-72.

224. Iwata N., Tsubuki S., Takaki Y., Sekiguchi M., Kosoki E., Kawashima-Morishima M., Lee H.J., Hama E., Sekine-Aizawa Y., Saido T.C. Identification of the major Abeta 1-42 degrading catabolic pathway in brain parenchyma: suppression leads to biochemical and pathological deposition. Nat Med 2000, 6(2), 143-50.

225. Jankowsky J.L., Fadale D.J., Anderson J., Xu G.M., Gonzales V., Jenkins N.A, Copeland N.G., Lee M.K., Younkin L.H., Wagner S.L., Younkin S.G., Borchelt D.R. Mutant presenilins specifically elevate the levels of the 42 residue beta-amyloid peptide in vivo: evidence for augmentation of a 42-specific gamma secretase. Hum Mol Genet. 2004, 13(2), 159-70.

226. Jellinger K.A., Attems J. Neuropathological evaluation of mixed dementia. J Neurol Sci. 2007, 257(1-2), 80-87.

227. Jhamandas J.H., Harris K.H., MacTavish D., Jassar B.S. Novel excitatory actions of galanin on rat cholinergic basal forebrain neurons: implications for its role in Alzheimer's disease. J Neurophysiol. 2002, 87(2), 696-704.

228. Jian C., Zou D., Luo C., Liu X., Meng L., Huang J., Li X., Huang R., Wu Y. Cognitive deficits are ameliorated by reduction in amyloid β accumulation in Tg2576/p75(NTR+/-) mice. Life Sci. 2016, 155, 167-73.

229. Johnson E.M. Jr, Taniuchi M., Clark H.B., Springer J.E., Koh S., Tayrien M.W., Loy R. Demonstration of the retrograde transport of nerve growth factor receptor in the peripheral and central nervous system. J Neurosci. 1987, 7(3), 923-29.

230. Jones B.E., Yang T.Z. The efferent projections from the reticular formation and the locus coeruleus studied by anterograde and retrograde axonal transport in the rat. J Comp Neurol. 1985, 242(1), 56-92.

231. Joyce J.N., Myers A.J., Gurevich E. Dompamine D2 receptor bands in normal human temporal cortex are absent in Alzheimer’s disease Brain Research, 1998, 784, 7-17

232. Kacza J., Grosche J., Seeger J., Brauer K., Brückner G., Härtig W. Laser scanning and electron microscopic evidence for rapid and specific in vivo labelling of cholinergic neurons in the rat basal forebrain with fluorochromated antibodies. Brain Res. 2000, 867(1-2), 232-38.

233. Kalb R. The protean actions of neurotrophins and their receptors on the life and death of neurons. Trends Neurosci. 2005, 28(1), 5-11.

234. Kamenetz F., Tomita T., Hsieh H., Seabrook G., Borchelt D., Iwatsubo T., Sisodia S., Malinow R. APP processing and synaptic function. Neuron. 2003, 37(6), 925-37.

235. Kane M.D., Lipinski W.J., Callahan M.J., Bian F., Durham R.A., Schwarz R.D., Roher A.E., Walker L.C. Evidence for seeding of beta -amyloid by intracerebral infusion of Alzheimer brain extracts in beta -amyloid precursor protein-transgenic mice. J Neurosci. 2000, 20(10), 3606-11.

236. Kang J.H., Ryoo N.Y., Shin D.W., Trojanowski J.Q., Shaw L.M. Role of cerebrospinal fluid biomarkers in clinical trials for Alzheimer's disease modifying therapies. Korean J Physiol Pharmacol. 2014, 18(6), 447-56

237. Kanning K.C., Hudson M., Amieux P.S., Wiley J.C., Bothwell M., Schecterson L.C. Proteolytic processing of the p75 neurotrophin receptor and two homologs generates C-terminal fragments with signaling capability. J Neurosci. 2003, 23(13), 5425-36.

238. Kantor B., McCown T., Leone P., Gray SJ. Clinical applications involving CNS gene transfer. Adv Genet. 2014, 87, 71-124.

239. Kaplan D.R, Stephens R.M. Neurotrophin signal transduction by the Trk receptor. J Neurobiol. 1994, 25(11), 1404-17.

240. Katzman R. The Prevalence and Malignancy of Alzheimer Disease A Major Killer. Arch Neurol. 1976, 33(4), 217-18.

241. Kawahara M. Neurotoxicity of β-amyloid protein: oligomerization, channel formation, and calcium dyshomeostasis. Curr Pharm Des. 2010, 16(25), 2779-89.

242. Kawahara M., Ohtsuka I., Yokoyama S., Kato-Negishi M., Sadakane Y. Membrane Incorporation, Channel Formation, and Disruption of Calcium Homeostasis by Alzheimer's β-Amyloid Protein. Int J Alzheimers Dis. 2011, 304583.

243. Kenchappa R.S., Tep C., Korade Z., Urra S., Bronfman F.C., Yoon S.O., Carter B.D. P75 neurotrophin receptor-mediated apoptosis in sympathetic neurons involves a biphasic activation of JNK and up-regulation of tumor necrosis factor-alpha-converting enzyme/ADAM17. J Biol Chem. 2010, 285(26), 20358-68.

244. Kesavapany S., Banner S.J., Lau K.F., Shaw C.E., Miller C.C., Cooper J.D., McLoughlin D.M. Expression of the Fe65 adapter protein in adult and developing mouse brain. Neuroscience. 2002, 115(3), 951-60.

245. Kester M.I., Goos J.D., Teunissen C.E., Benedictus M.R., Bouwman F.H., Wattjes M.P., Barkhof F., Scheltens P., Van der Flier W.M. Associations between cerebral small vessel disease and Alzheimer disease pathology as measured by cerebrospinal fluid biomarkers.JAMA Neurol 2014, 71(7), 855-62

246. Khachaturian Z.S. Hypothesis on the regulation of cytosol calcium concentration and the aging brain. Neurobiol Aging. 1987, 8(4), 345-46.

247. Khateb A., Mühlethaler M., Alonso A., Serafin M., Mainville L., Jones B.E. Cholinergic nucleus basalis neurons display the capacity for rhythmic bursting activity mediated by low-threshold calcium spikes. Neuroscience. 1992, 51(3), 489-94.

248. Kimberly W.T., LaVoie M.J., Ostaszewski B.L., Ye W., Wolfe M.S., Selkoe D.J. Gamma-secretase is a membrane protein complex comprised of presenilin, nicastrin, Aph-1, and Pen-2. Proc Natl Acad Sci U S A. 2003, 100(11), 6382-87.

249. Kim S.I., Yi J.S., Ko Y.G. Amyloid beta oligomerization is induced by brain lipid rafts. J Cell Biochem. 2006, 99(3), 878-89.

250. Kimura H., Tago H., Akiyama H., Hersh L.B., Tooyama I., McGeer P.L. Choline acetyltransferase immunopositive neurons in the lateral septum. Brain Res. 1990, 533(1), 165-70.

251. Kingwell K. Alzheimer disease: Joining the dots between APOE ε4 and late-onset Alzheimer disease via integrative genomics. Nat Rev Neurol. 2013, 9(9), 483.

252. Kiss J., McGovern J., Patel A.J. Immunohistochemical localization of cells containing nerve growth factor receptors in the different regions of the adult rat forebrain. Neuroscience. 1988, 27(3), 731-48.

253. Klein R., Jing S.Q., Nanduri V., O'Rourke E., Barbacid M. The trk proto-oncogene encodes a receptor for nerve growth factor. Cell. 1991, 65(1), 189-97.

254. Knobloch M., Mansuy I.M. Dendritic spine loss and synaptic alterations in Alzheimer's disease. Mol Neurobiol. 2008, 37(1), 73-82.

255. Koelliker A. Handbuch der Gewebelehre des Menschen, 2 Nervensystem; 6th ed. Leipzig: Engelmann; 1986.

256. Koffie R.M., Hyman B.T., Spires-Jones T.L. Alzheimer's disease: synapses gone cold. Mol Neurodegener. 2011, 26, 6(1), 63.

257. Koo E.H., Squazzo S.L. Evidence that production and release of amyloid beta protein involves the endocytic pathway. J Biol chem. 1994, 269(26), 17386-89.

258. Kook S.Y., Jeong H., Kang M.J., Park R., Shin H.J., Han S.H., Son S.M., Song H., Baik S.H., Moon M., Yi E.C., Hwang D., Mook-Jung I. Crucial role of calbindin-D28k in the pathogenesis of Alzheimer's disease mouse model. Cell Death Differ. 2014, 21(10), 1575-87.

259. Kordower J.H., Emborg M.E., Bloch J., Ma S.Y., Chu Y., Leventhal L., McBride J.,Chen E.Y., Palfi S., Roitberg B.Z., Brown W.D., Holden J.E., Pyzalski R., Taylor M.D., Carvey P., Ling Z., Trono D., Hantraye P., Deglon N., Aebischer. Neurodegeneration prevented by lentiviral vector delivery of GDNF in primate models of Parkinson's disease. Science. 2000, 290(5492), 767-73.

260. Kudo W., Petersen R.B., Lee H.G. Cellular prion protein and Alzheimer disease: link to oligomeric amyloid-β and neuronal cell death. Prion. 2013, 7(2), 114-16.

261. Kumar P., Woon-Khiong C. Optimization of lentiviral vectors generation for biomedical and clinical research purposes: contemporary trends in technology development and applications. Curr Gene Ther. 2011, 11(2), 144-53.

262. Kuner P., Schubenel R., Hertel C. Beta-amyloid binds to p57NTR and activates NFkappaB in human neuroblastoma cells. J Neurosci Res. 1998, 54(6), 798-804.

263. Lacy D.B., Stevens R.C. Recombinant expression and purification of the botulinum neurotoxin type A translocation domain. Protein Expr Purif. 1997, 11(2), 195-200.

264. LaFerla F.M., Green K.N., Oddo S. Intracellular amyloid-beta in Alzheimer's disease. Nat Rev Neurosci. 2007, 8(7), 499-509.

265. Lai A.Y., McLaurin J. Mechanisms of amyloid-Beta Peptide uptake by neurons: the role of lipid rafts and lipid raft-associated proteins. Int J Alzheimers Dis. 2010, 2011, 548380.

266. Lalli G., Schiavo G. Analysis of retrograde transport in motor neurons reveals common endocytic carriers for tetanus toxin and neurotrophin receptor p75NTR. J Cell Biol. 2002, 156(2), 233-39.

267. Lamballe F., Klein R., Barbacid M. The trk family of oncogenes and neurotrophin receptors. Princess Takamatsu Symp. 1991, 22, 153-70.

268. Lambert M.P., Barlow A.K., Chromy B.A., Edwards C., Freed R., Liosatos M., Morgan T.E., Rozovsky I., Trommer B., Viola K.L., Wals P., Zhang C., Finch C.E., Krafft G.A., Klein W.L. Diffusible, nonfibrillar ligands derived from Abeta1-42 are potent central nervous system neurotoxins. Proc Natl Acad Sci U S A. 1998, 95(11), 6448-53.

269. Lam F.C., Liu R., Lu P., Shapiro A.B., Renoir J.M., Sharom F.J., Reiner P.B. Beta-Amyloid efflux mediated by p-glycoprotein. J Neurochem 2001, 76(4), 1121-8.
224. Laske C. Blood-based biomarkers in Alzheimer disease. Arch Neurol. 2011, 68(5), 685-86

270. Lapchak P.A., Araujo D.M., Carswell S., Hefti F. Distribution of [125I]nerve growth factor in the rat brain following a single intraventricular injection: correlation with the topographical distribution of trkA messenger RNA-expressing cells. Neuroscience. 1993, 54(2), 445-60.

271. Lasagna-Reeves C.A., Castillo-Carranza D.L., Sengupta U., Clos A.L., Jackson G.R., Kayed R. Tau oligomers impair memory and induce synaptic and mitochondrial dysfunction in wild-type mice. Mol Neurodegener. 2011, 6-39

272. Laursen B., Mørk A., Plath N., Kristiansen U., Bastlund J.F. Cholinergic degeneration is associated with increased plaque deposition and cognitive impairment in APPswe/PS1dE9 mice. Behav Brain Res. 2013, 240, 146-52.

273. Laursen B., Mørk A., Plath N., Kristiansen U., Bastlund J.F. Impaired hippocampal acetylcholine release parallels spatial memory deficits in Tg2576 mice subjected to basal forebrain cholinergic degeneration. Brain Res. 2014, 1543, 253-62.

274. Lazarov O, Marr R.A. Neurogenesis and Alzheimer's disease: at the crossroads. Exp Neurol. 2010, 223(2), 267-81.

275. Lee J.H., Yu W.H., Kumar A., Lee S., Mohan P.S., Peterhoff C.M., Wolfe D.M., Martinez-Vicente M., Massey A.C., Sovak G., Uchiyama Y., Westaway D., Cuervo A.M., Nixon R.A. Lysosomal proteolysis and autophagy require presenilin 1 and are disrupted by Alzheimer-related PS1 mutations. Cell. 2010, 141(7), 1146-58.

276. Lee K.F., Li E., Huber L.J., Landis S.C., Sharpe A.H., Chao M.V., Jaenisch R. Targeted mutation of the gene encoding the low affinity NGF receptor p75 leads to deficits in the peripheral sensory nervous system. Cell. 1992, 69(5), 737-49.

277. Lee M.G., Hassani O.K., Alonso A., Jones B.E. Cholinergic basal forebrain neurons burst with theta during waking and paradoxical sleep. J Neurosci. 2005, 25 (17), 4365-69.

278. Lee R., Kermani P., Teng K.K., Hempstead B.L. Regulation of cell survival by secreted proneurotrophins. Science. 2001, 294(5548), 1945-48.

279. Lehrer S. Nasal NSAIDs for Alzheimer's Disease. Am J Alzheimers Dis Other Demen. 2014, 29(5),401-403.

280. Lemere C.A., Munger J.S., Shi G.P., Natkin L., Haass C., Chapman H.A., Selkoe D.J. The lysosomal cysteine protease, cathepsin S, is increased in Alzheimer's disease and Down syndrome brain. An immunocytochemical study. Am J Pathol., 1995, 146(4), 848-60

281. Leong S.W., Abas F., Lam K.W., Shaari K., Lajis N.H. 2-Benzoyl-6-benzylidenecyclohexanone analogs as potent dual inhibitors of acetylcholinesterase and butyrylcholinesterase. Bioorg Med Chem. 2016, 24(16), 3742-51

282. Lesnik E.A., Sampath R., Ecker D.J. Rev response elements (RRE) in lentiviruses: an RNAMotif algorithm-based strategy for RRE prediction. Med Res Rev. 2002, 22(6), 617-36.

283. Leuner K., Hauptmann S., Abdel-Kader R., Scherping I., Keil U., Strosznajder J.B., Eckert A., Müller W.E. Mitochondrial dysfunction: the first domino in brain aging and Alzheimer's disease? Antioxid Redox Signal. 2007, 9(10), 1659-75.

284. Levey A. Immunological localization of m1-m5 muscarinic acetylcholine receptors in peripheral tissues and brain. Life Sci. 1993, 52(5-6), 441-8.

285. Levin E.D., Rose J.E., McGurk S.R., Butcher L.L. Characterization of the cognitive effects of combined muscarinic and nicotinic blockade. Behav Neural Biol. 1990, 53(1), 103-12.

286. Levites Y., Jansen K., Smithson L.A., Dakin R., Holloway V.M., Das P., Golde T.E. Intracranial adeno-associated virus-mediated delivery of anti-pan amyloid beta, amyloid beta40, and amyloid beta42 single-chain variable fragments attenuates plaque pathology in amyloid precursor protein mice. J Neurosci. 2006, 26(46), 11923-28.

287. Levy J.R., Hannah S., Mooney R.L., Hug V., Stevens W. Sequence and functional characterization of the terminal exon of the human insulin receptor gene. Biochim Biophys Acta. 1995, 1263(3), 253-57.

288. Levy-Lahad E., Wasco W., Poorkaj P., Romano D.M., Oshima J., Pettingell W.H., Yu C.E., Jondro P.D., Schmidt S.D., Wang K. Candidate gene for the chromosome 1 familial Alzheimer's disease locus. Science. 1995, 269(5226), 973-77.

289. Li M., Husic N., Lin Y., Snider B.J. Production of lentiviral vectors for transducing cells from the central nervous system. J Vis Exp. 2012, (63), 4031.

290. Lilja A.M., Porras O., Storelli E., Nordberg A., Marutle A. Functional interactions of fibrillar and oligomeric amyloid-β with alpha7 nicotinic receptors in Alzheimer's disease. J Alzheimers Dis. 2011, 23(2), 335-47

291. Lipton S.A. The molecular basis of memantine action in Alzheimer's disease and other neurologic disorders: low-affinity, uncompetitive antagonism. Curr Alzheimer Res. 2005, 2(2), 155-65.

292. Liu A.K., Chang R.C., Pearce R.K., Gentleman S.M. Nucleus basalis of Meynert revisited: anatomy, history and differential involvement in Alzheimer's and Parkinson's disease. Acta Neuropathol. 2015, 129(4), 527-40

293. Liu Q., Huang Y., Xue F., Simard A., DeChon J., Li G., Zhang J., Lucero L., Wang M., Sierks M., Hu G., Chang Y., Lukas R.J., Wu J. A novel nicotinic acetylcholine receptor subtype in basal forebrain cholinergic neurons with high sensitivity to amyloid peptides. J Neurosci. 2009, 29(4), 918-29.

294. Liu Q., Kawai H., Berg D.K. beta -Amyloid peptide blocks the response of alpha 7-containing nicotinic receptors on hippocampal neurons. Proc Natl Acad Sci U S A. 2001, 98(8), 4734-39.

295. Llinás R., Sugimori M., Silver R.B. The concept of calcium concentration microdomains in synaptic transmission. Neuropharmacology. 1995, 34(11), 1443-51.

296. Luiten P.G., Gaykema R.P., Traber J., Spencer D.G.Jr. Cortical projection patterns of magnocellular basal nucleus subdivisions as revealed by anterogradely transported Phaseolus vulgaris leucoagglutinin. Brain Res. 1987, 413(2), 229-50.

297. Lustbader J.W., Cirilli M., Lin C., Xu H.W., Takuma K., Wang N., Caspersen C., Chen X., Pollak S., Chaney M., Trinchese F., Liu S., Gunn-Moore F., Lue L.F., Walker D.G., Kuppusamy P., Zewier Z.L., Arancio O., Stern D., Yan S.S., Wu H. ABAD directly links Abeta to mitochondrial toxicity in Alzheimer's disease. Science. 2004, 304(5669), 448-52.

298. Mandel R.J., Gage F.H., Clevenger D.G., Spratt S.K.., Snyder R.O., Leff S.E. Nerve growth factor expressed in the medial septum following in vivo gene delivery using a recombinant adeno-associated viral vector protects cholinergic neurons from fimbria-fornix lesion-induced degeneration. Exp Neurol. 1999, 155(1), 59-64.

299. Manders, E.M.M., Verbeek, F.J., Aten, J.A. 1993. Measurement of colocalization of objects in dual-color confocal images. J Microsc 1993, 169, 375-82.

300. Mann DMA, Neuropathology and neurochemical aspects of Alzheimer’s disease. In Inversen L.L., Iversen S.D., Synder S.H. (Eds.). Psychopharmacology of the aging nervous system: Plenum Press, New York, 1-67

301. Männistö P.T., Tuomainen P., Kutepova O., Borisenko S.A., Zolotov N., Voronina T. Effects of bilateral cholinotoxin infusions on the behavior and brain biochemistry of the rats. Pharmacol Biochem Behav. 1994, 49(1), 33-40.

302. Mantini D., Gerits A., Nelissen K., Durand J.B., Joly O., Simone L., Sawamura H., Wardak C., Orban G.A., Buckner R.L., Vanduffel W. Default mode of brain function in monkeys. J Neurosci. 2011, 31(36), 12954-62.

303. Marlin M.C., Li G. Biogenesis and Function of the NGF/TrkA Signaling Endosome. Int Rev Cell Mol Biol. 2015, 314, 239-57.

304. Martinez-Coria H., Green K.N., Billings L.M., Kitazawa M., Albrecht M., Rammes G., Parsons C.G., Gupta S., Banerjee P., LaFerla F.M. Memantine improves cognition and reduces Alzheimer's-like neuropathology in transgenic mice. Am J Pathol. 2010, 176(2), 870-80.

305. Martinez-Murillo, R, Rodrigo, J The localization of cholinergic neurons andmarkers in the CNS. In: Stone, TW eds. (1995) CNS Neurotransmitters and neuromodulators: Acetylcholine. CRC Press, Boca Raton, 1-38

306. Masters C.L., Simms G., Weinman N.A., Multhaup G., McDonald B.L., Beyreuther K. Amyloid plaque core protein in Alzheimer disease and Down syndrome. Proc Natl Acad Sci USA 1985, 82(12), 4245-49.

307. Matsunaga S., Kishi T., Iwata N. Combination Therapy with Cholinesterase Inhibitors and Memantine for Alzheimer's disease: A Systematic Review and Meta-analysis. Int J Neuropsychopharmacol. 2014, 28, 18(5).

308. Matsuzono K., Hishikawa N., Ohta Y., Yamashita T., Deguchi K., Nakano Y., Abe K. Combination Therapy of Cholinesterase Inhibitor (Donepezil or Galantamine) plus Memantine in the Okayama Memantine Study. J Alzheimers Dis. 2015, 45(3), 771-80.

309. Mattson M.P. Apoptosis in neurodegenerative disorders. Nat Rev Mol Cell Biol. 2000, 1(2), 120-29.

310. Mattson M.P, Magnus T. Ageing and neuronal vulnerability. Nat Rev Neurosci. 2006, 7(4), 278-94.

311. Mattson M.P., Rychlik B., Chu C., Christakos S. Evidence for calcium-reducing and excito-protective roles for the calcium-binding protein calbindin-D28k in cultured hippocampal neurons. Neuron. 1991, 6(1), 41-51.

312. McBrayer M., Nixon R.A. Lysosome and calcium dysregulation in Alzheimer's disease: partners in crime. Biochem Soc Trans. 2013, 41(6), 1495-502.

313. McGeer P.L., McGeer E.G., Suzuki J., Dolman C.E., Nagai T. Aging, Alzheimer's disease, and the cholinergic system of the basal forebrain. Neurology. 1984, 34(6), 741-45.

314. McKinney M, Jacksonville MC. Brain cholinergic vulnerability: relevance to behavior and disease. Biochem Pharmacol. 2005, 70(8), 1115-24. Neuron. 1991, 6(1), 41-51.

315. McLean C.A., Cherny R.A., Fraser F.W., Fuller S.J., Smith M.J., Beyreuther K., Bush A.I., Masters C.L. Soluble pool of Abeta amyloid as a determinant of severity of neurodegeneration in Alzheimer's disease. Ann Neurol. 1999, 46(6), 860-66.

316. McLellan M.E., Kajdasz S.T. Hyman B.T., Bacskai B.J. In vivo imaging of reactive oxygen species specifically associated with thioflavine S-positive amyloid plaques by multiphoton microscopy. J Neurosci 2003, 23(6), 2212-17

317. McLoughlin D.M., Miller C.C. The FE65 proteins and Alzheimer's disease. J Neurosci Res. 2008, 86(4), 744-54.

318. McQuiston A.R. Cholinergic modulation of excitatory synaptic input integration in hippocampal CA1. J Physiol. 2010, 588(19), 3727-42.

319. Melancon B.J., Tarr J.C., Panarese J.D., Wood M.R., Lindsley C.W. Allosteric modulation of the M1 muscarinic acetylcholine receptor: improving cognition and a potential treatment for schizophrenia and Alzheimer's disease. Drug Discov Today. 2013, 18(23-24), 1185-99.

320. Melander T., Staines W.A., Hökfelt T., Rökaeus A., Eckenstein F., Salvaterra P.M., Wainer B.H. Galanin-like immunoreactivity in cholinergic neurons of the septum-basal forebrain complex projecting to the hippocampus of the rat. Brain Res. 1985, 360(1-2), 130-38.

321. Mendoza-Oliva A., Zepeda A., Arias C. The complex actions of statins in brain and their relevance for Alzheimer's disease treatment: an analytical review. Curr Alzheimer Res. 2014, 11(9), 817-33.

322. Menting K.W., Claassen J.A. β-secretase inhibitor; a promising novel therapeutic drug in Alzheimer's disease. Front Aging Neurosci. 2014, 6, 165.

323. Mesulam M. The cholinergic lesion of Alzheimer's disease: pivotal factor or side show? Learn Mem. 2004, 11(1), 43-49.

324. Mesulam M.M., Mufson E.J., Levey A.I., Wainer B.H. Cholinergic innervation of cortex by the basal forebrain: cytochemistry and cortical connections of the septal area, diagonal band nuclei, nucleus basalis (substantia innominata), and hypothalamus in the rhesus monkey. J Comp Neurol. 1983, 214(2), 170-97.

325. Mesulam M.M., Mufson E.J., Wainer B.H., Levey A.I. Central cholinergic pathways in the rat – an overview based on an alternative nomenclature (Ch1- Ch6). Neuroscience 1983, 10, 1185-1201.

326. Mesulam M.M., Van Hoesen G.W. Acetylcholinesterase-rich projections from the basal forebrain of the rhesus monkey to neocortex. Brain Res. 1976, 109(1), 152-57.

327. Middlemas D.S., Lindberg R.A., Hunter T. TrkB, a neural receptor protein-tyrosine kinase: evidence for a full-length and two truncated receptors. Mol Cell Biol. 1991, 11(1), 143-53.

328. Miller G. Drug targeting, breaking down barriers. Science. 2002, 297(5584), 1116-18.

329. Minopoli G., de Candia P., Bonetti A., Faraonio R., Zambrano N., Russo T. The beta-amyloid precursor protein functions as a cytosolic anchoring site that prevents Fe65 nuclear translocation. J Biol Chem. 2001, 276(9), 6545-50.

330. Mintun M. A., Sacco D., Snyder A. Z., Couture L., Powers W.J., Hornbeck R., et al. Distribution of glycolysis in the resting healthy human brain correlates with distribution of beta-amyloid plaques in Alzheimer's disease. Soc. Neurosci. 2006, 707, 6.

331. Molinuevo J.L., Lladó A., Rami L. Memantine: targeting glutamate excitotoxicity in Alzheimer's disease and other dementias. Am J Alzheimers Dis Other Demen. 2005, 20(2), 77-85.

332. Momiyama T., Zaborszky L. Somatostatin presynaptically inhibits both GABA and glutamate release onto rat basal forebrain cholinergic neurons. J Neurophysiol. 2006, 96(2), 686-94.

333. Moore J.P., McKeating J.A., Weiss R.A., Sattentau Q.J. Dissociation of gp120from HIV-1 virions induced by soluble CD4. Science, 1990 (250), 1139-42.

334. Moretti M., Zoli M., George A.A., Lukas R.J., Pistillo F., Maskos U., Whiteaker P., Gotti C. The novel α7β2-nicotinic acetylcholine receptor subtype is expressed in mouse and human basal forebrain: biochemical and pharmacological characterization. Mol Pharmacol. 2014, 86(3), 306-17

335. Morimoto K., Yoshimi K., Tonohiro T., Yamada N., Oda T., Kaneko I. Co-injection of beta-amyloid with ibotenic acid induces synergistic loss of rat hippocampal neurons. Neuroscience. 1998, 84(2), 479-87.

336. Mormino E.C., Smiljic A., Hayenga A.O., Onami S.H., Greicius M.D., Rabinovici G.D., Janabi M., Baker S.L., Yen I.V., Madison C.M., Miller B.L., Jagust W.J. Relationships between β-amyloid and functional connectivity in different components of the default mode network in aging. Cereb Cortex. 2011, 21(10), 2399-407.

337. Mravec B., Lejavova K., Cubinkova V. Locus (coeruleus) minoris resistentiae in pathogenesis of Alzheimer's disease. Curr Alzheimer Res. 2014, 11(10), 992-1001.

338. Mufson E.J., Counts S.E., Fahnestock M., Ginsberg S.D. Cholinotrophic molecular substrates of mild cognitive impairment in the elderly. Curr Alzheimer Res. 2007, 4(4), 340-50.

339. Mufson E.J., Kordower J.H. Cortical neurons express nerve growth factor receptors in advanced age and Alzheimer disease. Proc Natl Acad Sci U S A. 1992, 89(2), 569-73.

340. Murchison D., Griffith W.H. Increased calcium buffering in basal forebrain neurons during aging. J Neurophysiol. 1998, 80(1), 350-64.

341. Murray S.S., Perez P., Lee R., Hempstead B.L., Chao M.V. A novel p75 neurotrophin receptor-related protein, NRH2, regulates nerve growth factor binding to the TrkA receptor. J Neurosci. 2004, 24(11), 2742-49.

342. Nagele R.G., D'Andrea M.R., Anderson W.J., Wang H.Y. Intracellular accumulation of beta-amyloid(1-42) in neurons is facilitated by the alpha 7 nicotinic acetylcholine receptor in Alzheimer's disease. Neuroscience. 2002, 110(2), 199-211.

343. Nakajima Y., Nakajima S., Obata K., Carlson C.G., Yamaguchi K. Dissociated cell culture of cholinergic neurons from nucleus basalis of Meynert and other basal forebrain nuclei. Proc Natl Acad Sci U S A. 1985, 82(18), 6325-29.

344. Nakamura S., Murayama N., Noshita T., Annoura H., Ohno T. Progressive brain dysfunction following intracerebroventricular infusion of beta(1-42)-amyloid peptide. Brain Res. 2001, 912(2), 128-36.

345. Nakayama H., Shioda S., Okuda H., Nakashima T., Nakai Y. Immunocytochemical localization of nicotinic acetylcholine receptor in rat cerebral cortex. Brain Res Mol Brain Res. 1995, 32(2), 321-28.

346. Nakaya K., Nakagawasai O., Arai Y., Onogi H., Sato A., Niijima F., Tan-No K., Tadano T. Pharmacological characterizations of memantine-induced disruption of prepulse inhibition of the acoustic startle response in mice: involvement of dopamine D2 and 5-HT2A receptors. Behav Brain Res. 2011, 218(1), 165-73.

347. Nanou A1, Azzouz M. Gene therapy for neurodegenerative diseases based on lentiviral vectors. Prog Brain Res. 2009, 175, 187-200.

348. Nardone R., Bergmann J., De Blasi P., Kronbichler M., Kraus J., Caleri F., Tezzon F., Ladurner G., Golaszewski S. Cholinergic dysfunction and amnesia in patients with Wernicke-Korsakoff syndrome: a transcranial magnetic stimulation study. J Neural Transm. 2010, 117(3), 385-91.

349. Nethercott H.E., Brick D.J., Schwartz P.H. Derivation of induced pluripotent stem cells by lentiviral transduction. Methods Mol Biol. 2011, 767, 67-85

350. Nath S., Agholme L., Kurudenkandy F.R., Granseth B., Marcusson J., Hallbeck M. Spreading of neurodegenerative pathology via neuron-to-neuron transmission of β-amyloid. J Neurosci. 2012, 32(26), 8767-77.

351. Naumann T., Casademunt E., Hollerbach E., Hofmann J., Dechant G., Frotscher M., Barde Y.A. Complete deletion of the neurotrophin receptor p75NTR leads to long-lasting increases in the number of basal forebrain cholinergic neurons. J Neurosci. 2002, 22(7), 2409-18.

352. Necula M., Kayed R., Milton S., Glabe C.G. Small molecule inhibitors of aggregation indicate that amyloid beta oligomerization and fibrillization pathways are independent and distinct. J Biol Chem. 2007, 282(14), 10311-24.

353. Niewiadomska G., Komorowski S., Baksalerska-Pazera M. Amelioration of cholinergic neurons dysfunction in aged rats depends on the continuous supply of NGF. Neurobiol Aging. 2002, 23(4), 601-13.

354. Nimmrich V., Grimm C., Draguhn A., Barghorn S., Lehmann A., Schoemaker H., Hillen H., Gross G., Ebert U., Bruehl C. Amyloid beta oligomers (A beta(1-42) globulomer) suppress spontaneous synaptic activity by inhibition of P/Q-type calcium currents. J Neurosci. 2008, 28(4), 788-97

355. Nishimura M., Satoh M., Matsushita K., Nomura F. How proteomic ApoE serotyping could impact Alzheimer's disease risk assessment: genetic testing by proteomics. Expert Rev Proteomics. 2014, 1-3

356. Nissl F. Ueber eine neue Untersuchungsmethode des Centralorgans zur Feststellung der Localisation der Nervenzellen. Neurologisches Centralblatt. 1894, 13, 507–8.

357. Nitsch R.M., Slack B.E., Wurtman R.J., Growdon J.H. Release of Alzheimer amyloid precursor derivatives stimulated by activation of muscarinic acetylcholine receptors. Science. 1992, 258(5080), 304-7.

358. Nitz D. Parietal cortex, navigation, and the construction of arbitrary reference frames for spatial information. Neurobiol Learn Mem. 2009, 91(2), 179-85.

359. Nixon R.A., Yang D.S., Lee J.H. Neurodegenerative lysosomal disorders: a continuum from development to late age. Autophagy. 2008, 4(5), 590-99

360. Nordberg A. Dementia in 2014: Towards early diagnosis in Alzheimer disease. Nat Rev Neurol. 2015.

361. Nykjaer A., Lee R., Teng K.K., Jansen P., Madsen P., Nielsen M.S., Jacobsen C., Kliemannel M., Schwarz E., Willnow T.E., Hempstead B.L., Petersen C.M. Sortilin is essential for proNGF-induced neuronal cell death. Nature. 2004, 427,843-48.

362. Nykjaer A., Willnow T.E. Sortilin: a receptor to regulate neuronal viability and function. Trends Neurosci. 2012, 35(4), 261-70.
363. O'Leary V.B., Ovsepian S.V., Bodeker M., Dolly J.O. Improved lentiviral transduction of ALS motor neurons in vivo via dual targeting. Mol Pharm. 2013, 10(11), 4195-206.

364. O'Meara G., Coumis U., Ma S.Y., Kehr J., Mahoney S., Bacon A., Allen S.J., Holmes F., Kahl U., Wang F.H., Kearns I.R., Ove-Ogren S., Dawbarn D., Mufson E.J., Davies C., Dawson G., Wynick D. Galanin regulates the postnatal survival of a subset of basal forebrain cholinergic neurons. Proc Natl Acad Sci U S A. 2000, 97(21), 11569-74.

365. Osuntokun B.O., Sahota A., Ogunniyi A.O., Gureje O., Baiyewu O., Adeyinka A., Oluwole S.O., Komolafe O., Hall K.S., Unverzagt F.W. Lack of an association

between apolipoprotein E epsilon 4 and Alzheimer's disease in elderly Nigerians. Ann Neurol. 1995, 38(3), 463-65.

366. Ovsepian S.V., Antyborzec I., O'Leary V.B., Zaborszky L., Herms J., Oliver Dolly J. Neurotrophin receptor p75 mediates the uptake of the amyloid beta (Aβ) peptide, guiding it to lysosomes for degradation in basal forebrain cholinergic neurons. Brain Struct Funct. 2014, 219(5), 1527-41

367. Ovespian S.V., Bodeker M., O'Leary V.B., Lawrence G.W., Oliver Dolly J. Internalization and retrograde axonal trafficking of tetanus toxin in motor neurons and trans-synaptic propagation at central synapses exceed those of its C-terminal-binding fragments. Brain Struct Funct. 2015;220(3):1825-38.

368. Ovsepian S.V., Dolly J.O. Dendritic SNAREs add a new twist to the old neuron theory. Proc Natl Acad Sci U S A. 2011, 108(48), 19113-20.

369. Ovsepian S.V., Dolly J.O., Zaborszky L. Intrinsic voltage dynamics govern the diversity of spontaneous firing profiles in basal forebrain noncholinergic neurons. J Neurophysiol. 2012, 108(2), 406-18

370. Ovsepian S.V., Herms J. Cholinergic neurons-keeping check on amyloid β in the cerebral cortex. Front Cell Neurosci. 2013, (7), 252.

371. Ovsepian S.V, Herms J. Drain of the brain: low-affinity p75 neurotrophin receptor affords a molecular sink for clearance of cortical amyloid β by the cholinergic modulator system. Neurobiol Aging. 2013, 34(11), 2517-24.

372. Ovsepian S.V., O'Leary V.B., Zaborszky L. Cholinergic Mechanisms in the Cerebral Cortex: Beyond Synaptic Transmission. Neuroscientist. 2016, 22(3), 238-51.

373. Page K.J., Saha A., Everitt B.J. Differential activation and survival of basal forebrain neurons following infusions of excitatory amino acids: studies with the immediate early gene c-fos. Exp Brain Res. 1993, 93(3), 412-22.

373. Palmer A.M., DeKosky S.T. Monoamine neurons in aging and Alzheimer s disease. Journal of Neural Transmission (Gen Sect), 1993, 91, 135-59.

374. Palmer A.M., Francis P.T., Benton J.S., Sims N.R., Mann D.M.A., Neary D., Snowden J.S., Bowen D.M. Presynaptic serotonergic dysfunction in patients with Alzheimer s disease. Brain Research, 1987, 48, 8-15.

375. Palmer A.M., Gershon S. Is the neuronal basis of Alzheimer's disease cholinergic or glutamatergic? FASEB J. 1990, 4(10), 2745-52.

376. Palop J.J., Jones B., Kekonius L., Chin J., Yu G.Q., Raber J., Masliah E., Mucke L. Neuronal depletion of calcium-dependent proteins in the dentate gyrus is tightly linked to Alzheimer's disease-related cognitive deficits. Proc Natl Acad Sci U S A. 2003, 100(16), 9572-77.

377. Palop J.J., Mucke L., Roberson E.D. Quantifying biomarkers of cognitive dysfunction and neuronal network hyperexcitability in mouse models of Alzheimer's disease: depletion of calcium-dependent proteins and inhibitory hippocampal remodeling. Methods Mol Biol. 2011, 670, 245-62.

378. Panula, P., Yang, H.Y., and Costa, E. Histamine-containing neurons in the rat hypothalamus. Proc. Natl. Acad. Sci. USA 1984, 81, 2572–76.

379. Park H., Han K.S., Seo J., Lee J., Dravid S.M., Woo J., Chun H., Cho S., Bae J., An H., Koh W., Yoon B.E., Berlinguer-Palmini R., Mannaioni G., Traynelis S.F., Bae Y., Choi S.Y., Lee C. Channel-mediated astrocytic glutamate modulates hippocampal synaptic plasticity by activating postsynaptic NMDA receptors. Mol Brain. 2015, 8(1),7.

380. Parri R.H., Dineley T.K. Nicotinic acetylcholine receptor interaction with beta-amyloid: molecular, cellular, and physiological consequences. Curr Alzheimer Res. 2010, 7(1), 27-39.

381. Patel A.N., Jhamandas J.H. Neuronal receptors as targets for the action of amyloid-beta protein (Aβ) in the brain. Expert Rev Mol Med. 2012, (14), 2.

382. Paula-Lima A.C., Brito-Moreira J., Ferreira S.T. Deregulation of excitatory neurotransmission underlying synapse failure in Alzheimer's disease. J Neurochem. 2013, 126(2), 191-202.

383. Paxinos G, Watson C (1998).The rat brain atlas. Fourth edition Academic Press.

384. Pellizzari R., Rossetto O., Schiavo G., Montecucco C. Tetanus and botulinum neurotoxins: mechanism of action and therapeutic uses. Philos Trans R Soc Lond B Biol Sci. 1999, 354(1381), 259-68.

385. Peng, S., Wuu, J., Mufson, E.J., and Fahnestock, M. Increased proNGF levels in subjects with mild cognitive impairment and mild Alzheimer disease. J. Neuropathol. Exp. Neurol.2004, 63, 641–49.

386. Pennanen C., Kivipelto M., Tuomainen S., Hartikainen P., Hänninen T., Laakso M.P., Hallikainen M., Vanhanen M., Nissinen A., Helkala E.L., Vainio P., Vanninen R., Partanen K., Soininen H. Hippocampus and entorhinal cortex in mild cognitive impairment and early AD. Neurobiol Aging. 2004, 25(3), 303-10.

387. Perez J.L., Carrero I., Gonzalo P., Arevalo-Serrano J., Sanz-Anquela J.M., Ortega J., Rodriguez M., Gonzalo-Ruiz A. Soluble oligomeric forms of beta-amyloid (Abeta) peptide stimulate Abeta production via astrogliosis in the rat brain. Exp Neurol. 2010, 223(2), 410-21.

388. Perez-Nievas B.G., Stein T.D., Tai H.C., Dols-Icardo O., Scotton T.C., Barroeta-Espar I., Fernandez-Carballo L., de Munain E.L., Perez J., Marquie M., Serrano-Pozo A., Frosch M.P., Lowe V., Parisi J.E., Petersen R.C., Ikonomovic M.D., López O.L., Klunk W., Hyman B.T., Gómez-Isla T. Dissecting phenotypic

traits linked to human resilience to Alzheimer's pathology. Brain. 2013, 136, (8), 2510-26.

389. Perry E., Walker M., Grace J., Perry R. Acetylcholine in mind: a neurotransmitter correlate of consciousness? Trends Neurosci. 1999, 22(6), 273-80.

390. Peyron C., Tighe D.K., van den Pol A.N., de Lecea L., Heller H.C., Sutcliffe J.G., Kilduff T.S. Neurons containing hypocretin (orexin) project to multiple neuronal systems. J Neurosci. 1998, 18(23), 9996-10015.

391. Piazza-Gardner A.K., Gaffud T.J., Barry A.E. The impact of alcohol on Alzheimer's disease: a systematic review. Aging Ment Health. 2013, 17(2), 133-46.

392. Pietrzik C.U., Yoon I.S., Jaeger S., Busse T., Weggen S., Koo E.H. FE65 constitutes the functional link between the low-density lipoprotein receptor-related protein and the amyloid precursor protein. J Neurosci. 2004, 24(17), 4259-65.

393. Podlisny M.B., Stephenson D.T., Frosch M.P., Tolan D.R., Lieberburg I., Clemens J.A., Selkoe D.J. Microinjection of synthetic amyloid S-protein in monkey cerebral cortex fails to produce acute neurotoxicity. Am. J. Pathol. 1993, 142, 17-24

394. Pongrac J.L., Rylett R.J. Molecular mechanisms regulating NGF-mediated enhancement of cholinergic neuronal phenotype: c-fos trans-activation of the choline acetyltransferase gene. J Mol Neurosci. 1998, 11(1), 79-93.

395. Pongrac J.L., Rylett R.J. Optimization of serum-free culture conditions for growth of embryonic rat cholinergic basal forebrain neurons. J Neurosci Methods. 1998, 84(1-2), 69-76.

396. Poo M.M. Neurotrophins as synaptic modulators. Nat Rev Neurosci. 2001, 2(1), 24-32.

397. Praticò D. Oxidative stress hypothesis in Alzheimer's disease: a reappraisal. Trends Pharmacol Sci. 2008, 29(12), 609-15.

398. Price D.L., Sisodia S.S. Mutant genes in familial Alzheimer's disease and transgenic models. Annu Rev Neurosci. 1998, 21, 479-505.

399. Puzzo D., Privitera L., Leznik E., Fà M., Staniszewski A., Palmeri A., Arancio O. Picomolar amyloid-beta positively modulates synaptic plasticity and memory in hippocampus. J Neurosci. 2008, 28(53), 14537-45

400. Quirion R. Cholinergic markers in Alzheimer disease and the autoregulation of acetylcholine release. J Psychiatry Neurosci. 1993, 18(5), 226-34.

401. Radhakrishnan P., Basma H., Klinkebiel D., Christman J., Cheng P.W. Cell type-specific activation of the cytomegalovirus promoter by dimethylsulfoxide and 5-aza-2'-deoxycytidine. Int J Biochem Cell Biol. 2008, 40(9), 1944-55.

402. Rafii M.S., Baumann T.L., Bakay R.A., Ostrove J.M., Siffert J., Fleisher A.S., Herzog C.D., Barba D., Pay M., Salmon D.P., Chu Y., Kordower J.H., Bishop K., Keator D., Potkin S., Bartus R.T. A phase1 study of stereotactic gene delivery of AAV2-NGF for Alzheimer's disease. Alzheimers Dement. 2014, 10(5), 571-81.

403. Raghunath A., Perez-Branguli F., Smith L., Dolly J.O. Adeno-associated virus transfer of a gene encoding SNAP-25 resistant to botulinum toxin A attenuates neuromuscular paralysis associated with botulism. J Neurosci. 2008, 28(14), 3683-88.

404. Rahim F., Javed M.T., Ullah H., Wadood A., Taha M., Ashraf M., Qurat-ul-Ain., Khan M.A., Khan F., Mirza S., Khan K.M. Synthesis, molecular docking, acetylcholinesterase and butyrylcholinesterase inhibitory potential of thiazole analogs as new inhibitors for Alzheimer disease. Bioorg Chem. 2015, 62, 106-16.

405. Rasmusson D.D. The role of acetylcholine in cortical synaptic plasticity. Behav Brain Res. 2000, 115(2), 205-18.

406. Ren K., King M.A., Liu J., Siemann J., Altman M., Meyers C., Hughes J.A., Meyer E.M. The alpha7 nicotinic receptor agonist 4OH-GTS-21 protects axotomized septohippocampal cholinergic neurons in wild type but not amyloid-overexpressing transgenic mice. Neuroscience. 2007, 148(1), 230-7

407. Ribot, T., 1881. Les Maladies de la Memoire. Felix Alcaan. Paris.

408. Richardson J.A., Burns D.K. Mouse models of Alzheimer's disease: a quest for plaques and tangles. ILAR J. 2002, 43(2), 89-99.

409. Richardson P.M., Issa V.M., Riopelle R.J. Distribution of neuronal receptors for nerve growth factor in the rat. J Neurosci. 1986, 6(8), 2312-21.

410. Ridley R.M., Baker H.F., Windle C.P., Cummings R.M. Very long term studies of the seeding of beta-amyloidosis in primates. J Neural Transm. 2006, 113(9), 1243-51

411. Rochester L., Yarnall A.J., Baker M.R., David R.V., Lord S., Galna B., Burn D.J. Cholinergic dysfunction contributes to gait disturbance in early Parkinson's disease. Brain. 2012, 135(9), 2779-88.

412. Roghani A., Feldman J., Kohan S.A., Shirzadi A., Gundersen C.B., Brecha N., Edwards R.H. Molecular cloning of a putative vesicular transporter for acetylcholine. Proc Natl Acad Sci U S A. 1994, 91(22), 10620-24.

413. Roher A.E., Kuo Y.M., Potter P.E., Emmerling M.R., Durham R.A., Walker D.G., Sue L.I., Honer W.G., Beach T.G. Cortical cholinergic denervation elicits vascular A beta deposition. Ann N Y Acad Sci. 2000, 903, 366-73.

414. Rohll J.B., Mitrophanous K.A., Martin-Rendon E., Ellard F.M., Radcliffe P.A., Mazarakis N.D., Kingsman S.M. Design, production, safety, evaluation, and clinical

applications of nonprimate lentiviral vectors. Methods Enzymol 2002, (346) 466-500.

415. Rosenberg M.B., Hawrot E., Breakefield X.O. Receptor binding activities of biotinylated derivatives of beta-nerve growth factor. J Neurochem. 1986, 46(2), 641-8.

416. Rosen R.F., Fritz J.J., Dooyema J., Cintron A.F., Hamaguchi T., Lah J.J., LeVine H., Jucker M., Walker L.C. Exogenous seeding of cerebral β-amyloid deposition in βAPP-transgenic rats. J Neurochem. 2012, 120(5), 660-66.

417. Rossner S., Härtig W., Schliebs R., Brückner G., Brauer K., Perez-Polo J.R., Wiley R.G., Bigl V. 192IgG-saporin immunotoxin-induced loss of cholinergic cells differentially activates microglia in rat basal forebrain nuclei. J Neurosci Res. 1995, 41(3), 335-46.

418. Rouse S.T., Edmunds S.M., Yi H., Gilmor M.L., Levey A.I.. Localization of M (2) muscarinic acetylcholine receptor protein in cholinergic and non-cholinergic terminals in rat hippocampus. Neurosci Lett. 2000, 284(3), 182-86.

419. Roux P.P., Bhakar A.L., Kennedy T.E., Barker P.A. The p75 neurotrophin receptor activates Akt (protein kinase B) through a phosphatidylinositol 3-kinase-dependent pathway. J Biol Chem. 2001, 276(25), 23097-104.

420. Ruberg M., Javoy-Agid F., Hirsch E., Scatton B., LHeureux R., Hauw J.J., Duyckaerts C., Gray F., Morel-Maroger A., Rascol A., et al. Dopaminergic and cholinergic lesions in progressive supranuclear palsy. Ann Neurol. 1985, 18(5), 523-29.

421. Rubinson D.A., Dillon C.P., Kwiatkowski A.V., Sievers C., Yang L., Kopinja J., Rooney D.L., Zhang M., Ihrig M.M., McManus M.T., Gertler F.B., Scott M.L., Van Parijs L. A lentivirus-based system to functionally silence genes in primary mammalian cells, stem cells and transgenic mice by RNA interference. Nat Genet. 2003, 33(3), 401-6.

422. Rush D.K. Scopolamine amnesia of passive avoidance: a deficit of information acquisition. Behav Neural Biol. 1988, 50(3), 255-74.

423. Rylett R.J., Ball M.J., Colhoun E.H. Evidence for high affinity choline transport in synaptosomes prepared from hippocampus and neocortex of patients with Alzheimer's disease. Brain Res. 1983, 289, 169-75.

424. Saavedra L., Mohamed A., Ma V., Kar S., de Chaves E.P. Internalization of beta-amyloid peptide by primary neurons in the absence of apolipoprotein E. J Biol Chem. 2007, 282(49), 35722-32.

425. Sabo S.L., Ikin A.F., Buxbaum J.D., Greengard P. The Alzheimer amyloid precursor protein (APP) and FE65, an APP-binding protein, regulate cell movement. J Cell Biol. 2001, 153(7), 1403-14.

426. Sabo S.L., Ikin A.F., Buxbaum J.D., Greengard P. The amyloid precursor protein and its regulatory protein, FE65, in growth cones and synapses in vitro and in vivo. J Neurosci. 2003, 23(13), 5407-15.

427. Sabo S.L., Lanier L.M., Ikin A.F., Khorkova O., Sahasrabudhe S., Greengard P., Buxbaum J.D. Regulation of beta-amyloid secretion by FE65, an amyloid protein precursor-binding protein. J Biol Chem. 1999, 274(12), 7952-7.

428. Sáez E.T., Pehar M., Vargas M.R., Barbeito L., Maccioni R.B. Production of nerve growth factor by beta-amyloid-stimulated astrocytes induces p75NTR-dependent tau hyperphosphorylation in cultured hippocampal neurons. J Neurosci Res. 2006, 84(5), 1098-106.

429. Sakurai T. The neural circuit of orexin (hypocretin): maintaining sleep and wakefulness. Nat Rev Neurosci. 2007, 8(3), 171-81.

430. Salama-Cohen P., Arévalo M.A., Meier J., Grantyn R., Rodríguez-Tébar A. NGF controls dendrite development in hippocampal neurons by binding to p75NTR and modulating the cellular targets of Notch. Mol Biol Cell. 2005, 16(1), 339-47.

431. Salehi A., Ocampo M., Verhaagen J., Swaab D.F. P75 neurotrophin receptor in the nucleus basalis of meynert in relation to age, sex, and Alzheimer's disease. Exp Neurol. 2000, 161(1), 245-58.

432. Salmon P., Trono D. Production and titration of lentiviral vectors. Curr Protoc Neurosci. 2006, Chapter 4: Unit 4.21.

433. Sanan D.A., Weisgraber K.H., Russell S.J., Mahley R.W., Huang D., Saunders A., Schmechel D., Wisniewski T., Frangione B., Roses A.D., et al. Apolipoprotein E associates with beta amyloid peptide of Alzheimer’s disease to form novel monofibrils. Isoform apoE4 associates more efficiently than apoE3.J Clin Invest. 1994, 94(2), 860-69

434. Sarter M., Hasselmo M.E., Bruno J.P., Givens B. Unravelling the attentional functions of cortical cholinergic inputs: interactions between signal-driven and cognitive modulation of signal detection. Brain Res Brain Res Rev. 2005, 48(1), 98-111.

435. Sasai N., Nakazawa Y., Haraguchi T., Sasai Y. The neurotrophin-receptor-related protein NRH1 is essential for convergent extension movements. Nat Cell Biol. 2004, 6(8), 741-48.

436. Sato A., Sato Y., Uchida S. Activation of the intracerebral cholinergic nerve fibres originating in the basal forebrain increases regional cerebral blood flow in the rat's cortex and hippocampus. Neurosci Lett. 2004, 361(1-3), 90-93.

437. Sawamura N., Morishima-Kawashima M., Waki H., Kobayashi K., Kuramochi T., Frosch M.P., Ding K., Ito M., Kim T.W., Tanzi R.E., Oyama F., Tabira T., Ando S., Ihara Y. Mutant presenilin 2 transgenic mice. A large increase in the levels of Abeta 42 is presumably associated with the low density membrane domain that

contains decreased levels of glycerophospholipids and sphingomyelin. J Biol Chem. 2000, 275(36), 27901-8.

438. Schellenberg G.D., Bird T.D., Wijsman E.M., Orr H.T., Anderson L., Nemens E., White J.A., Bonnycastle L., Weber J.L., Alonso M.E. Genetic linkage evidence for a familial Alzheimer's disease locus on chromosome 14. Science. 1992, 258(5082), 668-71.

439. Schliebs R., Arendt T. The significance of the cholinergic system in the brain during aging and in Alzheimer's disease. J Neural Transm. 2006, 113(11), 1625-44.

440. Schliebs R., Rossner S, Bigl V. Immunolesion by 192IgG-saporin of rat basal forebrain cholinergic system: a useful tool to produce cortical cholinergic dysfunction. Prog Brain Res. 1996, 109, 253-64.

441. Schneider J.A., Arvanitakis Z., Bang W., Bennett D.A. Mixed brain pathologies account for most dementia cases in community-dwelling older persons. Neurology. 2007, 69(24), 2197-204.

442. Schnitzler A.C., Lopez-Coviella I., Blusztajn J.K. Purification and culture of nerve growth factor receptor (p75)-expressing basal forebrain cholinergic neurons. Nat Protoc. 2008, 3(1), 34-40.

443. Schor N.F. The p75 neurotrophin receptor in human development and disease. Prog Neurobiol. 2005, 77(3), 201-14.

444. Schultz, S., Panzeri, S., Rolls, E., Treves, A. Quantitative analysis of a Schaffer collateral model. In Information Theory and the Brain, R., Baddeley, P., Hancock, P. Foldiak (Eds.). Cambridge University Press, UK,1998.

445. Schwaller B. Cytosolic Ca^{2+} buffers. Cold Spring Harb Perspect Biol. 2010, 2(11), 004051

446. Scoville W.B., Milner B. Loss of recent memory after bilateral hippocampal lesions. 1957. J Neuropsychiatry Clin Neurosci. 2000, 12(1), 103-13.

447. Seeger T., Fedorova I., Zheng F., Miyakawa T., Koustova E., Gomeza J., Basile A.S., Alzheimer C., Wess J. M2 muscarinic acetylcholine receptor knock-out mice show deficits in behavioral flexibility, working memory, and hippocampal plasticity. J Neurosci. 2004, 24(45), 10117-27.

448. Seidah N.G., Benjannet S., Pareek S., Savaria D., Hamelin J., Goulet B., Laliberte J., Lazure C., Chrétien M., Murphy R.A. Cellular processing of the nerve growth factor precursor by the mammalian pro-protein convertases. Biochem J. 1996, 15(314) , 951-60.

449. Selkoe D.J. Biochemistry and molecular biology of amyloid beta-protein and the mechanism of Alzheimer's disease. Handb Clin Neurol. 2008, 89, 245-60

450. Selkoe D.J. Cell biology of protein misfolding: the examples of Alzheimer's and Parkinson's diseases. Nat Cell Biol. 2004, 6(11), 1054-61.

451. Selkoe D.J. Folding proteins in fatal ways. Nature. 2003, 426(6968), 900-904.
452. Selkoe D.J. The ups and downs of Abeta. Nat Med. 2006, 12(7), 758-59

453. Semba K. Multiple output pathways of the basal forebrain: organization, chemical heterogeneity, and roles in vigilance. Behav. Brain Res. 2000, 115(2), 117-41

454. Sepulcre J., Sabuncu M.R., Becker A., Sperling R., Johnson K.A. In vivo characterization of the early states of the amyloid-beta network. Brain. 2013, 136, 2239-52

455. Serrano-Pozo A., Frosch M.P., Masliah E., Hyman B.T. Neuropathological alterations in Alzheimer disease. Cold Spring Harb Perspect Med. 2011, (1), 006189.

456. Seubert P., Vigo-Pelfrey F., Esch M., Lee H., Dovey D., Davis S., Sinha M., Schlossmacher J., Whaley C., Swindlehurst C. McCormack R., Wolfert R., Selkoe D., Lieberburg I., Schenk D. Isolation and quantification of soluble Alzheimer's beta-peptide from biological fluids. Nature, 1992, 359(6393), 325-27.

457. Shankar G.M., Bloodgood B.L., Townsend M., Walsh D.M., Selkoe D.J., Sabatini B.L. Natural oligomers of the Alzheimer amyloid-beta protein induce reversible synapse loss by modulating an NMDA-type glutamate receptor-dependent signaling pathway. J Neurosci. 2007, 27(11), 2866-75.

458. Shaughnessy L., Thomas M.B., Wakefield J., Chamblin B., Nair A., Koentgen F., Ramabhadran R. Lentiviral vector-based models of amyloid pathology: from cells to animals. Curr Alzheimer Res. 2005, 2(2), 239-47.

459. Sheng M., Ertürk A. Long-term depression: a cell biological view. Philos Trans R Soc Lond B Biol Sci. 2013, 369(1633), 20130138.

460. Shibata M., Yamada S., Kumar S.R., Calero M., Bading J., Franqione B., Holtzman D.M, Miller C.A., Strickland D.K., Ghiso J., Zlokovic B.V. Clearance of Alzheimer's amyloid-ss (1-40) peptide from brain by LDL receptor-related protein-1 at the blood brain barrier. J Clin Invest. 2000, 106(12), 1489-99.

461. Shimohama S., Taniguchi T., Fujiwara M., Kameyama M. Biochemical characterization of -adrenergic receptors in human brain and changes in Alzheimer-type dementia. Journal of Neurochemistry. 1986, 47, 1294-1301

462. Shimohama S., Taniguchi T., Fujiwara M., Kameyama M. Changes in nicotinic and muscarinic cholinergic receptors in Alzheimer-type dementia. J Neurochem. 1986, 46(1), 288-93.

463. Shoji M., Golde T.E., Ghiso J., Cheung T.T., Estus S., Shaffer L.M., Cai X.D., McKay D.M., Tintner R., Frangione B., et al. Production of the Alzheimer amyloid beta protein by normal proteolytic processing. Science. 1992, 258(5079), 126-9

464. Sihver W., Gillberg P.G., Svensson A.L., Nordberg A. Autoradiographic comparison of [3H](-)nicotine, [3H]cytisine and [3H]epibatidine binding in relation to vesicular acetylcholine transport sites in the temporal cortex in Alzheimer's disease. Neuroscience. 1999, 94(3), 685-96.

465. Simmons-Stern N.R., Deason R.G., Brandler B.J., Frustace B.S., O'Connor M.K., Ally B.A., Budson A.E. Music-based memory enhancement in Alzheimer's disease: promise and limitations. Neuropsychologia. 2012, 50(14), 3295-303.

466. Skeldal S., Matusica D., Nykjaer A., Culson E.J. Proteolytic processing of the p75 neurotrophin receptor: A prerequisite for signalling ? Bioessays. 2011, 33(8), 614-25.

467. Skovronsky D.M., Moore D.B., Milla M.E., Doms R.W., Lee V.M. Protein kinase C-dependent alpha-secretase competes with beta-secretase for cleavage of amyloid-beta precursor protein in the trans-golgi network. J Biol Chem. 2000, 275(4), 2568-75.

468. Sloan H.L., Good M., Dunnett S.B. Double dissociation between hippocampal and prefrontal lesions on an operant delayed matching task and a water maze reference memory task. Behav Brain Res. 2006, 171(1), 116-26.

469. Słomnicki LP, Leśniak W. A putative role of the Amyloid Precursor Protein Intracellular Domain (AICD) in transcription. Acta Neurobiol Exp (Wars). 2008, 68(2), 219-28.

470. Small D.H., Maksel D., Kerr M.L., Ng J., Hou X., Chu C., Mehrani H., Unabia S., Azari M.F., Loiacono R., Aguilar M.I., Chebib M. The beta-amyloid protein of Alzheimer's disease binds to membrane lipids but does not bind to the alpha7 nicotinic acetylcholine receptor. J Neurochem. 2007, 101(6), 1527-38.

471. Smith J.C., Nielson K.A., Woodard J.L., Seidenberg M., Durgerian S., Hazlett K.E., Figueroa C.M., Kandah C.C., Kay C.D., Matthews M.A., Rao S.M. Physical activity reduces hippocampal atrophy in elders at genetic risk for Alzheimer's disease. Front Aging Neurosci. 2014, 6, 61.

472. Solfrizzi V., Panza F., Frisardi V., Seripa D., Logroscino G., Imbimbo B.P., Pilotto A. Diet and Alzheimer's disease risk factors or prevention: the current evidence. Expert Rev Neurother. 2011, 11(5), 677-708.

473. Solodkin A., Veldhuizen S.D., Van Hoesen G.W. Contingent vulnerability of entorhinal parvalbumin-containing neurons in Alzheimer's disease. J Neurosci. 1996, 16(10), 3311-21.

474. Solomon P.R., Murphy C.A. Early diagnosis and treatment of Alzheimer's disease. Expert Rev Neurother. 2008, 8(5), 769-80

475. Soreq H., Seidman S. Acetylcholinesterase--new roles for an old actor. Nat Rev Neurosci. 2001, 2(4), 294-302.

476. Sotthibundhu A., Sykes A.M., Fox B., Underwood C.K., Thangnipon W., Coulson E.J. Beta-amyloid(1-42) induces neuronal death through the p75 neurotrophin receptor. J Neurosci. 2008, 28(15), 3941-46.

477. Sperling R.A., Dickerson B.C., Pihlajamaki M., Vannini P., LaViolette P.S., Vitolo O.V., Hedden T., Becker J.A., Rentz D.M., Selkoe D.J., Johnson K.A. Functional alterations in memory networks in early Alzheimer's disease. Neuromolecular Med. 2010, 12(1), 27-43.

478. Stein-Behrens B., Adams K., Yeh M., Sapolsky R. Failure of beta-amyloid protein fragment 25-35 to cause hippocampal damage in the rat. Neurobiol Aging. 1992,13(5), 577-9.

479. Sugino H., Watanabe A., Amada N., Yamamoto M., Ohgi Y., Kostic D., Sanchez R. Global Trends in Alzheimer Disease Clinical Development: Increasing the Probability of Success. Clin Ther. 2015, 37(8), 1632-42.

480. Sunderland T., Tariot P.N., Newhouse P.A. Differential responsivity of mood, behavior, and cognition to cholinergic agents in elderly neuropsychiatric populations. Brain Res. 1988, 472(4), 371-89.

481. Sun Y., Lu C., Chien K.L., Chen S.T., Chen R.C. Efficacy of multivitamin supplementation containing vitamins B6 and B12 and folic acid as adjunctive treatment with a cholinesterase inhibitor in Alzheimer's disease: a 26-week, randomized, double-blind, placebo-controlled study in Taiwanese patients. Clin Ther. 2007, 29(10), 2204-14.

482. Supnet C., Bezprozvanny I. Presenilins as endoplasmic reticulum calcium leak channels and Alzheimer's disease pathogenesis. Sci China Life Sci. 2011, 54(8), 744-51.

483. Sweeney J.E, Höhmann C.F, Oster-Granite M.L, Coyle J.T. Neurogenesis of the basal forebrain in euploid and trisomy 16 mice: an animal model for developmental disorders in Down syndrome. Neuroscience. 1989, 31(2), 413-25.

484. Szigeti C., Bencsik N., Simonka A.J., Legradi A., Kasa P., Gulya K. Long-term effects of selective immunolesions of cholinergic neurons of the nucleus basalis magnocellularis on the ascending cholinergic pathways in the rat: a model for Alzheimer's disease. Brain Res Bull. 2013, 94, 9-16.

485. Szutowicz A., Jankowska A., Tomaszewicz M. Disturbances of glucose metabolism in epilepsy and other neurodegenerative diseases. Neurol Neurochir Pol. 2000, 34(8), 59-66.

486. Takahashi R.H., Almeida C.G., Kearney P.F., Yu F., Lin M.T., Milner T.A., Gouras G.K. Oligomerization of Alzheimer's beta-amyloid within processes and synapses of cultured neurons and brain. J Neurosci. 2004, 24(14) 3592-99.

487. Takamori S., Rhee J.S., Rosenmund C., Jahn R. Identification of a vesicular glutamate transporter that defines a glutamatergic phenotype in neurons. Nature. 2000, 407(6801), 189-94.

488. Takei N., Torres E., Yuhara A., Jongsma H., Otto C., Korhonen L., Abiru Y., Skoglösa Y., Schütz G., Hatanaka H., Sofroniew M.V., Lindholm D. Pituitary adenylate cyclase-activating polypeptide promotes the survival of basal forebrain cholinergic neurons in vitro and in vivo: comparison with effects of nerve growth factor. Eur J Neurosci. 2000, 12(7), 2273-80.

489. Takeuchi A., Irizarry M.C., Duff K., Saido T.C., Hsiao Ashe K., Hasegawa M., Mann D.M., Hyman B.T., Iwatsubo T. Age-related amyloid beta deposition in transgenic mice overexpressing both Alzheimer mutant presenilin 1 and amyloid beta precursor protein Swedish mutant is not associated with global neuronal loss. Am J Pathol. 2000, 157(1), 331-39.

490. Talantova M., Sanz-Blasco S., Zhang X., Xia P., Akhtar M.W., Okamoto S., Dziewczapolski G., Nakamura T., Cao G., Pratt A.E., Kang Y.J., Tu S., Molokanova E., McKercher S.R., Hires S.A., Sason H., Stouffer D.G., Buczynski M.W., Solomon J.P., Michael S., Powers E.T., Kelly J.W., Roberts A., Tong G., Fang-Newmeyer T., Parker .J, Holland E.A., Zhang D., Nakanishi N., Chen H.S., Wolosker H., Wang Y., Parsons L.H., Ambasudhan R., Masliah E., Heinemann S.F., Piña-Crespo J.C., Lipton S.A. Aβ induces astrocytic glutamate release, extrasynaptic NMDA receptor activation, and synaptic loss. Proc Natl Acad Sci U S A. 2013, 110(27), 2518-27.

491. Tanaka K., Kelly C.E., Goh K.Y., Lim K.B., Ibáñez C.F. Death Domain Signaling by Disulfide-Linked Dimers of the p75 Neurotrophin Receptor Mediates Neuronal Death in the CNS. J Neurosci. 2016, 36(20), 5587-95.

492. Taniuchi M., Johnson E.M. Jr. Characterization of the binding properties and retrograde axonal transport of a monoclonal antibody directed against the rat nerve growth factor receptor. J Cell Biol. 1985, 101(3), 1100-6.

493. Terry R.D., Alzheimer's disease, R.L. Davis, D.M. Robertson, Editors , Textbook of Neuropathology, Williams and Wilkins, Baltimore 1985, 824–41.

494. Thal D.R., Rüb U., Orantes M., Braak H. Phases of A beta-deposition in the human brain and its relevance for the development of AD. Neurology. 2002, 58(12), 1791-800.

495. Tiscornia G., Singer O., Verma I.M. Production and purification of lentiviral vectors. NatProtoc. 2006, 1(1), 241-45.

496. Toledana A., Álvarez M.I. Lesion-induced vertebrate models of Alzheimer dementia. In: De Deyn PP, Van Dam D, editors. Animal Models of Dementia. New York: Springer Science + Business Media; 2010, 295–345.

497. Tsien R.W., Lipscombe D., Madison D.V., Bley K.R., Fox A.P. Multiple types of neuronal calcium channels and their selective modulation. Trends Neurosci. 1988, 11(10), 431-38.

498. Tucek S. Regulation of acetylcholine synthesis in the brain. J Neurochem. 1985, 44(1), 11-24.

499. Tuszynski M.H., Blesch A. Nerve growth factor: from animal models of cholinergic neuronal degeneration to gene therapy in Alzheimer's disease. Prog Brain Res. 2004, (146), 441-49.

500. Tuszynski M.H., Thal L., Pay M., Salmon D.P., U H.S., Bakay R., Patel P., Blesch A., Vahlsing H.L., Ho G., Tong G., Potkin S.G., Fallon J., Hansen L., Mufson E.J., Kordower J.H., Gall C., Conner J. A phase 1 clinical trial of nerve growth factor gene therapy for Alzheimer disease. Nat Med. 2005, 11(5), 551-5.

501. Tuszynski M.H., Yang J.H., Barba D., U H.S., Bakay R.A., Pay M.M., Masliah E., Conner J.M., Kobalka P., Roy S., Nagahara A.H. Nerve Growth Factor Gene Therapy: Activation of Neuronal Responses in Alzheimer Disease. JAMA Neurol. 2015, 72(10), 1139-47.

502. Ueda K., Shinohara S., Yagami T., Asakura K., Kawasaki K. Amyloid beta protein potentiates Ca2+ influx through L-type voltage-sensitive Ca2+ channels: a possible involvement of free radicals. J Neurochem. 1997, 68(1), 265-71.

503. Underwood C.K., Reid K., May L.M., Bartlett P.F., Coulson E.J. Palmitoylation of the C-terminal fragment of p75(NTR) regulates death signaling and is required for subsequent cleavage by gamma-secretase. Mol Cell Neurosci. 2008, 37(2), 346-58.

504. Upadhyay J., Baker S.J., Chandran P., Miller L., Lee Y., Marek G.J., Sakoglu U., Chin C.L., Luo F., Fox G.B., Day M. Default-mode-like network activation in awake rodents. PLoS One. 2011, 6(11), 27839

505. Urra S., Escudero C.A., Ramos P., Lisbona F., Allende E., Covarrubias P., Parraguez J.I., Zampieri N., Chao M.V., Annaert W., Bronfman F.C. TrkA receptor activation by nerve growth factor induces shedding of the p75 neurotrophin receptor followed by endosomal gamma-secretase-mediated release of the p75 intracellular domain. J Biol Chem. 2007, 282(10), 7606-15.

506. van Groen T., Kiliaan A.J., Kadish I. Deposition of mouse amyloid beta in human APP/PS1 double and single AD model transgenic mice. Neurobiol Dis. 2006, 23(3), 653-62.

507. Verdier Y., Penke B. Binding sites of amyloid beta-peptide in cell plasma membrane and implications for Alzheimer's disease. Curr Protein Pept Sci. 2004, 5(1), 19-31.

508. Vigna E., Cavalieri S., Ailles L., Geuna M., Loew R., Bujard H., Naldini L. Robust and efficient regulation of transgene expression in vivo by improved tetracycline-dependent lentiviral vectors. Robust and efficient regulation of transgene expression in vivo by improved tetracycline-dependent lentiviral vectors. Mol Ther. 2002, 5(3), 252-61.

509. Volosin M., Trotter C., Cragnolini A., Kenchappa R.S., Light M., Hempstead B.L., Carter B.D., Friedman W.J. Induction of proneurotrophins and activation of p75NTR-mediated apoptosis via neurotrophin receptor-interacting factor in hippocampal neurons after seizures. J Neurosci. 2008, 28(39), 9870-79.

510. von Schack D., Casademunt E., Schweigreiter R., Meyer M., Bibel M., Dechant G. Complete ablation of the neurotrophin receptor p75NTR causes defects both in the nervous and the vascular system. Nat Neurosci. 2001, 4(10), 977-78.

511. Wang B., Hu Q., Hearn M.G., Shimizu K., Ware C.B., Liggitt D.H., Jin L.W., Cool B.H., Storm D.R., Martin G.M. Isoform-specific knockout of FE65 leads to impaired learning and memory. J Neurosci Res. 2004, 75(1), 12-24.

512. Wang H.Y., Lee D.H., D'Andrea M.R., Peterson P.A., Shank R.P., Reitz A.B. beta-Amyloid(1-42) binds to alpha7 nicotinic acetylcholine receptor with high affinity. Implications for Alzheimer's disease pathology. J Biol Chem. 2000, 275(8), 5626-32.

513. Wang K.C., Kim J.A., Sivasankaran R., Segal R., He Z. P75 interacts with the Nogo receptor as a co-receptor for Nogo, MAG and OMgp. Nature. 2002, 420(6911), 74-78.

514. Wang K.K. Calpain and caspase: can you tell the difference? Trends Neurosci. 2000, 23(1), 20-26.

515. Wang Y.J., Wang X., Lu J.J., Li Q.X., Gao C.Y., Liu X.H., Sun Y., Yang M., Lim Y., Evin G., Zhong J.H., Masters C., Zhou X.F. p75NTR regulates Abeta deposition by increasing Abeta production but inhibiting Abeta aggregation with its extracellular domain. J Neurosci. 2011, 31(6), 2292-304.

516. Wang X., Shao Z., Zetoune F.S., Zeidler M.G., Gowrishankar K., Vincenz C. NRADD, a novel membrane protein with a death domain involved in mediating apoptosis in response to ER stress. Cell Death Differ. 2003, 10(5), 580-91.

517. Walsh D.M., Klyubin I., Fadeeva J.V., Cullen W.K., Anwyl R. Wolfe M.S., Rowan M.J., Selkoe D.J. Naturally secreted oligomers of amyloid beta protein potently inhibit hippocampal long-term potentiation in vivo. Nature 2002, 416(6880), 535-39.

518. Walsh D.M., Selkoe D.J. A beta oligomers - a decade of discovery. J Neurochem. 2007, 101(5), 1172-84.

519. Walsh D.M., Selkoe D.J. Deciphering the molecular basis of memory failure in Alzheimer's disease. Neuron. 2004, 44(1), 181-93.

520. Weiner M.W., Veitch D.P., Hayes J., Neylan T., Grafman J., Aisen P.S., Petersen R.C., Jack C., Jagust W., Trojanowski J.Q., Shaw L.M., Saykin A.J., Green R.C., Harvey D., Toga A.W., Friedl K.E., Pacifico A., Sheline Y., Yaffe K., Mohlenoff B.; Department of Defense Alzheimer's Disease Neuroimaging Initiative. Alzheimers Dement. 2014, 10(3), S226-35

521. Weingarten M.D., Lockwood A.H., Hwo S.Y., Kirschner M.W. A protein factor essential for microtubule assembly. Proc Natl Acad Sci U S A. 1975, 72(5), 1858-62.

522. Wenk G.L., McGann K., Hauss-Wegrzyniak B., Rosi S. The toxicity of tumor necrosis factor-alpha upon cholinergic neurons within the nucleus basalis and the role of norepinephrine in the regulation of inflammation: implications for Alzheimer's disease. Neuroscience. 2003, 121(3), 719-29.

523. Whitehouse P.J., Martino A.M., Antuono P.G., Lowenstein P.R., Coyle J.T., Price D.L., Kellar K.J. Nicotinic acetylcholine binding sites in Alzheimer's disease. Brain Res. 1986, 371(1), 146-51.

524. Whitehouse P.J., Price D.L., Clark A.W., Coyle J.T., DeLong M.R. Alzheimer disease: evidence for selective loss of cholinergic neurons in the nucleus basalis. Ann Neurol. 1981, 10(2), 122-26.

525. Wiley R.G., Oeltmann T.N., Lappi D.A. Immunolesioning: selective destruction of neurons using immunotoxin to rat NGF receptor. Brain Res. 1991, 562(1), 149-53.

526. Wiley R.G. Toxin-induced death of neurotrophin-sensitive neurons. Methods Mol Biol. 2001, 169, 217-22.

527. Winkler J., Suhr S.T., Gage F.H., Thal L.J, Fisher L.J. Essential role of neocortical acetylcholine in spatial memory. Nature. 1995, 375(6531), 484-87.

528. Wong J., Higgins M., Halliday G., Garner B. Amyloid beta selectively modulates neuronal TrkB alternative transcript expression with implications for Alzheimer's disease. Neuroscience. 2012, 17(210), 363-74.

529. Wong J., Rothmond D.A., Webster M.J., Weickert C.S. Increases in two truncated TrkB isoforms in the prefrontal cortex of people with schizophrenia. Schizophr Bull. 2013, 39(1), 130-40.

530. Wong Y.H., Lee C.M., Xie W., Cui B., Poo M.M. Activity-dependent BDNF release via endocytic pathways is regulated by synaptotagmin-6 and complexin. Proc Natl Acad Sci U S A. 2015, 112(32), E4475-84

531. Woolf, N.J. A possible role for cholinergic neurons of the basal forebrain and pontomesencephalon in consciousness. Consciousness and Cognition, 1997, 6, 574-96.

532. Woolf, N.J., Butcher, L.L. The cholinergic basal forebrain as a cognitive machine. In: Functions of the Basal Forebrain Cholinergic System. 1991, 347-80.

533. Woolf N.J. Cholinergic systems in mammalian brain and spinal cord. Prog. Neurobiol. 1991, 37, 475-524.

534. Woolf N.J., Gould E, Butcher L.L. Nerve growth factor receptor is associated with cholinergic neurons of the basal forebrain but not the pontomesencephalon. Neuroscience. 1989, 30(1), 143-52.

535. Wu, C.-K., Geula, C., 1997. Selective loss of calbindin D 28k from cholinergic neurons of human basal forebrain in aging and Alzheimer's disease. In: Iqbal, K., Winblad, B., Nishimura, T., Takeda, M., Wisniewski, H.M. (Eds.), Alzheimer's Disease: Biology, Diagnosis and Therapeutics. John Wiley and Sons Ltd., England, pp. 297– 302.

536. Wu G., Wu., Na S., Hershey J.C. Quantitative assessment of Aβ peptide in brain, cerebrospinal fluid and plasma following oral administration of γ-secretase inhibitor MRK-560 in rats. Int J Neurosci. 2015, 125(8), 616-24.

537. Wu H.Y., Hudry E., Hashimoto T., Kuchibhotla K., Rozkalne A., Fan Z., Spires-Jones T., Xie H., Arbel-Ornath M., Grosskreutz C.L., Bacskai B.J., Hyman B.T. Amyloid beta induces the morphological neurodegenerative triad of spine loss, dendritic simplification, and neuritic dystrophies through calcineurin activation. J Neurosci. 2010, 30(7), 2636-49.

538. Wurtzer S., Goubard A., Mammano F., Saragosti S., Lecossier D., Hance A.J., Clavel F. Functional central polypurine tract provides downstream protection of the human immunodeficiency virus type 1 genome from editing by APOBEC3G and APOBEC3B. J Virol. 2006, 80(7), 3679-83.

539. Wu Y.H., Feenstra M.G., Zhou J.N., Liu R.Y., Torano J.S. van Kann H.J., Fisher D.F., Ravid R., Swaab D.F. Molecular changes underlying reduced pineal melatonin levels in Alzheimer's disease: Alterations in preclinical and clinical stages. J. Clin. Enocr. Metab. 2003, 88, 5898-5906

540. Xie Y., Ye L.Y., Cui W., Xu K., Zhang X.B., Lou J.N., Hou X.P. Study on nerve growth factor liposomes on crossing blood-brain barrier in vitro and in vivo. Yao Xue Xue Bao. 2004, 39(11), 944-48.

541. Yaar M., Zhai S., Pilch P.F., Doyle S.M., Eisenhauer P.B., Fine R.E., Gilchrest B.A. Binding of beta-amyloid to the p75 neurotrophin receptor induces apoptosis. A possible mechanism for Alzheimer's disease. J Clin Invest. 1997, 100(9), 2333-40.

542. Yamasaki M., Matsui M., Watanabe M. Preferential localization of muscarinic M1 receptor on dendritic shaft and spine of cortical pyramidal cells and its anatomical evidence for volume transmission. J Neurosci. 2010, 30(12), 4408-18.

543. Yamashita T., Tucker K., Barde, Y. Neurotrophin binding to the p75 receptor modulates Rho activity and axonal outgrowth. Neuron 1999, 24, 585–93.

544. Yang J., Li S., He X.B., Cheng C., Le W. Induced pluripotent stem cells in Alzheimer's disease: applications for disease modeling and cell-replacement therapy. Mol Neurodegener. 2016, 11(1), 39.

545. Yang T., Knowles J.K., Lu Q., Zhang H., Arancio O., Moore L.A., Chang T., Wang Q., Andreasson K., Rajadas J., Fuller G.G., Xie Y., Massa S.M., Longo F.M. Small molecule, non-peptide p75 ligands inhibit Abeta-induced neurodegeneration and synaptic impairment. PLoS One. 2008, 3(11), 3604.

546. Yang R., Chen L., Wang H., Xu B., Tomimoto H., Chen L. Anti-amnesic effect of neurosteroid PREGS in Aβ25-35-injected mice through σ1 receptor- and α7nAChR-mediated neuroprotection. Neuropharmacology. 2012, 63(6), 1042-50.

547. Yang Z., Cool B.H., Martin G.M., Hu Q. A dominant role for FE65 (APBB1) in nuclear signaling. J Biol Chem. 2006, 281(7), 4207-14.

548. Yeo T.T., Yang T., Massa S.M., Zhang J.S., Honkaniemi J., Butcher L.L., Longo F.M. Deficient LAR expression decreases basal forebrain cholinergic neuronal size and hippocampal cholinergic innervation. J Neurosci Res. 1997, 47(3), 348-60.

449. Yiannopoulou K.G., Papageorgiou S.G. Current and future treatments for Alzheimer's disease. Ther Adv Neurol Disord. 2013, 6(1), 19-33.

550. Yoon S.O., Casaccia-Bonnefil P., Carter B., Chao M.V. Competitive signaling between TrkA and p75 nerve growth factor receptors determines cell survival. J Neurosci. 1998, 18(9), 3273-81.

551. Zaborszky L., Rosin D.L., Kiss J. Alpha-adrenergic receptor (alpha (2 A)) is colocalized in basal forebrain cholinergic neurons: a light and electron microscopic double immunolabeling study. J Neurocytol. 2004, 33(3), 265-76.

552. Zaborsky L., Van den Pol A., Gyengesi E. The basal forebrain cholinergic projection system in mice. Elsvier Inc., 2012, 28.

553. Zarow C, Lyness S.A., Mortimer J.A., Chui H.C. Neuronal loss is greater in the locus coeruleus than nucleus basalis and substantia nigra in Alzheimer and Parkinson diseases. Arch Neurol. 2003, 60(3), 337-41.

554. Zeng F., Lu J.J., Zhou X.F., Wang Y.J. Roles of p75NTR in the pathogenesis of Alzheimer's disease: a novel therapeutic target. Biochem Pharmacol. 2011, 82(10), 1500-9.

555. Zheng X.Y., Zhang H.L., Luo Q., Zhu J. Kainic acid-induced neurodegenerative model: potentials and limitations. J Biomed Biotechnol. 2011, 457079.

556. Zhou X.F., Wang Y.J. The p75NTR extracellular domain: a potential molecule regulating the solubility and removal of amyloid-β. Prion. 2011, 5(3), 161-63

557. Zufferey R., Dull T., Mandel R.J., Bukovsky A., Quiroz D., Naldini L., Trono D. Self-inactivating lentivirus vector for safe and efficient in vivo gene delivery. J Virol1998, (72), 9873-80.

558. Zussy C., Brureau A., Delair B., Marchal S., Keller E., Ixart G., Naert G., Meunier J., Chevallier N., Maurice T., Givalois L. Time-course and regional analyses of the physiopathological changes induced after cerebral injection of an amyloid β fragment in rats. Am J Pathol. 2011, 179(1), 315-34

I apologise other authors for not citing all the relevant literature to this topic.

7.3. Buffers and solutions used

AP buffer (5X)

14.6 NaCl; 30.25 g Tris; $MgCL_2x6H_2O$

Adjust pH to 9.5 with HCl

Brain tissue extraction buffer:

20mM Tris-HCl; 145 mM NaCl, 10% glycerol; 5 mM EDTA; 0.5% Nonidet

Before use add protease inhibitor cocktail (539134, Calbiochem)

PBS (10X)

0.02M NaH_2PO_4 (monobasic); 0.077 M Na_2HPO_4 (dibasic); 1.4M NaCl

4% PFA

Heat less than 100 ml H_2O and add 4g paraformaldehyde (weight with face mask on). Stir and heat to get clear solution. Add few drops 1M NaOH until the solution gets clear. Filter the solution through 0.45 μm filter. Add 10 ml (10X) PBS. Adjust pH to 7.4 with HCl or NaOH

Polyacrylamide gel (12.5%) (composition for 2 gels)

resolving gel: 3.75 ml Tris-SDS, pH=8.8; 4.75 ml H_20; 6.35 ml acrylamide; 12.5 μl Temed; 10 % APS

Stacking gel: 1.7 ml Tris-SDS, pH=6.8; 4.9 ml H_20; 925 μl acrylamide; 7.5 μl Temed; 75μl 10% APS

QIAfilter Plasmid Midi Kit buffers:

P1: 50 mM Tris-HCl, pH 8.0; 10 mM EDTA; 100 μg/ml RNase A

P2: 200 mM NaOH, 1% SDS (w/v)

P3: 3.0 M potassium acetate, pH 5.5

QBT: 750 mM NaCl, 50 mM MOPS, pH 7.0; 15% isopropanol (v/v); 0.15 % Triton X-100 (v/v)

QC: 1.0 M NaCl, 50 mM MOPS, pH 7.0; 15% isopropanol (v/v)

QF: 1.25 M NaCl, 50 mM Tris-Cl, pH 8.5; 15% isopropanol (v/v)

SDS-PAGE buffer (1L)

1M MOPS; 1M Tris base; 69.3 mM SDS; 20.5 mM EDTA

Or Tris base (30g); glycin (144g); SDS (10g)

TAE (Tris-acetate-EDTA buffer) (10X)

48.4 g of Tris Base, 11.4 ml of glacial acetic acid (17.4 M); 3.7 g of EDTA, disodium salt; deionized water up to 1L

TBS (10X)

50 mM Tris-HCl; 150 mM NaCl

pH to 7.4 with HCl or NaOH

TBST buffer for 1 L

100ml of TBS(10X) + 900 ml ultra-pure H_2O and 1ml of Tween 20

TE (Tris-EDTA buffer)

10 mM Tris, bring to pH 8.0 with HCl, 1 mM EDTA

Tris-SDS for polyacrylamide gels

Tris for resolving gel (1 L): Tris base 181.7 g; 10 % SDS, pH=8.8

Tris stacking gel for (1 L): Tris base 60.6 g; 10 % SDS, pH=6.8

WB transfer buffer for 1 L

100 ml Methanol; 3.04 g Tris base; 15 g glycine

All reagents were purchased from Sigma Aldrich: 30 % acrylamide (A3574), APS (A3678), EDTA (E6758), glacial acetic acid (1005706), glycerol (G6279), HCl (H1758), isopropanol (I9516), methanol (34860), $MgCL2x6H_2O$ (M9272), MOPS (69947), Na_2HPO_4 (30412), NaH_2PO_4 (S8282), NaCl (S7653,Sigma), NaOH (S0399), Nonidet (74385), Paraformaldehyde (P6148), Potassium acetate (P1190), SDS (L3771), Temed (T7024), Tris-HCl (T3253), Triton X-100 (T9284), Trizma base (93349), Tween 20 (P1379).

7.4. Plasmids' chart

A

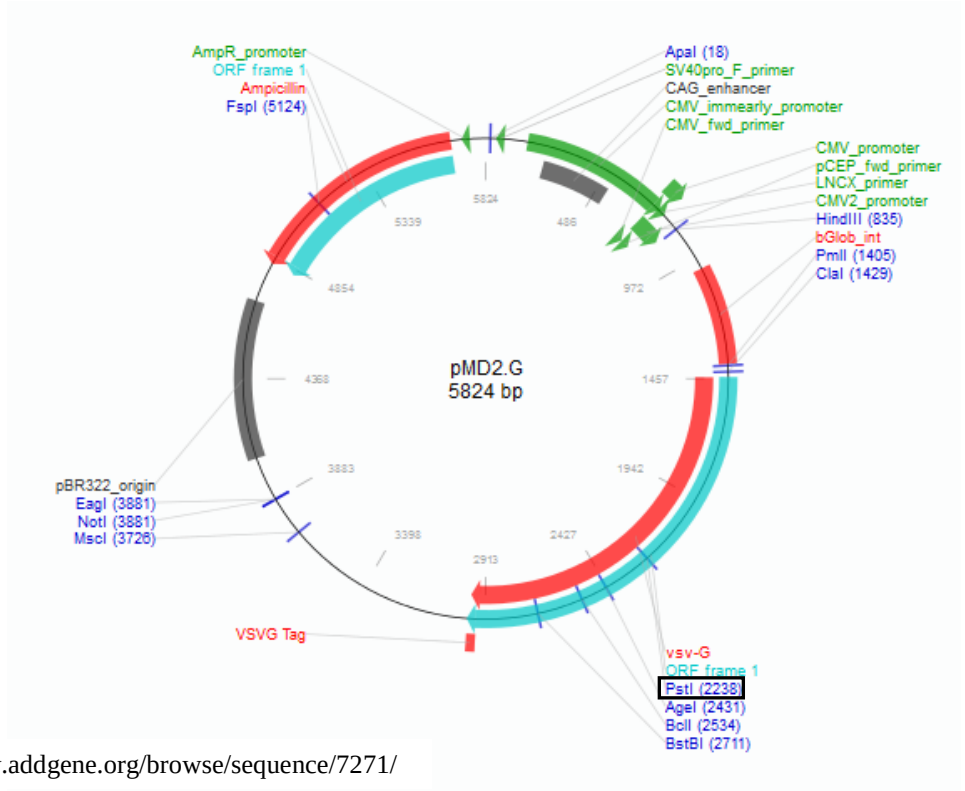

http://www.addgene.org/browse/sequence/7271/

B

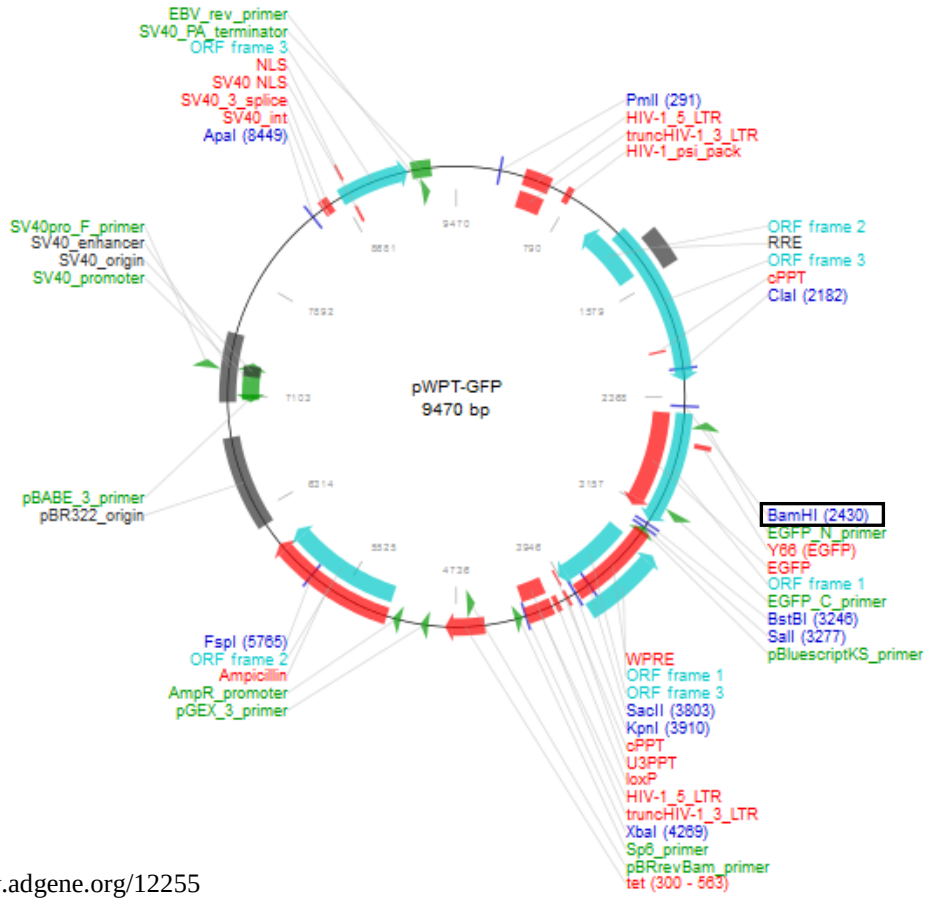

http://www.adgene.org/12255

C

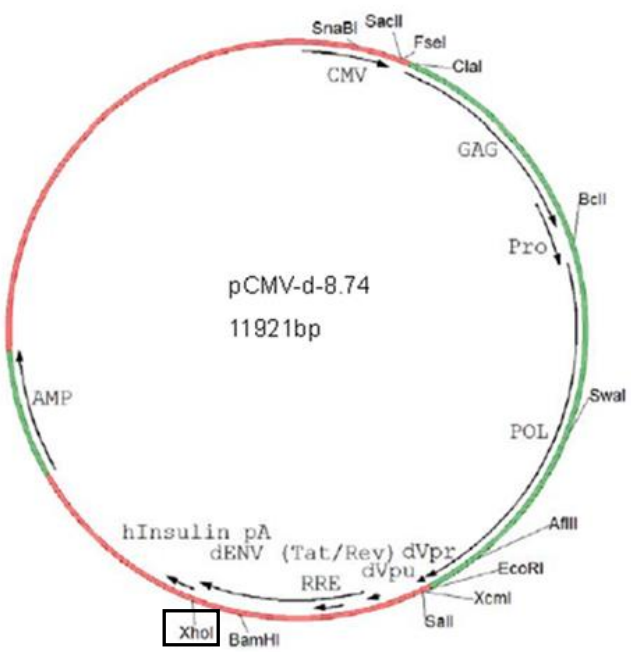

Schematic representation of pCMV-d-8.74 from ICNT library

D

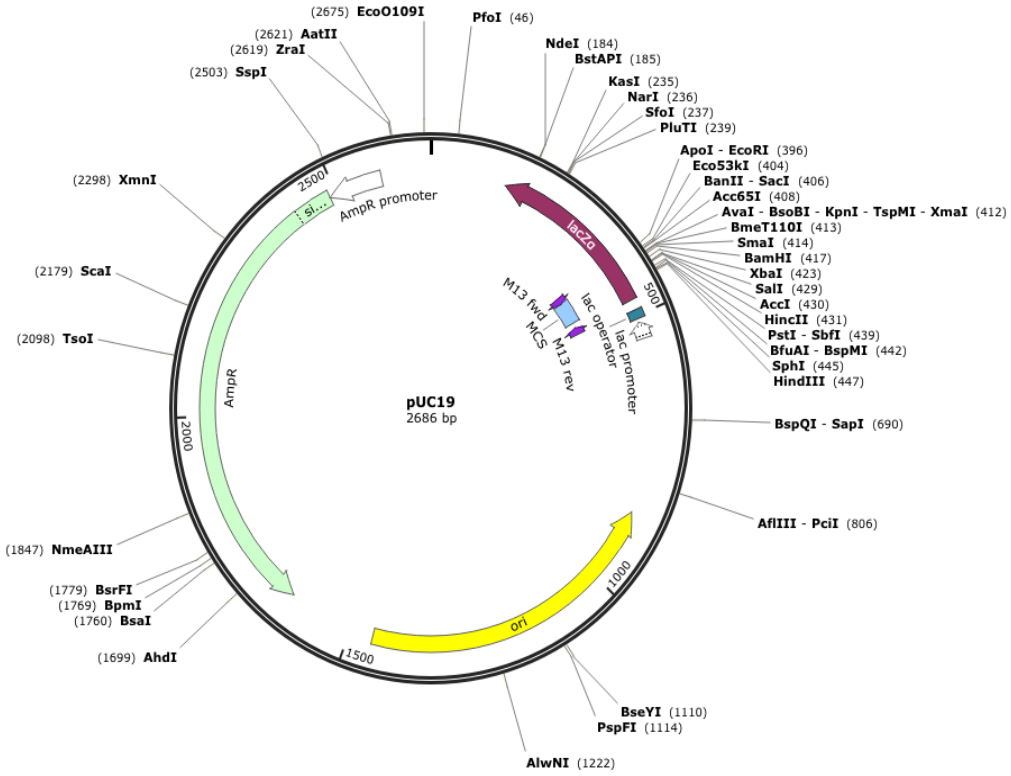

http://www.snapgene.com/resources/plasmid_files/basic_cloning_vectors/pUC19

Figure 70. Schematic representation of plasmids DNA with most important restriction sites indicated. A. pMD2G – envelope plasmid. B. pWPT-GFP – packaging plasmid. C. pCMV – helper plasmid. D. pUC19 – control plasmid. The source of each plasmid restriction map is given underneath each plasmid.

7.5. Posters

- "Basal forebrain cholinergic neurons as a target for gene therapy in Alzheimer's disease"

  (Bio)pharmaceutical and Pharmacological Sciences Conference Dublin City University, Ireland (2011)

- "$p75^{NTR}$ endocytosis as a potential route for amyloid β internalization in cholinergic neurons of basal forebrain"

  11th International Conference on Alzheimer's and Parkinson's Diseases (AD/PDTM 2013), Florence, Italy (2013)

- "Targeting $p75^{NTR}$ by lentiviral vectors as prerequisite for AD gene therapy"

  Careers in Neuroscience Symposium, National University of Ireland, Galway, Ireland (2014)

7.6. Publications and abstracts published

- Ovsepian S.V., Antyborzec I., O'Leary V.B., Zaborszky L., Herms J., Oliver Dolly J. Neurotrophin receptor p75 mediates the uptake of the amyloid beta (Aβ) peptide, guiding it to lysosomes for degradation in basal forebrain cholinergic neurons. Brain Struct Funct. 2014, 219(5), 1527-41.

- The publication was additionally mentioned in Targeting Trends 2013,14(4),3

- Antyborzec I., O'Leary V.B., Dolly J.O., Ovsepian S.V. Neurotherapeutics. Low-affinity neurotrophin receptor p75 promotes the transduction of targeted lentiviral vectors to cholinergic neurons of rat basal forebrain. 2016 May 24. [Epub ahead of print]

Abstract:

- "$P75^{NTR}$ Endocytosis as a Potential Route for Amyloid β Internalization in Cholinergic Neurons of Basal Forebrain" published as a supplement to the Neurodegenerative Diseases Journal, 2013, Vol. 11, Suppl. 1 - Alzheimer's and Parkinson's Diseases: Mechanisms, Clinical Strategies, and Promising Treatments of Neurodegenerative Diseases – also available online http://adpd.ekonnect.co/ADPD_443/poster_53219/program.aspx

7.7. Other contributions

Immuno-cytochemistry and cell counting for the publication below

Ovsepian S.V., Dolly J.O., Zaborszky L. Intrinsic voltage dynamics govern the diversity of spontaneous firing profiles in basal forebrain noncholinergic neurons. J Neurophysiol. 2012, 108(2), 406-18.